

**Spatial patterns of humus forms,  
soil organisms and soil biological activity at  
high mountain forest sites in the Italian Alps**

Doctoral dissertation



**Niels Hellwig**  
Osnabrück University





**Spatial patterns of humus forms,  
soil organisms and soil biological activity at  
high mountain forest sites in the Italian Alps**

Dissertation  
zur Erlangung des Grades  
Doktor der Naturwissenschaften (Dr. rer. nat.)  
am Fachbereich Kultur- und Sozialwissenschaften  
der Universität Osnabrück

**Niels Hellwig**  
Institute of Geography  
School of Cultural Studies and Social Sciences  
Osnabrück University

Osnabrück, 2018

**Cover photos:**

Niels Hellwig, 2014-2015

Background: Humus profile under branches at a north-facing slope near Rabbi Fonti (1620 m a.s.l., Val di Rabbi, Trentino, Italian Alps).

Front cover: 1) Treeline of the European larch (*Larix decidua*) next to Lago di Soprasasso at 2200 m a.s.l., in the upper part of the Valle di Valorz above the Valorz waterfalls near San Bernardo (Val di Rabbi, Trentino, Italian Alps); 2) View from the Valle di Valorz on the Val di Rabbi and San Bernardo (Trentino, Italian Alps).

Back cover: 1) View from Malga Polinar on investigated south-facing slope near San Bernardo (Val di Rabbi, Trentino, Italian Alps); 2) View from the Passo di Morbigai on the lower part of the Val di Rabbi and Malè in the Val di Sole (Trentino, Italian Alps).



## Abstract

The objective of the thesis is the model-based analysis of spatial patterns of decomposition properties on the forested slopes of the montane level (ca. 1200-2200 m a.s.l.) in a study area in the Italian Alps (Val di Sole / Val di Rabbi, Autonomous Province of Trento). The analysis includes humus forms and enchytraeid assemblages as well as pH values, activities of extracellular enzymes and C/N ratios of the topsoil. The first aim is to develop, test and apply data-based techniques for spatial modelling of soil ecological parameters. This methodological approach is based on the concept of digital soil mapping. The second aim is to reveal the relationships between humus forms, soil organisms and soil microbiological parameters in the study area. The third aim is to analyze if the spatial patterns of indicators of decomposition differ between the landscape scale and the slope scale.

At the landscape scale, sample data from six sites are used, covering three elevation levels at both north- and south-facing slopes. A knowledge-based approach that combines a decision tree analysis with the construction of fuzzy membership functions is introduced for spatial modelling. According to the sampling design, elevation and slope exposure are the explanatory variables.

The investigations at the slope scale refer to one north-facing and one south-facing slope, with 30 sites occurring on each slope. These sites have been derived using conditioned Latin Hypercube Sampling, and thus reasonably represent the environmental conditions within the study area. Predictive maps have been produced in a purely data-based approach with random forests.

At both scales, the models indicate a high variability of spatial decomposition patterns depending on the elevation and the slope exposure. In general, sites at high elevation on north-facing slopes almost exclusively exhibit the humus forms Moder and Mor. Sites on south-facing slopes and at low elevation exhibit also Mull and Amphimull. The predictions of those enchytraeid species characterized as Mull and Moder indicators match the occurrence of the corresponding humus forms well. Furthermore, referencing the mineral topsoil, the predictive models show increasing pH values, an increasing leucine-aminopeptidase activity, an increasing ratio alkaline/acid phosphomonoesterase activity and a decreasing C/N ratio from north-facing to south-facing slopes and from high to low elevation.

The predicted spatial patterns of indicators of decomposition are basically similar at both scales. However, the patterns are predicted in more detail at the slope scale because of a larger data basis and a higher spatial precision of the environmental covariates. These factors enable the observation of additional correlations between the spatial patterns of indicators of decomposition and environmental influences, for example slope angle and curvature. Both the corresponding results and broad model evaluations have shown that the applied methods are generally suitable for modelling spatial patterns of indicators of decomposition in a heterogeneous high mountain environment. The overall results suggest that the humus form can be used as indicator of organic matter decomposition processes in the investigated high mountain area.



## Zusammenfassung

Ziel der Dissertation ist die modellbasierte Analyse räumlicher Muster von Dekompositionscharakteristika in den bewaldeten Hangbereichen der montanen Stufe (ca. 1200-2200 m ü. NN) in einem Untersuchungsgebiet in den italienischen Alpen (Val di Sole / Val di Rabbi, Autonome Provinz Trient). Als Indikatoren für Dekompositionsprozesse werden Humusformen, Enchyträengemeinschaften sowie pH-Werte, Aktivitäten extrazellulärer Enzyme und C/N-Verhältnisse im Oberboden untersucht. Aufbauend auf dem Konzept des Digital Soil Mapping sollen datenbasierte Verfahren zur räumlichen Modellierung bodenökologischer Parameter entwickelt, getestet und angewendet werden. Die Modelle sollen zeigen, welche Zusammenhänge zwischen Humusformen, Bodenorganismen und bodenmikrobiologischen Parametern im Untersuchungsgebiet bestehen. Außerdem soll analysiert werden, inwiefern sich die räumlichen Dekompositionsmuster zwischen der Landschaftsebene und der Hangebene unterscheiden.

Auf Landschaftsebene werden Daten von sechs Standorten genutzt, die jeweils drei Höhenstufen an nord- und südexponierten Hängen abdecken. Für die räumliche Modellierung wird ein wissensbasierter Ansatz bestehend aus einer Entscheidungsbaumanalyse und der Konstruktion von Fuzzy-Zugehörigkeitsfunktionen vorgestellt. Entsprechend dem Sampling-Design dienen die Höhe und die Hangexposition als erklärende Variablen.

Die Untersuchungen auf Hangebene beziehen sich auf einen nord- und einen südexponierten Hang. Die Datenbasis umfasst jeweils 30 mittels Conditioned Latin Hypercube Sampling abgeleitete Standorte, die die Standortbedingungen im Untersuchungsgebiet möglichst gut repräsentieren. Zur Erstellung von Vorhersagekarten wird mit Random Forests ein rein datenbasierter Ansatz genutzt.

Die Modelle zeigen auf beiden Skalenebenen eine deutliche Variabilität der Dekompositionsmuster, die mit der Höhe und der Hangexposition zusammenhängt. Generell sind höhergelegene nordexponierte Standorte fast ausschließlich durch die Humusformen Moder und Rohhumus charakterisiert. An südexponierten sowie an tiefergelegenen Standorten sind ebenso Mull und Amphimull zu finden. Die Vorhersagen für die Muster von als Mull- und Moder-Indikatoren gekennzeichneten Enchyträenarten stimmen mit dem Auftreten der jeweiligen Humusformen weitgehend überein. Außerdem zeigen die Vorhersagemodelle von nordexponierten Hängen zu südexponierten Hängen und mit abnehmender Höhe für den Oberboden jeweils steigende pH-Werte, eine steigende Aktivität von Leucin-Aminopeptidase, ein steigendes Verhältnis der Aktivität alkalischer/saurer Phosphomonoesterase und ein abnehmendes C/N-Verhältnis.

Auf beiden Skalenebenen haben die Modelle prinzipiell ähnliche räumliche Muster ergeben. Aufgrund der größeren Datengrundlage und der besseren räumlichen Genauigkeit der Umweltvariablen sind die Vorhersagen der Dekompositionsmuster auf Hangebene jedoch detaillierter und ermöglichen die Erfassung weiterer Korrelationen dieser Muster z. B. mit der Hangneigung und der Hangkrümmung. Die miteinander korrespondierenden Ergebnisse sowie umfassende Modellevaluationen haben gezeigt, dass die angewendeten Methoden generell zur Modellierung räumlicher Dekompositionsmuster in einer heterogenen Hochgebirgslandschaft geeignet sind. Insgesamt legen die Ergebnisse nahe, dass die Humusform als universeller Indikator für Zersetzungsprozesse organischer Substanz an den untersuchten Hochgebirgsstandorten genutzt werden kann.





# Contents

<b>Chapter 1: Introduction</b> .....	1
1 Introduction.....	3
1.1 Soil ecological mechanisms .....	3
1.2 Indicators of decomposition.....	3
1.3 Digital soil mapping .....	5
1.4 DecAlp project.....	6
1.5 Objective.....	6
1.6 Structure of the thesis.....	6
2 Study area .....	8
3 Methodological overview.....	14
4 References .....	18
<b>Chapter 2: A fuzzy logic based method for modeling the spatial distribution of indicators of decomposition in a high mountain environment</b> .....	23
Abstract.....	25
Introduction.....	25
Methodological Framework.....	26
Construction of a Decision Tree.....	26
Fuzzy Logic Model .....	27
Case Study: Modeling of Humus Forms at Val di Rabbi (Trentino, Italy) .....	28
Study Area .....	28
Data Basis and Preprocessing .....	28
Modeling .....	31
Results .....	31
Discussion.....	34
Results from the Case Study.....	34
Application of Decision Trees and Fuzzy Logic.....	36
Uncertainties and Validity of Models .....	37
Conclusions .....	37
Acknowledgments.....	38
References Cited .....	38

<b>Chapter 3: Upscaling the spatial distribution of enchytraeids and humus forms in a high mountain environment on the basis of GIS and fuzzy logic</b>	43
Abstract	45
1. Introduction	46
2. Material and methods	47
2.1. Study area	47
2.2. Experimental design	47
2.3. Data analysis	49
2.4. Modeling	49
2.5. Model assessment	51
3. Results	52
3.1. Data analysis	52
3.2. Spatial modeling of enchytraeids	52
3.3. Spatial modeling of humus forms	56
3.4. Model assessment	57
4. Discussion	59
4.1. Spatial distribution of enchytraeids and humus forms	59
4.2. Model limitations	60
5. Conclusion	62
Acknowledgements	62
References	62
<b>Chapter 4: Humus Forms and Soil Microbiological Parameters in a Mountain Forest: Upscaling to the Slope Scale</b>	67
Abstract	69
1. Introduction	70
2. Material and Methods	71
2.1. Study Area	71
2.2. Sampling	72
2.3. Soil Analysis	73
2.4. Spatial Modeling	75
2.5. Model Assessment	76
3. Results	76
4. Discussion	81
4.1. Spatial Modeling of Humus Forms and Topsoil Acidity	81
4.2. Upscaling of Microbiological Parameters	84
4.3. Soil Ecological Implications	86
5. Conclusion	87
Acknowledgements	87
References	87



<b>Chapter 5: General discussion and conclusion</b> .....	93
1 Discussion.....	95
1.1. Spatial patterns of indicators of decomposition.....	95
1.2. Methods for digital mapping of indicators of decomposition .....	98
1.3. Model limitations.....	100
1.4. Future perspectives.....	101
2 Conclusion.....	102
3 References.....	104
Appendices.....	109
Acknowledgements.....	139
Curriculum vitae .....	141



# List of figures

## Chapter 1

Figure 1	Relationship between humus form and decomposer community .....	4
Figure 2	Location of the study area in Italy and the study sites .....	9
Figure 3	Geology of the study area .....	10
Figure 4	Climate graph of Peio .....	10
Figure 5	Climate graph of Passo Tonale .....	11
Figure 6	Spatial variability of climate parameters in the study area .....	12
Figure 7	Normalized Difference Vegetation Index (NDVI) of the study area .....	15
Figure 8	Extent of a study site and exemplary distribution of the investigated humus form profiles .....	15
Figure 9	Basic humus forms in forests of the Italian Alps .....	16
Figure 10	Data basis and methods for modelling at the landscape scale as developed in Chapter 2 and applied in Chapters 2 and 3 .....	17
Figure 11	Data basis and methods for modelling at the slope scale as applied in Chapter 4 .....	17

## Chapter 2

Figure 1	Illustration of a node split in a decision tree depending on the scale of measurement of the influencing variable $X_i \in \{X_1, \dots, X_a\}$ .....	27
Figure 2	Location of the study area and investigation sites in the Autonomous Province of Trentino (Italy) .....	29
Figure 3	Decision tree for the distribution model of OH horizons .....	32
Figure 4	Cumulative distribution functions for the values predicting the percentage of a humus form with an OH horizon in the two models that are compared .....	32
Figure 5	Fuzzy membership functions for the distribution model of OH horizons above 1300 m a.s.l., derived from the right subtree in Figure 3 .....	33
Figure 6	Weights for the synthesis of the elevation models .....	34
Figure 7	Comparison of the predicted spatial distribution of humus forms showing an OH horizon .....	35

## Chapter 3

Fig. 1	Location of the study area in the Autonomous Province of Trento (Italy) .....	47
Fig. 2	Life forms (H-type) of three selected enchytraeid species .....	49
Fig. 3	Decision tree for the distribution model of enchytraeids indicating mull humus forms .....	54
Fig. 4	Decision tree for the distribution model of enchytraeids indicating moder humus forms .....	54
Fig. 5	Prediction of the areas of dominance of mull- and moder-indicating enchytraeids .....	55
Fig. 6	Decision tree for the distribution of forest humus forms showing an OH horizon .....	56
Fig. 7	Prediction of the spatial distribution of forest humus forms showing an OH horizon .....	57



Fig. 8	Uncertainties of the predictions related to LS factor and TWI .....	59
--------	---	----

#### Chapter 4

Figure 1	Study area and investigation sites in the Italian Alps (Autonomous Province of Trento).....	72
Figure 2	Humus form classes and parameter values for modelling .....	74
Figure 3	Predicted distribution of biogenic soil structure in the mineral soil and of the presence of organic layers above the mineral soil .....	79
Figure 4	Predicted distribution of topsoil acidity .....	80
Figure 5	Predicted distributions of microbiological parameters.....	82
Figure 6	Standard error of predictions from linear model of leucine-aminopeptidase activity as a function of the pH value .....	83

#### Chapter 5

Figure 1	Landscape-scale distribution of indicators of decomposition from adverse to favorable environmental conditions in the forests of the study area Val di Sole / Val di Rabbi .....	98
Figure 2	Methodological approaches at the landscape versus slope scale depending on the data basis .....	99

#### Appendix 2 (Supplementary material of Chapter 3)

Figure S1	Similarity between the models of the spatial distribution of enchytraeid indicator classes and the occurrence of humus forms showing an OH horizon.....	118
Figure S2	Spatial distribution of RMSE values of 27 resampled model results for mull-indicating enchytraeids.....	119
Figure S3	Spatial distribution of RMSE values of 27 resampled model results for moder-indicating enchytraeids .....	120
Figure S4	Spatial distribution of RMSE values of 27 resampled model results for forest humus forms showing an OH horizon .....	121

#### Appendix 3 (Supplementary material of Chapter 4)

Figure S1	Results of the random forest model for the biogenic soil structure in the mineral soil.....	128
Figure S2	Results of the kriging procedure of the model residuals for the biogenic soil structure in the mineral soil.....	129
Figure S3	Results of the random forest model for the presence of organic layers above the mineral soil.....	130
Figure S4	Results of the kriging procedure of the model residuals for the presence of organic layers above the mineral soil .....	131
Figure S5	Results of the random forest model for the topsoil acidity .....	132
Figure S6	Results of the kriging procedure of the model residuals for the topsoil acidity.....	133
Figure S7	Standard error of predictions from linear model of the ratio alkaline/acid phosphomonoesterase activity as a function of the pH value.....	134
Figure S8	Standard error of predictions from linear model of the soil C/N ratio as a function of the pH value.....	135

# List of tables

## Chapter 1

Table 1	Study sites located at north- and south-facing slopes in Val di Sole / Val di Rabbi (Autonomous Province of Trento, Italy) and the related indicators of decomposition analyzed in this thesis .....	14
---------	--	----

## Chapter 2

Table 1	Soil cover types, dominating humus forms, and humus profiles at the investigation sites .....	29
Table 2	Data basis for modeling .....	30
Table 3	Validation sites: topographic position and percentage values (observed and modeled) of humus forms showing an OH horizon .....	30

## Chapter 3

Table 1	Dominant humus forms and profiles at the investigation sites .....	48
Table 2	Microannelid species found in the samples and their classification as indicators of mull or moder humus forms in the model .....	50
Table 3	Data basis for modeling .....	52
Table 4	Validation sites: topographic position and percentage values (observed and predicted) of modeled parameters.....	53
Table 5	Results of uncertainty analysis of input data .....	58

## Chapter 4

Table 1	Soil properties, related investigation sites and sampled objects .....	73
Table 2	Two-dimensional characterization of humus forms for modelling.....	75
Table 3	Input data for modelling from sampling of humus forms and topsoil acidity.....	77
Table 4	Chemical and microbiological properties of the soils collected at the six study sites at north- and south-facing areas (N1–N3 and S6–S8, respectively).....	78
Table 5	Quality measures of the random forest models.....	80
Table 6	Results of linear modelling of microbiological parameters and the soil C/N ratio as a function of the pH value .....	81
Table 7	Results of linear regression analysis between predictions for humus forms and predictions of topsoil acidity and microbiological parameters.....	84

## **Appendix 2 (Supplementary material of Chapter 3)**

Table S1	Sample data from the investigation sites N1-N3 (northern slope exposure) and S6-S8 (southern slope exposure) .....113
Table S2	Data basis for resampling.....114
Table S3	Sample plot raw data on microannelid species from the investigation sites N1-N3 (north-facing slopes) and S6-S8 (south-facing slopes).....115
Table S4	Sample plot raw data on humus profiles from the investigation sites N1-N3 (north-facing slopes) and S6-S8 (south-facing slopes) .....117

## **Appendix 3 (Supplementary material of Chapter 4)**

Table S1	Input data for linear models of soil C/N ratio and enzyme activities depending on pH values .....123
Table S2	Input data for linear model of the ratio bacterial / archaeal abundance depending on pH values .....125
Table S3	Humus forms and pH values sampled at 60 sites in Val di Rabbi (RN1–RN30 at a north-facing slope, RS1–RS30 at a south-facing slope) .....126



# Chapter 1

## Introduction



**Photo credits (previous page):**

Niels Hellwig, 3 August 2014

View from the Valle di Valorz on the Val di Rabbi and San Bernardo (Trentino, Italian Alps).

# 1 Introduction

## 1.1 Soil ecological mechanisms

Soil ecological mechanisms are an important building block of ecosystem functioning (Bardgett & van der Putten 2014; Paul 2015) and also relevant for the well-being of humans (Wall et al. 2015). Land-use practices and ongoing environmental changes such as climate warming and an increasing frequency of drought periods and sudden natural disasters trigger biodiversity losses, biological invasions and pests (IPCC 2014; Newbold et al. 2016). These developments also pose a threat to soil organisms and potentially impact soil ecological functions (Gardi et al. 2013; Bardgett & van der Putten 2014; Tsiafouli et al. 2015). As a result, soil ecological mechanisms have gained increasing attention, though they are complex and still poorly understood (Eisenhauer et al. 2017). It is essential to unveil those mechanisms and to clarify how they vary in a spatial context in order to be able to both mitigate losses of ecosystem services and implement measures to cope with prospective consequences.

With reference to ecosystem services and especially to soil functions, soil organic matter plays a central role (Adhikari & Hartemink 2016; Jackson et al. 2017). The formation and decomposition of soil organic matter is part of biogeochemical cycles, a component of soil fertility and important in the context of carbon sequestration and storage (Lal 2004; Paul 2016). Litter is decomposed by soil organisms; its constituents are either transformed into relatively stable organic compounds or gradually further metabolized and mineralized (Lehmann & Kleber 2015). Decomposition processes depend on various biotic and abiotic factors including litter quality and quantity, soil temperature and soil moisture (Coûteaux

et al. 1995; Aerts 1997; Reichstein et al. 2000; Sauvadet et al. 2017).

## 1.2 Indicators of decomposition

Soil organisms are the indispensable players in the system of organic matter decomposition. They interact with each other in complex food webs. By breaking down the plant residues and releasing nutrients to the soil, the detritivores are involved in nutrient cycles (de Vries et al. 2013). Previous studies provide evidence that a loss of functional diversity of soil organisms hampers decomposition (Hättenschwiler et al. 2005; Gessner et al. 2010; Handa et al. 2014; Wagg et al. 2014).

Earthworms and enchytraeids are of particular importance for decomposition (Hättenschwiler et al. 2005; Blouin et al. 2013; Pelosi & Römbke 2018). Enchytraeids (family Enchytraeidae) are small (about 2 to 40 mm long), saprophagous micro-annelid worms with high abundances in central European soils (annual average 20,000 to 60,000 individuals per m<sup>2</sup>) (Jänsch et al. 2005). Dependent on their species, enchytraeids have different life forms corresponding to their natural habitat, similar to the ecophysiological groups of earthworm species (epigeic, endogeic, anecic). The species composition of the enchytraeids assemblage is specific to every humus form and to every layer of the topsoil (Graefe & Schmelz 1999).

In addition to the soil fauna, microorganisms (bacteria, fungi, archaea) substantially contribute to organic matter decomposition (Baldrian 2017). They produce enzymes, which are partially secreted as extracellular enzymes to the soil water or bound to complexes with other soil components (Burns et al. 2013). Due to their activities including soil

organic matter mineralization, the organisms of the soil microbiological community have a pivotal position in biogeochemical cycles (Schimel & Schaeffer 2012; Isobe & Ohte 2014).

Humus forms are the morphological results of litter decomposition, including humification and mineralization in the topsoil. These encompass the uppermost mineral soil horizon and the overlying organic matter (O) horizons (OL = litter, OF = fragmented residues, OH = humified residues). According to the presence/absence and the morphological characteristics of these horizons, three basic humus forms are differentiated in most classifications: Mull, Moder and Mor. However, the species composition of the soil biological community has been reported to be dichotomous between Mull on one hand and Moder and Mor on the other (Graefe & Beylich 2006). This dichotomy is typically related to the topsoil acidity with a threshold at a pH value (CaCl<sub>2</sub>) of about 4.2 (Graefe & Beylich 2006).

Mull features a low accumulation of organic material above the mineral soil, which implies the absence of any OH horizon. The uppermost mineral horizon is less acidic as compared to Moder and Mor. Moreover, it is usually characterized by a bacterial-driven food web and a high biological activity (Frouz 2018). Mull humus forms evolve from biological activity and concomitantly provide a habitat for a high diversity of species including anecic earthworm species (Ponge 2003). This causes a well-structured soil with crumbly to polyhedral biogenic aggregates (Six et al. 2004).

Moder and Mor, on the other hand, feature a high accumulation of organic material above the mineral soil, meaning that there are continuous OL, OF and OH horizons. Due to a high acidity, the uppermost mineral horizon is typically characterized by a fungal-driven food web and a comparatively low biological

activity (Ponge 2003; Frouz 2018). Therefore, the soil is mostly lacking biogenic aggregates. The assignment of a humus form does not only reflect the fate of plant residues in the course of decomposition, but also indicates the species composition of the decomposer organisms and the microbiological, physical and chemical properties of the topsoil (Graefe & Beylich 2006; Andreetta et al. 2013; Ponge 2013). Humus forms and the activity of the decomposer community are highly interrelated (Figure 1). Both humus forms and the composition of the decomposer community indicate processes and properties of organic matter decomposition. Therefore, in this thesis they are referred to as 'indicators of decomposition'.

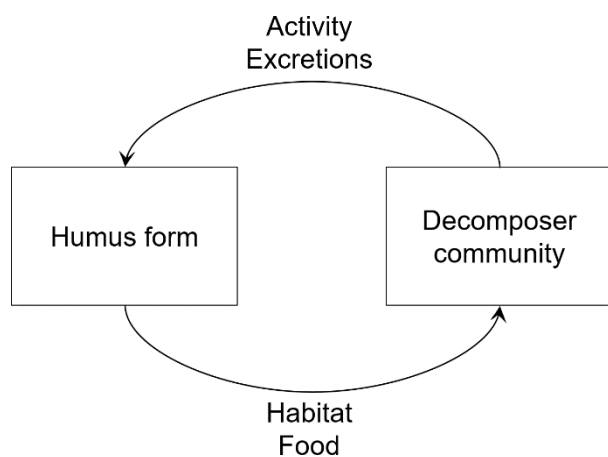


**Figure 1.** Relationship between humus form and decomposer community (modified from Hellwig et al. 2017).

Similar to pedogenesis, organic matter decomposition and, with that, also the development of humus forms are dependent on environmental influences. According to Jenny (1941), the state of the soil is a function of climate, organisms, relief, parent material and time. According to the variation of these influencing factors, humus forms are arranged in spatial patterns.

In the mountains, both climatic variables and vegetation composition are correlated with

topographical parameters such as elevation and slope exposure (Dobrowski 2011; Egli & Poulénard 2017). Therefore, the characteristics of organic matter decomposition at high mountain sites are especially influenced by the relief. Previous studies have shown that decomposition processes are favoured at south-facing slopes as compared with north-facing slopes in case there is no limitation by soil moisture at south-facing slopes (e.g. Egli et al. 2009; Ascher et al. 2012; Gómez-Brandón et al. 2017). Moreover, the high spatial variability of indicators of decomposition in the high mountains corresponds to a mosaic of microtopography and vegetation cover (Bednorz et al. 2000).

### 1.3 Digital soil mapping

Spatial patterns of soil taxonomic classes and soil properties have frequently been predicted by the application of modelling techniques related to the concept of digital soil mapping (Grunwald 2009; Minasny & McBratney 2016). Digital soil mapping – also referred to as predictive soil mapping (Scull et al. 2003) and soil-landscape modelling (Gessler et al. 1995) – includes numerical and statistical methods to quantitatively model the relationships between environmental data and soil data (from the field or laboratory) to derive predictions on spatial patterns of soil properties, typically presented as a digital map product (Scull et al. 2003; IUSS Working Group Digital Soil Mapping 2016). Methods used for digital soil mapping can be classified into factor-based approaches (i.e. methods considering soil-forming factors based on soil-landscape relationships), geostatistics and pedotransfer functions (McBratney et al. 2003; Behrens & Scholten 2006). Factor-based approaches rely on environmental covariates that represent the relevant factors of soil formation. These typically include terrain

attributes derived from a digital terrain model and/or existing climate, geology, vegetation and land-use maps. Here, digital soil mapping benefits from new techniques of data acquisition (e.g. modern remote sensing techniques) and data management (e.g. soil information systems and increasing computational power) (Grunwald et al. 2011; Brevik et al. 2016; Minasny & McBratney 2016). Furthermore, a high availability of environmental data from online platforms of public authorities helps to integrate various influencing parameters and achieve a quite realistic model. Methods frequently applied in a factor-based approach are generalized linear and additive models, data mining approaches such as tree-based models (e.g. random forest), artificial neural networks or support vector machines and fuzzy logic models (McBratney et al. 2003). Recent studies that compared several methods for digital soil mapping have shown that the method of choice depends on the dataset, the study area and the purpose of the model (Heung et al. 2016; Taghizadeh-Mehrjardi et al. 2016; Nussbaum et al. 2018). Digital soil mapping is applied for several purposes and on various scales. For example, digital soil mapping has been used to assess and optimize land-use practices (e.g. for precision agriculture, Söderström et al. 2016), to refine conventional soil maps (Yang et al. 2011; Sarmiento et al. 2017) or to evaluate the effects of environmental disturbances on soil parameters (Carré et al. 2007). Depending on the purpose, many studies are related to the farm or regional scale (Grunwald 2009). However, there are also promising advances for mapping soil parameters at high resolution on the global scale (Sanchez et al. 2009; Arrouays et al. 2014; Hengl et al. 2014). Due to the importance of soil ecological functions it is essential to map related soil parameters in order to enhance conservation of soil biodiversity (de Vries et al. 2013) and

management of environmental disturbances (Grunwald et al. 2011). This is of particular relevance in mountainous areas such as the European Alps, which are especially vulnerable to environmental changes (Beniston 2006; Mountain Research Initiative EDW Working Group 2015). Soil ecological processes in these areas are heterogeneous; thus, detailed, spatially explicit analyses of the correlations between humus forms, soil organisms and soil biological activity in high mountain regions are necessary (Broll 1998). However, few studies on mapping spatial patterns of soil ecological parameters exist to date (e.g. Rutgers et al. 2016).

## 1.4 DecAlp project

In order to better understand the fundamentals of organic matter decomposition in the high mountains, it is necessary to investigate soil ecological patterns and processes in an interdisciplinary context. This was the starting point of the research project 'Effect of climate on coarse woody debris decay dynamics and incorporation into the soils of forested Alpine areas' (DecAlp). DecAlp deals with soil fauna, soil microbiology, humus forms, coarse woody debris and spatial modelling (D.A.CH-DecAlp n.d.). The main objectives of DecAlp are:

- the investigation of the decomposition of dead wood and transformation into soil organic matter,
- the analysis of the relationships between environmental factors (especially climate) and indicators of decomposition and
- the analysis of spatial decomposition patterns.

As part of DecAlp, this thesis is related to the second and third objective of the project.

## 1.5 Objective

This thesis aims at investigating spatial patterns of organic matter decomposition in a study area in the Italian Alps. Indicators of decomposition such as humus forms, soil organisms and the soil biological activity are supposed to be predicted at the slope scale and at the landscape scale. The following research questions are addressed with reference to a study area in the Italian Alps:

- 1) Which methodological approaches are suitable for the data-based spatial modelling of indicators of decomposition processes and properties?
- 2) Which spatial patterns of decomposition properties can be predicted depending on the model scale from the slope to the landscape scale?
- 3) Which correlations can be found between the spatial distributions of humus forms, soil organisms of different decomposer communities and soil microbiological parameters?

As a whole, this thesis seeks to compile a methodological framework for digital mapping of soil ecological properties and apply this to unveil the correlations between spatial patterns of forest humus forms, soil organisms and soil biological activity in a study area in the Italian Alps. Each individual component of this thesis supports the overall objective.

## 1.6 Structure of the thesis

This chapter introduces the study area and gives a brief methodological overview. The Chapters 2, 3 and 4 include each one individual study. In Chapter 2, a methodological framework for digital mapping of indicators of decomposition at the landscape scale is

developed. This method is tested as a case study for the presence of OH horizons. Chapter 3 applies the new method presented in Chapter 2 to forest humus forms and enchytraeid species. The coincidence of Mull-like and Moder-like humus forms with specific compositions of the enchytraeid assemblage is analyzed. Chapter 4 focuses on one north-facing and one south-facing slope in the Val di Rabbi. That chapter contains a slope-scale analysis of spatial patterns of humus forms, topsoil acidity and microbiological parameters of the topsoil based on a data mining approach. Chapter 5 is composed of a discussion of the overall results of this thesis.

Spatial patterns of indicators of decomposition are discussed with reference to environmental influences, decomposition studies in the study area (mostly related to the DecAlp project), correlations between soil ecological parameters and the effects of the model scale. The methods for digital mapping of indicators of decomposition are discussed in terms of the factor-based approach of digital soil mapping, digital mapping of soil ecological parameters and the differences between the landscape scale and the slope scale. Additionally, the discussion includes remarks on model limitations and future perspectives.



## 2 Study area

The study area is located in the Italian Alps (between 46.25° N, 10.52° E and 46.49° N, 11.02° E) (Figure 2). It is part of the Autonomous Province of Trento and includes the valleys Val di Sole, Val di Rabbi, Val di Peio and Val di Vermiglio.

The mountains of the northern part of the study area belong to the Ortler Alps with the Monte Cevedale as highest point of the study area (3789 m a.s.l.). The main stream is the Noce River, flowing through the Val di Peio and the Val di Sole. The tributary stream entering from the Val di Rabbi is called Rabbies.

The study area is located in the southern part of the Central Alps, which are characterized by siliceous bedrock. The study area is dominated by paragneiss, schist and phyllite, with some outcrops of orthogneiss, amphibolite, chlorite schist and marble (Figure 3). All these materials yield acidic weathering products. The Periadriatic Seam runs directly through the Val di Sole and marks the border to the Southern Limestone Alps. The Val di Vermiglio borders the granites of the Adamello intrusion located in the south (von Seidlein 2000; Aberegge et al. 2009).

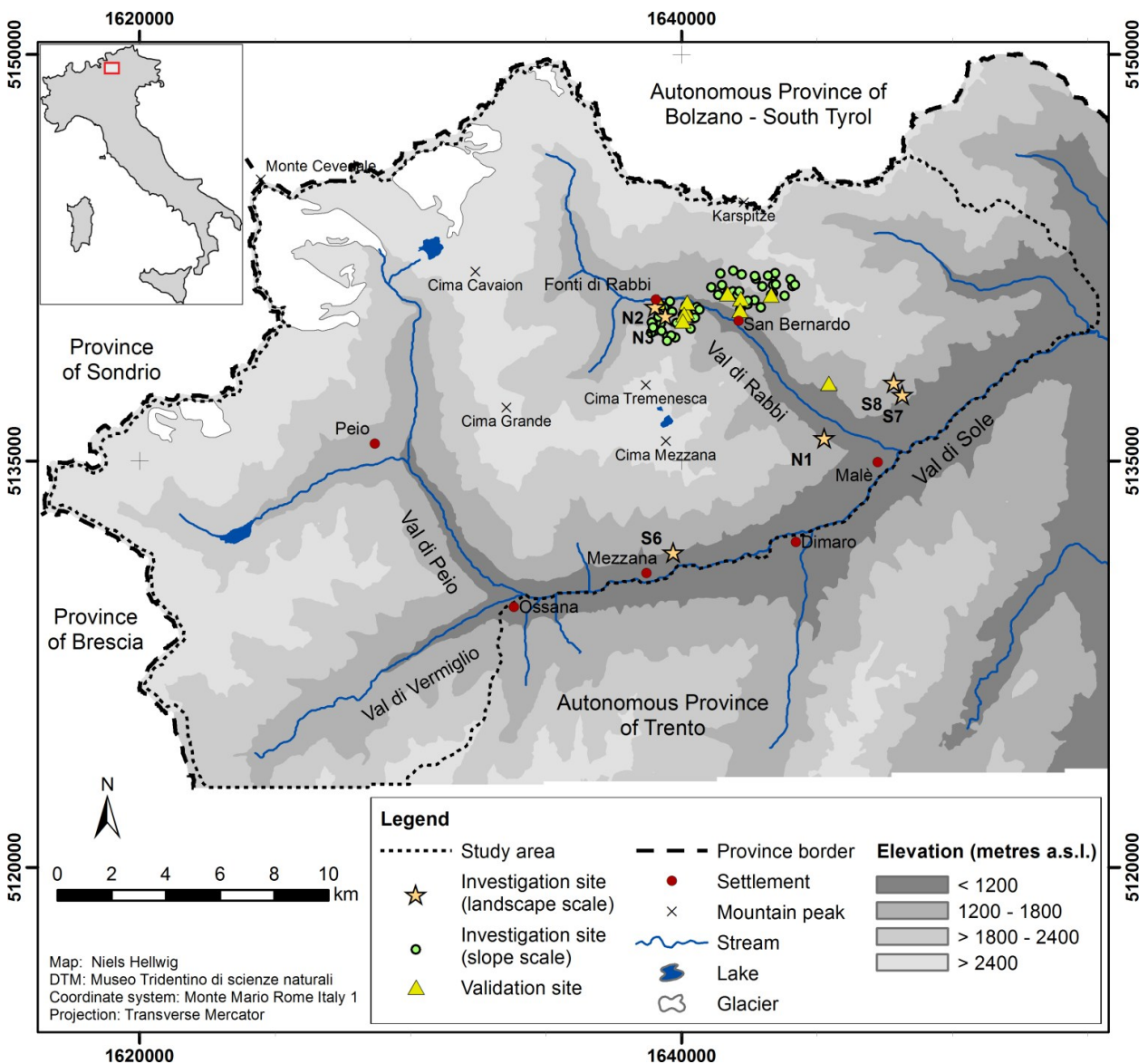


**Figure 2.** Location of the study area in Italy and the study sites.

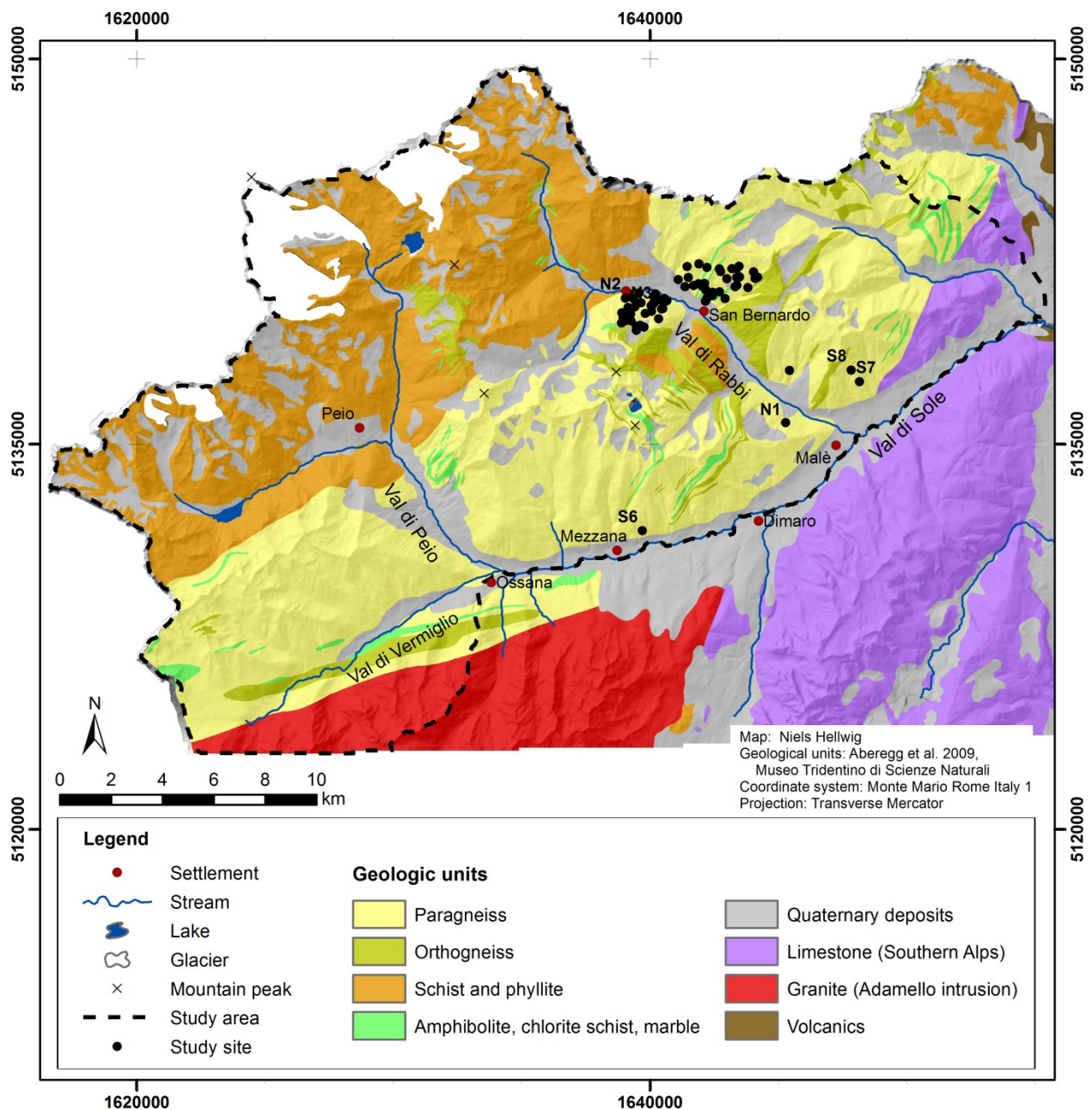


**Figure 3.** Geology of the study area (based on Aberegg et al. 2009, according to von Seidlein 2000).

The relief of the study area is glacially shaped. Current legacies of former glaciation are for example trough-shaped valleys, moraines and cirques. Recently, the relief has been reformed mainly by fluvio-glacial, fluvial and gravitational processes. This is shown by landforms such as talus deposits and alluvial fans. Patterns of erosive and accumulative characteristics also develop at small scales, especially on steep slopes. These patterns are normally

related to the vegetation cover, as roots, stems and shrubs stabilize the surface.

Throughout the study area, the mesoclimate is highly variable due to the pronounced mountainous relief. Sites at low elevation (e.g. Peio, Figure 4) generally exhibit higher temperatures as compared to sites at high elevation (e.g. Passo Tonale, Figure 5; see also Figure 6). As a consequence, there are also considerable differences between the valley

bottoms and the high-elevation sites with reference to the duration of snow cover and the growing season. Additionally, at high elevation the frost season is longer than at low elevation. For example, frost days are probable at Peio between October and May (Figure 4), at Passo Tonale between September and June (Figure 5).

The mean annual precipitation amounts to 1288 mm at Passo Tonale, which distinctly exceeds the precipitation at Peio (annual mean 935 mm). In high mountain areas of this kind, especially in the Alps, the spatial distribution of precipitation varies greatly, too (Figure 6) (Barry 2008). Regarding air temperature at the forest floor and topsoil temperature, the solar radiation has a considerable influence. Within the study area, the daily mean of solar radiation varies between ca. 100 W/m<sup>2</sup> and 230 W/m<sup>2</sup> – the spatial pattern of solar radiation principally traces back to the slope exposure (Figure 6). Accordingly, the soil temperature is significantly higher at south-facing

slopes as compared to north-facing slopes (Egli et al. 2016). Following Costantini et al. (2013) with reference to the whole of Italy, the study area can generally be assigned to the climatic region T1 (temperate continental, influenced by mountains). However, parts of the valleys belong to the climatic region T3 (temperate to warm temperate subcontinental, partly arid).

The soils developed in the areas of siliceous parent materials (Figure 3) are dominated by *Haplic Cambisols (Dystric)* and *Umbric Podzols* below 1900 m. Above, the typical soil types are *Entic Podzol*, *Albic Podzol* and *Umbric Podzol* (Sartori & Mancabelli 2009, classifications according to IUSS Working Group WRB 2006). Brunification is the dominant process at low parts of the south-facing slopes, whereas podzolization dominates on north-facing slopes and at high elevations. On glacial deposits in the valley bottom of Val di Sole, *Haplic Phaeozems* are found (Sartori & Mancabelli 2009).

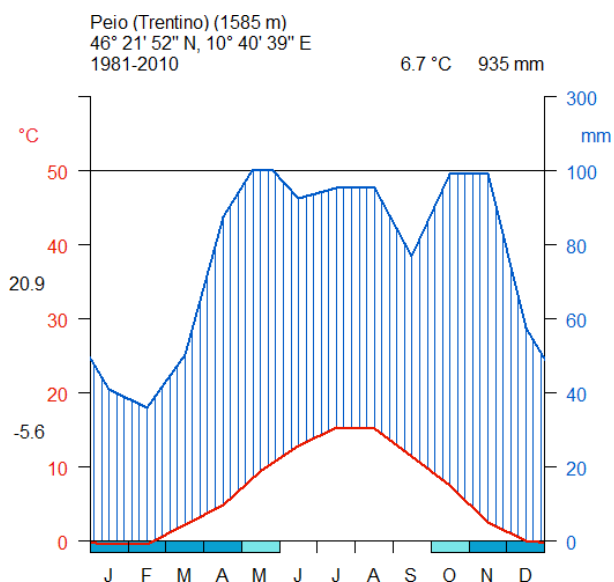


**Figure 4.** Climate graph of Peio (data from Provincia Autonoma di Trento 2014).

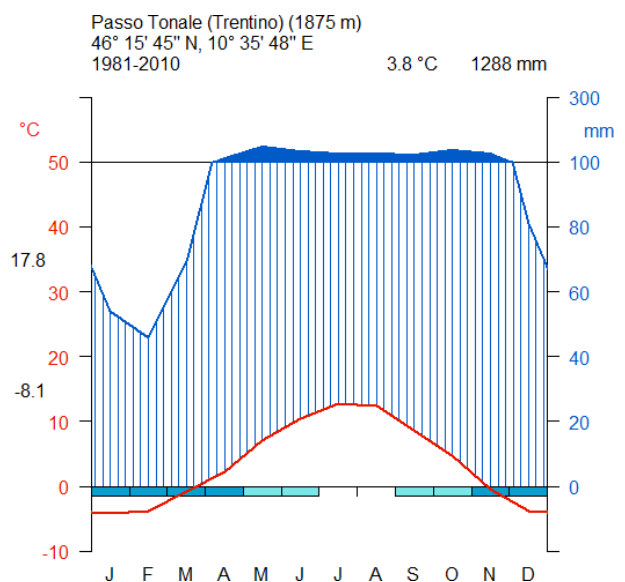


**Figure 5.** Climate graph of Passo Tonale (data from Provincia Autonoma di Trento 2014).



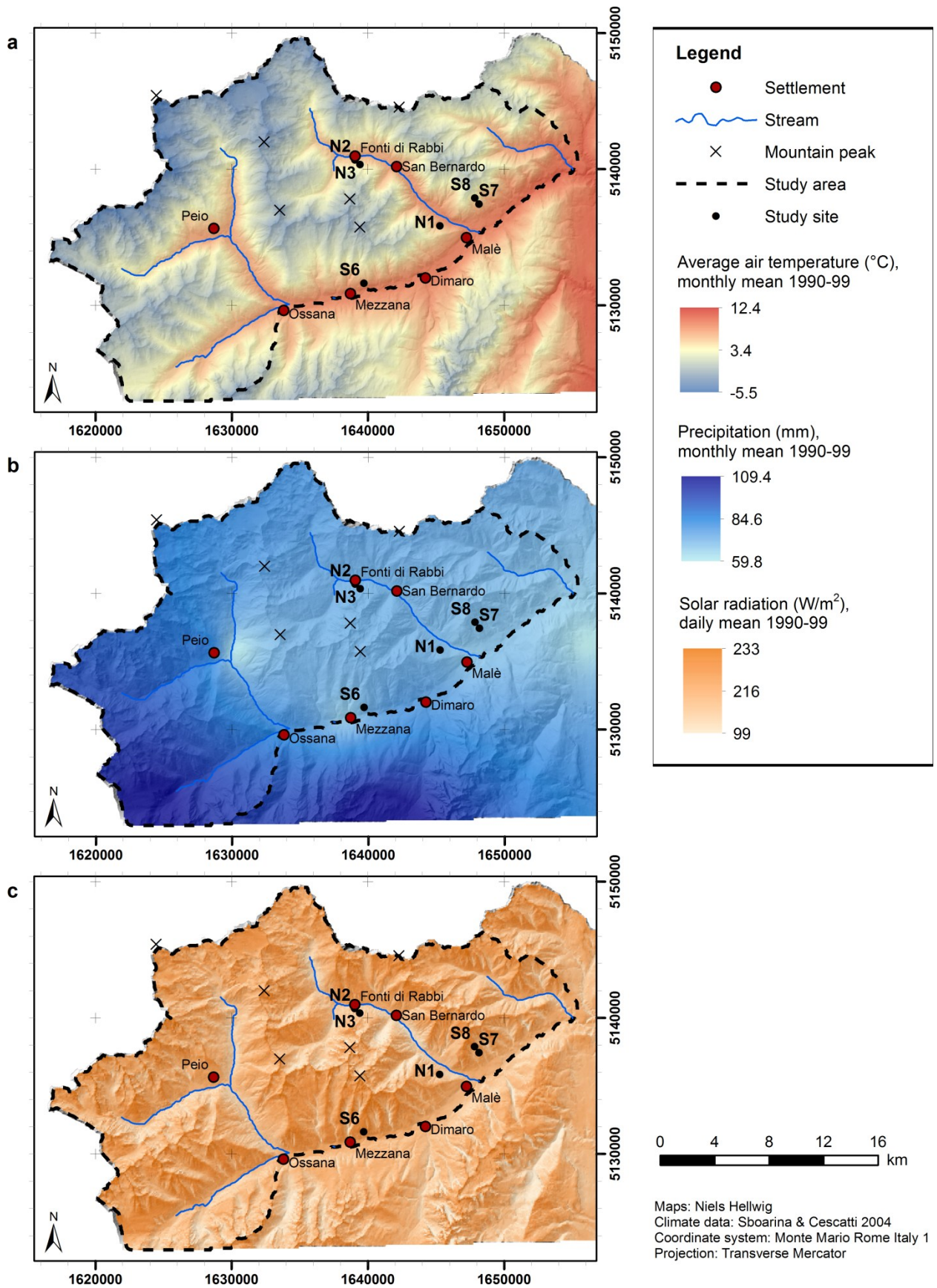


**Figure 6.** Spatial variability of climate parameters in the study area: (a) average air temperature, (b) precipitation, (c) solar radiation (all maps based on interpolation of data from 1990 to 1999, Sboarina & Cescatti 2004).

Owing to the variety of the terrain, the vegetation of the study area is also quite heterogeneous. Because of low temperatures, short growing seasons, a high degree of wind exposure, high rates of evaporation, varying exposure to light and steep slopes with initial soil development, the environmental conditions get more extreme for plant establishment and survival with increasing elevation. Vegetation zones according to elevation levels comprise different plant communities. The higher the elevation is, the sparser is the vegetation cover and the shorter is the growing season. This is indicated by a decrease of the mean values of the Normalized Difference

Vegetation Index (NDVI) with increasing elevation (Figure 7). The highest NDVI values appear at the forested valley slopes below the treeline. Throughout the study area, these forests consist of Norway spruce (*Picea abies*) and European larch (*Larix decidua*) as main tree species. Furthermore, there are very few patches where the main tree species are European silver fir (*Abies alba*), Scots pine (*Pinus sylvestris*), Austrian pine (*Pinus nigra*) and Swiss stone pine (*Pinus cembra*). Besides coniferous forests, there are also small patches of broadleaf forests close to the valley bottoms (Wagener 2014). The treeline in the study area is located

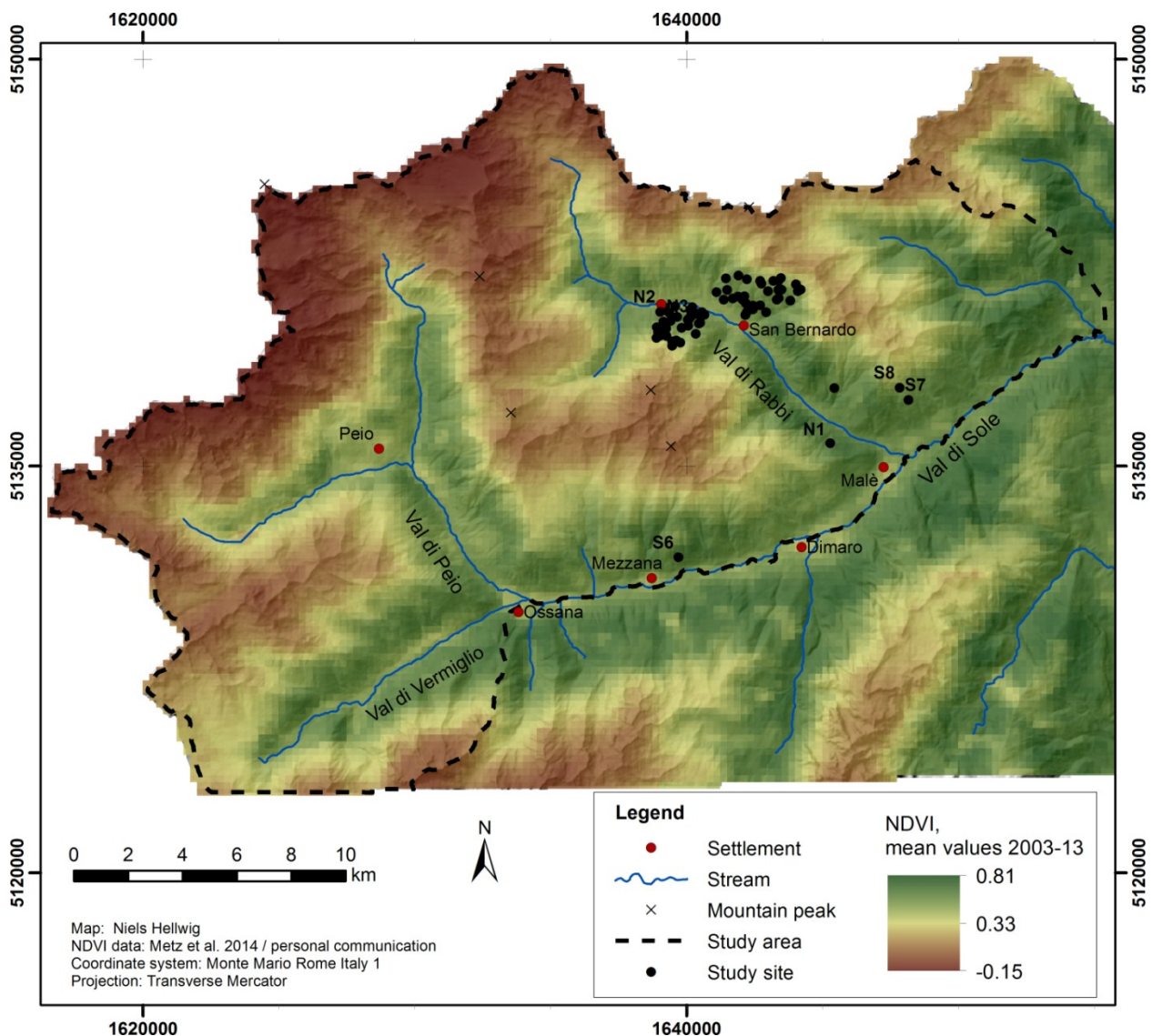


**Figure 7.** Normalized Difference Vegetation Index (NDVI) of the study area (based on data from 2003 to 2013, Metz et al. 2014, personal communication).

roughly between 1900 m and 2200 m a.s.l. The original treeline developed naturally due to interactions between limiting factors such as temperature, soil moisture, nutrient availability and geomorphological processes (Holtmeier & Broll 2007; Leonelli et al. 2016; Mayor et al. 2017). In contrast, the current treeline largely developed due to grazing and is therefore below the potential natural treeline.

The land use of the study area is characterized by developed areas and traffic areas, fruit cultivation and grassland farming. The forested slopes are used mostly for natural forestry. The areas close to the treeline are widely characterized by seasonal grazing of cattle and sheep in the context of transhumance.

### 3 Methodological overview

The investigations in this thesis rely on different sets of study sites (Table 1). All study sites are located in the coniferous forests on north- and south-facing slopes of the study area (Figure 2). The sites N1, N2, N3 (on north-facing slopes) and S6, S7, S8 (on south-facing slopes) were selected based on expert knowledge from previous studies (Egli et al. 2006). These sites were assumed as being relatively representative of the study area with respect to site conditions (Egli et al. 2006). The validation sites VN1, VN2, VS1, VS2 and V1-V6 were placed on nearby slopes for the evaluation of the spatial models. They resemble the sites N1, N2, N3, S6, S7, S8 in the

way that the site conditions are typical of the study area. The sites RN1-RN30 and RS1-RS30 were determined using conditioned Latin Hypercube Sampling (Minasny & McBratney 2006), which allows to include the spatial variability of environmental covariates to achieve a representative set of study sites. Details are given in Chapter 4.

All study sites encompassed an area of 25 m x 25 m (Figure 8). For every ground cover type of the site (litter, grass, moss, fern, shrubs), humus profiles were examined (width 50-100 cm). Humus forms were described and samples were collected for the analysis of indicators of decomposition.

**Table 1**

Study sites located at north- and south-facing slopes in Val di Sole / Val di Rabbi (Autonomous Province of Trento, Italy) and the related indicators of decomposition analyzed in this thesis.

Sites	Elevation range (m a.s.l.)	Slope exposure	Analyzed parameters	Data used in
N1-N3	1180-1620	north	Humus forms, Enchytraeids, pH values, Soil enzymatic activities, Total carbon and nitrogen, Bacterial and archaeal abundance	Chapters 2, 3, 4
S6-S8	1185-1660	south	Humus forms, Enchytraeids, pH values, Soil enzymatic activities, Total carbon and nitrogen, Bacterial and archaeal abundance	Chapters 2, 3, 4
VN1, VN2	1210-1380	north	Validation sites: Humus forms	Chapter 2
VS1, VS2	1340-1570	south	Validation sites: Humus forms	Chapter 2
V1-V3	1270-1650	north	Validation sites: Humus forms, Enchytraeids	Chapter 3
V4-V6	1240-1730	south	Validation sites: Humus forms, Enchytraeids	Chapter 3
RN1-RN30	1200-2100	north	Humus forms, pH values	Chapter 4
RS1-RS30	1200-2200	south	Humus forms, pH values	Chapter 4



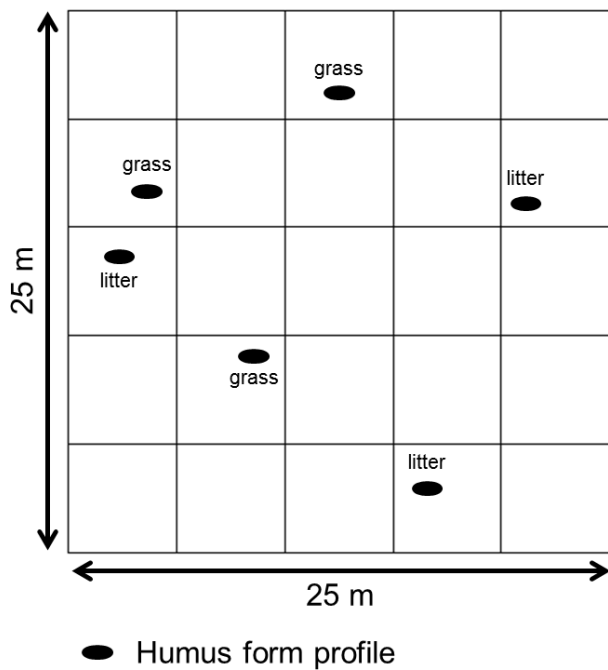


**Figure 8.** Extent of a study site and exemplary distribution of the investigated humus form profiles.

The classification of humus forms followed Ad-hoc-AG Boden (2005). Apart from the basic humus forms Mull and Moder, the classification of humus forms that was used for modelling in this thesis included the transitional humus form Mullmoder and the humus forms Amphimull and Eroded Moder. The humus form Mor was very sparsely found. Therefore and due to the similarity of soil biological properties, the humus forms Moder and Mor were not differentiated. The specification of humus forms was based on two dimensions: the presence of organic layers above the mineral soil and the biological activity as expressed by a biogenic soil structure in the mineral soil (Figure 9). More details on the methods that were applied for the analysis of indicators of decomposition (Table 1) are given in Chapters 2, 3 and 4.

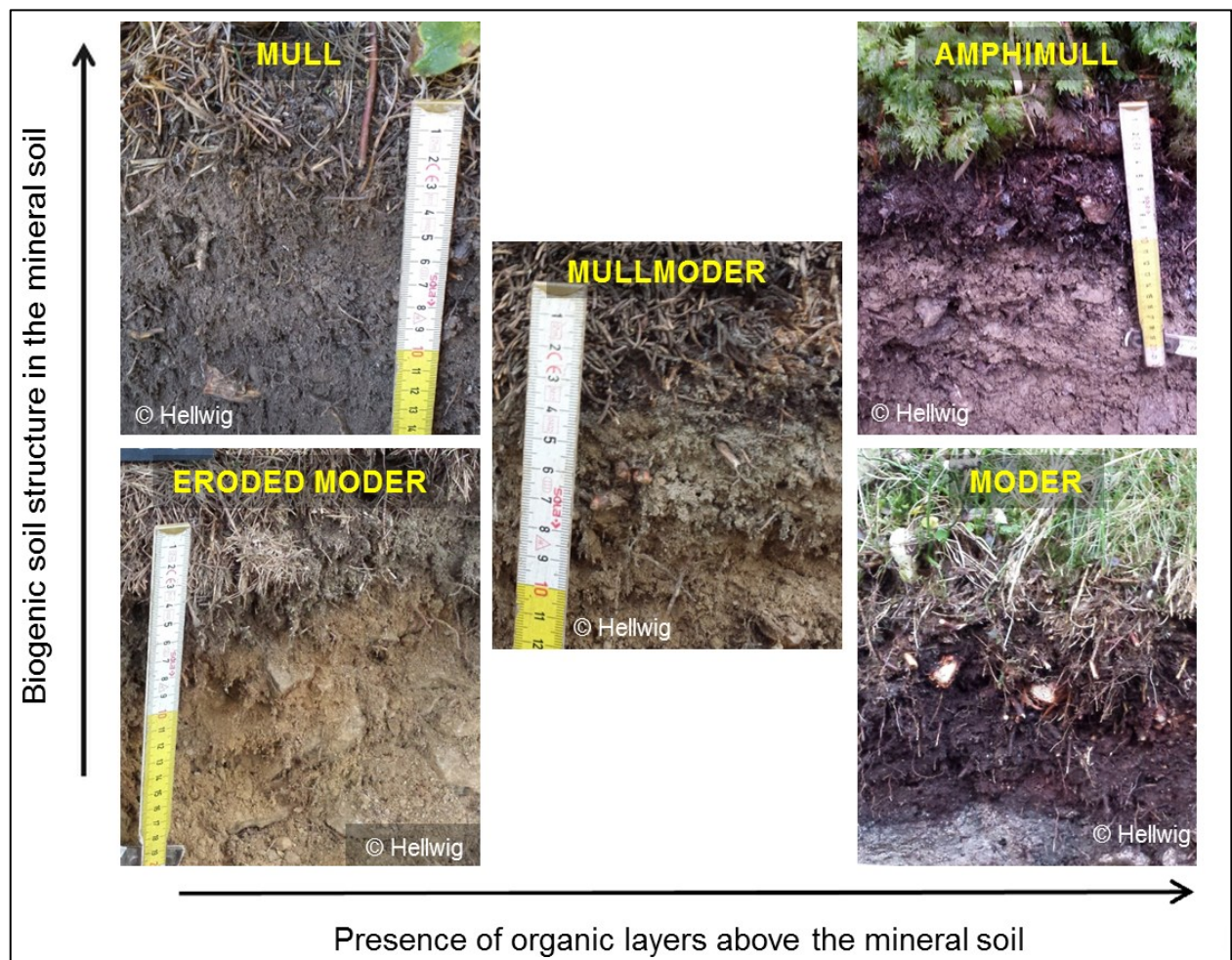


**Figure 9.** Basic humus forms in forests of the Italian Alps (modified from Hellwig et al. 2018).

Spatial modelling is realized depending on the data basis and the spatial scale. Landscape-scale models refer to the forested parts on the valley slopes of the whole study area (circa 500 km<sup>2</sup>, Figure 2). These models are based on data from the sites N1, N2, N3, S6, S7 and S8. Elevation and slope exposure are derived from a digital terrain model (DTM) with a grid width of 10 m and considered as covariates. The models are built using decision tree analysis (Breiman et al. 1984) and the tool ArcSIE (Shi et al. 2009) to parametrize fuzzy membership functions and produce predictive maps (Figure 10). Chapter 2 provides details on the modelling procedure. Additionally, Chapter 2 includes a case study of humus forms in Val di Rabbi (presence of OH horizons). In Chapter 3 this modelling

approach is refined to compare the spatial distribution of humus forms and enchytraeid species within the study area.

Slope-scale models refer to one north-facing slope (circa 2.5 km<sup>2</sup>) and one south-facing slope (circa 3.8 km<sup>2</sup>) next to San Bernardo in the Val di Rabbi. These models are based on data from the sites RN1-RN30 and RS1-RS30. Predictive maps are produced with spatial models using random forests (Breiman 2001). The environmental covariates include vegetation parameters and several terrain attributes derived from a DTM with a grid width of 1 m (Figure 11). Modelling at the slope scale is described in detail in Chapter 4. The maps provide predictions of humus forms and pH values, enzymatic activities and the C/N ratio of the topsoil.

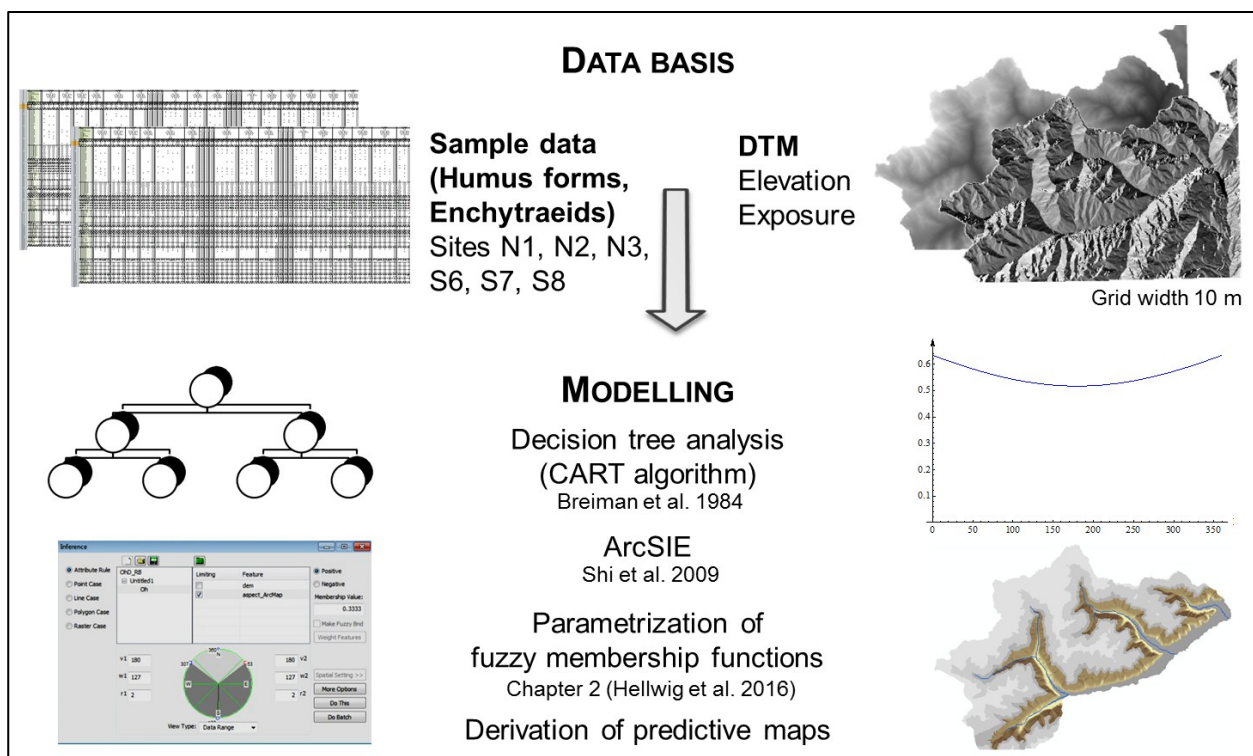


**Figure 10.** Data basis and methods for modelling at the landscape scale as developed in Chapter 2 and applied in Chapters 2 and 3 (modified from Hellwig et al. 2017).

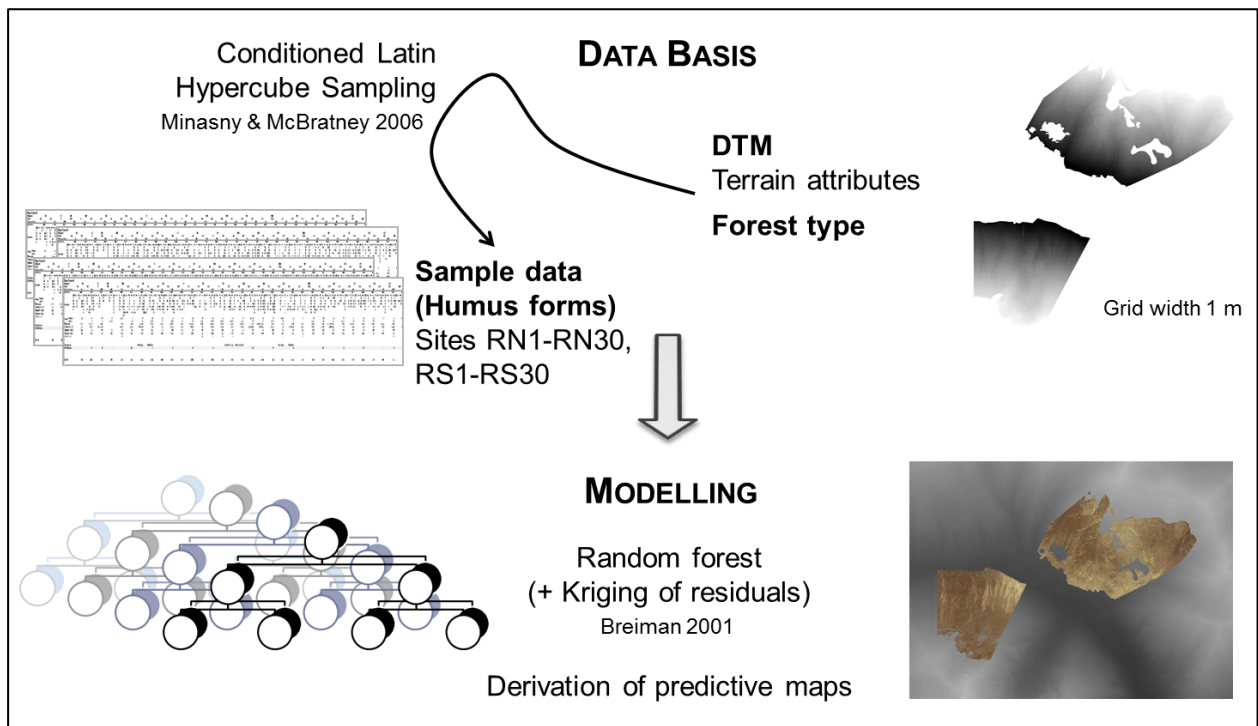


**Figure 11.** Data basis and methods for modelling at the slope scale as applied in Chapter 4 (modified from Hellwig et al. 2017).

## 4 References

- Aberegg, I., Egli, M., Sartori, G., Purves, R. (2009): Modelling spatial distribution of soil types and characteristics in a high Alpine valley (Val di Sole, Trentino, Italy). *Studi Trentini di Scienze Naturali* **85**, 39-50.
- Adhikari, K., Hartemink, A. E. (2016): Linking soils to ecosystem services – A global review. *Geoderma* **262**, 101-111.
- Ad-hoc-AG Boden (2005): *Bodenkundliche Kartieranleitung*. E. Schweizerbart'sche Verlagsbuchhandlung, Hannover, 5th edition.
- Aerts, R. (1997): Climate, Leaf Litter Chemistry and Leaf Litter Decomposition in Terrestrial Ecosystems: A Triangular Relationship. *Oikos* **79**(3), 439-449.
- Andreetta, A., Macci, C., Giansoldati, V., Masciandro, G., Carnicelli, S. (2013): Microbial activity and organic matter composition in Mediterranean humus forms. *Geoderma* **209-210**, 198-208.
- Arrouays, D., McKenzie, N., Hempel, J., Richer de Forges, A., McBratney, A. (2014): *GlobalSoilMap*. Basis of the global spatial soil information system. CRC Press/Balkema, London.
- Ascher, J., Sartori, G., Graefe, U., Thornton, B., Ceccherini, M. T., Pietramellara, G., Egli, M. (2012): Are humus forms, mesofauna and microflora in subalpine forest soils sensitive to thermal conditions? *Biology and Fertility of Soils* **48**, 709-725.
- Baldrian, P. (2017): Microbial activity and the dynamics of ecosystem processes in forest soils. *Current Opinion in Microbiology* **37**, 128-134.
- Bardgett, R. D., van der Putten, W. H. (2014): Belowground biodiversity and ecosystem functioning. *Nature* **515**, 505-511.
- Barry, R. G. (2008): *Mountain Weather and Climate*. Cambridge University Press, Cambridge, 3rd edition.
- Bednorz, F., Reichstein, M., Broll, G., Holtmeier, F.-K., Urfer, W. (2000): Humus Forms in the Forest-Alpine Tundra Ecotone at Stillberg (Dischmatal, Switzerland): Spatial Heterogeneity and Classification. *Arctic, Antarctic, and Alpine Research* **32**(1), 21-29.
- Behrens, T., Scholten, T. (2006): Digital soil mapping in Germany – a review. *Journal of Plant Nutrition and Soil Science* **169**, 434-443.
- Beniston, M. (2006): Mountain weather and climate: A general overview and a focus on climatic change in the Alps. *Hydrobiologia* **562**, 3-16.
- Blouin, M., Hodson, M. E., Delgado, E. A., Baker, G., Brussaard, L., Butt, K. R., Dai, J., Dendooven, L., Peres, G., Tondoh, J. E., Cluzeau, D., Brun, J.-J. (2013): A review of earthworm impact on soil function and ecosystem services. *European Journal of Soil Science* **64**(2), 161-182.
- Breiman, L. (2001): Random Forests. *Machine Learning* **45**, 5-32.
- Breiman, L., Friedman, J. H., Olshen, R. A., Stone, C. J. (1984): *Classification and regression trees*. Wadsworth, Belmont (= The Wadsworth Statistics/Probability Series).
- Brevik, E. C., Calzolari, C., Miller, B. A., Pereira, P., Kabala, C., Baumgarten, A., Jordán, A. (2016): Soil mapping, classification, and pedologic modeling: History and future directions. *Geoderma* **264**, 256-274.
- Broll, G. (1998): Diversity of soil organisms in Alpine and Arctic soils in Europe. Review and research needs. *Pirineos* **151-152**, 43-72.
- Burns, R. G., DeForest, J. L., Marxsen, J., Sinsabaugh, R. L., Stromberger, M. E., Wallenstein, M. D., Weintraub, M. N., Zoppini, A. (2013): Soil enzymes in a changing environment: Current knowledge and future directions. *Soil Biology & Biochemistry* **58**, 216-234.
- Carré, F., McBratney, A. B., Mayr, T., Montanarella, L. (2007): Digital soil assessments: Beyond DSM. *Geoderma* **142**, 69-79.
- Costantini, E. A. C., Fantappiè, M., L'Abate, G. (2013): Climate and pedoclimate of Italy. In: Costantini, E. A. C., Dazzi, C. (Eds.): *The Soils of Italy*. Springer, Dordrecht, 19-37.

- Coûteaux, M.-M., Bottner, P., Berg, B. (1995): Litter decomposition, climate and litter quality. *Trends in Ecology & Evolution* **10**(2), 63-66.
- D.A.CH-DecAlp (n.d.): D.A.CH-DecAlp. <https://www.dec alp.org/> (13/12/2017).
- de Vries, F. T., Thébault, E., Liiri, M., Birkhofer, K., Tsiafouli, M. A., Bjørnlund, L., Jørgensen, H. B., Brady, M. V., Christensen, S., de Ruiter, P. C., d'Hertefeldt, T., Frouz, J., Hedlund, K., Hemerik, L., Hol, W. H. G., Hotes, S., Mortimer, S. R., Setälä, H., Sgardelis, S. P., Uteseny, K., van der Putten, W. H., Wolters, V., Bardgett, R. D. (2013): Soil food web properties explain ecosystem services across European land use systems. *Proceedings of the National Academy of Science of the United States of America* **110**(35), 14296-14301.
- Dobrowski, S. Z. (2011): A climatic basis for microrefugia: the influence of terrain on climate. *Global Change Biology* **17**, 1022-1035.
- Egli, M., Poulénard, J. (2017): Soils of mountainous landscapes. In: Richardson, D., Castree, N., Goodchild, M. F., Kobayashi, A., Liu, W., Marston, R. A. (Eds.): *The International Encyclopedia of Geography: People, the Earth, Environment, and Technology*. Wiley, New York.
- Egli, M., Mirabella, A., Sartori, G., Zanelli, R., Bischof, S. (2006): Effect of north and south exposure on weathering rates and clay mineral formation in Alpine soils. *Catena* **67**(3), 155-174.
- Egli, M., Sartori, G., Mirabella, A., Favilli, F., Giaccari, D., Delbos, E. (2009): Effect of north and south exposure on organic matter in high Alpine soils. *Geoderma* **149**, 124-136.
- Egli, M., Hafner, S., Derungs, C., Ascher-Jenull, J., Camin, F., Sartori, G., Raab, G., Bontempo, L., Paolini, M., Ziller, L., Bardelli, T., Petrillo, M., Abiven, S. (2016): Decomposition and stabilisation of Norway spruce needle-derived material in Alpine soils using a <sup>13</sup>C-labelling approach in the field. *Biogeochemistry* **131**(3), 321-338.
- Eisenhauer, N., Antunes, P. M., Bennett, A. E., Birkhofer, K., Bissett, A., Bowker, M. A., Caruso, T., Chen, B., Coleman, D. C., de Boer, W., de Ruiter, P., DeLuca, T. H., Frati, F., Griffiths, B. S., Hart, M. M., Hättenschwiler, S., Haimi, J., Heethoff, M., Kaneko, N., Kelly, L. C., Leinaas, H. P., Lindo, Z., Macdonald, C., Rillig, M. C., Ruess, L., Scheu, S., Schmidt, O., Seastedt, T. R., van Straalen, N. M., Tiunov, A. V., Zimmer, M., Powell, J. R. (2017): Priorities for research in soil ecology. *Pedobiologia* **63**, 1-7.
- Frouz, J. (2018): Effects of soil macro- and mesofauna on litter decomposition and soil organic matter stabilization. *Geoderma* **332**, 161-172.
- Gardi, C., Jeffery, S., Saltelli, A. (2013): An estimate of potential threats levels to soil biodiversity in EU. *Global Change Biology* **19**, 1538-1548.
- Gessler, P. E., Moore, I. D., McKenzie, N. J., Ryan, P. J. (1995): Soil-landscape modelling and spatial prediction of soil attributes. *International Journal of Geographical Information Systems* **9**(4), 421-432.
- Gessner, M. O., Swan, C. M., Dang, C. K., McKie, B. G., Bardgett, R. D., Wall, D. H., Hättenschwiler, S. (2010): Diversity meets decomposition. *Trends in Ecology and Evolution*, **25**(6), 372-380.
- Gómez-Brandón, M., Ascher-Jenull, J., Bardelli, T., Fornasier, F., Sartori, G., Pietramellara, G., Arfaioli, P., Egli, M., Beylich, A., Insam, H., Graefe, U. (2017): Ground cover and slope exposure effects on micro- and mesobiota in forest soils. *Ecological Indicators* **80**, 174-185.
- Graefe, U., Beylich, A. (2006): Humus forms as tool for upscaling soil biodiversity data to landscape level? *Mitteilungen der Deutschen Bodenkundlichen Gesellschaft* **108**, 6-7.
- Graefe, U., Schmelz, R. M. (1999): Indicator values, strategy types and life forms of terrestrial Enchytraeidae and other microannelids. *Newsletter on Enchytraeidae* **6**, 59-67.
- Grunwald, S. (2009): Multi-criteria characterization of recent digital soil mapping and modeling approaches. *Geoderma* **152**, 195-207.
- Grunwald, S., Thompson, J. A., Boettinger, J. L. (2011): Digital Soil Mapping and Modeling at



- Continental Scales: Finding Solutions for Global Issues. *Soil Science Society of America Journal* **75**, 1201-1213.
- Handa, I. T., Aerts, R., Berendse, F., Berg, M. P., Bruder, A., Butenschoten, O., Chauvet, E., Gessner, M. O., Jabiol, J., Makkonen, M., McKie, B. G., Malmqvist, B., Peeters, E. T. H. M., Scheu, S., Schmid, B., van Ruijven, J., Vos, V. C. A., Hättenschwiler, S. (2014): Consequences of biodiversity loss for litter decomposition across biomes. *Nature* **509**, 218-221.
- Hättenschwiler, S., Tiunov, A. V., Scheu, S. (2005): Biodiversity and Litter Decomposition in Terrestrial Ecosystems. *Annual Review of Ecology, Evolution, and Systematics* **36**, 191-218.
- Hellwig, N., Anschlag, K., Broll, G. (2016): A fuzzy logic based method for modeling the spatial distribution of indicators of decomposition in a high mountain environment. *Arctic, Antarctic, and Alpine Research* **48**(4), 623-635. (= **Chapter 2 of this thesis**)
- Hellwig, N., Anschlag, K., Broll, G. (2017): Modellgestützte Analyse räumlicher Dekompositionsmuster im Hochgebirge. *Berichte der DBG (eprints)*, [http://eprints.dbges.de/1232/1/Hellwig%20et%20al\\_2017\\_DBG%20eprints\\_Dekompositionsmuster%20R%C3%A4umliche%20Modelle%20Hochgebirge.pdf](http://eprints.dbges.de/1232/1/Hellwig%20et%20al_2017_DBG%20eprints_Dekompositionsmuster%20R%C3%A4umliche%20Modelle%20Hochgebirge.pdf) (27/11/2017).
- Hellwig, N., Gómez-Brandón, M., Ascher-Jenull, J., Bardelli, T., Anschlag, K., Fornasier, F., Pietramellara, G., Insam, H., Broll, G. (2018): Humus forms and soil microbiological parameters in a mountain forest: Upscaling to the slope scale. *Soil Systems* **2**(1), 12. (= **Chapter 4 of this thesis**)
- Hengl, T., Mendes de Jesus, J., MacMillan, R. A., Batjes, N. H., Heuvelink, G. B. M., Ribeiro, E., Samuel-Rosa, A., Kempen, B., Leenaars, J. G. B., Walsh, M. G., Gonzalez, M. R. (2014): SoilGrids1km – Global Soil Information Based on Automated Mapping. *Plos ONE* **9**(8), e105992.
- Heung, B., Ho, H. C., Zhang, J., Knudby, A., Bulmer, C. E., Schmidt, M. G. (2016): An overview and comparison of machine-learning techniques for classification purposes in digital soil mapping. *Geoderma* **265**, 62-77.
- Holtmeier, F.-K., Broll, G. (2007): Treeline advance – driving processes and adverse factors. *Landscape Online* **1**, 1-33.
- IPCC (2014): Climate Change 2014: Synthesis Report. Contribution of Working Groups I, II and III to the Fifth Assessment Report of the Intergovernmental Panel on Climate Change. IPCC, Geneva.
- Isobe, K., Ohte, N. (2014): Ecological Perspectives on Microbes Involved in N-Cycling. *Microbes and Environments* **29**(1), 4-16.
- IUSS Working Group Digital Soil Mapping (2016): Digital Soil Mapping. <http://digitalsoilmapping.org/> (11/12/2017).
- IUSS Working Group WRB (2006): World reference base for soil resources 2006. World Soil Resources Reports No. 103. FAO, Rome.
- Jackson, R. B., Lajtha, K., Crow, S. E., Hugelius, G., Kramer, M. G., Piñeiro, G. (2017): The Ecology of Soil Carbon: Pools, Vulnerabilities, and Biotic and Abiotic Controls. *Annual Review of Ecology, Evolution, and Systematics* **48**, 419-445.
- Jänsch, S., Römbke, J., Didden, W. (2005): The use of enchytraeids in ecological soil classification and assessment concepts. *Ecotoxicology and Environmental Safety* **62**, 266-277.
- Jenny, H. (1941): Factors of Soil Formation – A System of Quantitative Pedology. McGraw-Hill, New York.
- Lal, R. (2004): Soil carbon sequestration to mitigate climate change. *Geoderma* **123**, 1-22.
- Lehmann, J., Kleber, M. (2015): The contentious nature of soil organic matter. *Nature* **528**, 60-68.
- Leonelli, G., Masseroli, A., Pelfini, M. (2016): The influence of topographic variables on treeline trees under different environmental conditions. *Physical Geography* **37**(1), 56-72.
- Mayor, J. R., Sanders, N. J., Classen, A. T., Bardgett, R. D., Clément, J.-C., Fajardo, A., Lavorel, S., Sundqvist, M. K., Bahn, M., Chisholm, C., Cieraad, E., Gedalof, Z., Grigulis, K., Kudo, G., Oberski, D. L., Wardle, D. A. (2017): Elevation alters ecosystem

- properties across temperate treelines globally. *Nature* **542**, 91-95.
- McBratney, A. B., Mendonça Santos, M. L., Minasny, B. (2003): On digital soil mapping. *Geoderma* **117**(1-2), 3-52.
- Metz, M., Rocchini, D., Neteler, M. (2014): Surface Temperatures at the Continental Scale: Tracking Changes with Remote Sensing at Unprecedented Detail. *Remote Sensing* **6**, 3822-3840.
- Minasny, B., McBratney, A. B. (2006): A conditioned Latin hypercube method for sampling in the presence of ancillary information. *Computers & Geosciences* **32**, 1378-1388.
- Minasny, B., McBratney, A. B. (2016): Digital soil mapping: A brief history and some lessons. *Geoderma* **264**, 301-311.
- Mountain Research Initiative EDW Working Group (2015): Elevation-dependent warming in mountain regions of the world. *Nature Climate Change* **5**, 424-430.
- Newbold, T., Hudson, L. N., Arnell, A. P., Contu, S., De Palma, A., Ferrier, S., Hill, S. L. L., Hoskins, A. J., Lysenko, I., Phillips, H. R. P., Burton, V. J., Chng, C. W. T., Emerson, S., Gao, D., Pask-Hale, G., Hutton, J., Jung, M., Sanchez-Ortiz, K., Simmons, B. I., Whitmee, S., Zhang, H., Scharlemann, J. P. W., Purvis, A. (2016): Has land use pushed terrestrial biodiversity beyond the planetary boundary? A global assessment. *Science* **353**(6296), 288-291.
- Nussbaum, M., Spiess, K., Baltensweiler, A., Grob, U., Keller, A., Greiner, L., Schaepman, M. E., Papritz, A. (2018): Evaluation of digital soil mapping approaches with large sets of environmental covariates. *SOIL* **4**, 1-22.
- Paul, E. A. (Ed.) (2015): *Soil Microbiology, Ecology, and Biochemistry*. Academic Press, Amsterdam, 4th edition.
- Paul, E. A. (2016): The nature and dynamics of soil organic matter: Plant inputs, microbial transformations, and organic matter stabilization. *Soil Biology & Biochemistry* **98**, 109-126.
- Pelosi, C., Römbke, J. (2018): Enchytraeids as bioindicators of land use and management. *Applied Soil Ecology* **123**, 775-779.
- Ponge, J. F. (2003): Humus forms in terrestrial ecosystems: a framework to biodiversity. *Soil Biology & Biochemistry* **35**, 935-945.
- Ponge, J. F. (2013): Plant-soil feedbacks mediated by humus forms: A review. *Soil Biology & Biochemistry* **57**, 1048-1060.
- Provincia Autonoma di Trento (2014): Tabelle degli indici climatici. [https://climatlas.fbk.eu/view/indici/\(04/12/2017\)](https://climatlas.fbk.eu/view/indici/(04/12/2017)).
- Reichstein, M., Bednorz, F., Broll, G., Kätterer, T. (2000): Temperature dependence of carbon mineralisation: conclusions from a long-term incubation of subalpine soil samples. *Soil Biology & Biochemistry* **32**, 947-958.
- Rutgers, M., Orgiazzi, A., Gardi, C., Römbke, J., Jänsch, S., Keith, A. M., Neilson, R., Boag, B., Schmidt, O., Murchie, A. K., Blackshaw, R. P., Pérès, G., Cluzeau, D., Guernion, M., Briones, M. J. I., Rodeiro, J., Piñero, R., Cosín, D. J. D., Sousa, J. P., Suhadolc, M., Kos, I., Krogh, P.-H., Faber, J. H., Mulder, C., Bogte, J. J., van Wijnen, H. J., Schouten, A. J., de Zwart, D. (2016): Mapping earthworm communities in Europe. *Applied Soil Ecology* **97**, 98-111.
- Sanchez, P. A., Ahamed, S., Carré, F., Hartemink, A. E., Hempel, J., Huising, J., Lagacherie, P., McBratney, A. B., McKenzie, N. J., Mendonça-Santos, M. L., Minasny, B., Montanarella, L., Okoth, P., Palm, C. A., Sachs, J. D., Shepherd, K. D., Vågen, T. G., Vanlauwe, B., Walsh, M. G., Winowiecki, L. A., Zhang, G. L. (2009): Digital Soil Map of the World. *Science* **325**(5941), 680-681.
- Sarmiento, E. C., Giasson, E., Weber, E. J., Flores, C. A., Hasenack, H. (2017): Disaggregating conventional soil maps with limited descriptive data: A knowledge-based approach in Serra Gaúcha, Brazil. *Geoderma Regional* **8**, 12-23.
- Sartori, G., Mancabelli, A. (2009): Carta dei suoli del Trentino: scala 1:250.000. Museo Tridentino di Scienze Naturali di Trento, Centro di Ricerca per l'Agrobiologia e la Pedologia di Firenze.

- Sauvadet, M., Chauvat, M., Brunet, N., Bertrand, I. (2017): Can changes in litter quality drive soil fauna structure and functions? *Soil Biology & Biochemistry* **107**, 94-103.
- Sboarina, C., Cescatti, A. (2004): Il clima del Trentino – Distribuzione spaziale delle principali variabili climatiche. *Report Centro Ecologia Alpina* **33**, 1-20.
- Schimel, J. P., Schaeffer, S. M. (2012): Microbial control over carbon cycling in soil. *Frontiers in Microbiology* **3**, 348.
- Scull, P., Franklin, J., Chadwick, O. A., McArthur, D. (2003): Predictive soil mapping: a review. *Progress in Physical Geography* **27**(2), 171-197.
- Shi, X., Long, R., Dekett, R., Philippe, J. (2009): Integrating Different Types of Knowledge for Digital Soil Mapping. *Soil Science Society of America Journal* **73**(5), 1682-1692.
- Six, J., Bossuyt, H., Degryze, S., Denef, K. (2004): A history of research on the link between (micro)aggregates, soil biota, and soil organic matter dynamics. *Soil & Tillage Research* **79**, 7-31.
- Söderström, M., Sohlenius, G., Rodhe, L., Piikki, K. (2016): Adaptation of regional digital soil mapping for precision agriculture. *Precision Agriculture* **17**, 588-607.
- Taghizadeh-Mehrjardi, R., Nabiollahi, K., Kerry, R. (2016): Digital mapping of soil organic carbon at multiple depths using different data mining techniques in Baneh region, Iran. *Geoderma* **266**, 98-110.
- Tsiafouli, M. A., Thébault, E., Sgardelis, S. P., de Ruiter, P. C., van der Putten, W. H., Birkhofer, K., Hemerik, L., de Vries, F. T., Bardgett, R., Brady, M. V., Bjornlund, L., Bracht Jørgensen, H., Christensen, S., D'Hertefeldt, T., Hotes, S., Hol, W. H. G., Frouz, J., Liiri, M., Mortimer, S. R., Setälä, H., Tzanopoulos, J., Uteseny, K., Pižl, V., Stary, J., Wolters, V., Hedlund, K. (2015): Intensive agriculture reduces soil biodiversity across Europe. *Global Change Biology* **21**(2), 973-985.
- von Seidlein, C. (2000): Petrographie und Struktur des ostalpinen Altkristallins südlich des Ultentales (Trentino, Nord-Italien). Doctoral dissertation at Ludwig-Maximilians-Universität München.
- Wagener, J. (2014): Die Vegetation der Region Val di Sole in den italienischen Alpen. Master thesis, University of Osnabrück, Osnabrück.
- Wagg, C., Bender, S. F., Widmer, F., van der Heijden, M. G. A. (2014): Soil biodiversity and soil community composition determine ecosystem multifunctionality. *Proceedings of the National Academy of Sciences of the United States of America* **111**(14), 5266-5270.
- Wall, D. H., Nielsen, U. N., Six, J. (2015): Soil biodiversity and human health. *Nature* **528**, 69-76.
- Yang, L., Jiao, Y., Fahmy, S., Zhu, A.-X., Hann, S., Burt, J. E., Qi, F. (2011): Updating Conventional Soil Maps through Digital Soil Mapping. *Soil Science Society of America Journal* **75**(3), 1044-1053.



## Chapter 2

A fuzzy logic based method for modeling the spatial distribution of indicators of decomposition in a high mountain environment



The online appendix can be found in Appendix 1 of this thesis.

**Citation:** Hellwig, N., Anschlag, K., Broll, G. (2016): A fuzzy logic based method for modeling the spatial distribution of indicators of decomposition in a high mountain environment. *Arctic, Antarctic, and Alpine Research* **48**(4), 623-635.

**Author contributions:** N.H. developed the methodological framework, performed data analysis, modeling and model assessment for the case study and wrote the paper; K.A. contributed to the realization of the case study; G.B. conceived and designed the experiments.

### **Copyright**

2016 Regents of the University of Colorado  
Reprinted with permission of the publisher

### **Photo credits (previous page):**

Niels Hellwig, 3 August 2014

Treeline of the European larch (*Larix decidua*) next to Lago di Soprasasso at 2200 m a.s.l., in the upper part of the Valle di Valorz above the Valorz waterfalls near San Bernardo (Val di Rabbi, Trentino, Italian Alps).

Photo published in the Arctic, Antarctic, and Alpine Research 2017 Calendar

# **A fuzzy logic based method for modeling the spatial distribution of indicators of decomposition in a high mountain environment**

NIELS HELLWIG<sup>1,\*</sup>, KERSTIN ANSCHLAG<sup>1</sup>, GABRIELE BROLL<sup>1</sup>

<sup>1</sup>Institute of Geography, University of Osnabrück, Seminarstraße 19ab, 49074 Osnabrück, Germany

\*Corresponding author

## **ABSTRACT**

Upscaling of sample data on indicators of decomposition to the landscape scale is often necessary for extensive ecological assessments. The amount of such data is mostly scarce even with high sampling efforts. Moreover, environmental conditions are very heterogeneous in high mountain regions. Therefore, the aim was to find a suitable technique for spatial modeling under these circumstances.

A method combining decision tree analysis and the construction of fuzzy membership functions is introduced for a GIS-based mapping of decomposition indicating parameters. It is compared with an approach solely based on decision trees. Within a case study in the Italian Alps the spatial distribution of humus forms, classified by the occurrence of an OH (humified residues) horizon, is examined. There appears to be a strong relationship with elevation and a minor correlation with slope exposition.

The fuzzy logic-based approach proves to be suitable for modeling the spatial distribution of indicators of decomposition. Mapping fuzzy values allows for the representation of small-scale variability and uncertainty of data due to a relatively low sample size in a very heterogeneous environment.

**Submitted:** 5 November 2015 – **Accepted:** 28 July 2016

## **INTRODUCTION**

Decomposition processes are of high significance for the functioning of terrestrial ecosystems. As part of various material cycles, these processes ensure the survival not only of decomposing but also of producing and consuming organisms (Swift et al., 1979). A prominent indicator with regard to decomposition are humus forms (Andreotta et al., 2012; Ascher et al., 2012; Graefe and Beylich, 2006; Ponge, 2013). They can be defined as

manifestations of dead organic matter at different stages of decomposition in the topsoil, which in forest ecosystems consist of organic layers (OL = litter, OF = fragmented residues, OH = humified residues) and the uppermost mineral horizon.

Analyzing and assessing the impacts of ecological processes and interactions are required at the landscape scale for numerous purposes. In contrast, ecological field data at the landscape scale is often scarce due to high costs and low accessibility, especially in high

mountain environments. Upscaling by means of spatial modeling allows for bridging the gap between the local study scale and the target landscape scale.

In terms of soil ecology, there is a wide range of such modeling methods associated with the concept of digital soil mapping (McBratney et al., 2003), comprising pedotransfer functions, geostatistical techniques, and factor-based approaches (Behrens and Scholten, 2006). Pedotransfer functions allow the derivation of soil variables from other factors easier to determine by means of mathematical formulas (Bouma, 1989; Wösten et al., 2001); thus a detailed quantitative comprehension of the correlations between environmental factors is prerequisite (McBratney et al., 2002). The application of geostatistical techniques (e.g., kriging, co-kriging) is particularly critical in areas with a high heterogeneity of environmental covariates. For these techniques an accordingly higher density of samples is indispensable (Heuvelink and Webster, 2001). Factor-based approaches are based on considering the soil properties as a system state, whose configuration is determined by the soil-forming factors (e.g., clorpt model, Jenny, 1941; scorpan model, McBratney et al., 2003). Different methods have been applied implementing the factor-based approach (Behrens and Scholten, 2007; McBratney et al., 2003), including linear regression and classification models, artificial neural networks, tree-based regression and classification models, support vector machines, and fuzzy logic models.

This study aims at refining a spatial knowledge-based modeling technique and establishing it for the prediction of indicators of decomposition processes and properties under a highly heterogeneous topography and a relatively small sample size. Decomposition processes are influenced by various environmental factors. In a high mountain environment these are in a large part mediated by the

elevation and the slope exposition, but for some factors in a nonlinear way (such as vegetation, where thresholds for different zones exist depending on the topography). Therefore a fuzzy logic approach based on a data mining decision tree algorithm accounting for nonlinearities is hypothesized to fit the situation.

The first part describes the methodological approach proposed in this study. It is followed by the presentation of a case study conducted in a study area in the Italian Alps. In this case study, the approach utilizing fuzzy logic is applied for modeling the occurrence of humus forms showing an OH horizon and comparing it with an approach solely utilizing decision tree analysis.

## METHODOLOGICAL FRAMEWORK

### Construction of a Decision Tree

Binary decision trees for data mining (i.e., classification and regression trees [CART]; Breiman et al., 1984) serve as a practicable and simply interpretable tool to statistically model complex and nonlinear dependencies between (environmental) influencing factors and a target variable on the basis of sample data (Aberegg et al., 2009; De'ath and Fabricius, 2000; McKenzie and Ryan, 1999; Mertens et al., 2002). Decision trees are constructed by recursively partitioning the sample set into pairwise disjoint subsets that show a higher rate of homogeneity with respect to the target variable. The rules for partitioning have the form  $x_i \leq c$ ,  $c \in V_i \subseteq \mathbb{R}$ , if the influencing factor  $X_i \in \{X_1, \dots, X_a\}$  taking values in  $V_i$  is interval or ratio scaled, and the form  $x_i \in S$  otherwise, with  $S$  covering a subset of the property values  $M_i = \{m_1, \dots, m_z\}$  of  $X_i$  ( $x_i$  is evaluated for every sample as the

value of  $X_i$ ) (Fig. 1). As part of the partitioning procedure, an inhomogeneity measure  $\iota$  is calculated in order to establish an appropriate decision rule. Each time, the difference of the inhomogeneity of a certain node  $v$  and the sum of the inhomogeneities of the successor nodes  $v_L$  and  $v_R$  are maximized:  $\max\{\iota[v] - [\iota(v_L) + \iota(v_R)]\}$ . For classification trees the gini index  $\iota_{Class}$  (Equation 1) serves as an estimator of the inhomogeneity of a node  $v$ , with the conditional probability  $p(y_i|v)$ ,  $i = 1, \dots, z$ , of a value of the target variable  $y_i \in Y$  in  $v$ . For regression trees the resubstitution error  $\iota_{Reg}$  (Equation 2) is used, where the number of all samples is denoted as  $N$  and the number of samples in  $v$  is denoted as  $N_v \leq N$ , with the related values of the target variable  $y_n$ ,  $n = 1, \dots, N_v$  (Breiman et al., 1984).

$$\iota_{Class}(v) = \sum_{k \neq l} p(y_k|v) \cdot p(y_l|v), y_k, y_l \in Y \quad (1)$$

$$\iota_{Reg}(v) = (1/N) \sum_{n=1}^{N_v} (y_n - \bar{y}(v))^2 \quad (2)$$

The recursive partitioning procedure is performed on all subsets. It terminates as soon as no higher degree of homogeneity can be

reached or a threshold of the number of elements in a node is undercut.

## Fuzzy Logic Model

The fuzzy logic model is based on the concept of fuzzy sets (Zadeh, 1965). Unlike ordinary sets, fuzzy sets enable their elements to show a partial degree of membership in the range from 0 (no membership) to 1 (full membership). In this way, fuzzy logic models are capable of representing continuous graduations from one class to another class (e.g., soil types, humus forms), which has been applied in soil science on numerous occasions (de Gruijter et al., 2011; McBratney and Odeh, 1997; Qi and Zhu, 2011; Zhu, 2006; Zhu et al., 1996, 2001). In the context of digital soil mapping, fuzzy logic models have been designed and applied for predicting various soil properties (Ashtekar and Owens, 2013; de Menezes et al., 2013). By means of fuzzy membership functions  $\mu: E_1 \times \dots \times E_n \rightarrow [0,1]$ ,  $(x_1, \dots, x_n) \mapsto \mu(x_1, \dots, x_n)$ , dependencies of a target variable on environmental covariates (with the domains  $E_1, \dots, E_n$ ) can be described. These functions refer membership degrees of

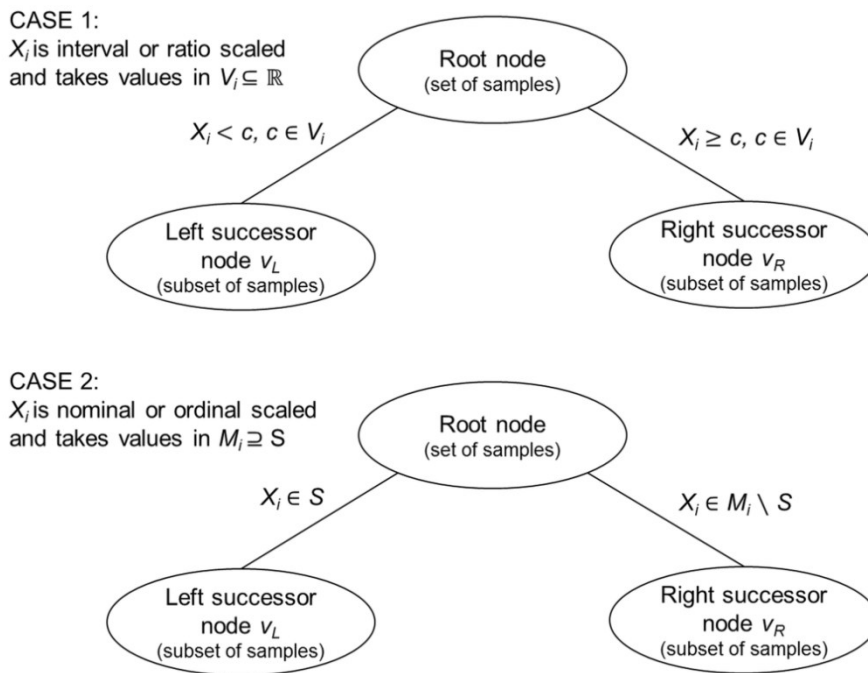


**Figure 1.** Illustration of a node split in a decision tree depending on the scale of measurement of the influencing variable  $X_i \in \{X_1, \dots, X_a\}$ .

the target variable to different environmental circumstances (McBratney and Odeh, 1997).

In order to derive suitable fuzzy membership functions from an existing decision tree, tuples containing the value that is inherited in a distinct tree node and the related values of the covariates are used to approximate a general function rule. In case of the fuzzy membership  $s_{ij,k,a}$  of a modeled variable  $k$  as a function of a single environmental variable  $a$  with the value  $z_{ij,a}$  at location  $(i,j)$ , a two-dimensional rule is needed, such as the bell-shaped function provided by Shi et al. (2009) and Shi (2013) (Equation 3), with the maximal membership  $max \in [0,1]$ , the central values of the function  $v_1$  and  $v_2$ , the inflection points  $w_1$  and  $w_2$ , and with  $r_1$  and  $r_2$  determining the steepness of the function parts.

In case of a continuously increasing or decreasing behavior of the modeled variable  $k$  along the gradient of an environmental variable  $a$ , a sigmoidal function can be derived from Equation 3 by utilizing only the increasing or decreasing function parts, respectively. Membership values between 0 and 1 can be derived from the fuzzy membership functions depending on the values of the environmental covariates. If information about these covariates is extensively available, membership values can be modeled for every site across the study area and for every class of the target variable.

Similar approaches based on a combination of decision trees and fuzzy logic have been described elsewhere (Chiang and Hsu, 2002; Suárez and Lutsko, 1999) and utilized for soil scientific purposes (Ai et al., 2013; Ribeiro et al., 2014; Qi and Zhu, 2011). To our knowledge, though, this is the first time that a

model combining decision tree analysis and fuzzy logic is applied for mapping indicators of decomposition.

## CASE STUDY: MODELING OF HUMUS FORMS AT VAL DI RABBI (TRENTINO, ITALY)

### Study Area

The study area (522.7 km<sup>2</sup>) belongs to the Autonomous Province of Trentino in northern Italy and encompasses the two Alpine valleys Val di Sole and Val di Rabbi (Fig. 2). The entire area is characterized by siliceous parent material, with paragneiss, mica schists and phyllites prevailing, and with some lenses of orthogneiss (Aberegge et al., 2009). In terms of soil classes, the range up to 1900 m a.s.l. is dominated by Haplic Cambisols (Dystric) and Umbric Podzols. At higher elevations, the prevalent classes are Entic Podzols, Albic Podzols, and Umbric Podzols (Sartori and Mancabelli, 2009).

### Data Basis and Preprocessing

Six investigation sites were located inside the closed coniferous forest along different elevations between 1180 and 1660 m a.s.l., three each at north-exposed slopes (N1, N2, N3) and south-exposed slopes (S6, S7, S8). They are comparable with respect to geology (all sites have paragneiss as parent material) and local topographical position (all sites are located on uniform slopes). The north-exposed sites are dominated by Norway spruce (*Picea abies*) and the south-exposed sites by European larch (*Larix decidua*). The site S6 was located in a former coppice.

$$\begin{cases} s_{ij,k,a} = max * \exp\left(\left[\frac{z_{ij,a} - v_1}{w_1}\right]^{r_1} \ln(0.5)\right) & \text{if } z_{ij,a} < v_1, \\ s_{ij,k,a} = max & \text{if } v_1 \leq z_{ij,a} \leq v_2, \\ s_{ij,k,a} = max * \exp\left(\left[\frac{z_{ij,a} - v_2}{w_2}\right]^{r_2} \ln(0.5)\right) & \text{if } z_{ij,a} > v_2 \end{cases} \quad (3)$$



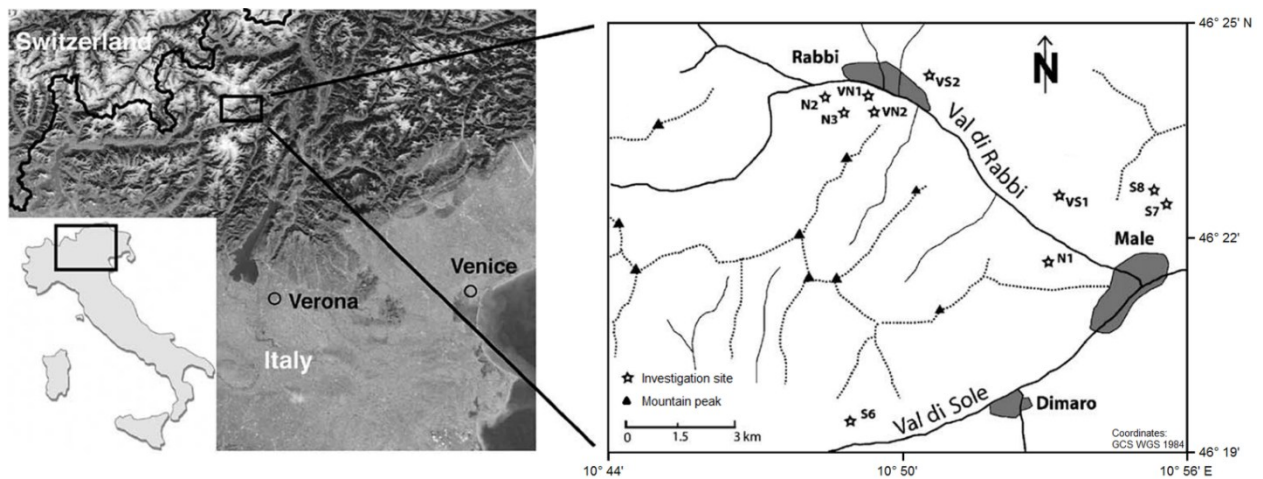


**Figure 2.** Location of the study area and investigation sites in the Autonomous Province of Trentino (Italy) (modified from Egli et al., 2006).

Every investigation site (~25 m<sup>2</sup>, depending on the local variability of site conditions) comprised three or six sampling plots, respectively (humus profiles at a length of up to 1 m), according to the number of different soil cover types (grass, moss, litter, fern). These plots also included different local slope dynamics (i.e., erosive and accumulative characteristics) at every investigation site. The total number of sampling plots amounted to  $n = 30$ . The humus profiles were dominated by

moder conditions (humus forms showing a continuous OH horizon), with transitions to Mull-like conditions (OH horizon missing), primarily at the lowest north-facing site N1 as well as at the south-facing sites (Table 1).

The model of humus forms addresses the occurrence of a humus form with an OH horizon. Data from the sampling plots were obtained, indicating the occurrence of an OH horizon with values from the interval [0,1] (Table 2). The value 1 was assigned to a

**Table 1**

Soil cover types, dominating humus forms, and humus profiles at the investigation sites (N1–N3, northern slope exposition; S6–S8, southern slope exposition) (according to Egli et al., 2006; personal communication, D. Tatti and G. Sartori).

Site	Elevation (m a.s.l.)	Soil cover types	Dominating humus form according to		Typical humus profile
			German classification (Ad-hoc-AG Boden, 2005)	Classification from Switzerland (Gobat et al., 2014)	
N1	1180-1195	moss (90 %), fern (10 %)	Mullartiger Moder	Hémimoder/Eumoder/Dysmoder	OL-OF-(OH-)AE
N2	1395-1410	moss (100 %)	Typischer Moder	Dysmoder	OL-OF-OH-AE
N3	1595-1605	grass (80 %), moss (20 %)	Typischer Moder	Dysmoder	OL-OF-OH-E
S6	1200-1220	litter (90 %), grass (10 %)	Mullartiger Moder	Eumésamphi	OL-OF-(OH-)A
S7	1380-1395	grass (100 %)	Mullartiger Moder	Hémimoder	OL-OF-(OH-)AE
S8	1650-1660	litter (80 %), grass (20 %)	Mullartiger Moder/Typischer Moder	Hémimoder	OL-OF-(OH-)AE

**Table 2**

Data basis for modeling. Values of topography and humus forms have been aggregated from all sampling plots per investigation site.

Site	Number of sampling plots	Elevation (m a.s.l.) <sup>1</sup>	Slope exposition	Percentage of humus forms showing an OH horizon
N1	6	1200	north (360°N)	15.00%
N2	3	1400	north (360°N)	66.67%
N3	6	1630	north (360°N)	60.00%
S6	6	1200	south (180°N)	6.67%
S7	3	1400	south (180°N)	50.00%
S8	6	1630	south (180°N)	53.33%

<sup>1</sup>From DTM, aggregated by plot elevations.

sample where a continuous OH horizon was present. If an OH horizon did not exist, the value 0 was assigned. For discontinuous OH horizons the small-scale presence and absence of an OH horizon often changed abruptly and irregularly (thus without the possibility to trace it back clearly to other factors). Therefore, the intermediate value 0.5 was used for this situation.

**Table 3**

Validation sites: topographic position and percentage values (observed and modeled) of humus forms showing an OH horizon.

Site	Elevation (m a.s.l.)	Slope exposition	Observed value	Decision tree model		Fuzzified decision tree model	
				Predicted value	Deviation	Predicted value	Deviation
VN1	1210	north	45.0%	10.8%	34.2%	11.2%	33.8%
VN2	1380	north	100.0%	51.7%	48.3%	62.0%	38.0%
VS1	1340	south	0.0%	63.3%	-63.3%	46.0%	-46.0%
VS2	1570	south	50.0%	51.7%	-1.7%	52.1%	-2.1%

In order to examine the combined effects of elevation and slope exposition, the particular elevation and slope exposition values were aggregated to three levels of elevation and two levels of exposition. For elevation, the intermediate values 1200 m, 1400 m, and 1630 m were derived from the elevation values of the related sampling plots. For slope exposition, north-exposed sites were assigned a value of 360°N (equal to 0°N), and south-exposed sites were assigned a value of 180°N (Table 2). The humus form data of each sampling plot was weighted according to the estimated percentage of its soil cover type in relation to the overall area at this site (Table 1).

Four additional sites for model validation were studied with a reduced number of sampling plots ( $n = 8$ ). Two sites each were located at north-facing (VN1, VN2) and south-facing (VS1, VS2) slopes (Table 3).

Information about the elevation in the study area was taken directly from a bare ground digital terrain model (DTM) with a grid width of 10 m (Aberegg et al., 2009; compiled by the Provincia Autonoma di Trento on the basis of the topographic map with the scale of 1:10,000). A model representing slope exposition values was derived from this DTM with the slope method by Horn (1981).



## Modeling

Two modeling approaches were juxtaposed. The first approach used results from decision tree analysis without any fuzzification process, and the second one combined decision trees and fuzzy logic. Decision trees were built using the statistical software R (R Core Team, 2015) and the R package `rpart` (Therneau et al., 2015). The routine can be found in the online appendix (file `DecTreeAnalysis.R` together with the data file `hf_data.txt`).

Bell-shaped fuzzy membership functions describing the occurrence of OH horizons in dependence on the elevation and slope exposition were formulated according to Equation 3. As the effects of two influencing variables (elevation and slope exposition) were examined, a two-step fuzzification procedure needed to be applied. With the first step, fuzzy membership functions were used to build submodels. These submodels correspond to the subtrees originating from the secondary split in the tree, thus they depend on the less influencing variable. The fuzzy membership functions were fitted by using values of the influencing variable together with the related percentages of a humus form with an OH horizon. With the second step, the submodels were combined by means of weighting functions that thereby realize fuzzification of the primary influencing variable. The resulting fuzzy membership functions were realized with the ArcGIS extension tool ArcSIE (Shi, 2013). This tool processed them to build maps that spatially predict the occurrence of OH horizons.

Modeling was conducted for the central part of Val di Rabbi. According to our field experience, the prediction area was selected to include the coniferous forest zone at the valley sides between 1100 m and 1800 m a.s.l.

The results from modeling were assessed with the mean error (Equation 4) and the root mean squared error (RMSE) (Equation 5) of the predictions at the validation sites:

$$ME = \frac{1}{n} \sum_{i=1}^n |y_i - \hat{y}_i| \quad (4)$$

$$RMSE = \sqrt{\frac{1}{n} \sum_{i=1}^n (y_i - \hat{y}_i)^2} \quad (5)$$

The number of samples for validation is  $n$ ,  $y_i$  are the observed values at the validation sites, and  $\hat{y}_i$  are the related values predicted by the model.

## RESULTS

The sample data on the spatial distribution of humus forms showing an OH horizon and the related data on elevation and slope exposition was used for the construction of a decision tree. This yielded a tree with a primary partition induced by the factor elevation at 1300 m a.s.l. (Fig. 3). The left subtree consisted of a single node, representing the relatively similar percentages of humus forms with an OH horizon at north-exposed and south-exposed slopes below 1300 m. The right subtree applied to elevations from 1300 m upwards and included another partition to distinguish between northern and southern slope expositions.

The nodes of the decision tree were obtained by recursive partitioning of the sample set. Each of the three leaf nodes held a subset with a prediction about the occurrence of OH horizons for the study area, which was specific to the related elevation and exposition range (Fig. 3):

- below 1300 m: 10.83% of the area exhibited a humus form with an OH horizon (based on 12 samples)

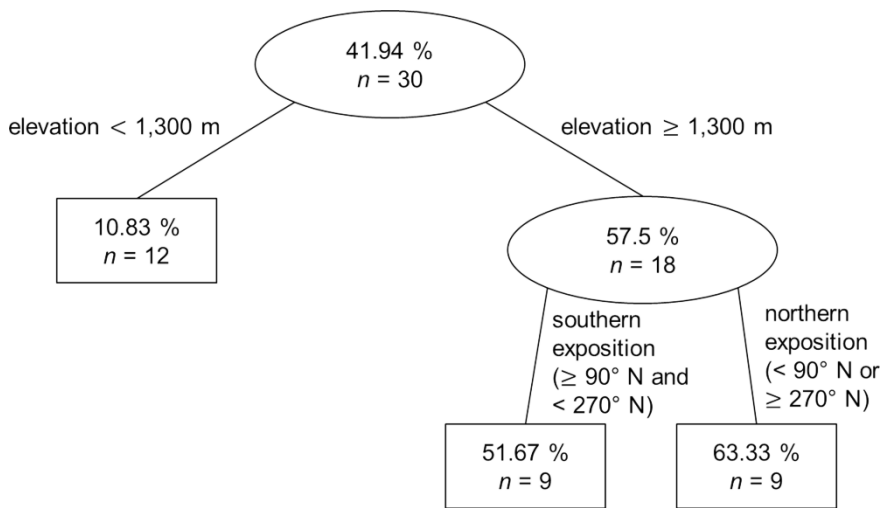


**Figure 3.** Decision tree for the distribution model of OH horizons. The upper value inside the tree nodes represents the projected percentage of the area with humus forms showing an OH horizon in relation to the overall area at this elevation and slope exposition. The lower value  $n$  indicates the number of related samples.

- at south-exposed slopes from 1300 m upwards: 51.67% of the area exhibited a humus form with an OH horizon (based on 9 samples)
- at north-exposed slopes from 1300 m upwards: 63.33% of the area exhibited a humus form with an OH horizon (based on 9 samples)

The first model variant simply used this separation and mapped the values from the leaf nodes to the related elevation and exposition ranges inside the study area. This caused a steplike behavior of the distribution function (Fig. 4).

The second model variant also originated from the values of the leaf nodes, but includes a fuzzification at the transitions between

different elevation and exposition ranges. As there are two variables influencing the occurrence of OH horizons, two steps of fuzzification need to be realized. With the first step, the two subtrees at tree level 2 were fuzzified, both being independent on elevation (Fig. 3). For elevations below 1300 m a.s.l. (left subtree) the constant value 10.83% was used for all slope expositions (constant function  $s_{ij,k,a} = 0.1083$ ). At higher elevations (right subtree) fuzzy membership functions were constructed, which covered the pairs  $(z_{ij,a}, s_{ij,k,a})$  referring to Equation 3 ( $z_{ij,a}$  = slope exposition in °N,  $s_{ij,k,a}$  = percentage of humus forms showing an OH horizon): (0, 0.6333), (180, 0.5167), (360, 0.6333). Figure 5 illustrates possible functions for different parameters  $r_1 / r_2$  (assuming  $r_1 =$

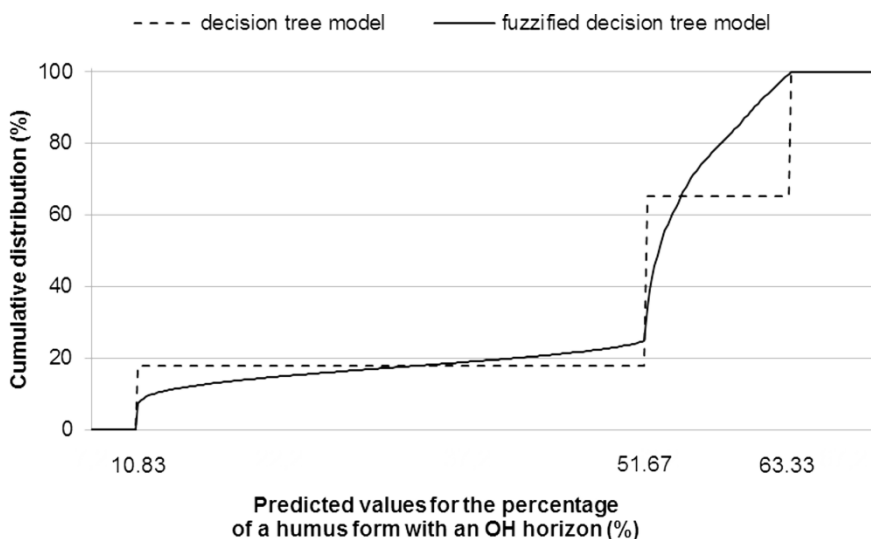


**Figure 4.** Cumulative distribution functions for the values predicting the percentage of a humus form with an OH horizon in the two models that are compared.

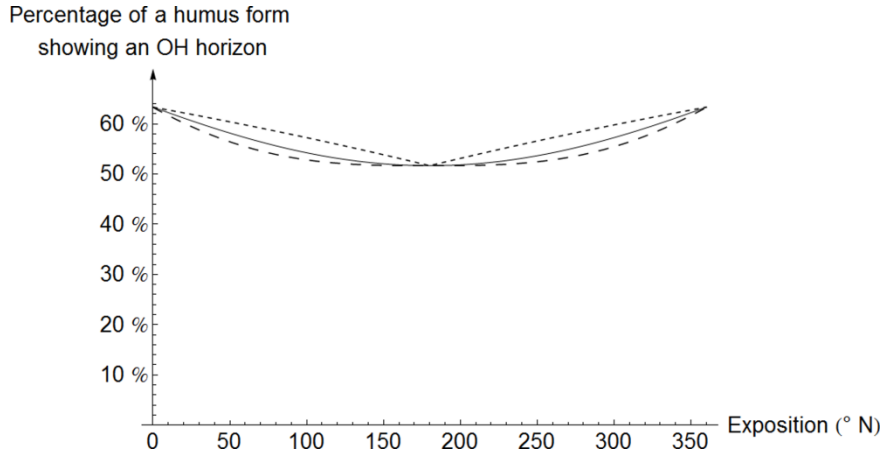


**Figure 5.** Fuzzy membership functions for the distribution model of OH horizons above 1300 m a.s.l., derived from the right subtree in Figure 3. The solid line represents the function with  $r_1 = r_2 = 2$ , the dashed lines have the parameters  $r_1 = r_2 = 1$  (short dashing) and  $r_1 = r_2 = 3$  (long dashing).

$r_2$ ). In this case the function with  $r_1 = r_2 = 2$  was chosen for further modeling, as a function with a median trend in the increasing occurrence of OH horizons from south to north exposition (Equation 6).

Under the assumption  $r_1 = r_2$  both of the functions for western and eastern slope expositions behaved equally ( $v_1 = v_2$  and  $w_1 = w_2$ ), so the system of equations Equation 6 reduced to a single equation (Equation 7).

The submodels for the two elevation ranges (1100–1300 m and 1300–1800 m) represent the (left and right) subtrees of the root node (Fig. 3), which both underwent fuzzification of the slope exposition. As a second fuzzification step the partition of the root node (where both submodels are connected) needs to be addressed. Fuzzification of the elevation was performed in the range between the examined investigation sites N1/S6 and N2/S7 (1200–1400 m a.s.l.), where predictions tend to be uncertain due to the lack of sampling data. It was accomplished by building functions associating the elevation with a weight between 0

and 1 (Fig. 6). These weighting functions were applied at the fuzzy membership functions of the submodels from the first fuzzification step. As a consequence of fuzzification, the distribution function of the second model showed a continuously increasing behavior without consecutive steps at the thresholds that stem from the decision tree (Fig. 4).

Prediction maps indicating the percentage of humus forms that show an OH horizon in the area selected for modeling were constructed for both model variants using ArcMap 10 and the extension ArcSIE (Fig. 7). According to the values of the fuzzy membership functions, the values of the prediction maps ranged from 10.8% to 63.3%. The lowest values were predicted for low elevation areas between 1100 m and 1200 m. At elevations from 1400 m upwards, where only the fuzzy membership functions for higher elevations was used (in consequence of the second fuzzification step, Fig. 6), there were significantly larger percentages of a humus form with an OH horizon (between 51.67% and 63.33%), with higher prediction values at north-exposed slopes.

$$\begin{cases} s_{ij,k,a} = 1 - 0.4833 * \exp\left(\left[\frac{z_{ij,a} - 180}{285}\right]^2 \ln(0.5)\right) & \text{if } z_{ij,a} < 180, \\ s_{ij,k,a} = 0.5167 & \text{if } z_{ij,a} = 180, \\ s_{ij,k,a} = 1 - 0.4833 * \exp\left(\left[\frac{z_{ij,a} - 180}{285}\right]^2 \ln(0.5)\right) & \text{if } z_{ij,a} > 180 \end{cases} \quad (6)$$

$$s_{ij,k,a} = 1 - 0.4833 * \exp\left(\left[\frac{z_{ij,a} - 180}{285}\right]^2 \ln(0.5)\right) \quad (7)$$

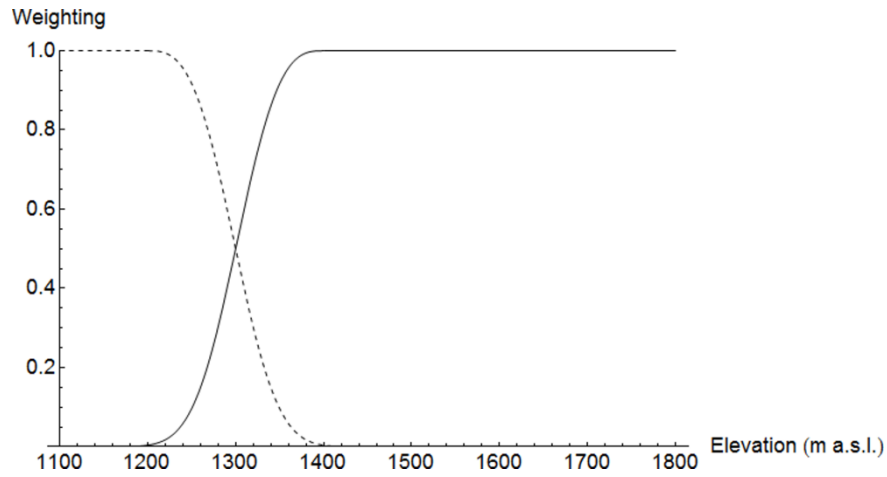


**Figure 6.** Weights for the synthesis of the elevation models. Dashed line: weights for the elevation model below 1300 m a.s.l.; solid line: weights for the elevation model from 1300 m a.s.l. upward. Parameter values of the model for lower elevations (dashed line):  $v_2 = 1200$ ,  $w_2 = 100$ ,  $r_2 = 3$ . Parameter values of the model for higher elevations (solid line):  $v_1 = 1400$ ,  $w_1 = 100$ ,  $r_1 = 3$ .

Model validation shows notable deviations for both models, which are highest at site VS1 (observed value 0.0 %, predicted value 63.3 % when using the decision tree model and 46.0 % when using the fuzzified decision tree model). The deviations for the sites VN1 and VN2 are moderate to high, the observed value for site VS2 corresponds best with the values predicted by the models (Table 3). When including fuzzification, validation results in a mean error of 30.0 % and an RMSE (root mean squared error) of 34.3 %. When predicting values only based on the decision tree, the mean error is 36.9 % and the RMSE is 43.3 %.

## DISCUSSION

### Results from the Case Study

The case study showed predictions for the occurrence of OH horizons that vary in accordance with the modeling approach. The model that includes a fuzzification procedure fitted the real situation potentially better than

the one without this procedure, as there were no abrupt changes in the projected values due to any threshold values from the decision tree, which cannot be justified based on the low data amount. Nevertheless, the structure of the decision tree was also reflected in the predictive map of the fuzzy logic model (Fig. 7).

Regarding the occurrence of OH horizons, modeling revealed differences primarily with a changing elevation. At higher elevations within the forest, north-exposed slopes were predicted to exhibit slightly larger percentages of a humus form with an OH horizon than south-exposed slopes. The validation showed that deviations of field observations from the model results were likely to occur in some places. Nevertheless the predicted trends of a higher occurrence of OH horizons with an increasing elevation and also at northern slope expositions were confirmed. The deviations at the validation sites suggested that further thresholds might exist depending on the elevation, which were still not well explained by the model.

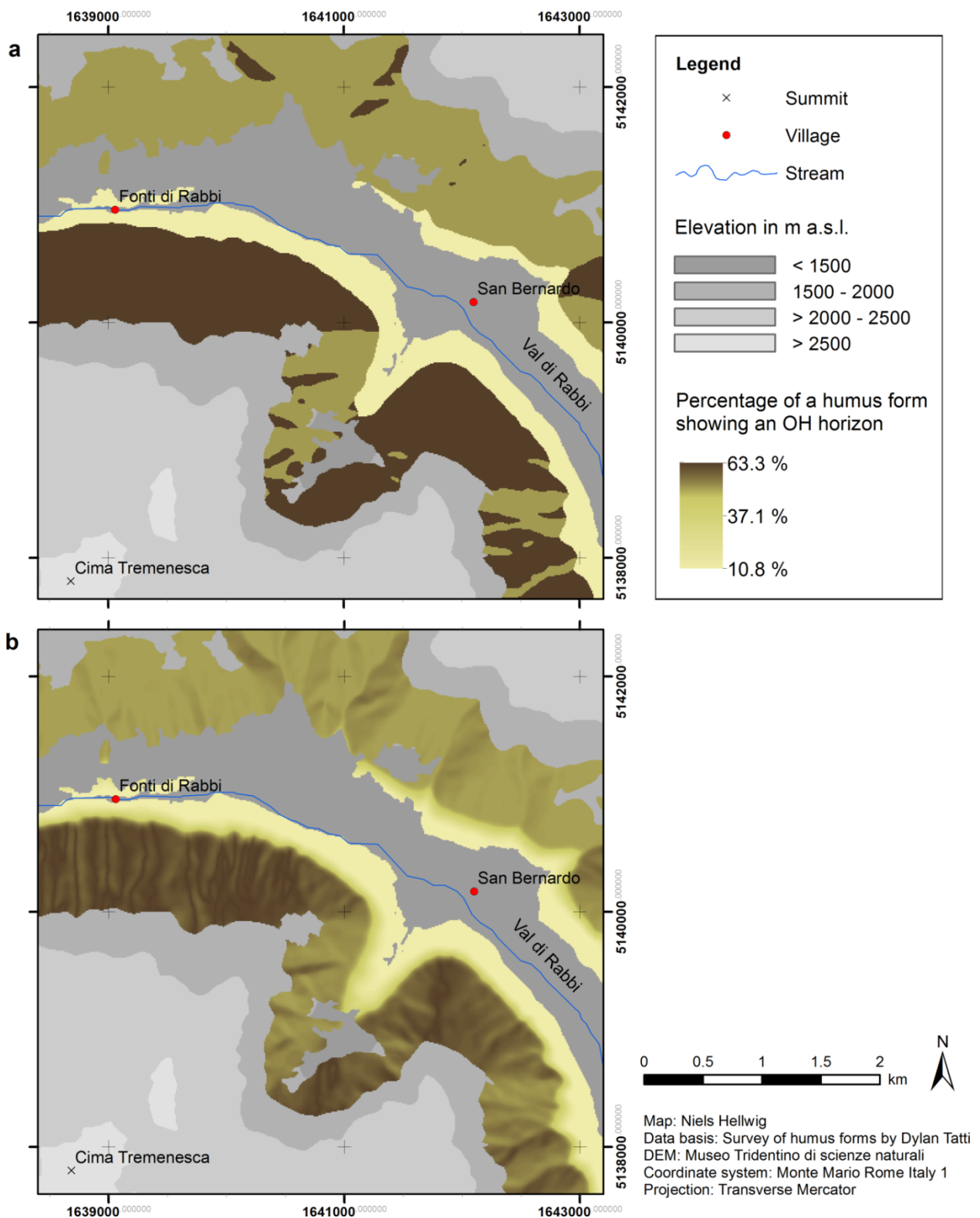


**Figure 7.** Comparison of the predicted spatial distribution of humus forms showing an OH horizon (a) using decision tree analysis without fuzzification procedure, and (b) combining decision tree analysis and fuzzy membership functions. In contrast to the first model (a), which only predicts three different percentage values, the second model (b) incorporates the gradual transitions in humus forms along different elevations and slope expositions. The modeled area includes areas with coniferous forest between 1100 m and 1800 m a.s.l. in the central part of Val di Rabbi (Trentino, Italy).

This predicted distribution depending on the elevation and slope exposition is in line with the findings of other investigations of forest ecosystems, for example higher accumulation of organic matter at north-facing compared to south-facing slopes (e.g., Aberegg et al., 2009; Ascher et al., 2012; Bernier, 1996; Egli et al., 2009, 2010a, 2010b). The correlation of humus forms and the relief parameters elevation and slope exposition emphasizes the influence of environmental factors such as solar radiation, temperature and vegetation on decomposition processes also in the study area. The effects of other covariates on decomposition such as parent material were not examined in the context of this study, thus modeling results are potentially subject to uncertainties at sites where environmental conditions deviate from the investigation sites (e.g., on mica schists). With a higher number of investigation sites the results could possibly be improved by integrating further potentially influencing variables.

## **Application of Decision Trees and Fuzzy Logic**

Modeling is exerted with a knowledge-based approach, built on the use of decision tree analysis and the concept of fuzzy logic. Decision trees have shown to be well suited for revealing relationships between sample data and environmental factors (Aberegg et al., 2009; De'ath and Fabricius, 2000; Gerlitz, 2015). In the case of a small sample size, decision tree analysis has to be frequently performed without any pruning procedure, since this would eliminate almost every partition of the sample set (for details on the pruning procedure, see Breiman et al., 1984). For that reason the number of sample elements is usually low especially in the leaf nodes, thus the direct use of maximum decision trees, which are not pruned, for prediction is criti-

cal. However, even these maximum trees are not generally overfitted, as long as the distinct places of the sampling plots have been determined directly in the field using the knowledge and experience of experts in the sector of decomposition.

The application of fuzzy logic helps to manage the limited predictive capability of the trees, as the divisions of the sample set and the related values of the covariates are fuzzified and do not act as strict thresholds. The use of a nonautomated fuzzification procedure also allows the integration of expert knowledge for the definition of fuzzy membership functions (e.g., when choosing free parameters; see Fig. 5). Because of the relatively low number of samples and the ensuing use of the results from a nonpruned tree, an automated fuzzification procedure does not seem to be appropriate (Gerlitz, 2015; Suárez and Lutsko, 1999).

With the help of fuzzy membership functions, the similarity of the environmental characteristics at a site in comparison to those at sites typical for one specific predicted value (e.g., OH horizon present) can be modeled in the form of a membership (de Menezes et al., 2013; Zhu, 1997). The usage of fuzzy membership values enables also the consideration of a high spatial heterogeneity. This allows, for example, for involving the small-scale variability, which has been shown to be an important characteristic of decomposition processes and properties in the Alps (Bednorz et al., 2000). Consequently, the predicted percentage values, arising from the fuzzy membership values, provide information about the local variability of humus forms, although it is not possible to get spatially differentiated predictions at a resolution higher than  $10 \times 10 \text{ m}^2$ .

The bell-shape functions used to model the dependency of indicators of decomposition on environmental factors show a high flexibility and can even manage factors that take

values in a cyclic range (such as slope exposition). Nevertheless, the application of a bell-shape function to map the relationship between the slope exposition and indicators of decomposition seems to be disadvantageous, as it shows different behavior for sites north exposed (near 0°N and 360°N) and south exposed (around 180°N) (see Fig. 5). A potentially more reasonable way for this would be the implementation of a trigonometrical function.

### **Uncertainties and Validity of Models**

For the application of environmental models it is essential to treat uncertainties, with respect to the acquisition of data on the one hand and to the modeling process on the other hand (Brown, 2010; Keenan et al., 2011). Within the modeled area of the case study, the results are subject to different magnitudes of uncertainty, depending on the similarity of the elevation and slope exposition values to those of the investigation sites. Accordingly, the highest uncertainties of the model results are located at eastern and western expositions and in elevation ranges midway between the investigation sites (e.g., 1300 m a.s.l., between 1200 m and 1400 m). This kind of uncertainty corresponds with the level of accordance of the fuzzy membership functions with the actual relationships in the modeled ecosystem. Other sources of potential uncertainties of the results are deviations of the elevation values in the DTM from the real values, errors due to the calculation procedure of exposition values and inaccuracies due to the discrete representation of the landscape in the form of a raster (Bocedi et al., 2012; Fisher and Tate, 2006; Wechsler, 2007). In the context of topographical and hydrological analyses, small errors in a DTM can result in major deviations when deriving relief parameters (Holmes et al., 2000; Zhou and Liu, 2004).

The validity of the results from the case study is constrained to the modeled forested areas in the range from 1100 m to 1800 m a.s.l. An explicit validation procedure is essential when having the intention to apply concrete predictions on indicators of decomposition (e.g., in the context of ecosystem management). This validation procedure also needs to consider the effect of additional environmental covariates that might be relevant for decomposition processes at places inside the area selected for prediction showing varying site conditions compared to the sampling locations. When planning to transfer the modeled effects of elevation and slope exposition on decomposition to woodless areas or other regions that exhibit different environmental conditions, a particular assessment of the transferability of the model is required (Wenger and Olden, 2012).

### **CONCLUSIONS**

Two modeling approaches for upscaling of sample data on indicators of decomposition from the local scale to the landscape scale have been juxtaposed. This study focused on an area characterized by a highly heterogeneous relief and data from a relatively small number of samples, which have been surveyed in places specified with expert knowledge. Combining decision tree analysis and the use of fuzzy membership functions has shown to serve as a suitable approach. Building decision trees helped to generate information about the influences of the environmental factors elevation and slope exposition. However, direct upscaling of information about decomposition processes from the results of decision tree analysis yielded partially unrealistic predictions that were manifested in abrupt transitions between areas differentiated by the tree.

Continuous and more realistic transitions can be achieved by further processing the results from decision tree analysis through an additional step that comprises the construction of bell-shape fuzzy membership functions. For the parameter slope exposition a future improvement of the mapping could be to leave the functionalities of ArcSIE and use another function type (e.g., trigonometric function). As the modeling approach is based on fuzzy logic, it accounts for small-scale variations in decomposition processes as well as for uncertainties caused by the inference from a few investigation sites to a large study area. Spatial modeling utilizing the technique presented in this paper is considered to be a useful tool to obtain a detailed insight into decomposition processes in a high mountain environment. Implementing such a model should include a validation procedure and an analysis of uncertainty. Apart from the humus form, this approach could be used to examine a variety of other related parameters on a landscape scale, such as the pH value and the composition of the decomposer community.

## ACKNOWLEDGMENTS

This study was realized in the context of the D.A.CH. project DecAlp and funded by the German Research Foundation (DFG, grant number BR 1106/23-1). The authors thank all colleagues of the project for an excellent cooperation. We are in particular grateful to Dylan Tatti (University of Neuchâtel) for sharing his data on humus forms and to Giacomo Sartori (Museo Tridentino di Scienze Naturale) for valuable discussions in the field. We also thank the anonymous reviewers for valuable comments on an earlier version of the manuscript.

## REFERENCES CITED

- Aberegg, I., Egli, M., Sartori, G., and Purves, R., 2009: Modelling spatial distribution of soil types and characteristics in a high Alpine valley (Val di Sole, Trentino, Italy). *Studi Trentini di Scienze Naturali*, 85: 39–50.
- Ad-hoc-AG Boden, 2005: *Bodenkundliche Kartieranleitung*. Fifth edition. Hannover: E. Schweizerbart'sche Verlagsbuchhandlung, 438 pp.
- Ai, L., Fang, N. F., Zhang, B., and Shi, Z. H., 2013: Broad area mapping of monthly soil erosion risk using fuzzy decision tree approach: integration of multi-source data within GIS. *International Journal of Geographic Information Science*, 27: 1251–1267.
- Andreetta, A., Macci, C., Ceccherini, M. T., Cecchini, G., Masciandaro, G., Pietramellara, G., and Carnicelli, S., 2012: Microbial dynamics in Mediterranean Moder humus. *Biology and Fertility of Soils*, 48: 259–270.
- Ascher, J., Sartori, G., Graefe, U., Thornton, B., Ceccherini, M. T., Pietramellara, G., and Egli, M., 2012: Are humus forms, mesofauna and microflora in subalpine forest soils sensitive to thermal conditions? *Biology and Fertility of Soils*, 48: 709–725.
- Ashtekar, J. M., and Owens, P. R., 2013: Remembering knowledge: an expert knowledge based approach to digital soil mapping. *Soil Horizons*, 54: doi <http://dx.doi.org/10.2136/sh13-01-0007>.
- Bednorz, F., Reichstein, M., Broll, G., Holtmeier, F.-K., and Urfer, W., 2000: Humus forms in the forest-alpine tundra ecotone at Stillberg (Dischmatal, Switzerland): spatial heterogeneity and classification. *Arctic, Antarctic, and Alpine Research*, 32: 21–29.
- Behrens, T., and Scholten, T., 2006: Digital soil mapping in Germany—A review. *Journal of Plant Nutrition and Soil Science*, 169: 434–443.
- Behrens, T., and Scholten, T., 2007: A comparison of data-mining techniques in predictive soil mapping. In Lagacherie, P., McBratney, A. B., and Voltz, M. (eds.), *Digital Soil Mapping—An Introductory Perspective*.



- Developments in Soil Science*, v. 31. Amsterdam: Elsevier, 353–366.
- Bernier, N., 1996: Altitudinal changes in humus form dynamics in a spruce forest at the montane level. *Plant and Soil*, 178: 1–28.
- Bocedi, G., Pe'er, G., Heikkinen, R. K., Matsinos, Y., and Travis, J. M. J., 2012: Projecting species' range expansion dynamics: sources of systematic biases when scaling up patterns and processes. *Methods in Ecology Evolution*, 3: 1008–1018.
- Bouma, J., 1989: Using soil survey data for quantitative land evaluation. In Stewart, B. A. (ed.), *Advances in Soil Science*, v. 9. New York: Springer-Verlag, 177–213.
- Breiman, L., Friedman, J. H., Olshen, R. A., and Stone, C. J., 1984: *Classification and Regression Trees*. Belmont: Wadsworth, 358 pp.
- Brown, J. D., 2010: Prospects for the open treatment of uncertainty in environmental research. *Progress in Physical Geography*, 34: 75–100.
- Chiang, I.-J., and Hsu, J. Y., 2002: Fuzzy classification trees for data analysis. *Fuzzy Sets and Systems*, 130: 87–99.
- De'ath, G., and Fabricius, K. E., 2000: Classification and regression trees: a powerful yet simple technique for ecological data analysis. *Ecology*, 81: 3178–3192.
- de Gruijter, J. J., Walvoort, D. J. J., and Bragato, G., 2011: Application of fuzzy logic to Boolean models for digital soil assessment. *Geoderma*, 166: 15–33.
- de Menezes, M. D., Silva, S. H. G., Owens, P. R., and Curi, N., 2013: Digital soil mapping approach based on fuzzy logic and field expert knowledge. *Ciência e Agrotecnologia*, 37: 287–298.
- Egli, M., Mirabella, A., Sartori, G., Zanelli, R., and Bischof, S., 2006: Effect of north and south exposure on weathering rates and clay mineral formation in Alpine soils. *Catena*, 67: 155–174.
- Egli, M., Sartori, G., Mirabella, A., Favilli, F., Giaccai, D., and Delbos, E., 2009: Effect of north and south exposure on organic matter in high Alpine soils. *Geoderma*, 149: 124–136.
- Egli, M., Sartori, G., Mirabella, A., and Giaccai, D., 2010a: The effects of exposure and climate on the weathering of late Pleistocene and Holocene Alpine soils. *Geomorphology*, 114: 466–482.
- Egli, M., Sartori, G., Mirabella, A., Giaccai, D., Favilli, F., Scherrer, D., Krebs, R., and Delbos, E., 2010b: The influence of weathering and organic matter on heavy metals lability in silicatic, Alpine soils. *Science of the Total Environment*, 408: 931–946.
- Fisher, P. F., and Tate, N. J., 2006: Causes and consequences of error in digital elevation models. *Progress in Physical Geography*, 30: 467–489.
- Gerlitz, L., 2015: Using fuzzified regression trees for statistical downscaling and regionalization of near surface temperatures in complex terrain. *Theoretical and Applied Climatology*, 122: 337–352.
- Gobat, J.-M., Le Bayon, C., and Tatti, D., 2014: *Clé de Sol—Principaux sols de Suisse*. Neuchâtel: Laboratoire Sol & Végétation, Université de Neuchâtel, Switzerland, 76 pp.
- Graefe, U., and Beylich, A., 2006: Humus forms as tool for upscaling soil biodiversity data to landscape level? *Mitteilungen der Deutschen Bodenkundlichen Gesellschaft*, 108: 6–7.
- Heuvelink, G. B. M., and Webster, R., 2001: Modelling soil variation: past, present, and future. *Geoderma*, 100: 269–301.
- Holmes, K. W., Chadwick, O. A., and Kyriakidis, P. C., 2000: Error in a USGS 30-meter digital elevation model and its impact on terrain modeling. *Journal of Hydrology*, 233: 154–173.
- Horn, B. K. P., 1981: Hill shading and the reflectance map. *Proceedings of the IEEE*, 69: 14–47.
- Jenny, H., 1941: *Factors of Soil Formation—A System of Quantitative Pedology*. New York: McGraw-Hill, 281 pp.
- Keenan, T. F., Carbone, M. S., Reichstein, M., and Richardson, A. D., 2011: The model-data fusion pitfall: assuming certainty in an uncertain world. *Oecologia*, 167: 587–597.

- McBratney, A. B., and Odeh, I. O. A., 1997: Application of fuzzy sets in soil science: fuzzy logic, fuzzy measurements and fuzzy decisions. *Geoderma*, 77: 85–113.
- McBratney, A. B., Minasny, B., Cattle, S. R., and Vervoort, R. W., 2002: From pedotransfer functions to soil inference systems. *Geoderma*, 109: 41–73.
- McBratney, A. B., Mendonça Santos, M. L., and Minasny, B., 2003: On digital soil mapping. *Geoderma*, 117: 3–52.
- McKenzie, N. J., and Ryan, P. J., 1999: Spatial prediction of soil properties using environmental correlation. *Geoderma*, 89: 67–94.
- Mertens, M., Nestler, I., and Huwe, B., 2002: GIS-based regionalization of soil profiles with Classification and Regression Trees (CART). *Journal of Plant Nutrition and Soil Science*, 165: 39–43.
- Ponge, J.-F., 2013: Plant-soil feedbacks mediated by humus forms: a review. *Soil Biology & Biochemistry*, 57: 1048–1060.
- Qi, F., and Zhu, A.-X., 2011: Comparing three methods for modeling the uncertainty in knowledge discovery from area-class soil maps. *Computers & Geosciences*, 37: 1425–1436.
- R Core Team, 2015: R: A language and environment for statistical computing. Vienna, Austria: R Foundation for Statistical Computing, <<http://www.R-project.org/>>, accessed 27 October 2015.
- Ribeiro, M. V., Cunha, L. M. S., Camargo, H. A., and Rodrigues, L. H. A., 2014: Applying a fuzzy decision tree approach to soil classification. In Laurent, A., Strauss, O., Bouchon-Meunier, B., and Yager, R. R. (eds.), *Information Processing and Management of Uncertainty in Knowledge-Based Systems. Communications in Computer and Information Science*, v. 442. Cham: Springer-Verlag, 87–96.
- Sartori, G., and Mancabelli, A., 2009: *Carta dei suoli del Trentino: scala 1:250.000*. Museo Tridentino di Scienze Naturali di Trento, Centro di Ricerca per l'Agrobiologia e la Pedologia di Firenze.
- Shi, X., 2013: ArcSIE, <<http://www.arcsie.com/Download/htm>>, accessed 11 October 2016.
- Shi, X. Long, R., Dekett, R., and Philippe, J., 2009: Integrating different types of knowledge for digital soil mapping. *Soil Science Society of America Journal*, 73: 1682–1692.
- Suárez, A., and Lutsko, J. F., 1999: Globally optimal fuzzy decision trees for classification and regression. *IEEE Transactions on Pattern Analysis and Machine Intelligence*, 21: 1297–1311.
- Swift, M. J., Heal, O. W., and Anderson, J. M., 1979: *Decomposition in Terrestrial Ecosystems*. Berkeley, Los Angeles: University of California Press, *Studies in Ecology*, v. 5, 372 pp.
- Therneau, T. M., Atkinson, E. J., and Foundation, M., 2015: An Introduction to Recursive Partitioning Using the RPART Routines. <<http://cran.r-project.org/web/packages/rpart/vignettes/longintro.pdf>>, accessed 27 October 2015.
- Wechsler, S. P., 2007: Uncertainties associated with digital elevation models for hydrologic applications: a review. *Hydrology and Earth System Sciences*, 11: 1481–1500.
- Wenger, S. J., and Olden, J. D., 2012: Assessing transferability of ecological models: an underappreciated aspect of statistical validation. *Methods in Ecology and Evolution*, 3: 260–267.
- Wösten, J. H. M., Pachepsky, Y. A., and Rawls, W. J., 2001: Pedotransfer functions: bridging the gap between available basic soil data and missing soil hydraulic characteristics. *Journal of Hydrology*, 251: 123–150.
- Zadeh, L. A., 1965: Fuzzy sets. *Information and Control*, 8: 338–353.
- Zhou, Q., and Liu, X., 2004: Analysis of errors of derived slope and aspect related to DEM data properties. *Computers & Geosciences*, 30: 369–378.
- Zhu, A.-X., 1997: A similarity model for representing soil spatial information. *Geoderma*, 77: 217–242.
- Zhu, A.-X., 2006: Fuzzy logic models. In Grunwald, S. (ed.), *Environmental Soil-Landscape Modeling. Geographic Information*

*Technologies and Pedometrics*. New York: CRC Press, 215–239.

Zhu, A.-X., Band, L. E., Dutton, B., and Nimlos, T. J., 1996: Automated soil inference under fuzzy logic. *Ecological Modelling*, 90: 123–145.

Zhu, A. X., Hudson, B., Burt, J., Lubich, K., and Simonson, D., 2001: Soil mapping using GIS, expert knowledge, and fuzzy logic. *Soil Science Society of America Journal*, 65: 1463–1472.



## Chapter 3

Upscaling the spatial distribution of enchytraeids and humus forms in a high mountain environment on the basis of GIS and fuzzy logic



Supplementary materials can be found in Appendix 2 of this thesis.

**Citation:** Hellwig, N., Graefe, U., Tatti, D., Sartori, G., Anschlag, K., Beylich, A., Gobat, J.-M., Broll, G. (2017): Upscaling the spatial distribution of enchytraeids and humus forms in a high mountain environment on the basis of GIS and fuzzy logic. *European Journal of Soil Biology* **79**, 1-13.

**Author contributions:** N.H. performed data analysis, modeling, model assessment and wrote the paper; N.H., U.G., D.T., G.S. and K.A. performed sampling; U.G. and A.B. analyzed micro-annelids; D.T. performed laboratory analyses for the final determination of humus forms; G.B. and J.-M.G. conceived and designed the experiments.

### **Copyright**

2017 Elsevier Masson SAS

Reprinted with permission of the publisher

### **Photo credits (previous page):**

Niels Hellwig, 1 August 2014

Humus profile under branches at a north-facing slope near Rabbi Fonti (1620 m a.s.l., Val di Rabbi, Trentino, Italian Alps).

# Upscaling the spatial distribution of enchytraeids and humus forms in a high mountain environment on the basis of GIS and fuzzy logic

NIELS HELLWIG <sup>a,\*</sup>, ULFERT GRAEFE <sup>b</sup>, DYLAN TATTI <sup>c,d</sup>, GIACOMO SARTORI <sup>e</sup>, KERSTIN ANSCHLAG <sup>a</sup>, ANNEKE BEYLICH <sup>b</sup>, JEAN-MICHEL GOBAT <sup>c</sup>, GABRIELE BROLL <sup>a</sup>

<sup>a</sup> Institute of Geography, University of Osnabrück, Seminarstraße 19ab, 49074 Osnabrück, Germany

<sup>b</sup> IFAB Institut für Angewandte Bodenbiologie GmbH, Tornberg 24a, 22337 Hamburg, Germany

<sup>c</sup> Functional Ecology Laboratory, University of Neuchâtel, Rue Emile-Argand 11, 2000 Neuchâtel, Switzerland

<sup>d</sup> Division Agronomie, Haute école des Sciences Agronomiques, Forestières et Alimentaires HAFL, Länggasse 85, 3052 Zollikofen, Switzerland

<sup>e</sup> Museo Tridentino di Scienze Naturali, Corso del Lavoro e della Scienza 3, 38122 Trento, Italy

\*Corresponding author

## ABSTRACT

The aim of this study was to map the spatial distribution of enchytraeids and humus forms in a study area in the Italian Alps by means of a knowledge-based modeling approach. The modeled area is located around Val di Sole and Val di Rabbi (Trentino, Italy) and includes the forested parts in the range between 1100 m and 1800 m a.s.l. Elevation and slope exposure are considered as environmental covariates. Models were implemented regarding the spatial distribution of three variables at the landscape scale: 1) enchytraeids indicating mull humus forms, 2) enchytraeids indicating moder/mor humus forms, 3) humus forms showing an OH horizon. All three models reveal a consistent trend of an increasing accumulation of plant residues and humus in organic layers from low to high elevations and from south-facing to north-facing slopes. Validation and uncertainty analysis of input data confirm these trends, although some deviations are to be expected (RMSE values from validation sites range from 26.3 to 36.2% points). Effects of additional potentially influencing variables may lead to uncertainties of the model predictions especially at positions with particular landforms (e.g. gullies and ridges). In the high mountains environmental conditions are often quite heterogeneous due to a highly variable topography, which also affects the species composition of the decomposer community and the occurrence of different humus forms.

**Keywords:** Decomposition; Soil mesofauna; Decomposer community; Knowledge-based modeling; Forest ecosystem; Italian Alps

**Submitted:** 30 August 2016 – **Revised:** 21 December 2016 – **Accepted:** 4 January 2017

## 1. INTRODUCTION

Soil organisms are of high relevance for the function of terrestrial ecosystems, driven by their response to environmental conditions and by a variety of interactions among themselves and with aboveground organisms [1,2]. With reference to decomposition, soil organisms can be classified into decomposer community types, i.e. typical, environmentally controlled species assemblages of decomposer organisms [3,4].

Enchytraeids are usually colorless worms belonging to the soil mesofauna (length ca. 2–40 mm) and inhabiting the topsoil [5]. As key members of the decomposer community enchytraeids strongly interact with other species within the soil food web. Thus an externally induced shift in the decomposer community (e.g. land-use change, soil acidification, invasion of earthworms) also alters the composition of the enchytraeid assemblage [6,7]. Hence, the species composition of the enchytraeid assemblage serves as indicator for the state of the entire decomposition system in the topsoil. The characteristic decomposer community of a particular site can be inferred from analyzing the annelid coenosis [8].

Variations in the activity of decomposing soil organisms also reflect differences in the kind of dead organic matter accumulated in the topsoil. In forest ecosystems, humus forms are distinguished by the presence of different organic layers (OL = litter, OF = fragmented residues, OH = humified residues) and by the characteristics of the uppermost horizon of the mineral soil [9]. As the relationship between decay processes and main features of the organic layers is obvious, humus forms are considered as indicators for soil ecological activity linked with decomposition [10]. Owing to this indicator function, humus forms serve as a valuable site-specific feature for the

investigation of environmental changes in ecosystems.

As to the annelid coenosis, it has been shown from investigations in the German lowlands that the occurrence of enchytraeid species varies according to the humus form, with a threshold between mull and moder/mor humus forms [8]. Mull humus forms are characterized by a high activity of soil organisms incorporating dead organic matter into the mineral soil, whereas moder/mor humus forms are characterized by the accumulation of highly decomposed dead organic matter above the mineral soil in the form of an OH horizon.

The spatial distribution of soil organisms and humus forms gives information about variations of soil quality including carbon stocks [11–15] and conditions for plant growth [10,16,17]. Hence, mapping has potential for tracing effects of climate and land-use changes as well as for supporting forest management [18]. Spatial modeling of indicators of decomposition such as humus forms and soil organisms is currently lacking [19], especially in high mountain areas [20,21], although these areas are known to be particularly affected by environmental changes [22]. Therefore, the development of such maps is required specifically for high mountain regions.

With this study, we aim at mapping the spatial distribution of enchytraeids and forest humus forms depending on the elevation and slope exposure in a study area located in the Italian Alps. Correlations between the occurrence of humus forms and the associated enchytraeid species are supposed to be revealed by means of a GIS-based modeling approach. In order to assess the current state of an ecosystem, it is often necessary to analyze patterns of decomposition processes at a scale higher than the local plot level. The focus of this study is a mountainous, highly topo-



graphically heterogeneous area that is mostly inaccessible due to the terrain. In this situation, upscaling of local information to the landscape scale faces challenges due to a relatively low number of sampling points and a high local variability of environmental parameters. Therefore, a spatial modeling technique specially designed to consider these issues is needed. We utilize a knowledge-based approach applying decision trees and fuzzy logic. Landscape-scale patterns of humus forms and enchytraeid species are compared to evaluate whether the composition of the enchytraeid assemblage is represented by the humus forms in a high mountain environment.

## 2. MATERIAL AND METHODS

### 2.1. Study area

The study area is located in the northern Italian Alps in the northwestern part of the Autonomous Province of Trento. It covers about 500 km<sup>2</sup> and includes most parts of the catchment area of Val di Sole (Fig. 1). The climatic conditions in the study area are temperate continental to subcontinental [23]. Local climatic conditions vary mainly according to the topography. Different slope angles

and exposures cause high variations of solar radiation [24]. The entire study area embraces a siliceous parent material, dominated by paragneiss, mica schists, phyllites and orthogneiss [21]. Soil classes differ primarily with the elevation: below ca. 1900 m a.s.l. Haplic Cambisols (Dystric) and Umbric Podzols prevail, above ca. 1900 m a.s.l. the predominant classes are Entic Podzols, Albic Podzols and Umbric Podzols [25].

The focus of this study was on the forested mid-elevation areas (between 1100 and 1800 m a.s.l.), which cover the slopes on both sides of the valleys. Norway spruce (*Picea abies*) and European larch (*Larix decidua*) are the prevailing tree species constituting these forests.

### 2.2. Experimental design

On the basis of previous research [26] and with the help of experts with local knowledge, six study sites (N1, N2, N3, S6, S7 and S8, ca. 25 m<sup>2</sup> each) were selected. They were located at three different elevations (on north and south exposed slopes respectively) and represented typical site conditions within the investigated slope areas. The main characteristics of these study sites are summarized in Table 1. Although the dominant humus forms differed between the sites, we often found a mosaic-like pattern of humus forms. This was

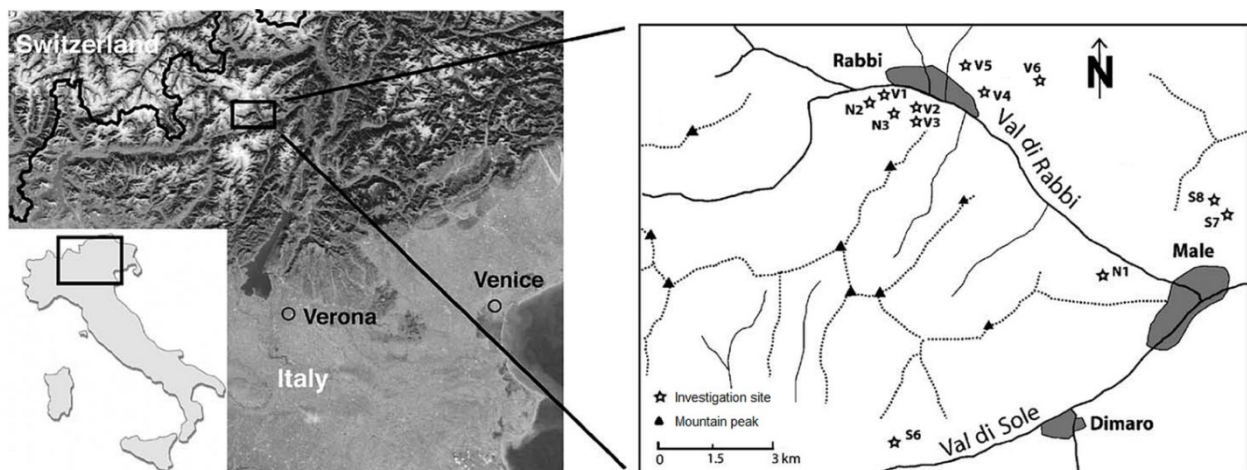


**Fig. 1.** Location of the study area in the Autonomous Province of Trento (Italy) (modified from Egli et al. [26]).

**Table 1**

Dominant humus forms and profiles at the investigation sites (N1-N3: northern slope exposure, S6-S8: southern slope exposure) (elevations according to Egli et al. [26]).

Site	Elevation (m a.s.l.)	Dominating humus form according to German classification [27]	Dominating humus form according to Swiss classification [28]	Typical humus profile
N1	1180	Mullartiger Moder	Hémimoder/Eumoder/Dysmoder/Dysmull	OL-OF-(OH-)AE
N2	1390	Typischer Moder	Dysmoder	OL-OF-OH-AE
N3	1620	Typischer Moder	Dysmoder	OL-OF-OH-E
S6	1185	Mullartiger Moder	Eumésamphi/Dysmull	OL-OF-(OH-)A
S7	1400	Mullartiger Moder	Hémimoder	OL-OF-(OH-)AE
S8	1660	Mullartiger Moder/ Typischer Moder	Hémimoder	OL-OF-(OH-)AE

manifested by the occurrence of humus forms with an OH horizon and a weak structure of the mineral soil (without biogenic features) right beside humus forms without OH horizon but with a well-structured A horizon inhabited by endogeic earthworms. The study sites were all located inside the coniferous forest. Norway spruce (*Picea abies*) prevailed at the north-exposed sites, whereas European larch (*Larix decidua*) was dominant at the south-exposed sites. In order to solidly detect the effects of elevation, we performed an intensive sampling at the lowest and highest study sites including six plots each (N1, N3, S6, S8). At the mid-elevation sites N2 and S7 three plots were sampled, respectively. Samples for this study were taken between June and August 2013.

At each plot ( $n = 30$  in total) humus forms were described in the field at topsoil profiles with a width of 50–100 cm using classifications and determination keys from Germany [27] and Switzerland [28]. Soil samples for the extraction of enchytraeids were acquired in the immediate vicinity of the profiles using a soil corer of 5 cm in diameter. Samples were

taken from the uppermost 15 cm of the soil starting at the top of the organic layer. As one of the samples at study site S6 could not be analyzed, a total of 29 plots remained.

Six additional validation sites V1-V6 were sampled with a reduced number of plots (three validation sites at different elevations on a north- and south-exposed slope, respectively). Samples for validation were taken in September 2015.

All samples for the investigation of enchytraeids were transported to the IFAB laboratory, where enchytraeids were extracted. The enchytraeid species were identified according to Schmelz and Collado [29]. Annelids from other families than Enchytraeidae but belonging to the same size class were recovered with the extraction as well. Thus we use the term ‘microannelids’ when we refer to all species determined. Species counting and determination were conducted at IFAB laboratory using dissecting and light microscopes. Additional laboratory analyzes for the final determination of humus forms were conducted at Functional ecology laboratory (University of Neuchâtel).

### 2.3. Data analysis

Because of the relatively low number of study sites, simplified representations of both the composition of the enchytraeid community and of humus forms were necessary. To evaluate the co-occurrence of enchytraeid species with different humus forms, the life form (H-type) of enchytraeids and other microannelids was applied. The concept of life form types indicates the typical habitat of species in the sequence of humus forms (represented by the four classes Mull, Mullmoder, Moder and Mor) together with their vertical distribution in the humus horizons [30]. The life forms of three species are presented as examples in Fig. 2. For the purpose of modeling, enchytraeid species were categorized as mull indicators or moder indicators based on expert knowledge. Species known to occur in mull but not in moder/moder were classified as mull indicators (e.g. *Fridericia bulboides*); species known to occur in moder/moder but not in mull were classified as moder indicators (e.g. *Cognettia sphagnetorum*); and species known to occur primarily in the intermediate humus form mullmoder or both in mull and moder were disregarded (e.g. *Enchytronia parva*), since they explicitly indicate neither mull nor moder/moder conditions. Table 2 specifies the enchytraeid species considered for modeling together with their mull and moder affinities. As one of the determining factors for humus forms and main criterion for the discrimina-

tion of mull-like and moder/moder-like humus forms, the occurrence of an OH horizon was used for modeling. Percentage values of humus forms showing an OH horizon were attributed to every plot. We applied a percentage of 100% to plots with a continuous OH horizon, a percentage of 50% to plots with a discontinuous OH horizon and a percentage of 0% to plots without OH horizon.

For modeling sample data on enchytraeids and humus forms were aggregated from all sampling plots per investigation site. This aggregation was accomplished by weighting the plot data according to the prevalence of the respective soil cover types at the investigation site (Table S1).

As variables influencing humus forms, the topographical parameters elevation and slope exposure were examined. Elevation values were transferred from a digital elevation model with a grid width of 10 m [21] (provided by Museo Tridentino di Scienze Naturali). Data on slope exposure were derived from the digital elevation model with the help of the aspect tool in ArcGIS [31].

### 2.4. Modeling

A methodological framework specifically designed to spatially predict indicators for decomposition processes was applied [20].

Modeling was based on binary decision trees built with the CART algorithm [32] using the statistical software R [33] and the R package

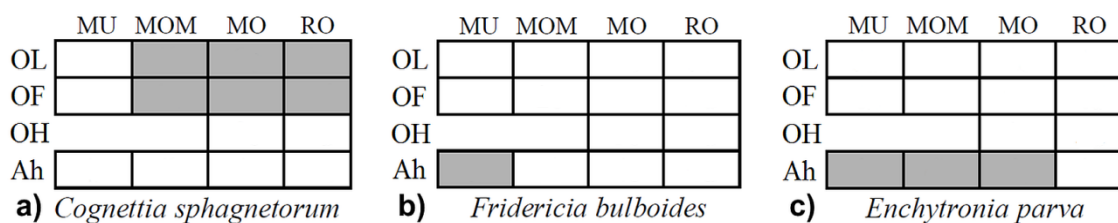


**Fig. 2.** Life forms (H-type) of three selected enchytraeid species (modified from Graefe and Schmelz [30]). Humus forms are indicated as follows: MU = Mull, MOM = Mullmoder, MO = Moder, RO = Mor ("Rohhumus"). The cells representing the typical habitat of the species are colored in grey. For modeling, species were characterized as a) mull indicators (life form including MU), b) moder indicators (life form including MO or RO), c) no indicators (life form including MU and MO).

rpart [34]. From these trees, bell-shaped or S-/Z-shaped fuzzy membership functions were derived referring to the concept of fuzzy logic [35–37]. Fuzzy logic was used because it enables elements to show a partial member-

ship of a set (in contrast to Boolean logic). Hence, complex relationships between the landscape and soil can be modeled in a continuous way. Many important soil properties are usually expressed as classified variables (e.g. soil types, humus forms, presence of an OH horizon). When using fuzzy logic an allocation of sharp boundaries between different soil properties, whose spatial positions are quite uncertain, is not required [38].

Prior to the construction of decision trees, values of elevation and slope exposure were aggregated from all sampling plots per investigation site. The exposure value 0° N was assigned to the sites at north-exposed slopes, the value 180° N was assigned to the sites at south-exposed slopes. For the three different elevation ranges the values 1200 m, 1400 m and 1630 m a.s.l. were used. These aggregations were necessary for avoiding unrealistic tree splits when the combined effects of elevation and slope exposure were analyzed.

The fuzzy membership functions described the distribution of enchytraeid indicator classes and the occurrence of humus forms showing an OH horizon in dependence on the elevation and the slope exposure, respectively. The parametrization of the functions utilized a multi-step procedure to incorporate the effects of both explanatory variables [20]: 1) construction of membership functions depending on the variable with lower explanatory power, 2) construction of weighting functions depending on the variable with higher explanatory power, 3) combination of the effects of both variables by applying the weighting functions from step 2 to the membership functions from step 1. Prediction maps were compiled with the ArcGIS extension tool ArcSIE [39].

The areas for modeling included all coniferous forests inside the study area, which are located between 1100 m and 1800 m a.s.l. (corresponding to the valley sides of Val di

**Table 2**

Microannelid species found in the samples and their classification as indicators of mull or moder humus forms in the model.

Species	Indicator class
<b>Enchytraeidae</b>	
<i>Achaeta danica</i> Nielsen & Christensen, 1959	Moder
<i>Achaeta</i> sp. (dzwi) <sup>a</sup>	Mull
<i>Bryodrilus ehlersi</i> Ude, 1892	Moder
<i>Buchholzia appendiculata</i> (Buchholz, 1862)	Mull
<i>Buchholzia simplex</i> Nielsen & Christensen, 1963	Mull
<i>Cognettia sphagnetorum</i> (Vejdovský, 1878)	Moder
<i>Enchytraeus buchholzi</i> Vejdovský, 1879	Mull
<i>Enchytraeus norvegicus</i> Abrahamsen, 1969	–
<i>Enchytronia christenseni</i> Dózsa-Farkas, 1970	Mull
<i>Enchytronia parva</i> Nielsen & Christensen, 1959	–
<i>Enchytronia</i> sp. (holo) <sup>a</sup>	Mull
<i>Euenchytraeus bisetosus</i> Bretscher, 1906	Moder
<i>Fridericia auritoides</i> Schmelz, 2003	Mull
<i>Fridericia benti</i> Schmelz, 2002	Mull
<i>Fridericia bisetosa</i> (Levinsen, 1884)	Mull
<i>Fridericia bulboides</i> Nielsen & Christensen, 1959	Mull
<i>Fridericia christeri</i> Rota & Healy, 1999	Mull
<i>Fridericia connata</i> Bretscher, 1902	Mull
<i>Fridericia miraflores</i> Sesma & Dózsa-Farkas, 1993	Mull
<i>Fridericia paroniana</i> Issel, 1904	Mull
<i>Fridericia ratzeli</i> (Eisen, 1872)	Mull
<i>Fridericia stephensoni</i> Moszyński, 1933	Mull
<i>Fridericia waldenstroemi</i> Rota & Healy, 1999	Mull
<i>Fridericia</i> sp. juv.	Mull
<i>Hemifridericia parva</i> Nielsen & Christensen, 1959	Mull
<i>Henlea nasuta</i> (Eisen, 1878)	Mull
<i>Henlea perpusilla</i> Friend, 1911	Mull
<i>Marionina clavata</i> Nielsen & Christensen, 1961	Moder
<i>Mesenchytraeus glandulosus</i> (Levinsen, 1884)	–
<i>Mesenchytraeus pelicensis</i> Issel, 1905	Moder
<b>Polychaeta</b>	
<i>Hrabeiella periglandulata</i> Pizl & Chalupský, 1984	–

<sup>a</sup> Species not yet formally described.

Sole, Val di Rabbi and adjacent valleys) and on siliceous bedrock.

## 2.5. Model assessment

The models of the spatial distribution of enchytraeid indicator classes and the occurrence of humus forms showing an OH horizon are compared by calculating a similarity index (1). At every location  $(x,y)$ ,  $d_{x,y}$  is the difference of the percentage of moder indicators and the percentage of mull indicators, normalized to the interval  $[0,1]$ , and  $h_{x,y}$  is the percentage of humus forms showing an OH horizon (also represented in the interval  $[0,1]$ ).

$$SI_{x,y} = \frac{d_{x,y}h_{x,y}}{d_{x,y}^2 + h_{x,y}^2 - d_{x,y}h_{x,y}} \quad (1)$$

In case of similar values  $d_{x,y}$  and  $h_{x,y}$  the index displays high values up to 1. If both values are dissimilar, the index shows low values down to 0.

The assessment of the model performance was accomplished in terms of different subjects: 1) the goodness of fit of the model; 2) the validity of the model structure (using a resampling approach) and of the prediction results (analyzing independent validation sites); 3) the uncertainty of the input data from the study sites; 4) the uncertainty of the model predictions regarding the applicability of the model for varying landform types.

The goodness of fit of the model and the prediction results at the validation sites were evaluated by calculating the mean error (ME) (2) and the root mean squared error (RMSE) (3) where  $n$  is the number of samples,  $y_i$  are the observed values and  $\hat{y}_i$  are the related values predicted by the model:

$$ME = \frac{1}{n} \sum_{i=1}^n |y_i - \hat{y}_i| \quad (2)$$

$$RMSE = \sqrt{\frac{1}{n} \sum_{i=1}^n (y_i - \hat{y}_i)^2} \quad (3)$$

Resampling was used to test the validity of the internal model structure. For each modeled variable (OH horizon, Mull indicators, Moder indicators) 27 models were built on the basis of a reduced number of sample plots per study site (2/3 of the original samples at every site) (Table S2).

Input data from the study sites are subject to uncertainties, as the ecology of the humus layers generally shows a high small-scale variability. Therefore, the effects of modified input site data sets on the model structure and results were studied using exemplary deviations of 20% points from the observed values. For all of the modeled variables (OH horizon, Mull indicators, Moder indicators) the observed percentage values were both diminished (simulating an overestimation in the model) and increased (simulating an underestimation in the model) by 20% points at each plot (as far as possible, up to 0% or 100%). The value of 20% points was chosen based on the magnitude of deviations of the observed values at the validation sites as compared to the corresponding study sites (Table 3, Table 4).

With reference to the predicted values, uncertainties are also caused as landform types different from those at the study sites might show deviations of soil ecological parameters from the modeled trends along gradients of elevation and slope exposure. In order to identify the relevant areas, two prominent topographic factors were examined: the LS factor (describing conditions for erosion by means of the slope length and steepness) and the Topographic Wetness Index (TWI) [40,41]. At the study sites both parameters attain intermediate values (the LS factor ranges between 9 and 13, the TWI ranges between 4 and 6.5). A measure of uncertainty was calculated by comparing the LS and TWI values of each position in the study area to those at the study sites: if the parameter values were

**Table 3**

Data basis for modeling. Percentages of microannelid indicator classes and humus forms with an OH horizon have been aggregated from all sampling plots per investigation site. See Table S1 for data of sampling plots, Table S3 and Table S4 for raw data of microannelid species and humus profiles.

Site	Number of sampling plots	Percentage of mull indicators to all microannelid individuals (%)	Percentage of moder indicators to all microannelid individuals (%)	Percentage of humus forms showing an OH horizon (%)
N1	6	15.07	44.93	18.33
N2	3	5.17	90.73	66.67
N3	6	20.53	73.55	90.00
S6	6 <sup>a</sup>	95.06	0.00	6.67
S7	3	62.12	5.31	50.00
S8	6	63.39	8.06	46.67

<sup>a</sup> At study site S6, the investigation of the enchytraeid indicator classes comprised only five samples.

similar to those at the study sites, a low uncertainty was attributed to the predictions (in this situation an uncertainty value close to 0 applies); if the parameter values deviated from those at the study sites, the uncertainty increased up to a maximum of 1. We indexed the uncertainty in proportion to the deviation of the parameter values from those at the study sites, applying Gaussian-shaped curves according to the uncertainty setting of Zhu et al. [42].

### 3. RESULTS

#### 3.1. Data analysis

At the south-exposed study sites we found high percentages of mull-indicating enchytraeids, whereas percentages of both moder-indicating enchytraeids and of forest humus forms showing an OH horizon are low (Table 3, Table S1). The highest percentage of mull indicators (ca. 95.1%) was found at the study site S6, located at low elevation. This coincides with the absence of moder indicators and with the low occurrence of humus forms with OH horizon (ca. 6.7%). Comparing the study sites S7 and S8 (at middle and high

elevations) with study site S6 (at low elevation), we found a lower percentage of mull indicators (ca. 62.1% and 63.4%) along with higher percentages of moder indicators (ca. 5.3% and 8.1%) and humus forms showing an OH horizon (ca. 50.0% and 46.7%).

The north-exposed study sites show generally lower percentages of mull indicators and higher percentages of both moder indicators and forest humus forms with OH horizon than the south-exposed sites (Table 3, Table S1). The highest percentage of moder indicators was found at the study site N2 (ca. 90.7%), whereas the highest percentage of humus forms with OH horizon occurs at site N3 (ca. 90.0%). The results at station N1 appear ambiguous: a relatively high percentage of moder indicators (ca. 44.9%) coincides with a relatively low percentage of humus forms with OH horizon (ca. 18.3%).

#### 3.2. Spatial modeling of enchytraeids

Decision trees revealing variations in the distribution of mull- and moder-indicating enchytraeids related to elevation and slope exposure have been accomplished by recursive partitioning of the sample set. They

**Table 4**

Validation sites: topographic position and percentage values (observed and predicted) of modeled parameters.

Site	Elevation (m a.s.l.)	Slope exposure	Observed value (%)	Predicted value (%)	Deviation (% points)
<i>OH horizon</i> (ME = 22.1% points, RMSE = 26.3% points)					
V1	1270	north	50.0	31.5	18.5
V2	1480	north	50.0	73.6	- 23.6
V3	1650	north	50.0	74.5	- 24.4
V4	1240	south	0.0	14.9	- 14.9
V5	1420	south	0.0	49.3	- 49.3
V6	1730	south	50.0	48.3	1.7
<i>Mull indicators</i> (ME = 26.1% points, RMSE = 36.2% points)					
V1	1270	north	90.2	9.9	80.3
V2	1480	north	0.0	14.5	- 14.5
V3	1650	north	0.0	21.4	- 21.4
V4	1240	south	88.3	76.2	12.1
V5	1420	south	87.5	63.6	23.9
V6	1730	south	60.9	56.6	4.3
<i>Moder indicators</i> (ME = 23.4% points, RMSE = 30.1% points)					
V1	1270	north	6.3	67.4	- 61.1
V2	1480	north	93.1	78.1	15.0
V3	1650	north	99.0	84.1	14.9
V4	1240	south	0.0	7.2	- 7.2
V5	1420	south	0.0	8.5	- 8.5
V6	1730	south	38.0	4.5	33.5

reflect the observations at the study sites as described above with the slope exposure being the more decisive factor for the spatial distribution of enchytraeids (first-level split in decision trees) in comparison with the elevation (second-level split in decision trees) (Fig. 3, Fig. 4).

Fuzzy membership functions are derived by deploying the results from these trees and fuzzifying them along the elevation gradient to two submodels for contrasting slope exposures (corresponding to the left and right subtrees in Figs. 3 and 4). The occurrence of mull indicators on south-exposed slopes is modeled with a Z-shape function, as it decreases with increasing elevation. The parametrization is realized by fitting the general function

rule based on the decision tree using the values 0.9506 at 1200 m (occurrence at site S6), 0.7352 at 1300 m (overall occurrence taken as approximation at the split value) and 0.6276 at 1515 m (mean occurrence at sites S7 and S8). Below 1200 m the function is fixed at the value 0.9506 because this was the maximum percentage of mull indicators found at south-exposed slopes and there were no investigation sites located further downhill. This leads to function (4) for south-exposed slopes. For north-exposed slopes an S-shape function is derived from the decision tree analogously, resulting in function (5). The fuzzy membership  $s_{ij,k,a}$  of a modeled variable  $k$  depends on the value  $z_{ij,a}$  of a single environmental variable  $a$  at location  $(i,j)$ .

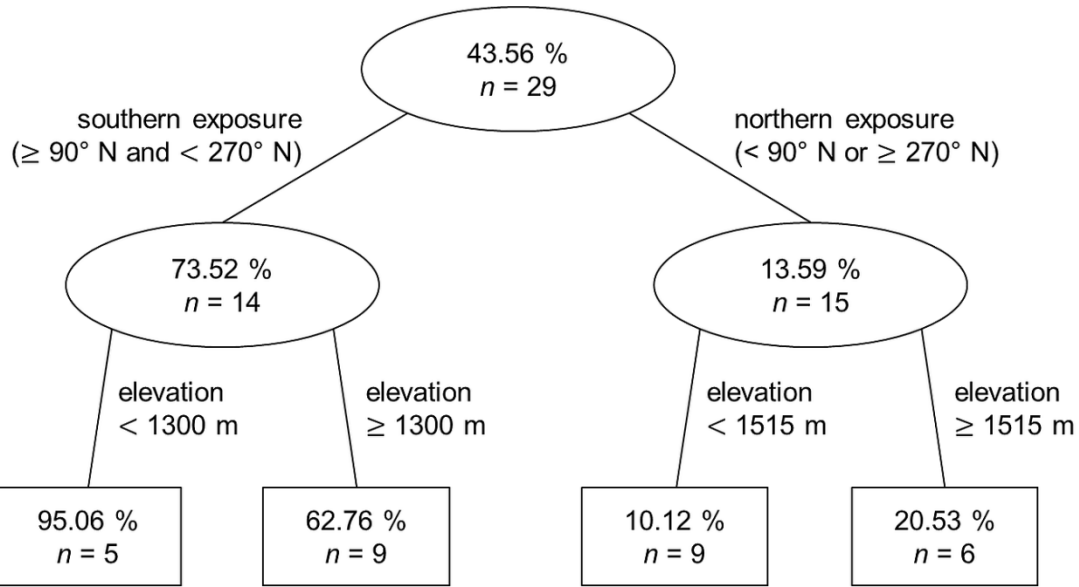


**Fig. 3.** Decision tree for the distribution model of enchytraeids indicating mull humus forms. The upper value inside the tree nodes represents the projected percentage of mull indicators in relation to all enchytraeids at this elevation and slope exposure, the lower value  $n$  indicates the number of related samples.

The occurrence of moder indicators is modeled with the function (6) for north-exposed slopes (derived in the same way as functions (4) and (5)). As in the decision tree there is no further split for south-exposed slopes (Fig. 4), a constant function is applied for these slopes ( $s_{ij,k,a} = 0.04457$ ).

Integrating the models for south- and north-

exposed sites is realized both for mull and moder indicators utilizing weighting functions depending on the local slope exposure  $x$ . The model for northern slope exposures is weighted with  $0.5 * \cos\left(x * \frac{\pi}{180}\right) + 0.5$ , the model for southern slope exposures with  $-0.5 * \cos\left(x * \frac{\pi}{180}\right) + 0.5$ . Cosine functions are utilized in order to reflect the similarity of the

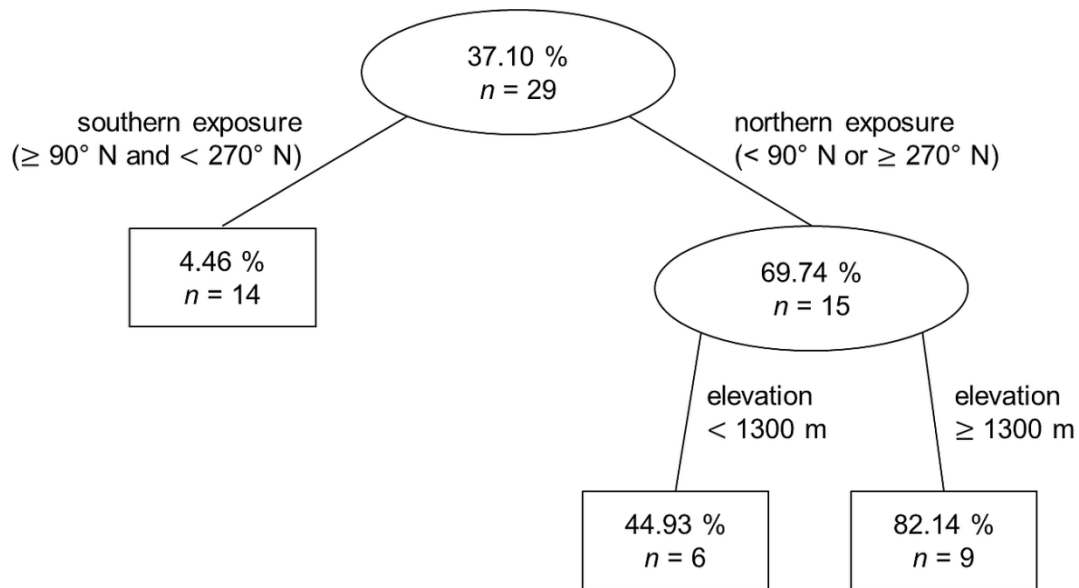


**Fig. 4.** Decision tree for the distribution model of enchytraeids indicating moder humus forms. The upper value inside the tree nodes represents the projected percentage of moder indicators in relation to all enchytraeids at this elevation and slope exposure, the lower value  $n$  indicates the number of related samples.



$$\begin{cases} s_{ij,k,a} = 0.9506 & \text{if } z_{ij,a} \leq 1200, \\ s_{ij,k,a} = 0.9506 * \exp\left(\left[\frac{(z_{ij,a} - 1200)}{1072.83}\right]^{0.418208} \ln(0.5)\right) & \text{if } z_{ij,a} > 1200 \end{cases} \quad (4)$$

$$\begin{cases} s_{ij,k,a} = 0.2053 * \exp\left(\left[\frac{(z_{ij,a} - 1630)}{317.15}\right]^{0.511492} \ln(0.5)\right) & \text{if } z_{ij,a} \leq 1630, \\ s_{ij,k,a} = 0.2053 & \text{if } z_{ij,a} > 1630 \end{cases} \quad (5)$$

$$\begin{cases} s_{ij,k,a} = 0.4493 & \text{if } z_{ij,a} \leq 1200, \\ s_{ij,k,a} = 1 - 0.5507 * \exp\left(\left[\frac{(z_{ij,a} - 1200)}{130.458}\right]^{0.550436} \ln(0.5)\right) & \text{if } z_{ij,a} > 1200 \end{cases} \quad (6)$$

slope exposure  $x$  in comparison with south and north exposure with regard to sunlight. The model results deliver predictions of the spatial distributions of mull and moder indicators in the study area. An evaluation of the predicted percentage values as emergent

areas of dominance of mull- and moder-indicating enchytraeids exhibits again a major relationship to the slope exposure and a minor relationship to the elevation, which is more pronounced at southern exposures (Fig. 5).

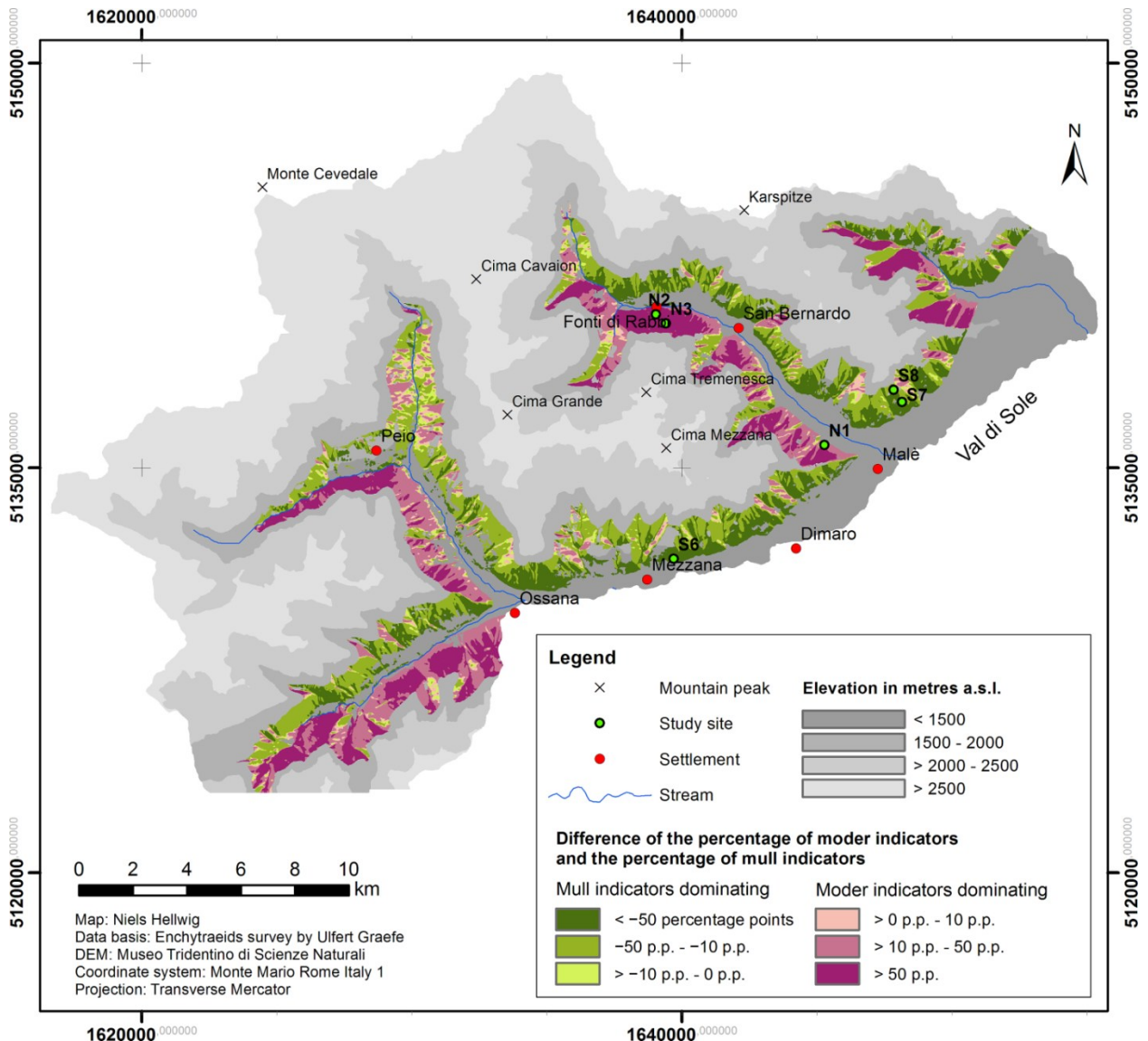


Fig. 5. Prediction of the areas of dominance of mull- and moder-indicating enchytraeids.

### 3.3. Spatial modeling of humus forms

Decision tree analysis and an ensuing fuzzification procedure examining the dependence of the distribution of forest humus forms showing an OH horizon on the factors elevation and slope exposure have been carried out similarly to those for enchytraeids. Unlike in the model of enchytraeids, elevation rather than slope exposure appears as the superior factor accounting for changes in the presence of an OH horizon (first-level split in the related decision tree) (Fig. 6).

The transformation to fuzzy membership functions (fuzzification along the slope exposure from 0° to 360° with reference to north exposure) yields the constant function  $s_{ij,k,a} = 0.125$  for elevations below 1300 m a.s.l. and the bell-shape-function (7) for elevations above 1300 m a.s.l.

For assembly of the submodels for these two elevation ranges, they are weighted depend-

ing on the local elevation value  $y$  for elevations between 1200 m and 1400 m a.s.l. (due to a lack of data at these elevations). The model for elevations below 1300 m a.s.l. is weighted with  $\exp(|(y - 1200) / 100|^3 \ln(0.5))$ , whereas the model for elevations above 1300 m a.s.l. is weighted with  $\exp(|(y - 1400) / 100|^3 \ln(0.5))$ .

A prediction map that depicts the spatial distribution of forest humus forms showing an OH horizon is obtained from the total model (Fig. 7). Corresponding with the domain of the fuzzy membership functions, the predicted percentage values range between 12.5% and 78.3%. The lowest values are to be found at low elevations. At high elevations (above 1300 m a.s.l.) the percentages of forest humus forms with OH horizon depend on the slope exposure: intermediate percentages around 50% are predicted at slopes with southern exposures, high percentages up to 78.3% arise at slopes with northern exposures.

$$s_{ij,k,a} = 1 - 0.5166 * \exp\left(\left[\frac{(z_{ij,a} - 180)}{161}\right]^2 \ln(0.5)\right) \quad (7)$$

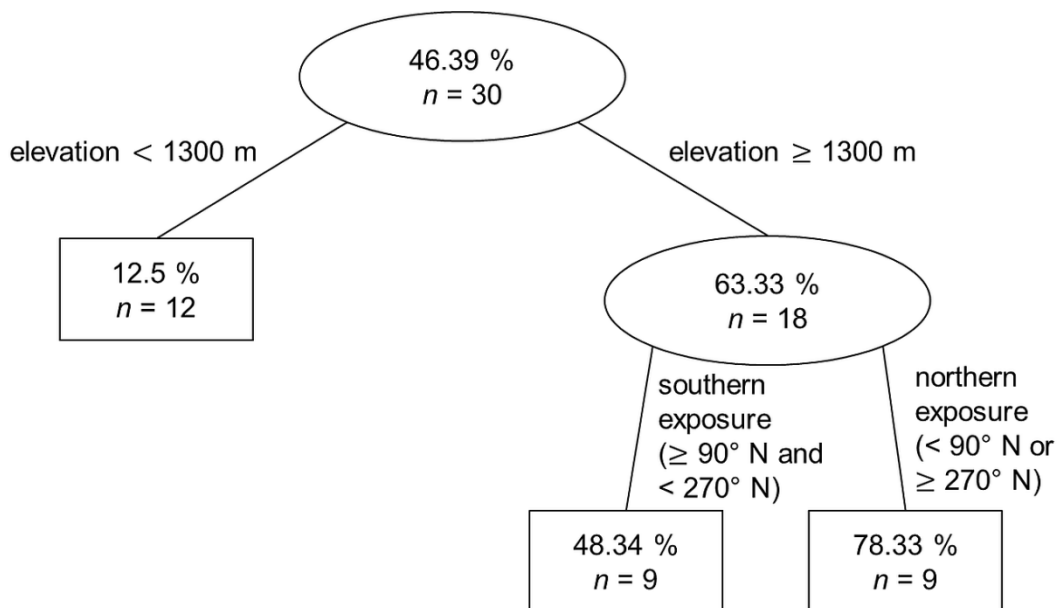


**Fig. 6.** Decision tree for the distribution of forest humus forms showing an OH horizon. The upper value inside the tree nodes represents the projected percentage of humus forms with OH horizon in relation to all humus forms at this elevation and slope exposure, the lower value  $n$  indicates the number of related samples.

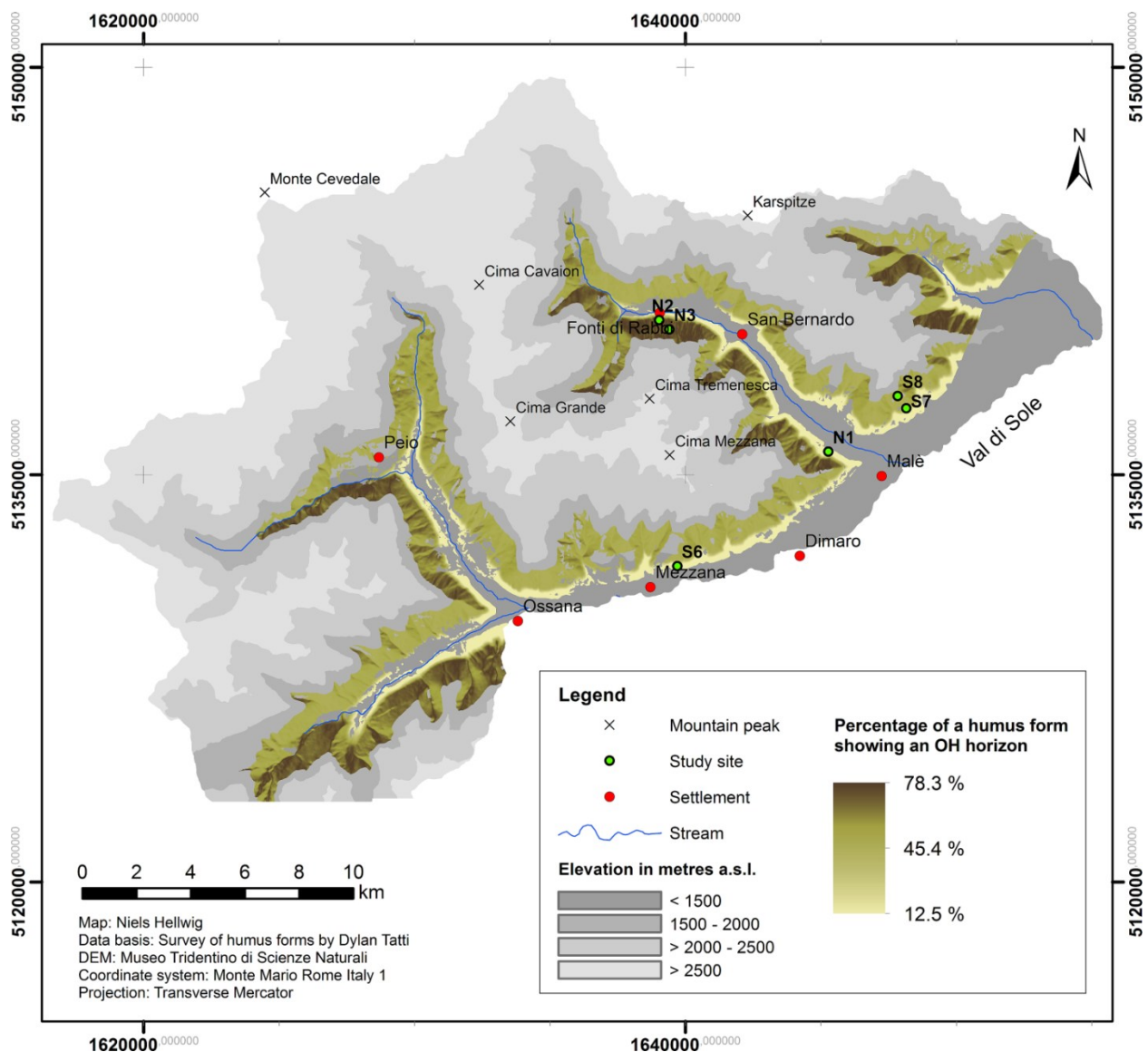


Fig. 7. Prediction of the spatial distribution of forest humus forms showing an OH horizon.

### 3.4. Model assessment

The comparison of the models of the spatial distribution of enchytraeid indicator classes and the occurrence of humus forms with an OH horizon revealed a high similarity in most parts of the study area. The distribution of enchytraeid species and the occurrence of OH horizons coincide generally better at north-facing than at south-facing slopes, with the exception of sites at low elevations where the overall lowest similarity values are found at north-facing slopes (Fig. S1).

The model shows a good fit to the observations: The RMSE values are 7.0% points both

for the model of humus forms with an OH horizon and for the model of mull-indicating enchytraeids. For moder-indicating enchytraeids the RMSE value is 8.0% points. The model residuals at the study sites are between 0 and 12.3% points for all three models. They are neither correlated among each other nor spatially autocorrelated.

Validation of the model structure shows a generally consistent model behavior when using different resampled data sets. This is reflected by a relatively low variability of the model results. Resampling shows RMSE values up to 11.34% points for mull-indicating enchytraeids. The highest variability occurs at

high elevations and south-exposed slopes (Fig. S2). For moder-indicating enchytraeids the maximum RMSE value is 16.46% points, which is found at low elevations on north-exposed slopes (Fig. S3). The resampled model results for humus forms with an OH horizon show RMSE values up to 19.39% points. They are highest at high elevations on south-exposed slopes and at middle elevations on north-exposed slopes (Fig. S4).

The assessment of the model results generally shows deviations of the predicted values from the observed values at the validation sites in the range of 5–25% points (Table 4). We found high deviations especially in the model addressing the distribution of humus forms with an OH horizon (up to 49.3% points at site V5) but also in the models of enchytraeids (especially at site V1: 80.3% points for mull indicators and 61.1% points for moder indicators). Because of the highest deviation at site V1 and the relatively high deviation at site V5 the RMSE is highest in the model of mull indicators (36.2% points). In the model of moder indicators the RMSE equals 30.1% points, whereas in the model of humus forms with an OH horizon it amounts to 26.3% points.

The results from uncertainty analysis of input data reveal a consistency regarding the structures of the decision trees for the majority of modifications of the data (Table 5). However, in some cases the structure of a tree changes, i.e. node splits are added, eliminated or modified (new splitting criteria). The absolute mean deviations in the predicted values range between 0.20 and 10.38% points, the absolute maximum deviation amounts to 29.99% points (when increasing the percentage of humus forms with an OH horizon by 20% points at station S8).

The uncertainties of the model predictions when considering landform types different from those at the study sites are derived

**Table 5**

Results of uncertainty analysis of input data. Values represent the deviations of the predicted values in percentage points as compared to the unmodified models. Underlined values indicate an alteration in the structure of the underlying decision tree (Figs. 3, 4, 6).

	Modified site					
	N1	N2	N3	S6	S7	S8
<i>OH horizon</i>						
Increase by 20% points						
Mean	1.59	4.23	1.96	1.59	5.26	<u>10.38</u>
SD	3.33	3.75	1.80	3.33	3.57	<u>12.48</u>
Maximum	10.00	10.11	5.03	10.00	10.00	<u>29.99</u>
Minimum	0.00	0.00	0.00	0.00	0.00	<u>-19.92</u>
Decrease by 20% points						
Mean	-1.46	<u>1.98</u>	-3.32	-0.53	-5.13	-5.13
SD	3.05	<u>11.56</u>	3.26	1.11	3.58	3.58
Maximum	0.00	<u>20.00</u>	0.00	0.00	0.00	0.00
Minimum	-9.17	<u>-29.92</u>	-9.91	-3.34	-10.01	-10.01
<i>Mull indicators</i>						
Increase by 20% points						
Mean	<u>-0.20</u>	<u>2.27</u>	4.46	0.24	<u>5.33</u>	<u>4.29</u>
SD	<u>6.23</u>	<u>3.16</u>	6.00	1.07	<u>6.83</u>	<u>4.72</u>
Maximum	<u>26.73</u>	<u>11.92</u>	20.00	4.94	<u>18.47</u>	<u>12.13</u>
Minimum	<u>-11.96</u>	<u>-0.27</u>	-2.24	-1.05	<u>-6.94</u>	<u>-6.94</u>
Decrease by 20% points						
Mean	-1.65	-0.58	<u>-5.00</u>	-0.94	-4.98	-4.98
SD	2.30	0.79	<u>5.89</u>	4.35	3.81	3.81
Maximum	0.40	0.03	<u>6.73</u>	4.52	0.01	0.01
Minimum	-7.59	-2.82	<u>-19.36</u>	-20.00	-11.90	-11.90
<i>Moder indicators</i>						
Increase by 20% points						
Mean	0.87	1.77	3.70	<u>1.93</u>	<u>5.99</u>	<u>5.87</u>
SD	3.61	1.60	3.35	<u>3.10</u>	<u>5.22</u>	<u>8.01</u>
Maximum	20.00	4.69	10.00	<u>15.54</u>	<u>16.35</u>	<u>23.60</u>
Minimum	-3.06	-0.28	-1.04	<u>-0.24</u>	<u>-4.46</u>	<u>-3.68</u>
Decrease by 20% points						
Mean	-0.98	-3.98	-3.98	- <sup>a</sup>	-0.97	-1.48
SD	3.57	3.58	3.58	- <sup>a</sup>	0.63	0.96
Maximum	2.17	0.15	0.15	- <sup>a</sup>	0.00	0.00
Minimum	-20.01	-10.90	-10.90	- <sup>a</sup>	-1.77	-2.69

<sup>a</sup> No moder indicators were found at study site S6.

from the values of the LS factor and the TWI. As the study sites, providing the data basis for modeling, are located on quite smooth slopes, the highest uncertainties appear at positions in gullies or on ridges. These topographical structures are clearly recognizable in the map illustrating the uncertainties of the model results (Fig. 8).

## 4. DISCUSSION

### 4.1. Spatial distribution of enchytraeids and humus forms

Processes of organic matter decomposition are influenced by the activity of decomposer

organisms [2,43,44]. Decomposition processes in turn affect the state of the topsoil; thus decomposition and the topsoil in its role as habitat of the decomposer organisms are interdependent. The state of the topsoil itself depends on the basic soil-forming factors climate, organisms, topography, parent material and time [45]. In our study area topography and vegetation are most important, as climatic differences are principally mediated by the topography and the parent material is relatively homogeneous (section 2.1). The factor time is of minor relevance for decomposition processes because decomposer organisms adapt relatively fast to environmental

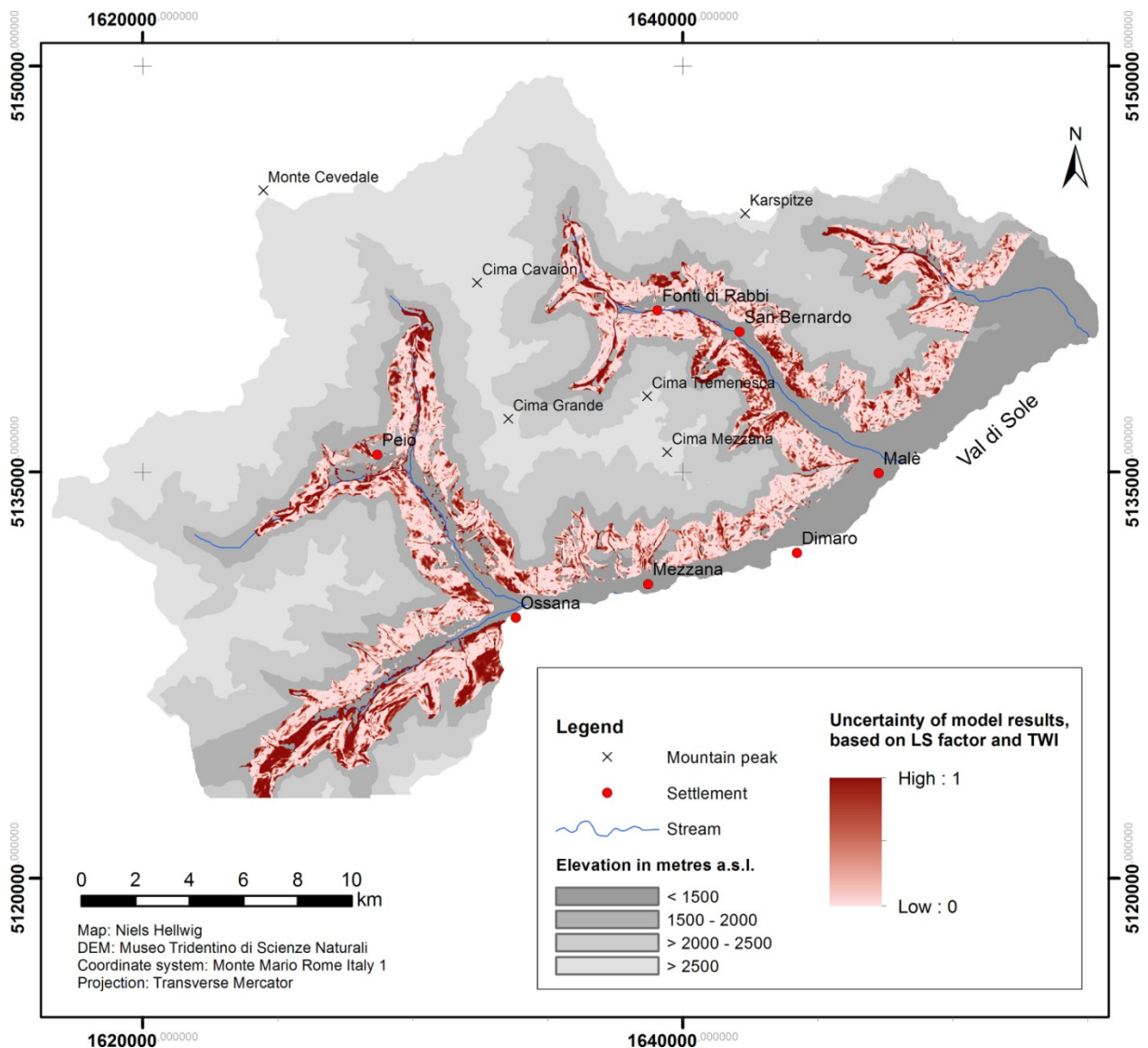


Fig. 8. Uncertainties of the predictions related to LS factor and TWI.

changes [46–49].

In this study, we examined the composition of the enchytraeid assemblage by proxy of the decomposer community on the one hand and the characteristics of humus forms as manifestations of dead organic matter at different stages of decomposition on the other hand. The occurrence of enchytraeids depends on factors such as soil pH, soil moisture, soil texture and soil organic matter content [30,50–52]. The connections between decomposer organisms like enchytraeids and humus forms are well known, also from investigations at the landscape scale [53,54]. The results of our study reveal a strong relationship between the occurrence of particular enchytraeid species and the spatial distribution of forest humus forms also under climatic conditions of the Alps. This relationship is obvious in all parts of the modeled areas except for north-facing slopes at low elevations (Figs. 5 and 7, see also Fig. S1).

The discrepancy between humus forms and enchytraeid indicator species in these places originates from the observations at study site N1. From our field experience this might be due to a small-scale spatial mosaic pattern of varying conditions in the topsoil. Another explanation could be the fact that the applied classification of life form types is based on observations from the German lowlands [30] and might not be completely transferable to the Alpine environment.

It has been previously shown that elevation and slope exposure have a major influence on the spatial distribution of forest humus forms and enchytraeids in the high mountains [12,55,56]. Our results confirm these findings and are in line with former investigations of humus forms and soil organic matter in the study area [21,57,58]. The sample data reveal a certain degree of local spatial heterogeneity of decomposition processes at all study sites (Table S1). In high mountain environments,

this local-scale variability of humus forms is connected to micro-topography and ground vegetation patterns [59,60]. The spatial model we presented emphasizes the landscape-scale patterns by yielding predictions for the entire slope areas of the study area. The application of fuzzy logic facilitates the representation of local spatial variability, as the percentage values reflect predicted mean values at an area of  $10 \times 10 \text{ m}^2$ .

In general, predicted percentages of moder/mor-indicating enchytraeids and related forest humus forms with an OH horizon increase from low to high elevations and from southern to northern exposures. At sites with high elevations and on north-exposed slopes, low temperatures apparently hinder the activity of those decomposers intermixing the topsoil and incorporating plant residues and humic substances into the mineral soil [61].

Models of the spatial distribution of soil properties based on landscape attributes have been formalized in the context of digital soil mapping [62–65]. Fuzzy logic-based approaches have been applied for modeling in several studies [20,38,66–69]. To our knowledge, this is the first time that the landscape-scale relationship between soil organisms and humus forms has been evaluated on the basis of spatial modeling. This study shows that in our study area the composition of the decomposer community can be approximated from the humus form. As a result, our findings contribute to demonstrating the ecological significance of humus forms in high mountain environments. Mapping of humus forms thus has great potential to be used for detecting environmental changes and understanding their impacts on high mountain ecosystems.

## 4.2. Model limitations

Humus forms were distinguished regarding the presence of an OH horizon, in congruity



with the discernment of enchytraeid species indicating mull and moder/mor. Although common humus form classifications provide a variety of subtypes [27,28,70], in this study we desisted from a further distinction due to the relatively low number of study sites. These simplifications do not allow the distinction of subtypes of humus forms or life forms of enchytraeids indicating different intermediate stages between the two classes mull and moder/mor, but enable the modeling of different degrees of similarity to both of these classes. Regarding seasonal dynamics, which might affect the abundance of enchytraeids, an interference with the model results presented in this study is unlikely because the composition of the enchytraeid assemblage does not vary much within the time span of sampling (June to September).

The validity of the model predictions is generally limited to areas between 1100 m and 1800 m a.s.l. that are located inside the coniferous forest. As for the results of the validation (from resampling and validation sites), they are ambiguous. The resampling procedure reveals low variation in the model results, thus the structure of the models is rather consistent. The analysis of the validation sites shows relatively high RMSE values, whereas the deviations of the observed values from the modeled values are relatively small (mostly up to ca. 25% points). The highest deviations are found at the sites V1 and V5. At site V1 this might originate from a small-scale mosaic of varying topsoil conditions. At site V5 the development of mull conditions might be promoted in comparison with S7 by gaps in the tree canopy, which potentially allows for a better thermal absorption of the topsoil.

The uncertainty analyses of input data show that effects of data modifications are attenuated in the model predictions, as there are only a few cases where the structure of the decision tree is moderately changed. This implies

that the predictions do not deviate tremendously from model results presented in our study even when assuming that the observations at the study sites do not reflect the exact percentage values of humus forms with an OH horizon and enchytraeid indicator classes. In general, these analyses confirm the predicted trends related to elevation and slope exposure.

The model results are also subject to uncertainties induced by both the selection of covariates and the set of values of the covariates at the study sites. Our study considered two basic topographic attributes (elevation, slope exposure) as influencing factors. Regarding these attributes, the uncertainties are expected to be the higher the more elevation and slope exposure of any site differ from the study sites (at east- and west-facing slopes or, for example, at 1300 m, midway between the study sites at 1200 m and 1400 m). The analysis of uncertainties referring to the landform type accounts for possible additional topographical influences on decomposition processes induced by erosion and accumulation (LS factor) or the distribution of water within the soil (TWI). In order to enhance the model a larger data basis is necessary, integrating for example sample sites with concave and convex landforms. Additionally, the integration of further possible influencing factors such as litter amount and composition (e.g. a data layer differentiating various forest units) could improve the model results. The consideration of irregular events affecting decomposition (e.g. dry/wet periods, windthrow, human influences) requires modeling on the basis of long-term data sets as well.

Future research should also address the effects of the model scale on the results. The investigations of this study refer to superordinate patterns of decomposition processes at the landscape scale, including the slopes of several Alpine valleys. However, decomposi-



tion processes show a considerable small-scale variability [59]. Thus we encourage investigations also at the slope scale, which should consider subordinate influencing variables (e.g. forest units, areas of erosion or accumulation), and at the local scale (e.g. 100 m<sup>2</sup>), where the micro-topography and local differences in the ground vegetation should be regarded.

## 5. CONCLUSION

The spatial distributions of enchytraeids and forest humus forms in a study area in the Italian Alps have been analyzed by means of a knowledge-based modeling approach, accommodating a relatively small amount of data samples and a high spatial heterogeneity of environmental variables. The predictions obtained from these models distinctly show the effects of slope exposure on different conditions for decomposition, which are characterized by the occurrence of different decomposer communities and forest humus forms. The highest percentages of forest humus forms with OH horizon occur at the uppermost north-exposed places inside the modeled area (up to 1800 m a.s.l.), where also a high dominance of moder-indicating enchytraeids over mull-indicating enchytraeids occurs. Those areas dominated by mull indicators are located at the lowest south-exposed sites of the modeled area (down to 1100 m a.s.l.). The models emphasize the coincidence of OH horizons with the related species of enchytraeids. This implies a high potential not only of humus forms and enchytraeids to be used for the prediction of decomposition patterns, but also of humus forms to serve as indicator of the enchytraeid assemblage, at least in our study area.

Although the modeling approach takes into account both the relatively small amount of

sample data and the small-scale variability of environmental conditions in the study area, the predictions are subject to uncertainties, which in some places can be high. However, the model allows the prediction of the overall trends in the distribution of forest humus forms and enchytraeids because the selected study sites seem to be representative. In most cases these trends were stable when modifying sample data in the context of uncertainty analyses. Uncertainties are usually to be expected in places where other environmental factors than elevation and slope exposure influence decomposition processes greatly (e.g. at landforms such as gullies and ridges).

## ACKNOWLEDGEMENTS

This work was realized in the context of the D.A.CH. project DecAlp and funded by the German Research Foundation (DFG, grant number BR 1106/23-1), the Swiss National Science Foundation (SNF, grant number 205321L\_141186) and the Austrian Science Fund (FWF). The authors thank all colleagues in the project for excellent cooperation. We are also grateful to Dott. Fabio Angeli (Ufficio Distrettuale Forestale di Malè) and the Stelvio National Park for supporting the field work and to Dr. Thomas Jarmer (University of Osnabrück) for valuable advice in the course of the model preparation.

## REFERENCES

- [1] D.A. Wardle, R.D. Bardgett, J.N. Klironomos, H. Setälä, W.H. van der Putten, D.H. Wall, Ecological linkages between aboveground and belowground biota, *Science* 304 (2004) 1629–1633.
- [2] S. Hättenschwiler, A.V. Tiunov, S. Scheu, Biodiversity and litter decomposition in terrestrial ecosystems, *Annu. Rev. Ecol. Evol. Syst.* 36 (2005) 191–218.

- [3] U. Graefe, Die Gliederung von Zersetzergesellschaften für die standortökologische Ansprache, *Mitt. Dtsch. Bodenkdl. Ges.* 69 (1993) 95–98.
- [4] A. Beylich, H.-C. Fründ, U. Graefe, Environmental monitoring of ecosystems and bioindication by means of decomposer communities, *Newsl. Enchytraeidae* 4 (1995) 25–34.
- [5] S. Jänsch, J. Römbke, W. Didden, The use of enchytraeids in ecological soil classification and assessment concepts, *Ecotoxicol. Environ. Saf.* 62 (2005) 266–277.
- [6] U. Graefe, A. Beylich, Critical values of soil acidification for annelid species and the decomposer community, *Newsl. Enchytraeidae* 8 (2003) 51–55.
- [7] J. Schlaghamerský, N. Eisenhauer, L.E. Frelich, Earthworm invasion alters enchytraeid community composition and individual biomass in northern hardwood forests of North America, *Appl. Soil Ecol.* 83 (2014) 159–169.
- [8] U. Graefe, Humusformengliederung aus bodenzoologischer Sicht, *Mitt. Dtsch. Bodenkdl. Ges.* 74 (1994) 41–44.
- [9] M. Chauvat, J.F. Ponge, V. Wolters, Humus structure during a spruce forest rotation: quantitative changes and relationship to soil biota, *Eur. J. Soil Sci.* 58 (2007) 625–631.
- [10] J.-F. Ponge, Plant-soil feedbacks mediated by humus forms: a review, *Soil Biol. Biochem.* 57 (2013) 1048–1060.
- [11] A. Andretta, R. Ciampalini, P. Moretti, S. Vingiani, G. Poggio, G. Matteucci, F. Tescari, S. Carnicelli, Forest humus forms as potential indicators of soil carbon storage in Mediterranean environments, *Biol. Fertil. Soils* 47 (2011) 31–40.
- [12] E. Bonifacio, G. Falsone, M. Petrillo, Humus forms, organic matter stocks and carbon fractions in forest soils of northwestern Italy, *Biol. Fertil. Soils* 47 (2011) 555–566.
- [13] O. Bojko, C. Kabala, Organic carbon pools in mountain soils d sources of variability and predicted changes in relation to climate and land use changes, *Catena* 149 (2017) 209–220.
- [14] C. De Nicola, A. Zanella, A. Testi, G. Fanelli, S. Pignatti, Humus forms in a Mediterranean area (Castelporziano Reserve, Rome, Italy): classification, functioning and organic carbon storage, *Geoderma* 235-236 (2014) 90–99.
- [15] B. De Vos, N. Cools, H. Ilvesniemi, L. Vesterdal, E. Vanguelova, S. Carnicelli, Benchmark values for forest soil carbon stocks in Europe: results from a large scale forest soil survey, *Geoderma* 251-252 (2015) 33–46.
- [16] J.-F. Ponge, Humus forms in terrestrial ecosystems: a framework to biodiversity, *Soil Biol. Biochem.* 35 (2003) 935–945.
- [17] A. Lalanne, J. Bardat, F. Lalanne-Amara, J.-F. Ponge, Local and regional trends in the ground vegetation of beech forests, *Flora* 205 (2010) 484–498.
- [18] B. Strandberg, S.M. Kristiansen, K. Tybirk, Dynamic oak-scrub to forest succession: effects of management on understorey vegetation, humus forms and soils, *For. Ecol. Manag.* 211 (2005) 318–328.
- [19] M. Rutgers, A. Orgiazzi, C. Gardi, J. Römbke, S. Jänsch, A.M. Keith, R. Neilson, B. Boag, O. Schmidt, A.K. Murchie, R.P. Blackshaw, G. Pérès, D. Cluzeau, M. Guernion, M.J.I. Briones, J. Rodeiro, R. Piñero, D.J. Díaz Cosín, J.P. Sousa, M. Suhadolc, I. Kos, P.-H. Krogh, J.H. Faber, C. Mulder, J.J. Bogte, H.J. van Wijnen, A.J. Schouten, D. de Zwart, Mapping earthworm communities in Europe, *Appl. Soil Ecol.* 97 (2016) 98–111.
- [20] N. Hellwig, K. Anschlag, G. Broll, A fuzzy logic based method for modelling the spatial distribution of indicators of decomposition in a high mountain environment, *Arct. Antarct. Alp. Res.* 48 (2016) 623–635.
- [21] I. Aberegg, M. Egli, G. Sartori, R. Purves, Modelling spatial distribution of soil types and characteristics in a high Alpine valley (Val di Sole, Trentino, Italy), *Studi Trent. Sci. Nat.* 85 (2009) 39–50.
- [22] Mountain Research Initiative EDW Working Group, Elevation-dependent warming in mountain regions of the world, *Nat. Clim. Chang.* 5 (2015) 424–430.

- [23] E.A.C. Costantini, M. Fantappiè, G. L'Abate, Climate and pedoclimate of Italy, in: E.A.C. Costantini, C. Dazzi (Eds.), *The Soils of Italy*, Springer, Dordrecht, 2013, pp. 19–37.
- [24] K. Zakšek, T. Podobnikar, K. Oštir, Solar radiation modelling, *Comput. Geosci.* 31 (2005) 233–240.
- [25] G. Sartori, A. Mancabelli, *Carta dei suoli del Trentino: scala 1:250.000*, Museo Tridentino di Scienze Naturali di Trento, Centro di Ricerca per l'Agrobiologia e la Pedologia di Firenze, 2009.
- [26] M. Egli, A. Mirabella, G. Sartori, R. Zanelli, S. Bischof, Effect of north and south exposure on weathering rates and clay mineral formation in Alpine soils, *Catena* 67 (2006) 155–174.
- [27] Ad-hoc-AG Boden, *Bodenkundliche Kartieranleitung*, in: E. Schweizerbart'sche Verlagsbuchhandlung, fifth, 2005. Hannover.
- [28] J.-M. Gobat, C. Le Bayon, D. Tatti, *Clé de Sol e Principaux sols de Suisse*, Laboratoire Sol & Végétation Université de Neuchâtel, Switzerland, 2014, 76 pages.
- [29] R. Schmelz, R. Collado, A guide to European terrestrial and freshwater species of Enchytraeidae (Oligochaeta), *Soil Org.* 82 (2010) 1–176.
- [30] U. Graefe, R.M. Schmelz, Indicator values, strategy types and life forms of terrestrial Enchytraeidae and other microannelids, *Newsl. Enchytraeidae* 6 (1999) 59–67.
- [31] ESRI, *ArcGIS Desktop, Release 10*, Environmental Systems Research Institute, Redlands, CA, 2011.
- [32] L. Breiman, J.H. Friedman, R.A. Olshen, C.J. Stone, *Classification and Regression Trees*, Wadsworth, Belmont, 1984.
- [33] R Core Team, *R: a Language and Environment for Statistical Computing*, R Foundation for Statistical Computing, 2016. Vienna, Austria, <http://www.Rproject.org/> (accessed 30.08.16).
- [34] T.M. Therneau, E.J. Atkinson, M. Foundation, *An Introduction to Recursive Partitioning Using the RPART Routines*, 2015. <http://cran.r-project.org/web/packages/rpart/vignettes/longintro.pdf> (accessed: 30.08.16).
- [35] L.A. Zadeh, Fuzzy sets, *Inf. Control* 8 (1965) 338–353.
- [36] A.B. McBratney, I.O.A. Odeh, Application of fuzzy sets in soil science: fuzzy logic, fuzzy measurements and fuzzy decisions, *Geoderma* 77 (1997) 85–113.
- [37] X. Shi, R. Long, R. Dekett, J. Philippe, Integrating different types of knowledge for digital soil mapping, *Soil Sci. Soc. Am. J.* 73 (2009) 1682–1692.
- [38] M.D. de Menezes, S.H.G. Silva, P.R. Owens, N. Curi, Digital soil mapping approach based on fuzzy logic and field expert knowledge, *Ciênc. Agrotec.* 37 (2013) 287–298.
- [39] X. Shi, *ArcSIE*, 2013. <http://www.arcsie.com/Download.htm> (accessed: 30.08.16).
- [40] I.D. Moore, R.B. Grayson, A.R. Ladson, Digital terrain modelling: a review of hydrological, geomorphological, and biological applications, *Hydrol. Process.* 5 (1991) 3–30.
- [41] J. Böhner, T. Selige, Spatial prediction of soil attributes using terrain analysis and climate regionalisation, in: J. Böhner, K.R. McCloy, J. Strobl (Eds.), *SAGA - Analysis and Modelling Applications* vol. 115, Göttinger Geogr. Abh., 2006, pp. 13–28. Goltze, Göttingen.
- [42] A.X. Zhu, J. Liu, F. Du, S.J. Zhang, C.Z. Qin, J. Burt, T. Behrens, T. Scholten, Predictive soil mapping with limited sample data, *Eur. J. Soil Sci.* 66 (2015) 535–547.
- [43] V. Huhta, T. Persson, H. Setälä, Functional implications of soil fauna diversity in boreal forests, *Appl. Soil Ecol.* 10 (1998) 277–288.
- [44] E. Edsberg, The quantitative influence of enchytraeids (Oligochaeta) and microarthropods on decomposition of coniferous raw humus in microcosms, *Pedobiologia* 44 (2000) 132–147.
- [45] H. Jenny, *Factors of Soil Formation: A System of Quantitative Pedology*, McGraw-Hill, New York, 1941.
- [46] J.C. Blankinship, P.A. Niklaus, B.A. Hungate, A meta-analysis of responses of soil

- biota to global change, *Oecologia* 165 (2011) 553–565.
- [47] N. Eisenhauer, S. Cesarz, R. Koller, K. Worm, P.B. Reich, Global change belowground: impacts of elevated CO<sub>2</sub>, nitrogen, and summer drought on soil food webs and biodiversity, *Glob. Chang. Biol.* 18 (2012) 435–447.
- [48] M. Holmstrup, R.M. Schmelz, N. Carrera, K. Dyrnum, K.S. Larsen, T.N. Mikkelsen, C. Beier, Responses of enchytraeids to increased temperature, drought and atmospheric CO<sub>2</sub>: results of an eight-year field experiment in dry heathland, *Eur. J. Soil Biol.* 70 (2015) 15–22.
- [49] S. Kataja-aho, F. Hannu, H. Jari, Short-term responses of soil decomposer and plant communities to stump harvesting in boreal forests, *For. Ecol. Manag.* 262 (2011) 379–388.
- [50] W.A.M. Didden, Ecology of terrestrial Enchytraeidae, *Pedobiologia* 37 (1993) 2–29.
- [51] P. Kapusta, Ł. Sobczyk, A. Rożen, J. Weiner, Species diversity and spatial distribution of enchytraeid communities in forest soils: effects of habitat characteristics and heavy metal contamination, *Appl. Soil Ecol.* 23 (2003) 187–198.
- [52] J. Römbke, S. Jänsch, H. Höfer, F. Horak, M. Roß-Nickoll, D. Russell, A. Toschki, State of knowledge of enchytraeid communities in German soils as a basis for biological soil quality assessment, *Soil Org.* 85 (2013) 123–146.
- [53] U. Graefe, A. Beylich, Humus forms as tool for upscaling soil biodiversity data to landscape level? *Mitt. Dtsch. Bodenkdl. Ges.* 108 (2006) 6–7.
- [54] S. Salmon, N. Artuso, L. Frizzera, R. Zampedri, Relationships between soil fauna communities and humus forms: response to forest dynamics and solar radiation, *Soil Biol. Biochem.* 40 (2008) 1707–1715.
- [55] N. Bernier, Altitudinal changes in humus form dynamics in a spruce forest at the montane level, *Plant Soil* 178 (1996) 1–28.
- [56] J. Ascher, G. Sartori, U. Graefe, B. Thornton, M.T. Ceccherini, G. Pietramellara, M. Egli, Are humus forms, mesofauna and microflora in subalpine forest soils sensitive to thermal conditions? *Biol. Fert. Soils* 48 (2012) 709–725.
- [57] M. Egli, G. Sartori, A. Mirabella, F. Favilli, D. Giaccai, E. Delbos, Effect of north and south exposure on organic matter in high Alpine soils, *Geoderma* 149 (2009) 124–136.
- [58] M. Egli, G. Sartori, A. Mirabella, D. Giaccai, The effects of exposure and climate on the weathering of late Pleistocene and Holocene Alpine soils, *Geomorphology* 114 (2010) 466–482.
- [59] F. Bednorz, M. Reichstein, G. Broll, F.-K. Holtmeier, W. Urfer, Humus forms in the forest-Alpine tundra ecotone at Stillberg (Dischmatal, Switzerland): spatial heterogeneity and classification, *Arct. Antarct. Alp. Res.* 32 (2000) 21–29.
- [60] B. Hiller, A. Mütterthies, F.-K. Holtmeier, G. Broll, Investigations on spatial heterogeneity of humus forms and natural regeneration of larch (*Larix decidua* Mill.) and Swiss stone pine (*Pinus cembra* L.) in an Alpine timberline ecotone (Upper Engadine, central Alps, Switzerland), *Geogr. Helv.* 57 (2002) 81–90.
- [61] R. Aerts, The freezer defrosting: global warming and litter decomposition rates in cold biomes, *J. Ecol.* 94 (2006) 713–724.
- [62] A.B. McBratney, M.L. Mendonça Santos, B. Minasny, On digital soil mapping, *Geoderma* 117 (2003) 3–52.
- [63] P. Scull, J. Franklin, O.A. Chadwick, D. McArthur, Predictive soil mapping: a review, *Prog. Phys. Geogr.* 27 (2003) 171–197.
- [64] S. Grunwald, J.A. Thompson, J.L. Boettinger, Digital soil mapping and modeling at continental scales: finding solutions for global issues, *Soil Sci. Soc. Am. J.* 75 (2011) 1201–1213.
- [65] E.C. Brevik, C. Calzolari, B.A. Miller, P. Pereira, C. Kabala, A. Baumgarten, A. Jordán, Soil mapping, classification, and pedologic modeling: history and future directions, *Geoderma* 264 (2016) 256–274.
- [66] C.E. Akumu, J.A. Johnson, D. Etheridge, P. Uhlig, M. Woods, D.G. Pitt, S. McMurray, GIS-fuzzy logic based approach in modeling soil texture: using parts of the Clay Belt and

- Hornepayne region in Ontario Canada as a case study, *Geoderma* 239-240 (2015) 13–24.
- [67] J.J. de Gruijter, D.J.J. Walvoort, G. Bragato, Application of fuzzy logic to Boolean models for digital soil assessment, *Geoderma* 166 (2011) 15–33.
- [68] E. Rodríguez, R. Peche, C. Garbisu, I. Gorostiza, L. Epelde, U. Artetxe, A. Irizar, M. Soto, J.M. Becerril, J. Etxebarria, Dynamic Quality Index for agricultural soils based on fuzzy logic, *Ecol. Indic.* 60 (2016) 678–692.
- [69] A.-X. Zhu, R. Wang, J. Qiao, C.-Z. Qin, Y. Chen, J. Liu, F. Du, Y. Lin, T. Zhu, An expert knowledge-based approach to landslide susceptibility mapping using GIS and fuzzy logic, *Geomorphology* 214 (2014) 128–138.
- [70] A. Zanella, B. Jabiol, J.F. Ponge, G. Sartori, R. De Waal, B. Van Delft, U. Graefe, N. Cools, K. Katzensteiner, H. Hager, M. Englisch, A. Brethes, G. Broll, J.M. Gobat, J.J. Brun, G. Mibert, E. Kolb, U. Wolf, L. Frizzera, P. Galvan, R. Kolli, R. Baritz, R. Kemmers, A. Vacca, G. Serra, D. Banas, A. Garlato, S. Chersich, E. Klimo, R. Langohr, European Humus Forms Reference Base, 2011. [http://hal.archives-ouvertes.fr/docs/00/56/17/95/PDF/Humus\\_Forms\\_ERB\\_31\\_01\\_2011.pdf](http://hal.archives-ouvertes.fr/docs/00/56/17/95/PDF/Humus_Forms_ERB_31_01_2011.pdf) (accessed: 30.08.16).

## Chapter 4

### Humus Forms and Soil Microbiological Parameters in a Mountain Forest: Upscaling to the Slope Scale



Supplementary materials can be found in Appendix 3 of this thesis.

**Citation:** Hellwig, N., Gómez-Brandón, M., Ascher-Jenull, J., Bardelli, T., Anschlag, K., Fornasier, F., Pietramellara, G., Insam, H., Broll, G. (2018): Humus Forms and Soil Microbiological Parameters in a Mountain Forest: Upscaling to the Slope Scale. *Soil Systems* 2(1), 12.

**Author contributions:** N.H. performed spatial modeling, model assessment and wrote the paper; N.H. and K.A. performed sampling and soil analysis of the sites RN1–RN30 and RS1–RS30; M.G.-B., J.A.-J. and T.B. performed sampling and soil analysis of the sites N1–N3 and S6–S8 and co-wrote the paper; F.F. and G.P. contributed to soil microbiological analysis; G.B. and H.I. conceived and designed the experiments.

### **Copyright**

2018 The authors

Reprinted under the Creative Common Attribution License (CC BY 4.0)

### **Photo credits (previous page):**

Niels Hellwig, 19 September 2015

View from Malga Polinar on investigated south-facing slope near San Bernardo (Val di Rabbi, Trentino, Italian Alps).



## Humus Forms and Soil Microbiological Parameters in a Mountain Forest: Upscaling to the Slope Scale

NIELS HELLWIG <sup>1,\*</sup>, MARÍA GÓMEZ-BRANDÓN <sup>2,3</sup>, JUDITH ASCHER-JENULL <sup>2,4</sup>, TOMMASO BARDELLI <sup>2,4</sup>, KERSTIN ANSCHLAG <sup>1</sup>, FLAVIO FORNASIER <sup>5</sup>, GIACOMO PIETRAMELLARA <sup>4</sup>, HERIBERT INSAM <sup>2</sup>, GABRIELE BROLL <sup>1</sup>

<sup>1</sup> Institute of Geography, Osnabrück University, Seminarstraße 19ab, 49074 Osnabrück, Germany

<sup>2</sup> Institute of Microbiology, University of Innsbruck, Technikerstraße 25d, 6020 Innsbruck, Austria

<sup>3</sup> Departamento de Ecología y Biología Animal, Universidad de Vigo, Vigo 36310, Spain

<sup>4</sup> Department of Agrifood and Environmental Science, University of Florence, Piazzale delle Cascine, 50144 Firenze, Italy

<sup>5</sup> Consiglio per la Ricerca e la Sperimentazione in Agricoltura, Centro di Ricerca per lo Studio delle Relazioni tra Pianti e Suolo (C.R.A.-R.P.S.), Via Trieste 23, 34170 Gorizia, Italy

\*Corresponding author

### ABSTRACT

Humus forms are the morphological results of organic matter decay and distribution in the topsoil, and thus important indicators for decomposer activities in forest ecosystems. The first aim was to examine if humus forms are suitable indicators of microbiological properties of the topsoil in a high mountain forest (Val di Rabbi, Trentino, Italian Alps). The second aim was to predict microbiological parameters based on the topsoil pH value on two slopes of the study area (ca. 1200-2200 m a.s.l.). We investigated humus forms and determined pH values and microbiological parameters (enzymatic activities, carbon/nitrogen (C/N) ratio and the ratio of bacterial/archaeal abundance) of the uppermost mineral horizon. The results reveal significant correlations between pH value and microbiological parameters (except for bacterial/archaeal abundance), which enable upscaling to the landscape scale using linear models. Based on a random forest with kriging of model residuals, predictive maps of humus form, pH value and microbiological parameters show that decomposition processes in our study area correspond with the topography. As compared to locations on south-facing slopes or close to the valley bottom, locations on north-facing slopes or close to the upper treeline exhibit Moder (scarcely Mull or Amphimull), more acidic topsoil (around pH 4), a lower activity of leucine-aminopeptidase, a lower ratio of alkaline/acid phosphomonoesterase activity and a higher soil C/N ratio (above 20). Our results suggest a high potential of humus forms to indicate soil microbiological properties in a high mountain forest. Together with the pH values of the topsoil, humus forms proved to be a useful tool as a basis for predictive maps of leucine-aminopeptidase activity, ratio of alkaline/acid phosphomonoesterase activity and C/N ratio of the mineral topsoil.

**Keywords:** spatial modeling; hydrolytic enzyme activities; soil acidity; random forest; forest ecosystem; Italian Alps

**Submitted:** 22 January 2018 – **Accepted:** 21 February 2018

## 1. INTRODUCTION

The humus form is an important indicator for decomposition in terrestrial ecosystems [1,2]. Humus forms are the morphological results of different biological activities in the topsoil. They thereby reflect the composition of the decomposer community [3]. Additionally, humus forms are well accepted as integrating indicators for changes in forest ecosystems [4]. Previous studies illustrated a strong correlation between the spatial distribution of enchytraeid species, humus forms and pH values of the topsoil (e.g. [5–7]), which has also been shown for high mountain environments [8]. Furthermore, extensive information on forest humus forms in a high mountain area can be used to upscale the spatial distribution of enchytraeid species to the landscape scale [9]. A high soil biological activity as derived from a well-structured mineral topsoil was connected with mull-indicating enchytraeid species at southern slope exposure (in case of sufficient soil moisture), whereas a low soil biological activity indicated by a poorly structured mineral topsoil was connected with moder-indicating enchytraeid species at northern slope exposure [9].

Due to the fact that changes in microbial communities can occur more quickly than remarkable changes in basic soil functions (e.g. filtering pollutants, storing nutrients), the study of microbial parameters is deemed a sensitive indicator when evaluating effects of soil disturbance [10]. In this sense, extracellular enzymes, which are biological catalysts of specific reactions, are considered as sensitive indicators of soil biological processes and soil fertility [11]. Abiotic factors like soil temperature, water potential, pH, substrate availability and complexity, along with biotic processes including enzyme synthesis and secretion, largely influence the activities of enzymes in natural environments [12].

Leucine-aminopeptidase activity has an important role in the nitrogen (N) cycle, as it catalyzes the hydrolysis of leucine and other amino acids from protein or peptide substrates [13]. Bacteria play a relevant role in the production of leucine-aminopeptidases [14] and, accordingly, Bardelli et al. [15] observed a greater activity in south-facing subalpine forest soils where a greater bacterial abundance was recorded in comparison with north-facing slopes.

Phosphorus (P) is taken up by microorganisms and plants largely as orthophosphate in soil solution. Since in many terrestrial ecosystems soil orthophosphate is limiting for plant productivity, the production of extracellular enzymes facilitating the mineralization of organic P compounds is therefore determined by the need for orthophosphate [16]. The phosphomonoesterases include acid and alkaline phosphatases, phytases and nucleotidases [17], and mineralize orthophosphate monoesters such as sugar phosphates, phytate and nucleotides. In particular, acid and alkaline phosphatases are responsible for the mineralization of organic P into phosphate by hydrolyzing phosphoric (mono) ester bonds under acid and alkaline conditions, respectively. They have an important role for P cycling in forest ecosystems, particularly where P availability may limit plant productivity [18]; and an increase in their activity can occur when P is limited, reflecting a demand for this macronutrient [16].

The soil carbon/nitrogen (C/N) ratio is among the most important properties of soil organic matter (SOM) and serves as a reliable proxy of the decomposition rate of SOM. The higher the ratio, the lower the decomposition rate, and as such, the soil C/N ratio can be considered as an estimator of microbial activity and overall as a proxy for soil quality and soil ecological conditions [15,19]. Soil microorganisms use carbon and nitrogen for metabolism,

with a C/N ratio of about 20:1 favoring SOM decomposition. The C/N ratio is influenced by a multitude of site-related factors (e.g. [20]). Soil microorganisms (bacteria, archaea and fungi) and their complex interplay are crucial in biogeochemical cycling in (forest) soils, especially in carbon (C) and nitrogen (N) cycling, as principal drivers of mineral weathering, decomposition/mineralization of organic matter (OM) and pedogenesis. Understanding the ecological role of microbial community dynamics for nutrient cycling is essential for understanding the functional stability of ecosystems and for predicting future scenarios due to changing environmental conditions [21]. Although bacteria and fungi are considered the primary decomposers of SOM, archaea have gained increasing interest as ecological indicators due to their adaptability to harsh environmental conditions (e.g. low temperatures, low pH, nutrient deficiency) and their role within the N cycle, owing to their ammonia oxidizing potential. In fact, ammonia oxidation, the first and rate-limiting step of nitrification, was only recently attributed also to archaea, thanks to the discovery of homologue ammonia monooxygenase (amo) genes [22–24]. The comparative assessment of bacteria and archaea provides important descriptive information about soil quality [25], as they can compete for the same nutrients [26] and due to different pH dependencies of fungi, bacteria and archaea [27]. In order to understand spatial decomposition patterns in a high mountain environment, it would be useful if humus forms could be applied as indicators not only of the distribution of enchytraeid species [9,28], but also of microbiological parameters [29]. Hence, the aims of this study were (i) to map humus forms and topsoil pH values in a mountain forest area in the Italian Alps as a basis for upscaling, (ii) to examine correlations between humus forms, pH values and micro-

biological parameters of the topsoil, (iii) to rank the examined parameters in terms of their usability for upscaling by proxy of humus forms and topsoil pH values, (iv) to upscale microbiological parameters utilizing humus forms and topsoil pH values if feasible according to (iii). In this study, upscaling refers to the extrapolation of microbiological data from the level of a study site to the slope scale using information on the spatial distribution of humus forms and pH values. The following microbiological parameters of the topsoil were addressed in this study: (1) the leucine-aminopeptidase activity as indicator of N cycle processes, (2) the ratio of alkaline/acid phosphomonoesterase activity as indicator of P cycle processes, (3) the C/N ratio as indicator of both C cycle and N cycle processes, (4) the ratio of bacterial/archaeal abundance as indicator of C cycle and N cycle processes, especially ammonia oxidation.

## 2. MATERIAL AND METHODS

### 2.1. Study Area

The study area is located in the northeastern Italian Alpine valley Val di Rabbi in the Autonomous Province of Trento (Fig. 1). With reference to geology, the study area is part of the Central Alps, characterized by siliceous bedrock. The dominant parent materials are acidic paragneiss, mica schists, phyllites and orthogneiss [30,31]. The climate of the study area is governed by the high relief intensity of the Alpine environment. Climatic variations are generally due to differences in elevation and slope exposure, with the local climatic situation being more complex [32]. The mean annual air temperature in the study area ranges from about 2°C close to the tree line to 7°C at the lowest sites near the valley bottom. The mean annual precipitation is about 800–850 mm [33]. The main soil classes in the

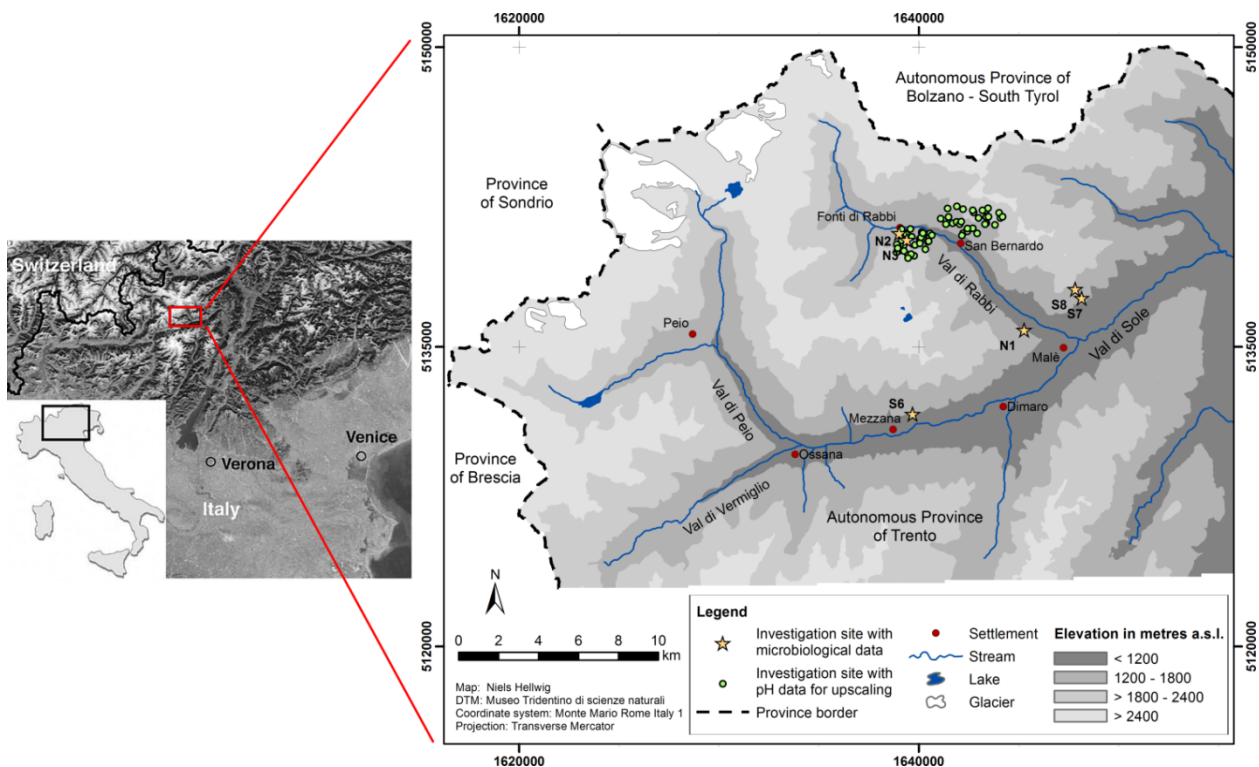


**Figure 1.** Study area and investigation sites in the Italian Alps (Autonomous Province of Trento) (left map: modified from Egli et al. [36]).

study area are Haplic Cambisols (Dystric) and Umbric Podzols below ca. 1900 m a.s.l., whereas Entic Podzols, Albic Podzols and Umbric Podzols are dominant in the forest above ([34], according to [35]).

Upscaling of local data refers to the forested parts of one north-facing slope (~ 1200–2100 m a.s.l., approx. 2.5 km<sup>2</sup>) and one south-facing slope (~ 1200–2200 m a.s.l., approx. 3.8 km<sup>2</sup>). The main tree species on these slopes are European larch (*Larix decidua*) and Norway spruce (*Picea abies*), both of them similarly prevalent at both slopes. Regarding the lower tree layer, Norway spruce is by far the dominant species, whereas young European larch trees only occur above 1800 m a.s.l. [37].

## 2.2. Sampling

For this study, we considered two sampling sets: the first set comprised 60 sampling sites for humus form determination and topsoil acidity analysis (RN1–RN30 and RS1–RS30); the second set comprised six additional sam-

pling sites for extensive microbiological analyses (N1–N3 and S6–S8) (Table 1).

Sampling of humus forms was carried out at a total of 60 sampling sites in Val di Rabbi. Among these sites, 30 of them were located on one north-facing (RN1–RN30) and 30 on one neighboring south-facing (RS1–RS30) slope, respectively (Fig. 1). These sites were determined based on conditioned Latin Hypercube Sampling (cLHS) [38]. The application of cLHS allowed to obtain a set of sampling sites most closely representing the investigated slopes in terms of the covariates elevation, slope gradient, slope exposure, slope curvature (planform, profile and general curvature), SAGA wetness index, LS factor (slope length and steepness) and forest type (details are given in [37]). Each of these sites comprised an area of 25 m x 25 m. The number of sampling plots corresponded to the number of ground cover types (one sample per available ground cover type: the ground cover types were litter, consisting of tree lit-

ter, mostly needles; grass; moss; fern; shrubs). For all of the ground cover types, percentages of their spatial distributions within the area of the site were estimated. At each sampling plot, a humus form profile was described and a sample for topsoil acidity analysis (two replicates) was collected from the uppermost mineral horizon directly beneath the organic layers. All analyses were carried out at these sites in September 2015.

For microbiological analyses, six additional sampling sites were chosen on the basis of local knowledge from experts involved in previous soil ecological studies (Fig. 1). They are located at three different elevations (~1200, 1400 and 1630 m a.s.l.) inside the closed forest, each half of them on north-facing (N1, N2, N3) and south-facing (S6, S7, S8) slopes, respectively. Further environmental characteristics of these sites have been specified elsewhere [15,39]. Soil sampling at these sites was comprised of three replicates with five subsamples each (for quantitative real-time PCR, the subsamples were pooled). A corer (diameter 5 cm) was used to sample three soil depths separately, including organic layers at the surface: 0–5 cm, 5–10 cm, 10–15 cm. Sampling was carried out at these sites in August 2012. All samples were bulked and sieved (<2 mm), aliquoted into 50-ml sterile conical centrifuge tubes, and stored at –20 °C. Apart from topsoil acidity, the analyses of these samples covered total C and N contents, soil enzymatic activities, abundance of bacteria and archaea.

### 2.3. Soil Analysis

Soil properties determined for the first sampling set (RN1–RN30 and RS1–RS30) comprised humus forms and topsoil acidity; the second sampling set (N1–N3 and S6–S8) was analyzed with respect to topsoil acidity, soil enzymatic activities, total C and N, bacterial and archaeal abundance (Table 1).

**Table 1.** Soil properties, related investigation sites and sampled objects.

Soil property	Sites	Sampled soil horizons/depths
Humus forms: Presence of organic layers	RN1–RN30, RS1–RS30	OL, OF, OH horizons
Humus forms: Soil structure	RN1–RN30, RS1–RS30	A horizon
pH value (H <sub>2</sub> O)	RN1–RN30, RS1–RS30	A horizon
pH value (H <sub>2</sub> O)	N1–N3, S6–S8	0–15 cm, depth increments of 5 cm
Leucine-aminopeptidase activity	N1–N3, S6–S8	0–15 cm, depth increments of 5 cm
Acid phospho-monoesterase activity	N1–N3, S6–S8	0–15 cm, depth increments of 5 cm
Alkaline phospho-monoesterase activity	N1–N3, S6–S8	0–15 cm, depth increments of 5 cm
Total C	N1–N3, S6–S8	0–15 cm, depth increments of 5 cm
Total N	N1–N3, S6–S8	0–15 cm, depth increments of 5 cm
Bacterial abundance	N1–N3, S6–S8	0–15 cm, depth increments of 5 cm
Archaeal abundance	N1–N3, S6–S8	0–15 cm, depth increments of 5 cm

#### 2.3.1. Humus Forms

Humus form profiles (width 50–100 cm) were described and classified according to [40]. In addition to the set of humus forms specified therein, the humus form Amphimull (AMU) was used whenever organic layers (OF and OH) existed above a well-structured soil in the uppermost mineral horizon (Fig. 2). Amphimull is a humus form usually not present under Central European climatic conditions, except for some mountain areas [41].

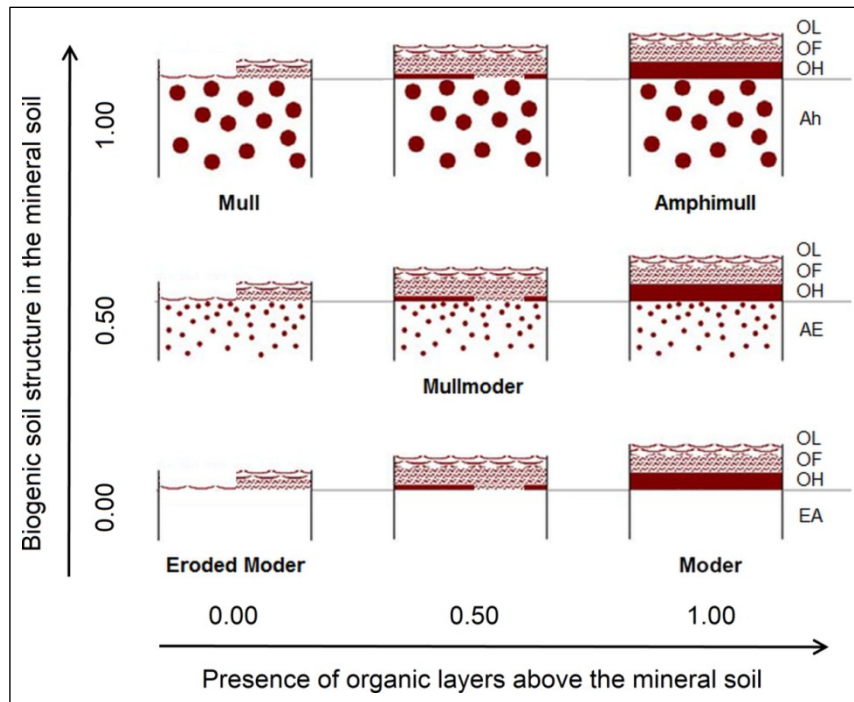


**Figure 2.** Humus form classes and parameter values for modeling (only names of described humus forms are given) (modified from Graefe [41]).

### 2.3.2. Topsoil Acidity

The pH values were determined in soil water extracts (1:10 m/v) from air-dried samples.

### 2.3.3. Soil Enzymatic Activities

A heteromolecular exchange principle [42] was used to desorb enzymes from soil in order to determine the leucine-aminopeptidase, acid and alkaline phosphomonoesterase potential activities, as described by Bardelli et al. [15]. For the disruption of soil aggregates and microbial cells the procedure involved the use of a 3% solution of lysozyme as desorbant and a bead-beating agent followed by centrifugation at 20,000g for 5 min. Afterwards, the supernatant containing desorbed enzymes was dispensed into 384-well microplates together with the appropriate buffer and the fluorometric quantification of the enzymes activities was done using 4-methyl-umbelliferyl (MUF) substrate. All the measurements were done in duplicate and the activities were expressed as nanomoles of MUF  $g^{-1}$  dry soil  $h^{-1}$ .

### 2.3.4. Total C and N

Soil samples were homogenized with a mortar prior to analysis. A CN analyzer (TruSpec CHN; LECO, Michigan, U.S.A.) was used to determine total C and N contents in oven-dried soil samples. The temperature used for CN analysis was 950 °C. Due to the siliceous bedrock throughout our study area, total C only includes organic C.

### 2.3.5. Quantitative Real-Time PCR

The DNA extraction and purification from soil samples (0.5 g, fresh weight) was done using a commercial kit (FastDNA Kit for Soil, MP-Biomedicals) as described in [43]. The Rotorgene 6000 Real Time Thermal Cycler (Corbett Research, Sydney, Australia) was used in combination with the Rotor-Gene Series Software 1.7 in order to quantify the 16S rRNA gene copy number of bacteria and archaea with the primer pairs 1055f/1392r (bacteria, [44]) and Parch519f/Arc915r (archaea, [45]). Standard curves for quantifica-

tion of both microbial domains were constructed as described by Bardelli et al. [15]. The reaction mix for each qPCR run was performed by using the 1X Sensimix™ SYBR® Hi-rox (Bioline, USA) based on the DNA-intercalating dye SYBR Green I as shown in [15]. Each run was accompanied by a melting analysis starting from 60°C to 95°C with temperature increments of 0.25°C and a transition rate of 5 s to check for product specificity and potential primer dimer formation. The purity of the amplified products was also checked by the presence of a single band of the expected length on a 1% agarose gel stained with the DNA stain Midori Green (Nippon Genetics, Germany) and visualized by UV-transillumination (Vilber Lourmat Deutschland GmbH). The efficiency for the bacterial and archaeal qPCR runs was in a range between 80–85%, indicating a good reproducibility.

## 2.4. Spatial Modeling

Humus forms were modeled in terms of two dimensions: 1) biogenic soil structure in the

mineral soil and 2) presence of organic layers above the mineral soil. Relative units (values from 0 to 1) were used for both dimensions according to the determined humus forms (Fig. 2, Table 2). At each site, the related samples were aggregated using weights according to the estimated relative distribution of different ground cover types. For example, at a site with Amphimull (AMU) under grass (70% occurrence) and Typischer Moder (MOA) under litter (30% occurrence), the dimension biogenic soil structure in the mineral soil amounts to  $0.7 \times 1.0 + 0.3 \times 0.0 = 0.7$  and the presence of organic layers above the mineral soil amounts to  $0.7 \times 1.0 + 0.3 \times 1.0 = 1.0$ . Spatial modeling consisted of a random forest [46] and ordinary kriging of the model residuals [47]. An approach combining a random forest and residuals kriging has been successfully applied in earlier digital soil mapping studies [48]. During the last years, random forest has been established as one of the most powerful approaches for spatial modeling in the context of predictive mapping in ecology and soil science [49–52]. In comparison with

**Table 2.** Two-dimensional characterization of humus forms for modeling. At each site, the relative distribution of different ground cover types provided weights, which were used to spatially aggregate the related samples.

Humus form (according to [40,41])	Humus form (according to Fig. 2)	Biogenic soil structure in the mineral soil (relative units according to Fig. 2)	Presence of organic layers above mineral soil (relative units according to Fig. 2)
F-Mull (MUO)	Mull	1.0	0.0
Mullartiger Moder (MOM)	Mullmoder	0.5	0.5
Typischer Moder (MOA, MOR)	Moder	0.0	1.0
Rohhumusartiger Moder (MRA, MRR)	Moder	0.0	1.0
Rohhumus (ROA, ROR)	Moder	0.0	1.0
Amphimull (AMU)	Amphimull	1.0	1.0
Graswurzelfilz-Moder (GMO)	Moder	0.0	1.0
Hagerhumus (HMO)	Eroded Moder	0.0	0.0



single-tree-based models, the use of a random forest avoids overfitting tendencies, yet includes the concurrent influences of a large set of environmental variables. In this study, environmental variables included topographic and vegetation parameters. Terrain attributes were derived from a digital terrain model with a grid width of 1 m (Provincia Autonoma di Trento, Ufficio Sistemi Informativi – Servizio autorizzazioni e valutazioni ambientali, LiDAR data from 2006–2008, available at <http://dati.trentino.it/dataset/lidar-rilievo-2006-2007-2008-link-al-servizio-di-download>). These attributes included elevation, slope, slope exposure, general curvature, profile and plan-form curvature (all slope parameters derived according to [53]) and LS factor (following [54]). Vegetation characteristics included forest type and forest density (obtained from Provincia Autonoma di Trento, Servizio Foreste e Fauna). The random forest models of the humus form parameters and the pH value thereby accounted for the highly heterogeneous conditions of relief and vegetation in the study area. In all random forest models, the number of trees amounted to 10,000 and the terminal nodes had a minimum size of 3 elements. Spatial modeling was performed with the statistical software R [55] and the R package randomForest [56].

Linear models were used to quantify the relationships between the pH value and microbiological parameters. These models were based on the data from the sites N1–N3 and S6–S8. For each sample from these sites, data was taken from that soil depth at which the uppermost mineral horizon was found (Tables S1 and S2). Those linear models with a highly significant correlation ( $p < 0.01$ ) were used to derive spatial models of the microbiological parameters from the model of topsoil acidity.

## 2.5. Model Assessment

The random forest models (used for humus form parameters and topsoil acidity) were evaluated by the mean value of the squared model residuals and the explained variance of the model [56]. The predicted values of the model refer to the out-of-bag samples, respectively, i.e., the set of trees where a sample does not belong to the data used for model training.

The linear models underlying the upscaling procedure of microbiological parameters were evaluated with the standard errors of the predictions. Maps of the standard errors were generated to reveal the spatially variable precision of the predicted values.

In order to assess the transferability of the upscaling results from pH values to humus forms, the relationships between the predictions of humus form parameter values on the one hand and pH values, enzyme activities and the soil C/N ratio on the other hand were examined using linear regression analyses.

## 3. RESULTS

The results from sampling of humus forms and topsoil acidity at the sites RN1–RN30 and RS1–RS30 show a distinct dominance of moder humus forms (particularly in the higher parts of the study area). Mullmoder and mull humus forms occur especially at south-facing sites and Amphimull can be found only below 1600 m a.s.l. The pH values in the uppermost mineral soil horizon range from 4 (at site RN27) to 6 (at site RN1). The data basis for the spatial modeling of humus forms (as characterized by the biogenic soil structure in the mineral soil and the presence of organic layers above the mineral soil) and of topsoil acidity is shown in Table 3 (raw data is presented in Table S3).

**Table 3.** Input data for modeling from sampling of humus forms and topsoil acidity.

Site	Humus form (according to Fig. 2)	Biogenic soil structure in the mineral soil (relative units according to Fig. 2)	Presence of organic layers above mineral soil (relative units according to Fig. 2)	pH in A horizon H <sub>2</sub> O (1:10)
RN1	Amphimull	1.0	1.0	6.06
RN2	Mullmoder	0.5	0.5	5.18
RN3	Moder	0.0	1.0	4.88
RN4	Amphimull	1.0	1.0	5.20
RN5	Amphimull, Mull	1.0	0.7	5.14
RN6	Eroded Moder, Moder	0.0	0.5	4.63
RN7	Moder	0.0	1.0	4.82
RN8	Moder	0.0	1.0	4.63
RN9	Moder	0.0	1.0	5.00
RN10	Amphimull	1.0	1.0	4.62
RN11	Moder, Mullmoder	0.25	0.75	4.57
RN12	Mullmoder, Moder	0.4	0.6	4.47
RN13	Moder	0.0	1.0	4.42
RN14	Moder	0.0	1.0	4.45
RN15	Moder	0.0	1.0	4.68
RN16	Moder	0.0	1.0	4.80
RN17	Moder	0.0	1.0	4.20
RN18	Moder	0.0	1.0	4.25
RN19	Moder	0.0	1.0	4.67
RN20	Moder	0.0	1.0	4.73
RN21	Moder	0.0	1.0	4.17
RN22	Moder	0.0	1.0	4.24
RN23	Moder	0.0	1.0	4.46
RN24	Moder	0.0	1.0	4.22
RN25	Mullmoder, Moder	0.4	0.6	4.67
RN26	Moder	0.0	1.0	4.74
RN27	Moder	0.0	1.0	4.02
RN28	Moder	0.0	1.0	4.52
RN29	Mullmoder, Moder	0.4	0.6	4.70
RN30	Moder	0.0	1.0	4.05
RS1	Mull	1.0	0.0	5.70
RS2	Moder	0.0	1.0	5.80
RS3	Amphimull	1.0	1.0	4.43
RS4	Moder, Amphimull	0.4	1.0	4.75
RS5	Amphimull	1.0	1.0	5.79
RS6	Mull	1.0	0.0	5.36
RS7	Mullmoder, Mull	0.65	0.35	4.79
RS8	Moder, Amphimull	0.3	1.0	4.90
RS9	Amphimull	1.0	1.0	5.45
RS10	Mull	1.0	0.0	5.95
RS11	Mullmoder	0.5	0.5	5.39
RS12	Mullmoder	0.5	0.5	4.72
RS13	Mullmoder	0.5	0.5	5.30
RS14	Moder	0.0	1.0	4.61
RS15	Moder, Eroded Moder	0.0	0.6	4.76
RS16	Moder	0.0	1.0	4.66
RS17	Moder, Mull	0.3	0.7	4.86
RS18	Moder	0.0	1.0	4.72
RS19	Moder	0.0	1.0	4.49
RS20	Mull	1.0	0.0	5.30
RS21	Moder, Mull	0.5	0.5	4.71
RS22	Mullmoder	0.5	0.5	5.15
RS23	Mull	1.0	0.0	5.02
RS24	Moder	0.0	1.0	4.96
RS25	Moder	0.0	1.0	4.78
RS26	Moder	0.0	1.0	5.95
RS27	Moder	0.0	1.0	4.61
RS28	Moder	0.0	1.0	4.55
RS29	Moder	0.0	1.0	4.67
RS30	Moder	0.0	1.0	4.59

Chemical and microbiological analyses at the sites N1–N3 and S6–S8 show distinct variations of the investigated parameters with soil depth (especially for the ratio of bacterial/archaeal abundance and the enzymatic activities) (Table 4). At these sites, the range of pH values is comparable to the other 60 sites (from 4.2 to 6.0). In addition, the ratio of alkaline/acid phosphomonoesterase activity shows an increasing trend from northern exposure and high elevation to southern exposure and low elevation. The C/N ratio increases from south-facing to north-facing sites (Table 4).

Maps of humus form parameters (presence of organic layers above the mineral soil and biogenic soil structure in the mineral soil) were obtained from spatial modeling. According to the predictions, organic layers are present

almost throughout the whole north-facing slope (values close to 1), whereas there is a relatively heterogeneous pattern at the south-facing slope (Fig. 3a). The predictions of the biogenic soil structure in the uppermost mineral horizon embrace a distinct decreasing trend with elevation at the north-facing slope. This holds partially true for the south-facing slope, where the predicted percentage of biogenic soil structure is generally higher as compared to the north-facing slope (Fig. 3b). The predicted distribution of pH values of the A horizon is presented in Fig. 4. Apart from considerable local patterns of variability, these predictions show a general trend of decreasing topsoil acidity from high to low elevation and from northern to southern slope exposure.

The results of the submodels (random forests

**Table 4.** Chemical and microbiological properties of the soils collected at the six study sites at north- and south-facing areas (N1–N3 and S6–S8, respectively). The results are shown pairwise, i.e., the couples of north- and south-facing sites at the same elevation (N1–S6; N2–S7; N3–S8). Values are means ( $n = 3$ )  $\pm$  standard deviations. Data are expressed on a dry weight basis. At all sites, soil C only includes organic C ( $C_{org}$ ). Nitrogen values used for calculation of the soil C/N ratio refer to total nitrogen ( $N_t$ ).

Site	Soil depth (cm)	pH H <sub>2</sub> O (1:10)	Leucine-aminopeptidase activity (nmol MUF g <sup>-1</sup> dry soil h <sup>-1</sup> )	Ratio of alkaline/acid phosphomonoesterase activity	Total C content (%)	Soil C <sub>org</sub> /N <sub>t</sub> ratio	Ratio of bacterial/archaeal abundance
N1	0–5	4.8 $\pm$ 0.4	368.9 $\pm$ 184.9	0.14 $\pm$ 0.1	24.6 $\pm$ 2.4	26.9 $\pm$ 3.9	11.8 $\pm$ 11.9
	5–10	4.8 $\pm$ 0.4	85.5 $\pm$ 48.9	0.08 $\pm$ 0.1	10.6 $\pm$ 6.2	20.6 $\pm$ 2.2	6.4 $\pm$ 3.5
	10–15	4.8 $\pm$ 0.3	31.5 $\pm$ 21.9	0.04 $\pm$ 0.1	4.4 $\pm$ 1.9	18.1 $\pm$ 3.7	1.7 $\pm$ 0.4
S6	0–5	6.0 $\pm$ 0.5	283.6 $\pm$ 56.6	0.83 $\pm$ 1.0	10.2 $\pm$ 3.7	19.9 $\pm$ 3.3	42.6 $\pm$ 43.3
	5–10	5.7 $\pm$ 0.6	94.5 $\pm$ 27.9	0.52 $\pm$ 0.6	4.0 $\pm$ 0.5	17.4 $\pm$ 2.8	20.9 $\pm$ 7.4
	10–15	5.6 $\pm$ 0.5	57.1 $\pm$ 19.5	0.40 $\pm$ 0.4	2.6 $\pm$ 0.8	15.4 $\pm$ 1.9	10.0 $\pm$ 7.8
N2	0–5	4.7 $\pm$ 0.8	393.7 $\pm$ 300.7	0.17 $\pm$ 0.2	42.8 $\pm$ 9.8	23.8 $\pm$ 4.2	232.4 $\pm$ 332.8
	5–10	4.3 $\pm$ 0.6	115.5 $\pm$ 45.4	0.04 $\pm$ 0.1	33.1 $\pm$ 13.5	24.8 $\pm$ 4.0	55.7 $\pm$ 54.6
	10–15	4.5 $\pm$ 0.6	38.9 $\pm$ 8.8	0.02 $\pm$ 0.02	11.3 $\pm$ 8.4	20.0 $\pm$ 1.8	14.5 $\pm$ 22.2
S7	0–5	5.7 $\pm$ 0.2	866.8 $\pm$ 80.9	0.56 $\pm$ 0.2	23.1 $\pm$ 1.0	18.1 $\pm$ 2.0	650.2 $\pm$ 446.5
	5–10	5.8 $\pm$ 0.2	207.5 $\pm$ 77.9	0.62 $\pm$ 0.2	9.0 $\pm$ 2.3	15.9 $\pm$ 1.5	250.4 $\pm$ 356.0
	10–15	5.8 $\pm$ 0.3	131.0 $\pm$ 75.5	0.67 $\pm$ 0.4	5.6 $\pm$ 1.6	14.9 $\pm$ 2.0	17.2 $\pm$ 14.9
N3	0–5	4.6 $\pm$ 0.3	375.3 $\pm$ 115.1	0.07 $\pm$ 0.04	46.3 $\pm$ 2.3	22.5 $\pm$ 2.2	340.6 $\pm$ 548.3
	5–10	4.2 $\pm$ 0.2	123.8 $\pm$ 25.8	0.02 $\pm$ 0.01	38.7 $\pm$ 12.9	22.0 $\pm$ 2.3	24.7 $\pm$ 6.1
	10–15	4.2 $\pm$ 0.3	77.4 $\pm$ 8.7	0.02 $\pm$ 0.01	18.8 $\pm$ 8.1	21.1 $\pm$ 1.8	17.2 $\pm$ 15.2
S8	0–5	5.4 $\pm$ 0.4	289.5 $\pm$ 144.1	0.16 $\pm$ 0.2	24.0 $\pm$ 11.4	21.0 $\pm$ 0.8	75.7 $\pm$ 94.4
	5–10	5.4 $\pm$ 0.2	70.8 $\pm$ 19.9	0.07 $\pm$ 0.02	10.1 $\pm$ 5.9	16.7 $\pm$ 2.0	19.1 $\pm$ 3.6
	10–15	5.4 $\pm$ 0.3	90.9 $\pm$ 6.5	0.07 $\pm$ 0.1	6.1 $\pm$ 0.5	14.2 $\pm$ 1.7	6.8 $\pm$ 10.9

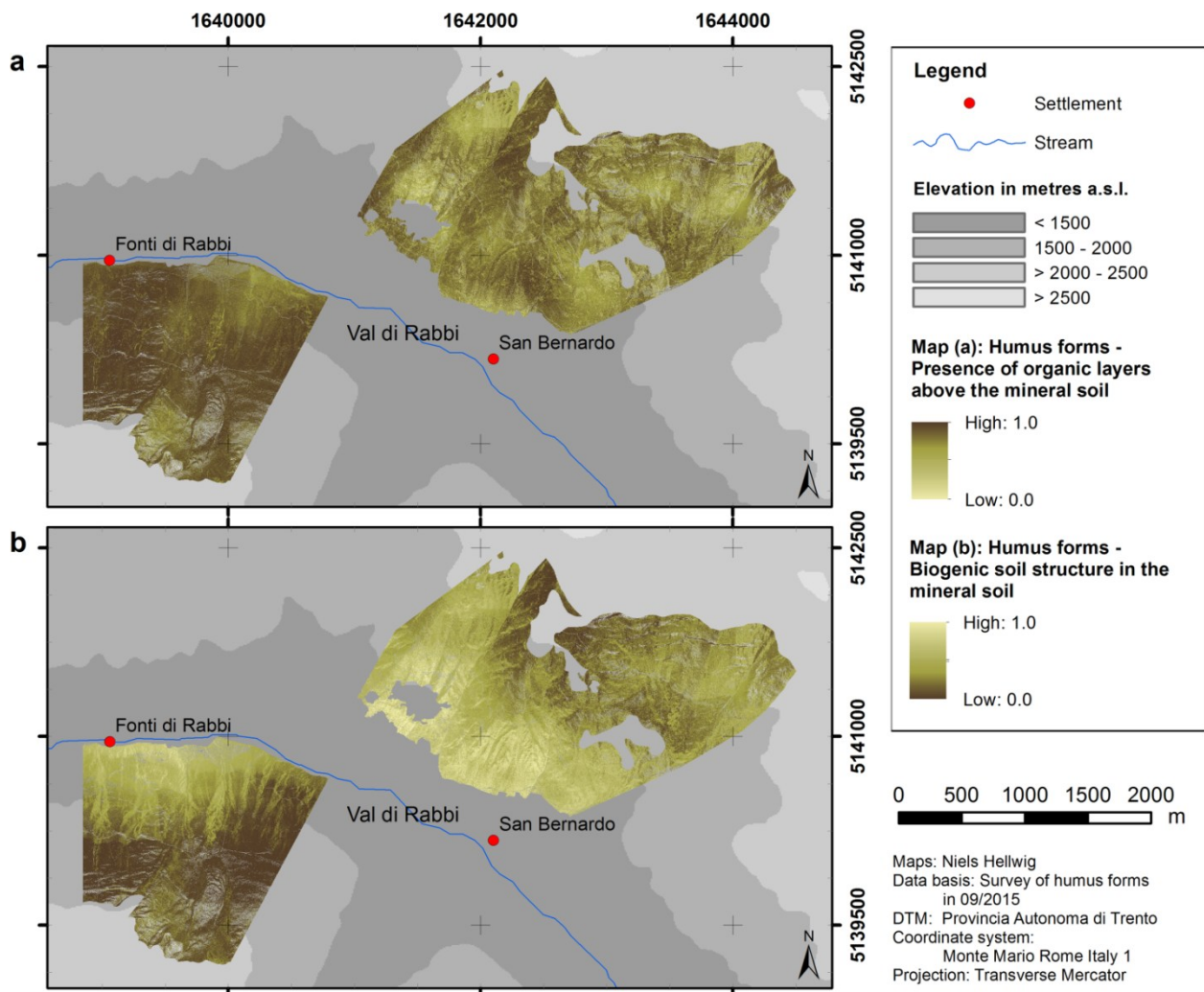


**Figure 3.** Predicted distribution of the two modeled humus form dimensions: (a) presence of organic layers above the mineral soil; (b) biogenic soil structure in the mineral soil.

and kriging procedures) are shown in Figs. S1–S6. Mean values of the squared residuals and explained variances of the underlying random forest models are shown in Table 5.

The relationships between the pH value and microbiological parameters as quantified by linear models are summarized in Table 6. On the basis of the *P* values of the linear models, the leucine-aminopeptidase activity, the ratio of alkaline/acid phosphomonoesterase activity and the C/N ratio are rated as usable parameters for upscaling, whereas the ratio of bacterial/archaeal abundance is rated as not usable.

The results of upscaling of the enzyme activities as well as the C/N ratio are presented as predictive maps (Fig. 5). Because of the linear

relationship to the topsoil pH value, the patterns concur with the predicted distribution of pH values (Fig. 4). The predicted activity of leucine-aminopeptidase in the uppermost mineral horizon ranges from 22.0 to 310.4 nmol MUF g<sup>-1</sup> dry soil h<sup>-1</sup>; the ratio of alkaline/acid phosphomonoesterase has values up to 1.0 (where the activity of alkaline phosphomonoesterase is predicted to equal the activity of acid phosphomonoesterase). Within our study area, both parameters are generally predicted to be lower at northern slope exposure and high elevation as compared to southern slope exposure and low elevation. The predicted values of the C/N ratio range from 16 at south-facing sites with low elevation to 23 at north-facing sites.

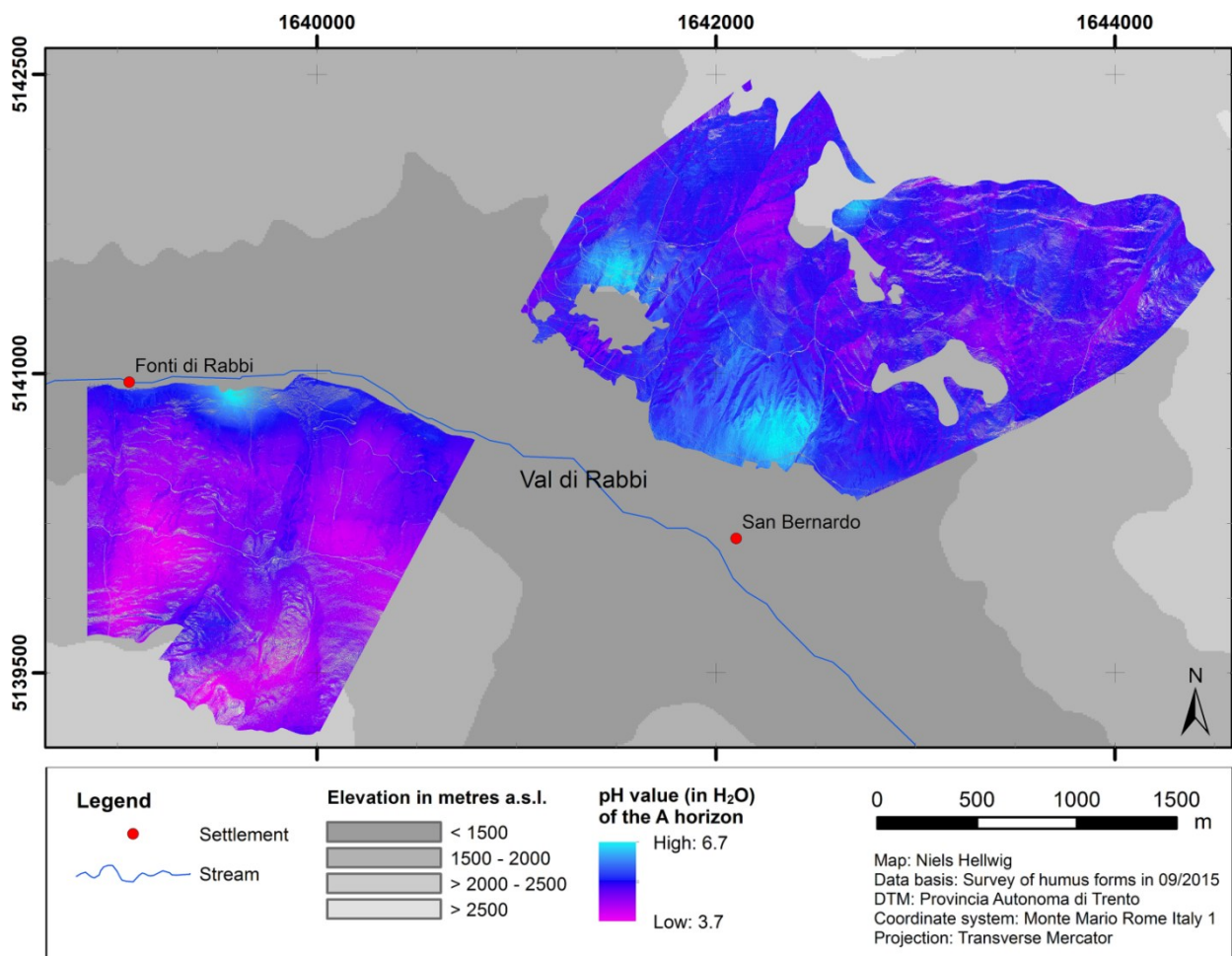


**Figure 4.** Predicted distribution of topsoil acidity.

Fig. 6 shows the standard error of the predictions from upscaling using the example of leucine-aminopeptidase (see Figs. S7 and S8

**Table 5.** Quality measures of the random forest models.

Parameter	Mean values of squared residuals	Explained variance (%)
Presence of organic layers above the mineral soil	0.079	18.05
Biogenic soil structure in the mineral soil	0.118	24.18
pH value (H <sub>2</sub> O)	0.140	37.04

for alkaline/acid phosphomonoesterase and C/N ratio). The predictions from linear modeling tend to be more imprecise at sites with predicted values below ca. pH 4.2 and above ca. pH 6.0 than at sites with intermediate pH values.

The linear regression models used for the analysis of the transferability of upscaling results from the pH value to humus forms revealed moderate, but highly significant relationships between the predictions of humus form dimensions (biogenic soil structure in the mineral soil and presence of organic layers above the mineral soil) on the one hand and the predicted pH values, enzyme activities and soil C/N ratio on the other hand (Table 7).

**Table 6.** Results of linear modeling of microbiological parameters and the soil C/N ratio as a function of the pH value ( $n$  = number of observations).

Parameter	$n$	Linear regression equation	Residual standard error	$R^2$	$P$ value
Leucine-aminopeptidase activity	89	$y = 98.87x - 348.57$	171.9	0.1569	<0.001
Ratio of alkaline/acid phosphomonoesterase activity	88	$y = 0.45988x - 2.05861$	0.2882	0.5889	<0.001
Soil C/N ratio	87	$y = -3.4416x + 37.2690$	3.51	0.3425	<0.001
Ratio of bacterial/archaeal abundance	18	$y = 61.08x - 258.55$	149.5	0.0914	0.223

## 4. DISCUSSION

### 4.1. Spatial Modeling of Humus Forms and Topsoil Acidity

The spatial models illustrate that humus forms, as well as pH values of the A horizon, in our study area are arranged in patterns corresponding to topographical features. The distributions of both humus form dimensions (presence of organic layers above the mineral soil and biogenic soil structure in the mineral soil) are related to slope exposure. Nevertheless, spatial patterns of both humus form dimensions are relatively dissimilar (Fig. 3). This implies that effects of topographic characteristics on the biological activity in the mineral soil are different from those on the formation of organic layers. For example, the percentage of biogenic soil structure in the mineral soil distinctly decreases within the forested area from low to high elevation (which indicates a decline of burrowing and mixing activities of soil organisms), whereas the presence of organic layers does not show discernible variations in terms of elevation. It would be interesting to analyze in more detail, if the climatic conditions in our study area have a higher effect on the biogenic soil structure in the mineral soil as compared to the presence of organic layers. The results

generally emphasize the dominance of moder-like humus forms on the north-exposed slope, especially at high elevation. Mull-like humus forms, on the contrary, mainly occur at the south-exposed slope, especially at low elevation. However, the correlations of the topography with the biogenic soil structure and with the presence of organic layers are different. Therefore, the humus forms Amphimull and Eroded Moder are also common in our study area.

The distribution of pH values of the A horizon likewise relates to the topographical situation, which influences the microclimatic conditions and the kind of litter: low pH values (around 4.0–4.5) are clearly dominant on the north-exposed slope (except for the very lowest part). In contrast, on the south-exposed slope there is a trend of relatively high pH values (around 6.5) decreasing with elevational gain to lower average values (around 4.5–5.0). Consequently, the analogous distributions of humus forms and pH values generally turn out as expected [6]: the presence of mull-like humus forms characterized by a high biological activity in the mineral soil coincides with higher pH values as compared to moder-like humus forms. Altogether, these findings at the slope scale confirm and amplify the trends from modeling at broader scales [9,57].



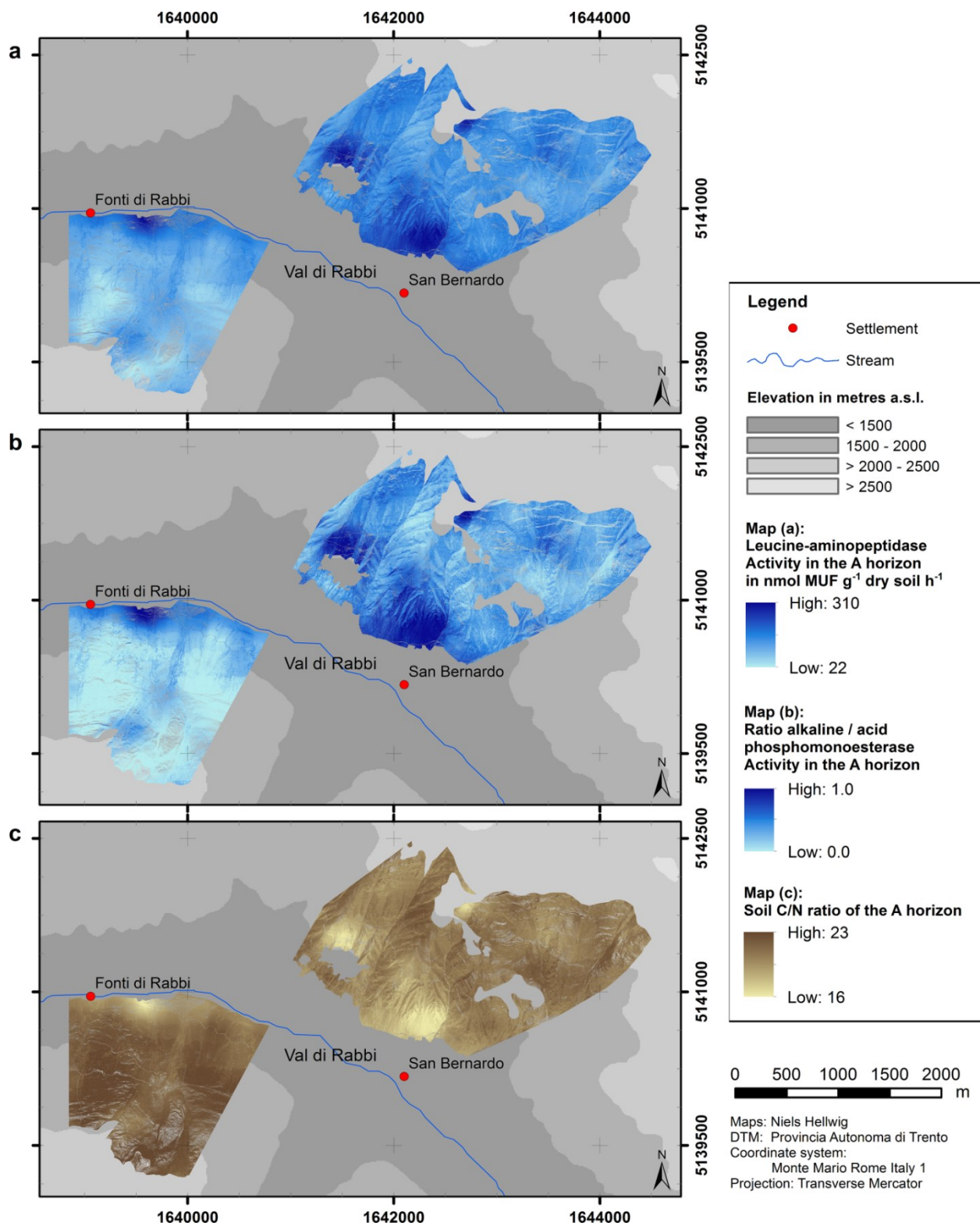


**Figure 5.** Predicted distributions of microbiological parameters.

Regarding the quality of the presented models, the mean values of the squared residuals from the random forest models are low in relation to the total ranges of values. Nevertheless, the random forest models show relatively low explained variances (about 18–

37%). Therefore, we addressed the local variability in the data (which the random forest models were not able to cover) by means of a kriging procedure of the model residuals (Figs. S2, S4 and S6). This way, the deviations of the observed values from those values



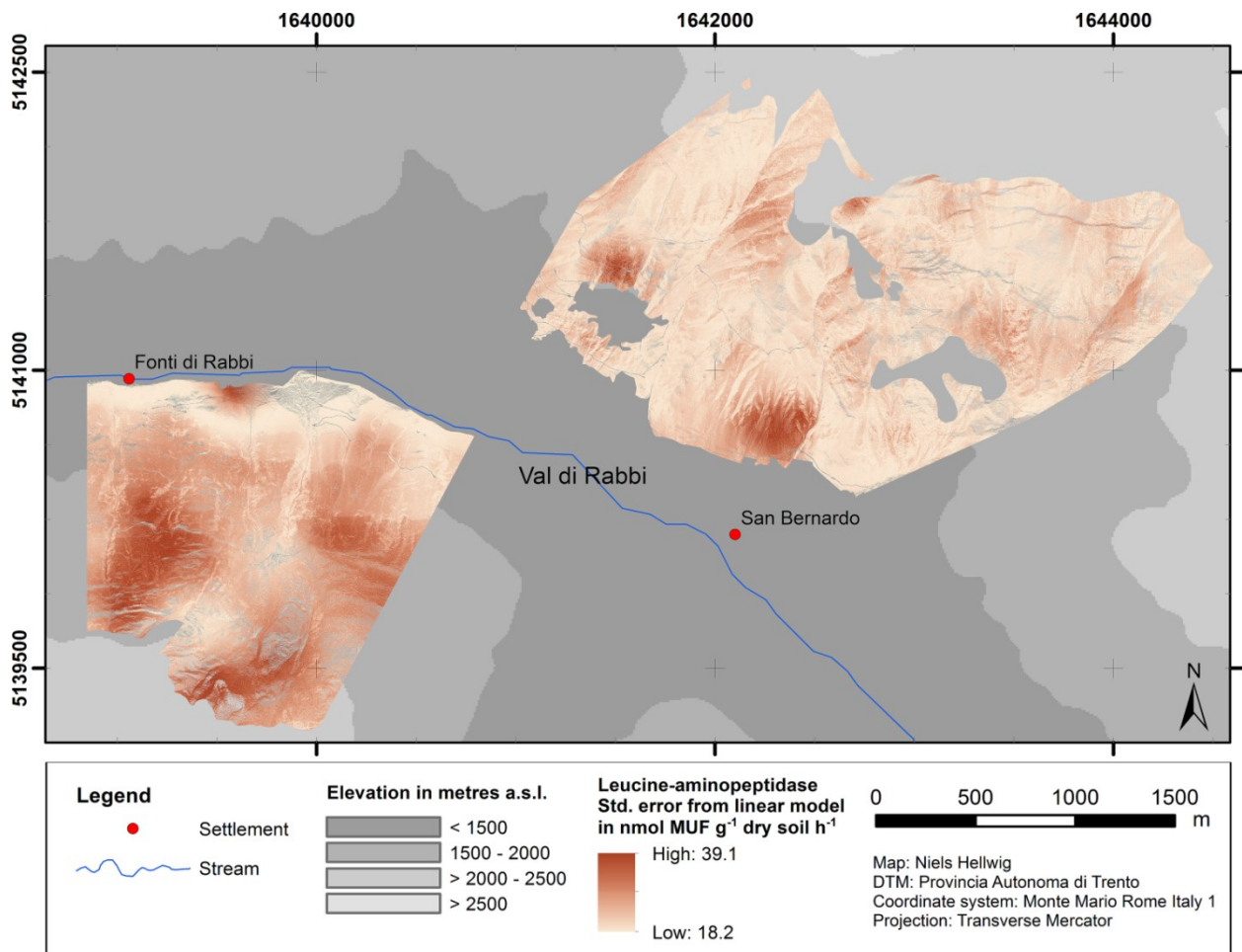


**Figure 6.** Standard error of predictions from linear model of leucine-aminopeptidase activity as a function of the pH value.

predicted by the random forest model (based on out-of-bag samples) could be included in the final predictions. Therefore, the quality of the presented models is altogether rated as high. However, the model results only account for the effects of topographic variation and spatial forest patterns (random forest models) together with deviations given by the kriging of the model residuals. This implies that the models do not reflect possible effects of variation of siliceous bedrock (as geological conditions are similar throughout the study area). Furthermore, the models are not representative of local peculiarities of un-sampled locations within the study area (e.g. totally different percentages of ground cover types or local disturbances).

Until now, only a few studies have considered spatial modeling of humus forms or

organic horizons in high mountain areas. Aberegg et al. [30] used a classification tree approach to model the distribution of mull, moder and mor humus forms. In a more recent study, Hellwig et al. [57] introduced an approach based on decision tree analysis and fuzzy logic for modeling humus forms. This approach was specially designed for highly heterogeneous areas in the high mountains, where only a low amount of sample data is available due to poor accessibility. Recent implementations of this model addressed the presence of OH horizons [9,57]. The humus form model presented in this study also involves the biological activity in the mineral soil, thus accounting for the properties of five different humus form classes (Fig. 2).

The lack of studies on spatial modeling of humus forms and other soil parameters relat-

**Table 7.** Results of linear regression analysis between predictions for humus forms ( $x_1$  = presence of organic layers above the mineral soil,  $x_2$  = biogenic soil structure in the mineral soil) (Fig. 3) and predictions of topsoil acidity and microbiological parameters (Figs. 4 and 5) ( $n = 5891366$ , number of predicted pixels).

Parameter	Linear regression equation	Residual standard error	Adj. $R^2$	$P$ value
pH value	$y = -0.53x_1 + 0.68x_2 + 5.05$	0.2156	0.4332	<0.001
Leucine-aminopeptidase activity	$y = -60.80x_1 + 67.97x_2 + 159.70$	30.54	0.3009	<0.001
Ratio of alkaline/acid phosphomonoesterase activity	$y = -0.27x_1 + 0.29x_2 + 0.31$	0.1259	0.3084	<0.001
Soil C/N ratio	$y = 2.12x_1 - 2.37x_2 + 19.58$	1.063	0.3009	<0.001

ed to organic matter decomposition contradicts the benefits of spatial models as compared to conventional mapping approaches. Soil analysis in the field is often time-consuming and costly. This is especially true for high mountain areas, where the spatial variation of soil properties is complex due to highly heterogeneous environmental conditions. In this context, digital soil mapping techniques are valuable tools to utilize and combine extensive information on soil-forming factors, for example from remote sensing [58].

#### 4.2. Upscaling of Microbiological Parameters

Topsoil pH values appear to be useful for upscaling three out of the four parameters investigated in this study: leucine-aminopeptidase activity, ratio of alkaline/acid phosphomonoesterase activity and C/N ratio. The significant correlations that we found between pH values, C/N ratio and enzyme activities correspond to the study of Leifeld and von Lützwow [59], who found that microbial soil organic matter decomposition depended on pH and substrate C/N ratio rather than on inherent chemical substrate properties. As linear models depending on pH value were used for upscaling (Table 6), the predicted spatial pat-

terns of enzyme activities and C/N ratio are arranged in the same spatial patterns as the pattern of pH values (Fig. 5). The significant relationships that we found between predicted humus form dimensions on the one hand and predicted pH values, enzyme activities and soil C/N ratio on the other hand suggest that also humus forms are a suitable indicator of microbiological processes related to organic matter decomposition.

Regarding leucine-aminopeptidase activity, the positive relationship with topsoil pH values aligns with Sinsabaugh et al. [60], who found an increase of this activity with increasing soil pH levels (pH 4 to 8.5). Furthermore, the slope exposure had a significant impact on leucine-aminopeptidase activity, even though such exposure-effect was elevation-dependent and a higher activity was registered at south than at north exposure only at 1400 m a.s.l. This suggests that at this specific elevation this enzymatic activity might have been more sensitive to the differences in soil temperature between both slopes, bearing in mind that also in alpine soils temperature is an important factor in the regulation of soil N mineralization [61]. In addition, the type of vegetation could also have influenced the potential activity of the leucine-aminopeptidase, since the proportion of easily available

monomers and polymers that enter the soil varies greatly depending on plant community composition as pointed out by Sanaullah et al. [62].

Similar to the activity of leucine-aminopeptidase, the ratio of alkaline/acid phosphomonoesterase activity shows a positive relationship with topsoil pH values. This implies that the activity of alkaline phosphomonoesterase increases as compared to the activity of acid phosphomonoesterase under less acidic conditions, which is consistent with earlier studies [63,64]. The ratio of alkaline/acid phosphomonoesterase activity has also previously been reported as being closely related to the soil pH value [65]. Our results confirm this relationship for high mountain forests of the Central Alps.

The soil C/N ratio of the A horizon is significantly, positively correlated with the pH value. Similarly to the results of this study, other studies from mountain areas have shown an increasing C/N ratio of the topsoil with elevation depending on the kind of litter [66–68]. Moreover, Cools et al. [20] found a distinct relationship between the topsoil C/N ratio and the humus form.

The linear models used to quantify the relationships between the pH value and the microbiological parameters are all highly significant, but differ in the explained variation as indicated by the coefficient of determination ( $R^2$ ) (Table 6). Accordingly, a ranking of the parameters can be deduced with regard to the quality of the predictions and to the usability for upscaling by proxy of humus forms and topsoil pH values. The ratio of alkaline/acid phosphomonoesterase activity is ranked first; the C/N ratio follows in the second position; the leucine-aminopeptidase activity takes the third position.

Additionally, standard errors of the predictions from the linear models were determined to assess the accuracy of the predicted values

in respect of its spatial variability. Although the pattern of the standard errors corresponds with the independent variable (pH value), the maps indicate those areas, where predictions are less accurate (mostly at the north-facing slope). Furthermore, they provide quantitative accuracy values, which allow for the consideration of the magnitude of deviations when using predicted values.

Contrary to the aforementioned parameters, upscaling based on pH values is infeasible for the ratio of bacterial/archaeal abundance ( $P$  value ca. 0.22). Prosser and Nicol [23] suggested ammonia limitation, mixotrophy, and pH as the main factors providing niche specialization and differentiation between soil ammonia oxidizing archaea (AOA) and ammonia oxidizing bacteria (AOB) in a wide range of soil types. In a study of forest soils along an elevation gradient in South Tyrol (Italian Alps), Siles and Margesin [69] found that bacterial and fungal diversity properties and community structures were highly correlated to topsoil pH values. However, archaeal, bacterial and fungal abundances were not significantly related to pH values [69]. Corresponding to these findings, the results of our study do not identify a significant relationship between the pH values and the ratio of bacterial/archaeal abundance in the topsoil of a high mountain forest. This might be due to the complex interactions and ecological functions of soil microorganisms or caused by the range of low pH values, in particular at the north-facing slope. Especially for undisturbed forest soils, our knowledge of its autochthonous microorganisms – even in the era of high throughput molecular ecology – remains limited [18,70].

Upscaling of microbiological parameters is based on two sampling sets and two steps of modeling (random forest model together with kriging of the residuals and linear regression analysis). Therefore, the model results are

subject to potential uncertainty due to limitations both of the sample data and of the models. The sampling set used for microbiological analyses comprises considerably less investigation sites than the sampling set used for the determination of humus forms. Hence, that sampling set is less representative in terms of factors such as elevation. In addition, those samples for microbiological analyses partly were collected at sites within a few kilometers distance from the slopes where humus forms were described (Fig. 1). With respect to upscaling, the spatial patterns of the pH value are used to derive predictions of the microbiological parameters with a linear model. The model evaluation revealed that this is feasible for all parameters except for the ratio of bacterial/archaeal abundance. Nevertheless, the actual relationship remains uncertain (whether linear or not) and other factors potentially relevant for microbiological properties of the mineral soil (e.g. soil C content, depth of the A horizon) are not part of these models.

### 4.3. Soil Ecological Implications

In mountain ecosystems, topography causes a high spatial variability of microclimatic conditions and slope dynamics. The results of this study emphasize the considerable effects of topography on decomposition processes as expressed by the distribution of humus forms, topsoil pH values and microbiological parameters. Bojko and Kabala [71] established a significant relationship between soil organic carbon pools and humus forms of mountain soils. In that regard, our results confirm the findings from earlier studies that demonstrated the pivotal role of topography (alongside with factors such as vegetation and climate) for the formation of soil organic carbon patterns in high mountain areas [72–74]. Spatial variation of organic matter decomposition has

been reported to be engendered by differences of soil temperature [75–78], soil moisture [79–82], litter quality and quantity [83–85], slope processes [86] and seasonality. These factors are likely to be strongly affected by the topographic diversity in our study area, thus they potentially govern also spatial differences that we found in the models of this study.

Furthermore, the results of this study are in line with the patterns of humus forms and soil pH values described in previous studies of mountain forests. Egli et al. [87] investigated mountain soils also within the area of this study and found a higher percentage of weakly degraded organic matter as well as higher soil organic carbon concentrations at northern slope exposure as compared to southern slope exposure. Other studies described patterns similar to this study regarding humus forms, pH values and soil C/N ratio along an elevation gradient (e.g. [66,88]).

However, random forest models alone are not sufficient to predict the spatial distribution of humus forms and pH values. Most of the variance in humus forms and pH values is not explained by those models depending on climatic, topographic and vegetation influences. This insight points to the importance of additional, currently undiscovered mechanisms determining decomposition processes. These may include rather local effects of decomposer organisms [89,90], caused by e.g. litter affinity of decomposer organisms [91,92], temporal shifts of decomposer communities during decomposition [93] and responses to different levels of litter species diversity [81,94].

The results of this study show a strong relationship between topography on the one hand and enzyme activities and the C/N ratio of the topsoil on the other hand (Fig. 5). This relationship might be relevant to consider also for

projections of future landscape development, as C and N cycling are predicted to be affected by climate change, especially at high-elevation sites [95,96].

When integrated with those of previous studies [8,9,28], our findings show that the humus form proves to be a comprehensive indicator for soil ecological processes in a high mountain environment of the Central Alps, including soil macro- and mesofaunal as well as microbiological properties.

## 5. CONCLUSION

Variations of humus forms, pH values and microbiological parameters investigated in this study are arranged in patterns that are related to topography. Although the underlying random forest models explain only between 18 and 37% of the variances of humus form parameters and pH values, the predictive maps reveal distinct patterns especially corresponding to elevation and slope exposure. These patterns are also reflected by the spatial models of microbiological parameters. Unlike the ratio of bacterial/archaeal abundance, all parameters are highly significantly correlated with the pH value. Regarding their usability for upscaling by proxy of humus forms and topsoil pH values, they can be ranked as follows: 1) the ratio of alkaline/acid phosphomonoesterase activity, 2) the C/N ratio, 3) the leucine-aminopeptidase activity.

With this study, we applied concepts from digital soil mapping to the field of soil microbiology. This study illustrates both the capability and the high value of modeling techniques to cope with soil ecological research questions in a spatial context. Thus, we encourage further usage of soil-landscape modeling in the context of soil ecological studies.

## ACKNOWLEDGEMENTS

This work was realized in the context of the D.A.CH. project DecAlp and funded by the German Research Foundation (DFG, grant number BR 1106/23-1), the Austrian Science Fund (FWF, I989-B16) and the Swiss National Science Foundation (SNF). The authors thank all colleagues in the project for excellent cooperation. We also thank Dott. Fabio Angeli (Ufficio Distrettuale Forestale di Malè) and the Stelvio National Park for supporting the field work. We are grateful to Alison Simerly for proofreading. María Gómez-Brandón acknowledges support by the Programa Ramón y Cajal (RYC-2016-21231; Ministerio de Economía y Competitividad).

## REFERENCES

1. Ponge, J.F. Plant-soil feedbacks mediated by humus forms: A review. *Soil Biol. Biochem.* **2013**, *57*, 1048–1060.
2. Graefe, U.; Beylich, A. Humus forms as tool for upscaling soil biodiversity data to landscape level? *Mitt. Dtsch. Bodenkd. Ges.* **2006**, *108*, 6–7.
3. Ponge, J.F. Humus forms in terrestrial ecosystems: a framework to biodiversity. *Soil Biol. Biochem.* **2003**, *35*, 935–945.
4. Moscatelli, M.C.; Bonifacio, E.; Chiti, T.; Cudlin, P.; Dinca, L.; Gömöryova, E.; Grego, S.; La Porta, N.; Karlinski, L.; Pellis, G.; Rudawska, M.; Squartini, A.; Zhiyanski, M.; Broll, G. Soil properties as indicators of treeline dynamics in view of anthropogenic pressure and climate change. *Clim. Res.* **2017**, *73*, 73–84.
5. Graefe, U.; Schmelz, R.M. Indicator values, strategy types and life forms of terrestrial Enchytraeidae and other microannelids. *Newsl. Enchytraeidae* **1999**, *6*, 59–67.

6. Labaz, B.; Galka, B.; Bogacz, A.; Waroszewski, J.; Kabala, C. Factors influencing humus forms and forest litter properties in the mid-mountains under temperate climate of southwestern Poland. *Geoderma* **2014**, *230–231*, 265–273.
7. Andreetta, A.; Cecchini, G.; Bonifacio, E.; Cornolli, R.; Vingiani, S.; Carnicelli, S. Tree or soil? Factors influencing humus form differentiation in Italian forests. *Geoderma* **2016**, *264*, 195–204.
8. Ascher, J.; Sartori, G.; Graefe, U.; Thornton, B.; Ceccherini, M.T.; Pietramellara, G.; Egli, M. Are humus forms, mesofauna and microflora in subalpine forest soils sensitive to thermal conditions? *Biol. Fertil. Soils* **2012**, *48*, 709–725.
9. Hellwig, N.; Graefe, U.; Tatti, D.; Sartori, G.; Anschlag, K.; Beylich, A.; Gobat, J.M.; Broll, G. Upscaling the spatial distribution of enchytraeids and humus forms in a high mountain environment on the basis of GIS and fuzzy logic. *Eur. J. Soil Biol.* **2017**, *79*, 1–13.
10. Baldrian, P. Microbial activity and the dynamics of ecosystem processes in forest soils. *Curr. Opin. Microbiol.* **2017**, *37*, 128–134.
11. Gianfreda, L.; Rao, M.A. *Enzymes in Agricultural Sciences*; OMICS Group International: Foster City, CA, United States of America, 2014.
12. Burns, R.G.; DeForest, J.L.; Marxsen, J.; Sinsabaugh, R.L.; Stromberger, M.E.; Wallenstein, M.D.; Weintraub, M.N.; Zoppini, A. Soil enzymes in a changing environment: current knowledge and future directions. *Soil Biol. Biochem.* **2013**, *58*, 216–234.
13. Matsui, M.; Fowler, J.H.; Walling, L.L. Leucine aminopeptidases: diversity in structure and function. *Biol. Chem.* **2006**, *387*, 1535–1544.
14. Burke, D.J.; Weintraub, M.N.; Hewins, C.R.; Kalisz, S. Relationship between soil enzyme activities, nutrient cycling and soil fungal communities in a northern hardwood forest. *Soil Biol. Biochem.* **2011**, *43*, 795–803.
15. Bardelli, T.; Gómez-Brandón, M.; Ascher-Jenull, J.; Fornasier, F.; Arfaioli, P.; Francioli, D.; Egli, M.; Sartori, G.; Insam, H.; Pietramellara, G. Effects of slope exposure on soil physico-chemical and microbiological properties along an altitudinal climosequence in the Italian Alps. *Sci. Total Environ.* **2017**, *575*, 1041–1055.
16. Salazar, S.; Sánchez, L.E.; Alvarez, J.; Valverde, A.; Galindo, P.; Igual, J.M.; Peix, A.; Santa-Regina, I. Correlation among soil enzyme activities under different forest ecosystem management practices. *Ecol. Eng.* **2011**, *37*, 1123–1131.
17. Nannipieri, P.; Giagnoni, L.; Renella, G.; Puglisi, E.; Ceccanti, B.; Masciandaro, G.; Fornasier, F.; Moscatelli, M.C.; Marinari, S. Soil enzymology: classical and molecular approaches. *Biol. Fertil. Soils* **2012**, *48*, 743–762.
18. Nannipieri, P.; Ascher, J.; Ceccherini, M.T.; Landi, L.; Pietramellara, G.; Renella, G. Microbial diversity and soil functions. *Eur. J. Soil Sci.* **2003**, *54*, 655–670.
19. Yamakura, T.; Sahunalu, P. Soil Carbon/Nitrogen Ratio as a Site Quality Index for Some South-East Asian Forests. *J. Trop. Ecol.* **1990**, *6*, 371–377.
20. Cools, N.; Vesterdal, L.; De Vos, B.; Vanguelova, E.; Hansen, K. Tree species is the major factor explaining C:N ratios in European forest soils. *For. Ecol. Manag.* **2014**, *311*, 3–16.
21. Bardgett, R.D.; Freeman, C.; Ostle, N.J. Microbial contributions to climate change through carbon cycle feedbacks. *ISME J.* **2008**, *2*, 805–814.
22. Venter, J.C.; Remington, K.; Heidelberg, J.F.; Halpern, A.L.; Rusch, D.; Eisen, J.A.; Wu, D.; Paulsen, I.; Nelson, K.E.; Nelson, W.; Fouts, D.E.; Levy, S.; Knap, A.H.; Lomas, M.W.; Nealson, K.; White, O.; Peterson, J.; Hoffman, J.; Parsons, R.; Baden-Tillson, H.; Pfannkoch, C.; Rogers, Y.H.; Smith, H.O. Environmental Genome Shotgun Sequencing of the Sargasso Sea. *Science* **2004**, *304*, 66–74.
23. Prosser, J.I.; Nicol, G.W. Archaeal and bacterial ammonia-oxidisers in soil: the quest for niche specialisation and differentiation. *Trends Microbiol.* **2012**, *20*, 523–531.
24. Isobe, K.; Ohte, N. Ecological Perspectives on Microbes Involved in N-Cycling. *Microbes Environ.* **2014**, *29*, 4–16.

25. Sterngren, A.E.; Hallin, S.; Bengtson, P. Archaeal Ammonia Oxidizers Dominate in Numbers, but Bacteria Drive Gross Nitrification in N-amended Grassland Soil. *Front. Microbiol.* **2015**, *6*, 1350.
26. Bengtson, P.; Barker, J.; Grayston, S.J. Evidence of a strong coupling between root exudation, C and N availability, and stimulated SOM decomposition caused by rhizosphere priming effects. *Ecol. Evol.* **2012**, *2*, 1843–1852.
27. Rousk, J.; Bååth, E.; Brookes, P.C.; Lauber, C.L.; Lozupone, C.; Caporaso, J.G.; Knight, R.; Fierer, N. Soil bacterial and fungal communities across a pH gradient in an arable soil. *ISME J.* **2010**, *4*, 1340–1351.
28. Gómez-Brandón, M.; Ascher-Jenull, J.; Bardelli, T.; Fornasier, F.; Sartori, G.; Pietramellara, G.; Arfaioli, P.; Egli, M.; Beylich, A.; Insam, H.; Graefe, U. Ground cover and slope exposure effects on micro- and mesobiota in forest soils. *Ecol. Indic.* **2017**, *80*, 174–185.
29. Andreetta, A.; Macci, C.; Giansoldati, V.; Masciandaro, G.; Carnicelli, S. Microbial activity and organic matter composition in Mediterranean humus forms. *Geoderma* **2013**, *209–210*, 198–208.
30. Aberegg, I.; Egli, M.; Sartori, G.; Purves, R. Modelling spatial distribution of soil types and characteristics in a high Alpine valley (Val di Sole, Trentino, Italy). *Stud. Trent. Sci. Nat.* **2009**, *85*, 39–50.
31. von Seidlein, C. Petrographie und Struktur des ostalpinen Altkristallins südlich des Ultentales (Trentino, Nord-Italien). Dissertation, Ludwig-Maximilians-Universität München, Munich, Germany, March 2000.
32. Dobrowski, S.Z. A climatic basis for microrefugia: the influence of terrain on climate. *Glob. Chang. Biol.* **2011**, *17*, 1022–1035.
33. Sboarina, C.; Cescatti, A. *Il clima del Trentino – Distribuzione spaziale delle principali variabili climatiche*, Report Centro Ecologia Alpina 33; Centro di ecologia alpina: Sardinia (Trento), Italy, 2004; 1–20.
34. Sartori, G.; Mancabelli, A. *Carta dei suoli del Trentino: scala 1:250.000*. Museo Tridentino di Scienze Naturali di Trento, Centro di Ricerca per l'Agrobiologia e la Pedologia di Firenze: Trento, Italy, 2009.
35. IUSS Working Group WRB. *World reference base for soil resources 2006*, World Soil Resources Report 103; FAO: Rome, Italy, 2006.
36. Egli, M.; Mirabella, A.; Sartori, G.; Zanelli, R.; Bischof, S. Effect of north and south exposure on weathering rates and clay mineral formation in Alpine soils. *Catena* **2006**, *67*, 155–174.
37. Anschlag, K.; Tatti, D.; Hellwig, N.; Sartori, G.; Gobat, J.M.; Broll, G. Vegetation-based bioindication of humus forms in coniferous mountain forests. *J. Mt. Sci.* **2017**, *14*, 662–673.
38. Minasny, B.; McBratney, A.B. A conditioned Latin hypercube method for sampling in the presence of ancillary information. *Comput. Geosci.* **2006**, *32*, 1378–1388.
39. Egli, M.; Hafner, S.; Derungs, C.; Ascher-Jenull, J.; Camin, F.; Sartori, G.; Raab, G.; Bontempo, L.; Paolini, M.; Ziller, L.; Bardelli, T.; Petrillo, M.; Abiven, S. Decomposition and stabilisation of Norway spruce needle-derived material in Alpine soils using a <sup>13</sup>C-labelling approach in the field. *Biogeochem.* **2016**, *131*, 321–338.
40. Ad-hoc-AG Boden. *Bodenkundliche Kartieranleitung*, 5th ed. E. Schweizerbart'sche Verlagsbuchhandlung: Hannover, Germany, 2005; ISBN 978-3-510-95920-4.
41. Graefe, U. Gibt es in Deutschland die Humusform Amphi? *Mitt. Dtsch. Bodenkd. Ges.* **2007**, *110*, 459–460.
42. Fornasier, F.; Margon, A. Bovine serum albumin and Triton X-100 greatly increase phosphomonoesterases and arylsulphatase extraction yield from soil. *Soil Biol. Biochem.* **2007**, *39*, 2682–2684.
43. Ascher, J.; Ceccherini, M.T.; Pantani, O.L.; Agnelli, A.; Borgogni, F.; Guerri, G.; Nannipieri, P.; Pietramellara, G. Sequential extraction and genetic fingerprinting of a forest soil metagenome. *Appl. Soil Ecol.* **2009**, *42*, 176–181.
44. Ferris, M.J.; Muyzer, G.; Ward, D.M. Denaturing gradient gel electrophoresis



- profiles of 16S rRNA-defined populations inhabiting a hot spring microbial mat community. *Appl. Environ. Microbiol.* **1996**, *62*, 340–346.
45. Coolen, M.J.L.; Hopmans, E.C.; Rijpstra, W.I.C.; Muyzer, G.; Schouten, S.; Volkman, J.K.; Damste, J.S.S. Evolution of the methane cycle in Ace Lake (Antarctica) during the Holocene: response of methanogens and methanotrophs to environmental change. *Org. Geochem.* **2004**, *35*, 1151–1167.
  46. Breiman, L. Random Forests. *Mach. Learn.* **2001**, *45*, 5–32.
  47. Heuvelink, G.B.M.; Webster, R. Modelling soil variation: past, present, and future. *Geoderma* **2001**, *100*, 269–301.
  48. Guo, P.T.; Li, M.F.; Luo, W.; Tang, Q.F.; Liu, Z.W.; Lin, Z.M. Digital mapping of soil organic matter for rubber plantation at regional scale: An application of random forest plus residuals kriging approach. *Geoderma* **2015**, *237–238*, 49–59.
  49. Prasad, A.M.; Iverson, L.R.; Liaw, A. Newer Classification and Regression Tree Techniques: Bagging and Random Forests for Ecological Prediction. *Ecosyst.* **2006**, *9*, 181–199.
  50. Cutler, D.R.; Edwards, Jr., T.C.; Beard, K.H.; Cutler, A.; Hess, K.T.; Gibson, J.C.; Lawler, J.J. Random Forests for Classification in Ecology. *Ecol.* **2007**, *88*, 2783–2792.
  51. Grimm, R.; Behrens, T.; Märker, M.; Elsenbeer, H. Soil organic carbon concentrations and stocks on Barro Colorado Island – Digital soil mapping using Random Forest analysis. *Geoderma* **2008**, *146*, 102–113.
  52. Heung, B.; Bulmer, C.E.; Schmidt, M.G. Predictive soil parent material mapping at a regional-scale: A Random Forest approach. *Geoderma* **2014**, *214–215*, 141–154.
  53. Zevenbergen, L.W.; Thorne, C.R. Quantitative analysis of land surface topography. *Earth Surf. Process. Landf.* **1987**, *12*, 47–56.
  54. Moore, I.D.; Grayson, R.B.; Ladson, A.R. Digital terrain modelling: a review of hydrological, geomorphological, and biological applications. *Hydrol. Process.* **1991**, *5*, 3–30.
  55. R Core Team. R: a Language and Environment for Statistical Computing. R Foundation for Statistical Computing: Vienna, Austria, 2016, <http://www.R-project.org/>.
  56. Liaw, A.; Wiener, M. Classification and Regression by randomForest. *R News* **2002**, *2*, 18–22.
  57. Hellwig, N.; Anschlag, K.; Broll, G. A fuzzy logic based method for modeling the spatial distribution of indicators of decomposition in a high mountain environment. *Arct. Antarct. Alp. Res.* **2016**, *48*, 623–635.
  58. Baruck, J.; Nestroy, O.; Sartori, G.; Baize, D.; Traidl, R.; Vrščaj, B.; Bräm, E.; Gruber, F.E.; Heinrich, K.; Geitner, C. Soil classification and mapping in the Alps: The current state and future challenges. *Geoderma* **2016**, *264*, 312–331.
  59. Leifeld, J.; von Lützw, M. Chemical and microbial activation energies of soil organic matter decomposition. *Biol. Fertil. Soils* **2014**, *50*, 147–153.
  60. Sinsabaugh, R.L.; Lauber, C.L.; Weintraub, M.N.; Ahmed, B.; Allison, S.D.; Crenshaw, C.; Contosta, A.R.; Cusack, D.; Frey, S.; Gallo, M.E.; Gartner, T.B.; Hobbie, S.E.; Holland, K.; Keeler, B.L.; Powers, J.S.; Stursova, M.; Takacs-Vesbach, C.; Waldrop, M.P.; Wallenstein, M.D.; Zak, D.R.; Zeglin, L.H. Stoichiometry of soil enzyme activity at global scale. *Ecol. Lett.* **2008**, *11*, 1252–1264.
  61. Koch, O.; Tscherko, D.; Kandeler, E. Temperature sensitivity of microbial respiration, nitrogen mineralization, and potential soil enzyme activities in organic alpine soils. *Glob. Biogeochem. Cycles* **2007**, *21*, GB4017.
  62. Sanaullah, M.; Blagodatskaya, E.; Chabbi, A.; Rumpel, C.; Kuzyakov, Y. Drought effects on microbial biomass and enzyme activities in the rhizosphere of grasses depend on plant composition. *Appl. Soil Ecol.* **2011**, *48*, 38–44.
  63. Eivazi, F.; Tabatabai, M.A. Phosphatases in Soils. *Soil Biol. Biochem.* **1977**, *9*, 167–172.
  64. Juma, N.G.; Tabatabai, M.A. Distribution of Phosphomonoesterases in Soils. *Soil Sci.* **1978**, *126*, 101–108.
  65. Dick, W.A.; Cheng, L.; Wang, P. Soil acid and alkaline phosphatase activity as pH

- adjustment indicators. *Soil Biol. Biochem.* **2000**, *32*, 1915–1919.
66. Badía, D.; Ruiz, A.; Girona, A.; Martí, C.; Casanova, J.; Ibarra, P.; Zufiaurre, R. The influence of elevation on soil properties and forest litter in the Siliceous Moncayo Massif, SW Europe. *J. Mt. Sci.* **2016**, *13*, 2155–2169.
67. Tashi, S.; Singh, B.; Keitel, C.; Adams, M. Soil carbon and nitrogen stocks in forests along an altitudinal gradient in the eastern Himalayas and a meta-analysis of global data. *Glob. Chang. Biol.* **2016**, *22*, 2255–2268.
68. Müller, M.; Oelmann, Y.; Schickhoff, U.; Böhner, J.; Scholten, T. Himalayan treeline soil and foliar C:N:P stoichiometry indicate nutrient shortage with elevation. *Geoderma* **2017**, *291*, 21–32.
69. Siles, J.A.; Margesin, R. Abundance and Diversity of Bacterial, Archaeal, and Fungal Communities Along an Altitudinal Gradient in Alpine Forest Soils: What Are the Driving Factors? *Microb. Ecol.* **2016**, *72*, 207–220.
70. Nannipieri, P.; Ascher-Jenull, J.; Ceccherini, M.T.; Giagnoni, L.; Pietramellara, G.; Renella, G. Microbial diversity and soil functions. *Eur. J. Soil Sci.* **2017**, *68*, 12–26.
71. Bojko, O.; Kabala, C. Organic carbon pools in mountain soils – Sources of variability and predicted changes in relation to climate and land use changes. *Catena* **2017**, *149*, 209–220.
72. Oueslati, I.; Allamano, P.; Bonifacio, E.; Claps, P. Vegetation and Topographic Control on Spatial Variability of Soil Organic Carbon. *Pedosphere* **2013**, *23*, 48–58.
73. Prietzel, J.; Christophel, D. Organic carbon stocks in forest soils of the German Alps. *Geoderma* **2014**, 221–222, 28–39.
74. Chen, L.-F.; He, Z.-B.; Du, J.; Yang, J.-J.; Zhu, X. Patterns and environmental controls of soil organic carbon and total nitrogen in alpine ecosystems of northwestern China. *Catena* **2016**, *137*, 37–43.
75. Davidson, E.A.; Janssens, I.A. Temperature sensitivity of soil carbon decomposition and feedbacks to climate change. *Nature* **2006**, *440*, 165–173.
76. Conant, R.T.; Ryan, M.G.; Ågren, G.I.; Birge, H.E.; Davidson, E.A.; Eliasson, P.E.; Evans, S.E.; Frey, S.D.; Giardina, C.P.; Hopkins, F.M.; Hyvönen, R.; Kirschbaum, M.U.F.; Lavalley, J.M.; Leifeld, J.; Parton, W.J.; Steinweg, J.M.; Wallenstein, M.D.; Wetterstedt, J.Å.M.; Bradford, M.A. Temperature and soil organic matter decomposition rates – synthesis of current knowledge and a way forward. *Glob. Chang. Biol.* **2011**, *17*, 3392–3404.
77. von Lützw, M.; Kögel-Knabner, I. Temperature sensitivity of soil organic matter decomposition – what do we know? *Biol. Fertil. Soils* **2009**, *46*, 1–15.
78. Klimek, B.; Jelonkiewicz, Ł.; Niklińska, M. Drivers of temperature sensitivity of decomposition of soil organic matter along a mountain altitudinal gradient in the Western Carpathians. *Ecol. Res.* **2016**, *31*, 609–615.
79. A’Bear, A.D.; Jones, T.H.; Kandeler, E.; Boddy, L. Interactive effects of temperature and soil moisture on fungal-mediated wood decomposition and extracellular enzyme activity. *Soil Biol. Biochem.* **2014**, *70*, 151–158.
80. Brockett, B.F.T.; Prescott, C.E.; Grayston, S.J. Soil moisture is the major factor influencing microbial community structure and enzyme activities across seven biogeoclimatic zones in western Canada. *Soil Biol. Biochem.* **2012**, *44*, 9–20.
81. Santonja, M.; Fernandez, C.; Proffit, M.; Gers, C.; Gauquelin, T.; Reiter, I.M.; Cramer, W.; Baldy, V. Plant litter mixture partly mitigates the negative effects of extended drought on soil biota and litter decomposition in a Mediterranean oak forest. *J. Ecol.* **2017**, *105*, 801–815.
82. García-Palacios, P.; Prieto, I.; Ourcival, J.-M.; Hättenschwiler, S. Disentangling the Litter Quality and Soil Microbial Contribution to Leaf and Fine Root Litter Decomposition Responses to Reduced Rainfall. *Ecosyst.* **2016**, *19*, 490–503.
83. De Long, J.R.; Dorrepaal, E.; Kardol, P.; Nilsson, M.C.; Teuber, L.M.; Wardle, D.A. Understory plant functional groups and litter species identity are stronger drivers of litter decomposition than warming along a boreal

- forest post-fire successional gradient. *Soil Biol. Biochem.* **2016**, *98*, 159–170.
84. Makkonen, M.; Berg, M.P.; Handa, I.T.; Hättenschwiler, S.; van Ruijven, J.; van Bodegom, P.M.; Aerts, R. Highly consistent effects of plant litter identity and functional traits on decomposition across a latitudinal gradient. *Ecol. Lett.* **2012**, *15*, 1033–1041.
85. Hättenschwiler, S.; Gasser, P. Soil animals alter plant litter diversity effects on decomposition. *Proc. Natl. Acad. Sci. U. S. A.* **2005**, *102*, 1519–1524.
86. Berhe, A.A.; Harden, J.W.; Torn, M.S.; Harte, J. Linking soil organic matter dynamics and erosion-induced terrestrial carbon sequestration at different landform positions. *J. Geophys. Res.* **2008**, *113*, G04039.
87. Egli, M.; Sartori, G.; Mirabella, A.; Favilli, F.; Giaccai, D.; Delbos, E. Effect of north and south exposure on organic matter in high Alpine soils. *Geoderma* **2009**, *149*, 124–136.
88. Bayranvand, M.; Kooch, Y.; Hosseini, S.M.; Alberti, G. Humus forms in relation to altitude and forest type in the Northern mountainous regions of Iran. *For. Ecol. Manag.* **2017**, *385*, 78–86.
89. Bradford, M.A.; Berg, B.; Maynard, D.S.; Wieder, W.R.; Wood, S.A. Understanding the dominant controls on litter decomposition. *J. Ecol.* **2016**, *104*, 229–238.
90. Prescott, C.E.; Maynard, D.G.; Laiho, R. Humus in northern forests: friend or foe? *For. Ecol. Manag.* **2000**, *133*, 23–36.
91. Austin, A.T.; Vivanco, L.; González-Arzac, A.; Pérez, L.I. There's no place like home? An exploration of the mechanisms behind plant litter–decomposer affinity in terrestrial ecosystems. *New Phytol.* **2014**, *204*, 307–314.
92. Milcu, A.; Manning, P. All size classes of soil fauna and litter quality control the acceleration of litter decay in its home environment. *Oikos* **2011**, *120*, 1366–1370.
93. García-Palacios, P.; Shaw, E.A.; Wall, D.H.; Hättenschwiler, S. Temporal dynamics of biotic and abiotic drivers of litter decomposition. *Ecol. Lett.* **2016**, *19*, 554–563.
94. Setiawan, N.N.; Vanhellemont, M.; De Schrijver, A.; Schelfhout, S.; Baeten, L.; Verheyen, K. Mixing effects on litter decomposition rates in a young tree diversity experiment. *Acta Oecologia* **2016**, *70*, 79–86.
95. Gutiérrez-Girón, A.; Díaz-Pinés, E.; Rubio, A.; Gavilán, R.G. Both altitude and vegetation affect temperature sensitivity of soil organic matter decomposition in Mediterranean high mountain soils. *Geoderma* **2015**, *237–238*, 1–8.
96. Dawes, M.A.; Schleppei, P.; Hättenschwiler, S.; Rixen, C.; Hagedorn, F. Soil warming opens the nitrogen cycle at the alpine treeline. *Glob. Chang. Biol.* **2017**, *23*, 421–434.

# Chapter 5

## General discussion and conclusion



**Photo credits (previous page):**

Niels Hellwig, 3 August 2014

View from the Passo di Morbigai on the lower part of the Val di Rabbi and Malè in the Val di Sole (Trentino, Italian Alps).

# 1 Discussion

## 1.1 Spatial patterns of indicators of decomposition

### Environmental influences

Spatial patterns of soil ecological properties have been poorly studied for a long time (Kandeler et al. 2001; Ettema & Wardle 2002; Baldrian 2014); only recently they have gained increasing attention (e.g. O'Brien et al. 2016; Rutgers et al. 2016). As a result, specific relationships between environmental factors and decomposition processes at different spatial scales in high mountain forest ecosystems are still unclear. In the high mountains, patterns and processes of organic matter decomposition are affected by environmental factors in multiple, interactive ways (especially climate, relief, vegetation, land use and geology, see Chapter 1). This thesis contributes to an enhanced understanding of environmental influences on decomposition processes at the landscape and slope scale in the study area in the Italian Alps.

The mesoclimate at sites of high elevation (close to the treeline) and at north-facing slopes is generally colder than at sites of low elevation (~ 1200 m a.s.l.) and at south-facing slopes. This entails a longer frost period and longer duration of snow cover at high elevation and north-exposed sites, which affects the activities of the decomposer community. For example, Zhang et al. (2017) found that seasonal frost periods at high mountain forest sites in China lead to a reduced abundance of topsoil microorganisms and a loss of bacterial and archaeal diversity. Deep snow cover provides insulation for the topsoil (Edwards et al. 2007). However, the effects of a typically patchy distribution of snow cover in the high mountains (Holtmeier & Broll 1992) together

with a varying snow cover depth on decomposition processes are more complex (Löffler et al. 2008; Baptist et al. 2010; Saccone et al. 2013). Additionally, the activities of the decomposer community are influenced by further variations of season (Didden 1993; Baldrian et al. 2013). North-facing slopes are less prone to drought periods in the summer as compared to south-facing slopes, where the solar radiation is much higher. Ascher et al. (2012) studied humus forms, enchytraeids and soil microbiological properties at high mountain sites (Val di Fassa, Trentino) and found a relationship with climate according to the elevations and slope exposures of the sites. Spatial patterns of soil temperature and moisture in the high mountains are expected to change in the context of global warming (Gobiet et al. 2014; Mountain Research Initiative EDW Working Group 2015). Accordingly, patterns of indicators of decomposition are also likely to change (Gavazov 2010).

At steep slopes of high mountain forests, there are often mosaics of ground vegetation at the small scale, which correlate with erosive and accumulative conditions. A dense vegetation cover hampers erosion (Guerra et al. 2017). Twigs, needles and other dead plant materials that accumulate at the surface are (locally) moved downhill and deposited on small terraces or above barriers such as rocks, trunks and stubs. Spatial patterns of humus forms are related to these mosaics (Anschlag et al. 2017). Furthermore, beside ground vegetation, the tree species composition is a main factor for decomposition processes in forest ecosystems, as it determines the litter quality (Cools et al. 2014; Dawud et al. 2016). For example, Schelfhout et al. (2017) found that the density and biomass of earthworm ecological groups differed between six

common European tree species. These differences were found to be related to the topsoil pH value and to the concentrations of exchangeable soil Al and litter Ca (Schelfhout et al. 2017). Moreover, changes in spatial patterns of indicators of decomposition are often induced by land-use changes, e.g. pasture abandonment followed by forest succession (Hiller & Mütterthies 2005; Strandberg et al. 2005). In managed forests, the temporal development of those patterns coincides with the forest cycle (Bernier 1996; Salmon 2018).

Apart from the organic matter, the habitat of decomposer organisms is shaped by the weathering products from the geological parent material. Sites on siliceous bedrocks generally exhibit more acidic soils as compared to sites on calcareous bedrocks. The species composition of the decomposer community is sensitive to changes in topsoil acidity. Depending on the combination of all environmental factors and their local variability, different lime contents of the parent material may thus lead to different mosaics of humus forms (Graefe & Beylich 2003; Bothe 2015).

### **Indicators of decomposition in the study area**

In the study area of this thesis, climatic influences largely depend on the relief (see Chapter 1). Variable climatic conditions are also the reason for vegetation zones with different species compositions. Besides, the vegetation is affected by the land use. Nowadays, natural forestry is dominant within the forested areas of the study area. However, the Southern Alps have undergone a long history of alpine pastures, especially at south-facing slopes. The first pastures were created in the Prehistoric era (Pini et al. 2017). In the last decades, they have frequently been abandoned and recolonized by forest (Sitzia 2009). Thus, former land-use practices might have contributed to the current forest structure at

sites within the study area (Bebi et al. 2017). Therefore, forest type and density were included as covariates in the slope-scale model (see Chapter 4). The results of this thesis have revealed that indicators of decomposition are arranged in spatial patterns according to elevation and slope exposure (Chapters 2, 3 and 4). Moreover, curvature, slope angle and forest type are at least partially relevant to patterns of humus forms and microbiological topsoil properties at the slope scale (Chapter 4; Hellwig et al. 2017).

Regarding humus forms, the analysis of the random forest models (conducted by Hellwig et al. 2017) has shown that slope angle, profile curvature and partly the LS factor (indicating the potential of erosion by means of slope length and steepness) are more important for the accumulation of organic material above the mineral soil than for the biological activity in the mineral soil. Erosion and accumulation processes might explain this. At sites where erosion occurs frequently there is much less litter decay as compared to sites with accumulative features (due to litter relocation). Thus, there is more parent material of organic layers at sites where litter accumulates as compared to those sites where litter is lost (Hellwig et al. 2017). Furthermore, the analysis revealed a high importance of elevation in the model of biological activity in the mineral soil. In contrast, elevation was a negligible factor for the modelled accumulation of organic material above the mineral soil. This points to a higher dependence of the biological activity on climatic conditions mediated by elevation as opposed to the formation of organic layers (Hellwig et al. 2017).

The spatial patterns of indicators of decomposition predicted in this thesis are in line with other recent studies that investigated organic matter decomposition within the study area Val di Sole / Val di Rabbi in the Italian Alps. Inside the forests of the study area, Aberegg



et al. (2009) found Moder as dominant humus form. At sites nearby the study area, Chersich et al. (2007) studied the dependence of humus forms on the forest development phase and found a high presence of Amphimull and Moder inside the forests, with a higher accumulation of organic carbon and a lower pH value at northern as compared to southern slope exposure.

Studies on soil organic matter indicated that there are generally higher organic matter contents on north-facing slopes as compared to south-facing slopes (Egli et al. 2009). Based on studies of mesocosms, Egli et al. (2016) found that soil organic matter decomposition is limited by temperature at elevations above 1700 m a.s.l. (higher decomposition rate on south-facing slopes than on north-facing slopes). Below 1700 m a.s.l., it is limited by soil moisture (higher decomposition rate on north-facing slopes than on south-facing slopes) (Egli et al. 2016). Rodeghiero et al. (2010) only found weak correlations between soil organic carbon pools and temperature, precipitation and elevation in a regional-scale forest carbon inventory study, but did not consider the relationship to soil moisture.

An exemplary comparison of the enchytraeid assemblages on north-facing and south-facing slopes of the study area and their relationships to the ground cover type and topsoil acidity was conducted by Gómez-Brandón et al. (2017a). Bardelli et al. (2017) investigated the soil microbiological properties at different elevations and slope exposures. The results from those studies correspond to the results of this thesis, indicating more acid conditions and slow organic matter decomposition on north-facing slopes and high elevation as compared to south-facing slopes and low elevation.

Additional studies showed that the decay of deadwood in the study area depends on soil moisture and temperature, which was reflect-

ed in varying deadwood chemical and microbiological properties according to elevation and slope exposure (Petrillo et al. 2015; Fravolini et al. 2016; Gómez-Brandón et al. 2017b). Deadwood from European larch (*Larix decidua*) was found to have longer residence times than deadwood from Norway spruce (*Picea abies*), especially at north-facing slopes (Petrillo et al. 2016). The concept of lignoforms (= humus forms related to deadwood) was introduced in the context of fieldwork in the study area to describe morphological differences in the incorporation of deadwood into the soil (Tatti et al. 2018).

### **Correlations between humus forms, soil organisms and soil biological activity**

This thesis has found strong correlations between humus forms, soil organisms and soil biological activity in the study area in the Italian Alps. Enchytraeid species, extracellular enzymes, the pH value and the C/N ratio of the topsoil are known to be key parameters in the context of soil biological and biogeochemical processes (e.g. Didden 1993; Ponge 2003; Burns et al. 2013). The spatial distribution of all these indicators of decomposition has shown to be related to elevation and slope exposure (Figure 1).

Altogether, the results of this thesis give clear evidence that the humus form is a good indicator of soil biological and biogeochemical processes in the study area. This is in line with previous studies that reported humus forms as meaningful indicators of soil biological and ecological processes at high mountain sites (Salmon et al. 2008; Ascher et al. 2012; Moscatelli et al. 2017).

### **Effects of scale**

Spatial patterns of indicators of decomposition are dependent on the model scale. Pat-

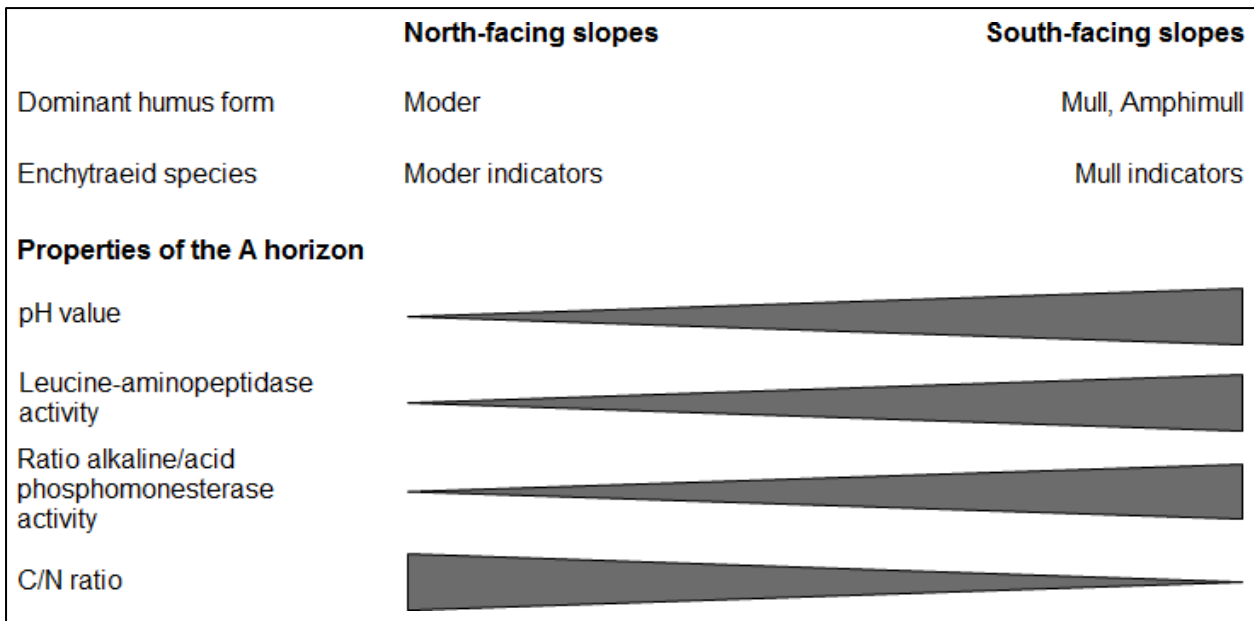


**Figure 1.** Landscape-scale distribution of indicators of decomposition from adverse to favorable environmental conditions in the forests of the study area Val di Sole / Val di Rabbi.

terns at the landscape scale mostly depend on macro-topographical features, especially elevation and slope exposure (see Chapters 2 and 3). Environmental conditions at low elevation (~ 1200 m a.s.l.) and on south-facing slopes are favorable for organic matter decomposition as compared to high elevation (close to the treeline) and north-facing slopes, where accumulation of organic matter is high. At the slope scale this trend is also evident – additional spatial variations of indicators of decomposition were found to be related to curvature, slope angle and forest type (Hellwig et al. 2017). Still the (dis)similarity between landscape-scale effects and slope-scale effects on spatial patterns of indicators of decomposition is difficult to evaluate because of disparate sampling designs and the accompanying different approaches for modelling (see Chapters 2, 3 and 4).

Gradients of elevation and slope exposure are low at the local scale (= scale of one sampling site, 25 m x 25 m). Here the data analysis revealed a high variability of humus forms according to micro-topography and ground vegetation (see Chapter 3; Anschlag et al.

2017). Soil ecological processes are driven by complex interactions at the micro-scale. These are subject to a high spatial variability due to micro-scale differences in soil aggregation, pore space and organic matter content (Nunan 2017). This mosaic of micro-habitats might simultaneously trigger and arise from mosaic-like differences of humus layers that were observable at the scale of a sampling site (see Chapters 2, 3 and 4).

## 1.2 Methods for digital mapping of indicators of decomposition

### Factor-based approach to digital soil mapping

This thesis presents a novel method for digital soil mapping with limited sample data based on expert knowledge for an area with a highly heterogeneous landscape. In the last decade, digital soil mapping has shifted from research studies to common practice (Minasny & McBratney 2016). However, specific issues such as digital soil mapping with limited data (Zhu et al. 2015; Stumpf et al. 2016) and in heterogeneous, hardly accessible areas

(Cambule et al. 2013) have only been the focus of recent studies. In this situation, it is particularly important to select an appropriate modelling method and a thorough model evaluation (Zhu et al. 2015; Beguin et al. 2017).

The concept of digital soil mapping includes a wide array of methods for the spatial prediction of soil parameters (McBratney et al. 2003). In this thesis, spatial patterns of humus forms, soil organisms and soil biological activity were modelled utilizing factor-based approaches for digital soil mapping. Factor-based approaches integrate relationships between environmental influences and the target soil properties into spatial modelling (McBratney et al. 2003). Purely geostatistical approaches were not appropriate in this study area due to the high heterogeneity of the mountainous landscape both at the local scale and at the landscape scale. Factor-based approaches appeared useful, though, as it is well established that factors such as climate and litter quality influence indicators of decomposition (Bradford et al. 2016). Therefore, modelling was based on the spatial variation of those environmental covariates that were expected to affect decomposition processes in the study area (especially terrain attributes, see Chapters 2, 3 and 4).

### Digital mapping of indicators of decomposition

This thesis contributes to digital mapping of soil ecological parameters. Maps of these

parameters are useful to evaluate the effects of environmental changes or disturbances on ecosystem functioning. Organic matter decomposition is among the most fundamental processes for ecosystem functioning, which are conceptualized as ecosystem services (Costanza et al. 2017). Consequently, maps of indicators of decomposition also provide information on spatial variations of ecosystem services. With regard to high mountain forest ecosystems, this study appears to be the first instance of employing digital mapping techniques to investigate soil ecological relationships on such a broad scale.

Digital soil mapping is most frequently utilized for the prediction of soil taxonomic classes, soil texture, hydraulic properties and chemical elements or substances in soils (McBratney et al. 2003; Scull et al. 2003; Grunwald 2009). Moreover, there are several studies on spatial modelling of pH values (e.g. Laslett et al. 1987; Baltensweiler et al. 2017; Robinson et al. 2017). Other indicators of decomposition have only rarely been addressed. Pino (2016) mapped the diversity of microorganisms in soils of New South Wales. Delgado-Baquerizo et al. (2018) analyzed ecological groups of soil bacteria at the global scale and built maps of the major bacterial clusters. Furthermore, recent studies mapped spatial patterns of extracellular enzyme activities in soils at the local scale (Baldrian et al. 2010; Baldrian 2014; Boeddinghaus et al. 2015). Aberegg et al. (2009) mapped humus form classes in the same study area as in this

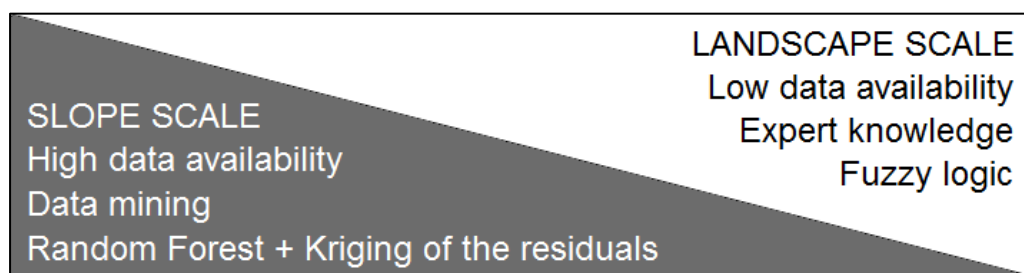


**Figure 2.** Methodological approaches at the landscape versus slope scale depending on the data basis (modified from Hellwig et al. 2017).

thesis (including woodless areas). This thesis advances predictive mapping of humus forms, soil organisms and soil biological activity at the landscape and slope scales.

### **Methods at the landscape versus slope scale**

According to the data availability different methods were applied at the landscape scale and at the slope scale (Figure 2). Modelling at the landscape scale relies on a small amount of data (sites N1-N3, S6-S8, see Chapters 2 and 3). The sampling sites were determined on the basis of expert knowledge. They cover an elevational gradient and opposing slope exposures (north-facing and south-facing slopes). This implied that for the prediction of indicators of decomposition it was only possible to include elevation and slope exposure as covariates. In this situation, an approach combining decision tree analysis with fuzzy logic performed better than an approach solely based on decision trees (see Chapter 2).

At the slope scale, 30 sites per slope were determined with conditioned Latin Hypercube Sampling. This allowed using a data mining approach, since the sampling method yielded a sampling set that represented the environmental conditions of the whole study area relatively well.

As compared to the decision tree models at the landscape scale, the random forest models at the slope scale are more robust, since they have a lower tendency to overfit the training data and they alleviate the influence of extremes in the data (Breiman 2001; Prasad et al. 2006). Nevertheless, the methodological framework comprising a decision tree analysis and fuzzy membership functions has appeared to be a suitable approach for predicting indicators of decomposition when the landscape is heterogeneous. The random forest models were coupled with a kriging of the residuals, which accounts for the spatial variation in the training data that cannot be

explained by the environmental covariates. This proved to be a suitable approach for predicting indicators of decomposition when the training dataset is an accurate representation of the variation in environmental conditions in the study area.

## **1.3 Model limitations**

### **Data uncertainties**

The sample data are subject to different sources of uncertainty. A high small-scale variability of ground cover (litter, grass, moss, fern, shrubs) and humus forms indicates that single samples for the analysis of biological and biogeochemical parameters might not be typical of the entire site. Therefore, a set of several samples was taken per site considering visible variations of the ground cover (see Chapters 2, 3 and 4). Furthermore, side effects of the transport and laboratory analyses of the samples cannot completely be excluded, although samples were treated thoroughly. Integrating all samples used for modelling, the data are deemed transferable to typical sites throughout the study area.

Regarding the environmental data, errors and uncertainty arise from the compilation of the digital terrain models. Both topographic maps and LiDAR data provide approximations to actual elevation values (Fisher & Tate 2006; Wechsler 2007). Additionally, all environmental data are spatially imprecise, as they contain spatially aggregated values according to their resolution.

The results from this thesis are related to the study area Val di Sole / Val di Rabbi in the Italian Alps. Spatial patterns of indicators of decomposition are not directly transferable to study areas with different parent materials, climatic conditions, forest types or land-use practices. However, this thesis provides a methodological framework that can be used similarly to analyze spatial patterns of in-

dicators of decomposition in other study areas characterized by a heterogeneous landscape.

### **Model evaluations**

Due to the high uncertainty of both sampling and environmental data, the results of spatial modelling needed to be evaluated extensively. The methods used for the evaluation of the spatial models presented in this thesis were chosen depending on the modelling methods. Although frequently disregarded, model evaluations are generally important to interpret and potentially use the results for further purposes (Bennett et al. 2013).

All models showed a satisfying reliability (see Chapters 2, 3 and 4). However, due to the data scarcity, the landscape-scale predictions are especially dependent on single observations. The distinctly higher deviations of the predictions from the observations at the validation sites as compared to the goodness of fit of the model indicate that there is a risk of overfitting the sample data (see Chapter 2). Therefore, the landscape-scale models have been evaluated considering the goodness of fit, resampling of the training data, observations from validation sites, systematic manipulation of the input data to account for uncertainties and deviations of landform types from the training data (see Chapter 3). In this context, the mean error (ME) and the root mean squared error (RMSE) were used as quantitative metrics. Both metrics are commonly used and appropriate to evaluate the performance of models (Chai & Draxler 2014). The random forest models revealed spatial patterns at the slope scale depending on several environmental factors with explained

variances between 18 % and 37 %. Kriging of the model residuals enabled to increase the goodness of predictions of the modelled parameters (see Chapter 4).

## **1.4 Future perspectives**

Soil ecological mechanisms relevant for ecosystem functioning in high mountain forests are still not well understood (Broll 1998; Baldrian 2017; van der Wal & de Boer 2017; Frouz 2018). Thus it is necessary to examine further parameters related to organic matter decomposition in high mountain forests (e.g. focusing on soil food webs, litter traits or root-soil interactions). Presuming an enhanced understanding of soil ecological processes, future models of the system of organic matter decomposition may employ mechanism-based simulation approaches in place of purely data-based mapping approaches (Cuddington et al. 2013; Sarmiento Cabral et al. 2017).

Future spatial models of soil ecological parameters need to meet new demands to support ecosystem management in the face of environmental changes. First, they should be able to cross spatial scales from the local scale up to the landscape scale. Second, they should integrate the temporal dimension (e.g. Stockmann et al. 2015) to map changes over time and to calculate future scenarios. This is particularly important in view of expected responses of soil organisms involved in the carbon cycle to a changing climate (Reichstein et al. 2013; Frank et al. 2015; Coyle et al. 2017). Third, spatial models should always be communicated together with limitations and estimates of uncertainty.

## 2 Conclusion

This thesis focused on spatial patterns of humus forms, soil organisms and soil biological activity in a study area in the Italian Alps. Modelling methods frequently used in the context of digital soil mapping have been refined to derive predictive maps of indicators of decomposition based on correlations between sample data and environmental data. Models have been developed and evaluated both at the landscape scale and at the slope scale.

The first research question asked for suitable methods for data-based spatial modelling of indicators of decomposition. The study area of this thesis is located in the high mountains, a quite heterogeneous landscape in terms of environmental conditions. The study of parameters related to organic matter decomposition has shown that predictive mapping in such a landscape requires a specific methodological design depending on the data availability and the model scale. Factor-based approaches from digital soil mapping appeared suitable for mapping indicators of decomposition, as they are designed to include extensively available data on environmental influencing factors. At the landscape scale, the data basis was characterized by a small amount of sample data achieved in an expert-based sampling design. Modelling thus demands a knowledge-based approach. The application of fuzzy logic has shown to be adequate in deriving membership functions from decision trees. Predictive maps are produced by combining all functions depending on the different environmental parameters that are considered as covariates. At the slope scale, the data basis consisted of a relatively large amount of sample data that were acquired in a model-based sampling design.

This allows for the application of random forest as a data mining method for spatial modelling, which integrates several environmental covariates.

The second research question concerned the dependence of spatial patterns of indicators of decomposition on the model scale. With regard to the described patterns, the model results at the landscape scale and at the slope scale are similar. However, together with a high availability of sample data, the higher level of detail at the slope scale allows to capture the effects of additional topographical parameters such as curvature and slope angle. Due to limited data availability at the landscape scale, it remains unclear if these topographical parameters influence the patterns of indicators of decomposition similarly at the landscape scale. Therefore, spatial models at the landscape scale have a higher uncertainty. At the slope scale, geostatistical analyses such as kriging of the model residuals from random forest may help to derive realistic predictions. Sample data acquired at the local scale indicate that micro-topography and ground vegetation, but not the tree species composition, are the most important factors for small-scale variability of decomposition processes.

The third research question targeted the correlations between the spatial distributions of humus forms, soil organisms of different decomposer communities and soil microbiological parameters. The respective spatial patterns have been shown to be distinctly correlated among each other and with environmental conditions.

On north-facing slopes, there are generally adverse environmental conditions for decomposition processes. This is evident, as the

spatial models show that topsoils at these sites are characterized by low pH values, a decomposer community dominated by Moder-indicating enchytraeids, a relatively high C/N ratio, a low activity of leucine-aminopeptidase and a low ratio of the activities of alkaline and acid phosphomonoesterase. In this situation, the spatial models of humus forms indicate almost exclusively Moder (partly eroded) and Mor. Decomposition on north-facing slopes is probably limited by soil temperature. Therefore, decomposition processes are hampered more at high elevations near the treeline than at low elevations close to the valley bottoms.

On south-facing slopes, environmental conditions are generally rather favorable for decomposition processes. The spatial models show that topsoils on south-facing slopes are characterized by relatively high pH values, a decomposer community dominated by Mull-indicating enchytraeids, a low C/N ratio, a high activity of leucine-aminopeptidase and a high ratio of the activities of alkaline and acid phosphomonoesterase. In this situation, the

spatial models of humus forms indicate a high presence of Mull and Amphimull. Spatial variations of indicators of decomposition along the elevational gradient are not as pronounced on the south-facing slopes when compared to those of the north-facing slopes. This indicates that decomposition processes on south-facing slopes are probably limited by both soil temperature and soil moisture. Decomposition processes are hampered by drought periods during the summer especially at the highly irradiated, warm sites at low elevation on south-facing slopes.

Altogether, environmental conditions for organic matter decomposition in the study area vary significantly according to the topographical position, especially between different elevations and slope exposures. The relatively high coincidence of spatial patterns of humus forms and of ecological properties of the topsoil suggests that the humus form can be used as indicator of organic matter decomposition processes in the investigated high mountain area.



### 3 References

- Aberegg, I., Egli, M., Sartori, G., Purves, R. (2009): Modelling spatial distribution of soil types and characteristics in a high Alpine valley (Val di Sole, Trentino, Italy). *Studi Trentini di Scienze Naturali* **85**, 39-50.
- Anschlag, K., Tatti, D., Hellwig, N., Sartori, G., Gobat, J.-M., Broll, G. (2017): Vegetation-based bioindication of humus forms in coniferous mountain forests. *Journal of Mountain Science* **14**(4), 662-673. **(The abstract of this reference can be found in Appendix 4 of this thesis.)**
- Ascher, J., Sartori, G., Graefe, U., Thornton, B., Ceccherini, M. T., Pietramellara, G., Egli, M. (2012): Are humus forms, mesofauna and microflora in subalpine forest soils sensitive to thermal conditions? *Biology and Fertility of Soils* **48**, 709-725.
- Baldrian, P. (2014): Distribution of Extracellular Enzymes in Soils: Spatial Heterogeneity and Determining Factors at Various Scales. *Soil Science Society of America Journal* **78**, 11-18.
- Baldrian, P. (2017): Forest microbiome: diversity, complexity and dynamics. *FEMS Microbiology Reviews* **41**(2), 109-130.
- Baldrian, P., Merhautová, V., Cajthaml, T., Petránková, M., Šnajdr, J. (2010): Small-scale distribution of extracellular enzymes, fungal, and bacterial biomass in *Quercus petraea* forest topsoil. *Biology and Fertility of Soils* **46**(7), 717-726.
- Baldrian, P., Šnajdr, J., Merhautová, V., Dobiášová, P., Cajthaml, T., Valášková, V. (2013): Responses of the extracellular enzyme activities in hardwood forest to soil temperature and seasonality and the potential effects of climate change. *Soil Biology & Biochemistry* **56**, 60-68.
- Baltensweiler, A., Walthert, L., Ginzler, C., Sutter, F., Purves, R. S., Hanewinkel, M. (2017): Terrestrial laser scanning improves digital elevation models and topsoil pH modelling in regions with complex topography and dense vegetation. *Environmental Modelling & Software* **95**, 13-21.
- Baptist, F., Yoccoz, N. G., Choler, P. (2010): Direct and indirect control by snow cover over decomposition in alpine tundra along a snowmelt gradient. *Plant and Soil* **328**, 397-410.
- Bardelli, T., Gómez-Brandón, M., Ascher-Jenull, J., Fornasier, F., Arfaioli, P., Francioli, D., Egli, M., Sartori, G., Insam, H., Pietramellara, G. (2017): Effects of slope exposure on soil physico-chemical and microbiological properties along an altitudinal climosequence in the Italian Alps. *Science of the Total Environment* **575**, 1041-1055.
- Bebi, P., Seidl, R., Motta, R., Fuhr, M., Firm, D., Krumm, F., Conedera, M., Ginzler, C., Wohlgemuth, T., Kulakowski, D. (2017): Changes of forest cover and disturbance regimes in the mountain forests of the Alps. *Forest Ecology and Management* **388**, 43-56.
- Beguin, J., Fuglstad, G. A., Mansuy, N., Paré, D. (2017): Predicting soil properties in the Canadian boreal forest with limited data: Comparison of spatial and non-spatial statistical approaches. *Geoderma* **306**, 195-205.
- Bennett, N. D., Croke, B. F. W., Guariso, G., Guillaume, J. H. A., Hamilton, S. H., Jakeman, A. J., Marsili-Libelli, S., Newham, L. T. H., Norton, J. P., Perrin, C., Pierce, S. A., Robson, B., Seppelt, R., Voinov, A. A., Fath, B. D., Andreassian, V. (2013): Characterising performance of environmental models. *Environmental Modelling & Software* **40**, 1-20.
- Bernier, N. (1996): Altitudinal changes in humus form dynamics in a spruce forest at the montane level. *Plant and Soil* **178**, 1-28.
- Boeddinghaus, R. S., Nunan, N., Berner, D., Marhan, S., Kandeler, E. (2015): Do general spatial relationships for microbial biomass and soil enzyme activities exist in temperate grassland soils? *Soil Biology & Biochemistry* **88**, 430-440.
- Bothe, H. (2015): The lime-silicate question. *Soil Biology & Biochemistry* **89**, 172-183.
- Bradford, M. A., Berg, B., Maynard, D. S., Wieder, W. R., Wood, S. A. (2016): Understanding the dominant controls on litter

- decomposition. *Journal of Ecology* **104**(1), 229-238.
- Breiman, L. (2001): Random Forests. *Machine Learning* **45**, 5-32.
- Broll, G. (1998): Diversity of soil organisms in Alpine and Arctic soils in Europe. Review and research needs. *Pirineos* **151-152**, 43-72.
- Burns, R. G., DeForest, J. L., Marxsen, J., Sinsabaugh, R. L., Stromberger, M. E., Wallenstein, M. D., Weintraub, M. N., Zoppini, A. (2013): Soil enzymes in a changing environment: Current knowledge and future directions. *Soil Biology & Biochemistry* **58**, 216-234.
- Cambule, A. H., Rossiter, D. G., Stoorvogel, J. J. (2013): A methodology for digital soil mapping in poorly-accessible areas. *Geoderma* **192**, 341-353.
- Chai, T., Draxler, R. R. (2014): Root mean square error (RMSE) or mean absolute error (MAE)? – Arguments against avoiding RMSE in the literature. *Geoscientific Model Development* **7**, 1247-1250.
- Chersich, S., Galvan, P., Frizzera, L., Scattolin, L. (2007): Variabilità delle forme di humus in due siti campione di pecceta altimontana trentina. *Forest@* **4**(2), 220-226.
- Cools, N., Vesterdal, L., De Vos, B., Vanguelova, E., Hansen, K. (2014): Tree species is the major factor explaining C:N ratios in European forest soils. *Forest Ecology and Management* **311**, 3-16.
- Costanza, R., de Groot, R., Braat, L., Kubiszewski, I., Fioramonti, L., Sutton, P., Farber, S., Grasso, M. (2017): Twenty years of ecosystem services: How far have we come and how far do we still need to go? *Ecosystem Services* **28**, 1-16.
- Coyle, D. R., Nagendra, U. J., Taylor, M. K., Campbell, J. H., Cunard, C. E., Joslin, A. H., Mundepi, A., Phillips, C. A., Callahan Jr., M. A. (2017): Soil fauna responses to natural disturbances, invasive species, and global climate change: Current state of the science and a call to action. *Soil Biology & Biochemistry* **110**, 116-133.
- Cuddington, K., Fortin, M.-J., Gerber, L. R., Hastings, A., Liebhold, A., O'Connor, M., Ray, C. (2013): Process-based models are required to manage ecological systems in a changing world. *Ecosphere* **4**(2), 20.
- Dawud, S. M., Raulund-Rasmussen, K., Domisch, T., Finér, L., Jaroszewicz, B., Vesterdal, L. (2016): Is Tree Species Diversity or Species Identity the More Important Driver of Soil Carbon Stocks, C/N Ratio, and pH? *Ecosystems* **19**(4), 645-660.
- Delgado-Baquerizo, M., Oliverio, A. M., Brewer, T. E., Benavent-González, A., Eldridge, D. J., Bardgett, R. D., Maestre, F. T., Singh, B. K., Fierer, N. (2018): A global atlas of the dominant bacteria found in soil. *Science* **359**(6373), 320-325.
- Didden, W. A. M. (1993): Ecology of terrestrial Enchytraeidae. *Pedobiologia* **37**, 2-29.
- Edwards, A. C., Scalenghe, R., Freppaz, M. (2007): Changes in the seasonal snow cover of alpine regions and its effect on soil processes: A review. *Quaternary International* **162-163**, 172-181.
- Egli, M., Sartori, G., Mirabella, A., Favilli, F., Giaccari, D., Delbos, E. (2009): Effect of north and south exposure on organic matter in high Alpine soils. *Geoderma* **149**, 124-136.
- Egli, M., Hafner, S., Derungs, C., Ascher-Jenuell, J., Camin, F., Sartori, G., Raab, G., Bontempo, L., Paolini, M., Ziller, L., Bardelli, T., Petrillo, M., Abiven, S. (2016): Decomposition and stabilisation of Norway spruce needle-derived material in Alpine soils using a <sup>13</sup>C-labelling approach in the field. *Biogeochemistry* **131**(3), 321-338.
- Ettema, C. H., Wardle, D. A. (2002): Spatial soil ecology. *Trends in Ecology & Evolution* **17**(4), 177-183.
- Fisher, P. F., Tate, N. J. (2006): Causes and consequences of error in digital elevation models. *Progress in Physical Geography* **30**(4), 467-489.
- Frank, D., Reichstein, M., Bahn, M., Frank, D., Mahecha, M. D., Smith, P., Thonicke, K., van der Velde, M., Vicca, S., Babst, F., Beer, C., Buchmann, N., Canadell, J. G., Ciais, P., Cramer, W., Ibrom, A., Miglietta, F., Poulter, B., Rammig, A., Seneviratne, S. I., Walz, A., Wattenbach, M., Zavala, M. A., Zscheischler, J. (2015): Effects of climate extremes on the

- terrestrial carbon cycle: concepts, processes and potential future impacts. *Global Change Biology* **21**, 2861-2880.
- Fravolini, G., Egli, M., Derungs, C., Cherubini, P., Ascher-Jenull, J., Gómez-Brandón, M., Bardelli, T., Tognetti, R., Lombardi, F., Marchetti, M. (2016): Soil attributes and microclimate are important drivers of initial deadwood decay in sub-alpine Norway spruce forests. *Science of the Total Environment* **569-570**, 1064-1076.
- Frouz, J. (2018): Effects of soil macro- and mesofauna on litter decomposition and soil organic matter stabilization. *Geoderma* **332**, 161-172.
- Gavazov, K. S. (2010): Dynamics of alpine plant litter decomposition in a changing climate. *Plant and Soil* **337**(1-2), 19-32.
- Gobiet, A., Kotlarski, S., Beniston, M., Heinrich, G., Rajczak, J., Stoffel, M. (2014): 21st century climate change in the European Alps—A review. *Science of the Total Environment* **493**, 1138-1151.
- Gómez-Brandón, M., Ascher-Jenull, J., Bardelli, T., Fornasier, F., Sartori, G., Pietramellara, G., Arfaioli, P., Egli, M., Beylich, A., Insam, H., Graefe, U. (2017a): Ground cover and slope exposure effects on micro- and mesobiota in forest soils. *Ecological Indicators* **80**, 174-185.
- Gómez-Brandón, M., Ascher-Jenull, J., Bardelli, T., Fornasier, F., Fravolini, G., Arfaioli, P., Ceccherini, M. T., Pietramellara, G., Lamorski, K., Sławiński, C., Bertoldi, D., Egli, M., Cherubini, P., Insam, H. (2017b): Physico-chemical and microbiological evidence of exposure effects on *Picea abies* – Coarse woody debris at different stages of decay. *Forest Ecology and Management* **391**, 376-389.
- Graefe, U., Beylich, A. (2003): Critical values of soil acidification for annelid species and the decomposer community. *Newsletter of Enchytraeidae* **8**, 51-55.
- Grunwald, S. (2009): Multi-criteria characterization of recent digital soil mapping and modeling approaches. *Geoderma* **152**, 195-207.
- Guerra, A. J. T., Fullen, M. A., Jorge, M. C. O., Bezerra, J. F. R., Shokr, M. S. (2017): Slope Processes, Mass Movement and Soil Erosion: A Review. *Pedosphere* **27**(1), 27-41.
- Hellwig, N., Anschlag, K., Broll, G. (2017): Modellgestützte Analyse räumlicher Dekompositionsmuster im Hochgebirge. *Berichte der DBG (eprints)*, [http://eprints.dbges.de/1232/1/Hellwig%20et%20al\\_2017\\_DBG%20eprints\\_Dekompositionsmuster%20R%C3%A4umliche%20Modelle%20Hochgebirge.pdf](http://eprints.dbges.de/1232/1/Hellwig%20et%20al_2017_DBG%20eprints_Dekompositionsmuster%20R%C3%A4umliche%20Modelle%20Hochgebirge.pdf) (27/11/2017).
- Hiller, B., Mütterthies, A. (2005): Humus Forms and Reforestation of an Abandoned Pasture at the Alpine Timberline (Upper Engadine, Central Alps, Switzerland). In: Broll, G., Keplin, B. (Eds.): *Mountain Ecosystems. Studies in Treeline Ecology*. Springer, Berlin, Heidelberg, 203-218.
- Holtmeier, F.-K., Broll, G. (1992): The Influence of Tree Islands and Microtopography on Pedoecological Conditions in the Forest-Alpine Tundra Ecotone on Niwot Ridge, Colorado Front Range, U.S.A. *Arctic and Alpine Research* **24**(3), 216-228.
- Kandeler, E., Tschirko, D., Stemmer, M., Schwarz, S., Gerzabek, M. H. (2001): Organic matter and soil microorganisms – Investigations from the micro- to the macro-scale. *Die Bodenkultur* **52**(2), 117-131.
- Laslett, G. M., McBratney, A. B., Pahl, P. J., Hutchinson, M. F. (1987): Comparison of several spatial prediction methods for soil pH. *Journal of Soil Science* **38**, 325-341.
- Löffler, U. C. M., Cypionka, H., Löffler, J. (2008): Soil microbial activity along an arctic-alpine altitudinal gradient from a seasonal perspective. *European Journal of Soil Science* **59**, 842-854.
- McBratney, A. B., Mendonça Santos, M. L., Minasny, B. (2003): On digital soil mapping. *Geoderma* **117**(1-2), 3-52.
- Minasny, B., McBratney, A. B. (2016): Digital soil mapping: A brief history and some lessons. *Geoderma* **264**, 301-311.
- Moscatelli, M. C., Bonifacio, E., Chiti, T., Cudlín, P., Dinca, L., Gömöryova, E., Grego, S., La Porta, N., Karlinski, L., Pellis, G., Rudawska, M., Squartini, A., Zhiyanski, M., Broll, G. (2017): Soil properties as indicators of treeline

- dynamics in relation to anthropogenic pressure and climate change. *Climate Research* **73**(1-2), 73-84.
- Mountain Research Initiative EDW Working Group (2015): Elevation-dependent warming in mountain regions of the world. *Nature Climate Change* **5**, 424-430.
- Nunan, N. (2017): The microbial habitat in soil: Scale, heterogeneity and functional consequences. *Journal of Plant Nutrition and Soil Science* **180**(4), 425-429.
- O'Brien, S. L., Gibbons, S. M., Owens, S. M., Hampton-Marcell, J., Johnston, E. R., Jastrow, J. D., Gilbert, J. A., Meyer, F., Antonopoulos, D. A. (2016): Spatial scale drives patterns in soil bacterial diversity. *Environmental Microbiology* **18**(6), 2039-2051.
- Petrillo, M., Cherubini, P., Sartori, G., Abiven, S., Ascher, J., Bertoldi, D., Camin, F., Barbero, A., Larcher, R., Egli, M. (2015): Decomposition of Norway spruce and European larch coarse woody debris (CWD) in relation to different elevation and exposure in an Alpine setting. *iForest* **9**, 154-164.
- Petrillo, M., Cherubini, P., Fravolini, G., Marchetti, M., Ascher-Jenull, J., Schärer, M., Synal, H.-A., Bertoldi, D., Camin, F., Larcher, R., Egli, M. (2016): Time since death and decay rate constants of Norway spruce and European larch deadwood in subalpine forests determined using dendrochronology and radiocarbon dating. *Biogeosciences* **13**, 1537-1552.
- Pini, R., Ravazzi, C., Raiteri, L., Guerreschi, A., Castellano, L., Comolli, R. (2017): From pristine forests to high-altitude pastures: an ecological approach to prehistoric human impact on vegetation and landscapes in the western Italian Alps. *Journal of Ecology* **105**, 1580-1597.
- Pino, V. (2016): Soil microbial diversity across different agroecological zones in New South Wales. PhD thesis at the University of Sydney.
- Ponge, J.-F. (2003): Humus forms in terrestrial ecosystems: a framework to biodiversity. *Soil Biology & Biochemistry* **35**, 935-945.
- Prasad, A. M., Iverson, L. R., Liaw, A. (2006): Newer Classification and Regression Tree Techniques: Bagging and Random Forests for Ecological Prediction. *Ecosystems* **9**, 181-199.
- Reichstein, M., Bahn, M., Ciais, P., Frank, D., Mahecha, M. D., Seneviratne, S. I., Zscheischler, J., Beer, C., Buchmann, N., Frank, D. C., Papale, D., Rammig, A., Smith, P., Thonicke, K., van der Velde, M., Vicca, S., Walz, A., Wattenbach, M. (2013): Climate extremes and the carbon cycle. *Nature* **500**, 287-295.
- Robinson, N. J., Benke, K. K., Norng, S., Kitching, M., Crawford, D. M. (2017): Improving the information content in soil pH maps: a case study. *European Journal of Soil Science* **68**, 592-604.
- Rodeghiero, M., Tonolli, S., Vescovo, L., Gianelle, D., Cescatti, A., Sottocornola, M. (2010): INFOCARB: A regional scale forest carbon inventory (Provincia Autonoma di Trento, Southern Italian Alps). *Forest Ecology and Management* **259**, 1093-1101.
- Rutgers, M., Orgiazzi, A., Gardi, C., Römcke, J., Jänsch, S., Keith, A. M., Neilson, R., Boag, B., Schmidt, O., Murchie, A. K., Blackshaw, R. P., Pérès, G., Cluzeau, D., Guernion, M., Briones, M. J. I., Rodeiro, J., Piñero, R., Cosín, D. J. D., Sousa, J. P., Suhadolc, M., Kos, I., Krogh, P.-H., Faber, J. H., Mulder, C., Bogte, J. J., van Wijnen, H. J., Schouten, A. J., de Zwart, D. (2016): Mapping earthworm communities in Europe. *Applied Soil Ecology* **97**, 98-111.
- Saccone, P., Morin, S., Baptist, F., Bonneville, J.-M., Colace, M.-P., Domine, F., Faure, M., Geremia, R., Lochet, J., Poly, F., Lavorel, S., Clément, J.-C. (2013): The effects of snowpack properties and plant strategies on litter decomposition during winter in subalpine meadows. *Plant and Soil* **363**, 215-229.
- Salmon, S. (2018): Changes in humus forms, soil invertebrate communities and soil functioning with forest dynamics. *Applied Soil Ecology* **123**, 345-354.
- Salmon, S., Artuso, N., Frizzera, L., Zampedri, R. (2008): Relationship between soil fauna communities and humus forms: Response to forest dynamics and solar radiation. *Soil Biology & Biochemistry* **40**, 1707-1715.
- Sarmiento Cabral, J., Valente, L., Hartig, F. (2017): Mechanistic simulation models in

- macroecology and biogeography: state-of-art and prospects. *Ecography* **40**, 267-280.
- Schelfhout, S., Mertens, J., Verheyen, K., Vesterdal, L., Baeten, L., Muys, B., De Schrijver, A. (2017): Tree Species Identity Shapes Earthworm Communities. *Forests* **8**(3), 85.
- Scull, P., Franklin, J., Chadwick, O. A., McArthur, D. (2003): Predictive soil mapping: a review. *Progress in Physical Geography* **27**(2), 171-197.
- Sitzia, T. (2009): Ecologia e gestione dei boschi di neoformazione nel paesaggio del Trentino. Provincia Autonoma di Trento – Servizio Foreste e Fauna, Trento.
- Stockmann, U., Padarian, J., McBratney, A., Minasny, B., de Brogniez, D., Montanarella, L., Hong, S. Y., Rawlins, B. G., Field, D. J. (2015): Global soil organic carbon assessment. *Global Food Security* **6**, 9-16.
- Strandberg, B., Kristiansen, S. M., Tybirk, K. (2005): Dynamic oak-scrub to forest succession: Effects of management on understorey vegetation, humus forms and soils. *Forest Ecology and Management* **211**(3), 318-328.
- Stumpf, F., Schmidt, K., Behrens, T., Schönbrodt-Stitt, S., Buzzo, G., Dumperth, C., Wadoux, A., Xiang, W., Scholten, T. (2016): Incorporating limited field operability and legacy soil samples in a hypercube sampling design for digital soil mapping. *Journal of Plant Nutrition and Soil Science* **179**(4), 499-509.
- Tatti, D., Fatton, V., Sartori, L., Gobat, J.-M., Le Bayon, R.-C. (2018): What does 'lignoform' really mean? *Applied Soil Ecology* **123**, 632-645.
- van der Wal, A., de Boer, W. (2017): Dinner in the dark: Illuminating drivers of soil organic matter decomposition. *Soil Biology & Biochemistry* **105**, 45-48.
- Wechsler, S. P. (2007): Uncertainties associated with digital elevation models for hydrologic applications: a review. *Hydrology and Earth System Sciences* **11**, 1481-1500.
- Zhang, L., Wang, A., Yang, W., Xu, Z., Wu, F., Tan, B., Liu, Y., Chen, L. (2017): Soil microbial abundance and community structure vary with altitude and season in the coniferous forests, China. *Journal of Soils and Sediments* **17**, 2318-2328.
- Zhu, A. X., Liu, J., Du, F., Zhang, S. J., Qin, C. Z., Burt, J., Behrens, T., Scholten, T. (2015): Predictive soil mapping with limited sample data. *European Journal of Soil Science* **66**(3), 535-547.

## Appendices

Appendix 1	Online appendix of Chapter 2 .....	111
Appendix 2	Supplementary material of Chapter 3.....	113
Appendix 3	Supplementary material of Chapter 4.....	123
Appendix 4	Abstract of co-authored article (Anschlag et al. 2017) .....	137





## Appendix 1: Online appendix of Chapter 2

### Code from the file DecTreeAnalysis.R

```
# Use R package rpart (Therneau et al., 2015)
library(rpart)
# Select folder that contains file 'hf_data.txt'
setwd(choose.dir(default=".", caption="Select data folder"))

# Load data
hf_data <- read.delim("hf_data.txt")
# Apply weights for different soil cover types
hf_data_w <- data.frame(hf_data[rep(seq_len(dim(hf_data)[1]), hf_data$weight), ,
drop = FALSE], row.names = NULL)

# Build decision tree
dec_tree <- rpart(OH ~ elevation + exposition, method="anova", data=hf_data_w,
minsplit = 50)
plot(dec_tree, uniform = TRUE, compress = TRUE, main="Decision tree: OH horizon",
margin = 0.1, nspace = 1, branch = 0.5)
text(dec_tree, use.n = FALSE, all = TRUE, fancy = TRUE, fwidth = 6, fheight =
2.0, cex = 1.0, adj = c(0.5,0.8))

# Derive fuzzy membership function (bell-shape) for areas higher than 1300 m
a.s.l.:
f <- function(x, c, b) 1-(1-0.5167)*exp(abs((x-180)/b)^c*log(0.5))

# Minimize deviation at north-exposed sites (exposition = 360 degrees), where OH
= 63.33 % (see decision tree)
f_app1 <- function(c, b) abs(f(360, c, b) - 0.6333)

# Choose intermediate value c = 2
optimize(f_app1, c(0,10000), tol = 0.01, c = 2) # Minimum for b = 285

# Different behaviour of fuzzy membership function for other c values
optimize(f_app1, c(0,10000), tol = 0.01, c = 1) # Minimum for b = 452
optimize(f_app1, c(0,10000), tol = 0.01, c = 3) # Minimum for b = 245
```

### Data from the file hf\_data.txt

site	OH	elevation	exposition	weight
N1F1	0	1200	360	1
N1F2	0	1200	360	1
N1F3	0	1200	360	1
N1M1	0	1200	360	9
N1M2	0.5	1200	360	9
N1M3	0	1200	360	9
N2M1	1	1400	360	10
N2M2	1	1400	360	10
N2M3	0	1400	360	10
N3G1	1	1630	360	8
N3G2	1	1630	360	8
N3G3	0	1630	360	8
N3M1	0	1630	360	2
N3M2	1	1630	360	2
N3M3	0	1630	360	2
S6G1	0	1200	180	1
S6G2	1	1200	180	1
S6G3	1	1200	180	1
S6L1	0	1200	180	9
S6L2	0	1200	180	9
S6L3	0	1200	180	9
S7G1	0.5	1400	180	10
S7G2	0.5	1400	180	10
S7G3	0.5	1400	180	10
S8G1	0	1630	180	2
S8G2	0	1630	180	2
S8G3	0	1630	180	2
S8L1	1	1630	180	8
S8L2	0	1630	180	8
S8L3	1	1630	180	8



## Appendix 2: Supplementary material of Chapter 3

**Table S1** Sample data from the investigation sites N1-N3 (northern slope exposure) and S6-S8 (southern slope exposure)

Site	Soil cover types (weighting for aggregation)	Sample	Percentage of mull indicators to all microannelid individuals (%)	Percentage of moder indicators to all microannelid individuals (%)	Percentage of humus forms showing an OH horizon (%)
N1	moss (90 %)	M1	31.91	36.17	0.00
		M2	0.00	90.80	50.00
		M3	5.26	8.77	0.00
	fern (10 %)	F1	76.92	19.23	100.00
		F2	2.86	77.14	0.00
		F3	37.80	29.92	0.00
N2	moss (100 %)	M1	0.00	98.63	100.00
		M2	15.52	81.03	100.00
		M3	0.00	92.54	0.00
N3	grass (80 %)	G1	11.36	81.82	100.00
		G2	21.19	68.64	100.00
		G3	44.44	55.56	100.00
	moss (20 %)	M1	0.00	100.00	100.00
		M2	0.00	82.00	50.00
		M3	0.00	97.14	0.00
S6	litter (90 %)	L1	91.07	0.00	0.00
		L2	100.00	0.00	0.00
		L3	100.00	0.00	0.00
	grass (10 %)	G1	59.09	0.00	0.00
		G2	95.74	0.00	100.00
		G3	-	-	100.00
S7	grass (100 %)	G1	63.41	2.44	50.00
		G2	29.49	11.54	50.00
		G3	93.46	1.96	50.00
S8	litter (80 %)	L1	10.34	17.24	100.00
		L2	90.00	5.00	0.00
		L3	96.77	0.00	50.00
	grass (20 %)	G1	83.33	0.00	100.00
		G2	21.05	15.79	0.00
		G3	58.06	16.13	0.00

**Table S2** Data basis for resampling (designations of the sample plots refer to soil cover types: M = moss, F = fern, G = grass, L = litter)

Model no.	Samples left out in resampled data set					
	N1	N2	N3	S6	S7	S8
1	M1, F1	M1	G1, M1	L1, G1	G1	L1, G1
2	M1, F1	M1	G2, M2	L1, G1	G1	L2, G2
3	M1, F1	M1	G3, M3	L1, G1	G1	L3, G3
4	M1, F1	M2	G1, M1	L1, G1	G2	L1, G1
5	M1, F1	M2	G2, M2	L1, G1	G2	L2, G2
6	M1, F1	M2	G3, M3	L1, G1	G2	L3, G3
7	M1, F1	M3	G1, M1	L1, G1	G3	L1, G1
8	M1, F1	M3	G2, M2	L1, G1	G3	L2, G2
9	M1, F1	M3	G3, M3	L1, G1	G3	L3, G3
10	M2, F2	M1	G1, M1	L2, G2	G1	L1, G1
11	M2, F2	M1	G2, M2	L2, G2	G1	L2, G2
12	M2, F2	M1	G3, M3	L2, G2	G1	L3, G3
13	M2, F2	M2	G1, M1	L2, G2	G2	L1, G1
14	M2, F2	M2	G2, M2	L2, G2	G2	L2, G2
15	M2, F2	M2	G3, M3	L2, G2	G2	L3, G3
16	M2, F2	M3	G1, M1	L2, G2	G3	L1, G1
17	M2, F2	M3	G2, M2	L2, G2	G3	L2, G2
18	M2, F2	M3	G3, M3	L2, G2	G3	L3, G3
19	M3, F3	M1	G1, M1	L3, G3	G1	L1, G1
20	M3, F3	M1	G2, M2	L3, G3	G1	L2, G2
21	M3, F3	M1	G3, M3	L3, G3	G1	L3, G3
22	M3, F3	M2	G1, M1	L3, G3	G2	L1, G1
23	M3, F3	M2	G2, M2	L3, G3	G2	L2, G2
24	M3, F3	M2	G3, M3	L3, G3	G2	L3, G3
25	M3, F3	M3	G1, M1	L3, G3	G3	L1, G1
26	M3, F3	M3	G2, M2	L3, G3	G3	L2, G2
27	M3, F3	M3	G3, M3	L3, G3	G3	L3, G3

**Table S3** Sample plot raw data on microannelid species from the investigation sites N1-N3 (north-facing slopes) and S6-S8 (south-facing slopes). Designations of the sample plots refer to soil cover types: M = moss, F = fern, G = grass, L = litter)

Species	Sample plot														
	N1M1	N1M2	N1M3	N1F1	N1F2	N1F3	N2M1	N2M2	N2M3	N3G1	N3G2	N3G3	N3M1	N3M2	N3M3
<i>Achaeta danica</i>	15	6	-	10	-	14	33	11	18	-	-	-	-	-	-
<i>Achaeta</i> sp. (dzwi)	-	-	-	-	-	-	-	-	-	-	-	-	-	-	-
<i>Bryodrilus ehlersi</i>	-	-	-	-	-	-	-	1	7	-	4	8	-	-	-
<i>Buchholzia appendiculata</i>	7	-	3	38	-	45	-	-	-	-	9	10	-	-	-
<i>Cognettia sphagnetorum</i>	2	73	5	5	27	24	17	16	37	71	20	12	27	25	64
<i>Enchytraeus buchholzi</i>	-	-	-	-	-	-	-	-	-	-	-	-	-	-	-
<i>Enchytraeus norvegicus</i>	2	-	13	-	-	2	-	2	4	-	1	-	-	-	-
<i>Enchytronia parva</i>	7	-	36	3	1	13	-	-	1	-	10	-	-	-	-
<i>Enchytronia</i> sp. (holo)	-	-	-	-	-	-	-	-	-	-	-	-	-	-	-
<i>Euenchytraeus bisetosus</i>	-	-	-	-	-	-	-	-	-	-	-	-	-	-	4
<i>Fridericia auritoides</i>	-	-	-	-	-	-	-	-	-	-	-	-	-	-	-
<i>Fridericia bentii</i>	-	-	-	1	-	2	-	-	-	-	-	-	-	-	-
<i>Fridericia bisetosa</i>	1	-	-	-	-	-	-	-	-	-	-	-	-	-	-
<i>Fridericia bulboides</i>	5	-	-	-	-	-	-	9	-	3	-	1	-	-	-
<i>Fridericia christeri</i>	-	-	-	-	-	-	-	-	-	-	-	-	-	-	-
<i>Fridericia connata</i>	2	-	-	8	-	1	-	-	-	-	-	-	-	-	-
<i>Fridericia miraflores</i>	-	-	-	2	-	-	-	-	-	-	-	-	-	-	-
<i>Fridericia paroniana</i>	-	-	-	1	-	-	-	-	-	-	-	-	-	-	-
<i>Fridericia ratzeli</i>	-	-	-	-	-	-	-	-	-	-	-	-	-	-	-
<i>Fridericia stephensoni</i>	-	-	-	-	-	-	-	-	-	-	-	-	-	-	-
<i>Fridericia waldenstroemi</i>	-	-	-	-	-	-	-	-	-	-	-	-	-	-	-
<i>Fridericia</i> sp. juv.	-	-	-	8	1	-	-	-	-	-	3	-	-	-	-
<i>Hemifridericia parva</i>	-	-	-	-	-	-	-	-	-	-	13	5	-	-	-
<i>Henlea nasuta</i>	-	-	-	-	-	-	-	-	-	-	-	-	-	-	-
<i>Henlea perpusilla</i>	-	-	-	2	-	-	-	-	-	7	-	-	-	-	-
<i>Marionina clavata</i>	-	-	-	-	-	-	22	19	-	1	57	-	14	16	-
<i>Mesenchytraeus glandulosus</i>	6	8	-	-	6	26	1	-	-	6	1	-	-	9	2
<i>Mesenchytraeus pelicensis</i>	-	-	-	-	-	-	-	-	-	-	-	-	1	-	-
<i>Hrabeiella periglandulata</i>	-	-	-	-	-	-	-	-	-	-	-	-	-	-	-
Total of extracted animals	47	87	57	78	35	127	73	58	67	88	118	36	42	50	70

Table S3 Continued

Species	Sample plot														
	S6L1	S6L2	S6L3	S6G1	S6G2	S6G3	S7G1	S7G2	S7G3	S8L1	S8L2	S8L3	S8G1	S8G2	S8G3
<i>Achaeta danica</i>	-	-	-	-	-	-	-	-	-	-	-	-	-	-	-
<i>Achaeta</i> sp. (dzwi)	-	-	-	-	-	-	-	-	-	1	-	-	-	-	-
<i>Bryodrillus ehlersi</i>	-	-	-	-	-	-	-	-	-	-	-	-	-	-	-
<i>Buchholzia appendiculata</i>	211	-	303	-	190	-	2	9	40	-	-	21	-	-	1
<i>Cognettia sphagnetorum</i>	-	-	-	-	-	-	1	9	1	5	1	-	-	3	3
<i>Enchytraeus buchholzi</i>	3	11	9	8	-	-	-	-	9	-	-	-	-	-	-
<i>Enchytraeus norvegicus</i>	-	-	-	11	1	-	-	2	-	5	1	-	-	6	8
<i>Enchytronia parva</i>	36	-	-	22	15	-	14	44	7	16	-	1	2	6	-
<i>Enchytronia</i> sp. (holo)	-	-	-	8	-	-	1	-	3	-	-	-	-	-	-
<i>Euenchytraeus bisetosus</i>	-	-	-	-	-	-	-	-	-	-	-	-	-	-	-
<i>Fridericia auritoides</i>	-	25	-	-	-	-	-	-	-	-	-	-	-	-	-
<i>Fridericia benti</i>	-	-	-	-	-	-	-	-	-	-	-	-	-	-	-
<i>Fridericia bisetosa</i>	1	-	-	-	-	-	-	-	6	-	1	2	-	-	-
<i>Fridericia bulboides</i>	13	-	4	-	3	-	5	4	15	-	-	5	3	-	14
<i>Fridericia christeri</i>	-	1	8	-	1	-	-	-	1	-	-	-	-	-	-
<i>Fridericia connata</i>	3	-	15	2	1	-	1	7	-	1	-	-	-	-	-
<i>Fridericia miraflores</i>	-	-	-	-	-	-	5	-	1	-	-	-	-	-	-
<i>Fridericia paroniana</i>	59	21	48	6	106	-	-	-	7	-	-	-	-	-	-
<i>Fridericia ratzeli</i>	-	-	-	-	-	-	-	-	1	-	-	-	-	-	-
<i>Fridericia stephensoni</i>	-	-	-	-	-	-	-	-	-	-	-	-	-	-	3
<i>Fridericia waldenstroemi</i>	-	1	-	11	-	-	-	-	8	-	-	-	-	-	-
<i>Fridericia</i> sp. juv.	69	30	54	17	59	-	12	3	43	-	15	2	7	-	-
<i>Hemifridericia parva</i>	-	-	-	-	-	-	-	-	-	-	-	-	-	-	-
<i>Henlea nasuta</i>	8	-	-	-	-	-	-	-	-	-	-	-	-	-	-
<i>Henlea perpusilla</i>	-	-	-	-	-	-	-	-	9	1	2	-	-	4	-
<i>Marionina clavata</i>	-	-	-	-	-	-	-	-	-	-	-	-	-	-	-
<i>Mesenchytraeus glandulosus</i>	-	-	-	-	-	-	-	-	-	-	-	-	-	-	-
<i>Mesenchytraeus pelicensis</i>	-	-	-	-	-	-	-	-	2	-	-	-	-	-	2
<i>Hrabeiella periglandulata</i>	-	-	-	3	-	-	-	-	-	-	-	-	-	-	-
Total of extracted animals	403	89	441	88	376	-	41	78	153	29	20	31	12	19	31

**Table S4** Sample plot raw data on humus profiles from the investigation sites N1-N3 (north-facing slopes) and S6-S8 (south-facing slopes). Designations of the sample plots refer to soil cover types: M = moss, F = fern, G = grass, L = litter

Sample plot	Presence of organic horizons			Dominant humus form according to Swiss classification [28]	Dominant humus form according to German classification [27]
	OL	OF	OH		
N1M1	yes	yes	no	Dysmull	
N1M2	yes	yes	partial	Eumesoamphi	
N1M3	yes	yes	no	Dysmull	Mullartiger Moder
N1F1	yes	yes	yes	Eumesoamphi	
N1F2	yes	yes	no	Dysmull	
N1F3	yes	yes	no	Dysmull	
N2M1	yes	yes	yes	Dysmoder	
N2M2	yes	yes	yes	Dysmoder	Typischer Moder
N2M3	yes	yes	no	Dysmoder	
N3G1	yes	yes	yes	Dysmoder	
N3G2	yes	yes	yes	Dysmoder (folic)	Typischer Moder
N3G3	yes	yes	yes	Dysmoder	
N3M1	yes	yes	yes	Dysmoder (folic)	
N3M2	yes	yes	partial	Hemimoder	
N3M3	yes	yes	no	Hemimoder	
S6L1	yes	yes	no	Dysmull	
S6L2	yes	yes	no	Dysmull (Amphi)	Mullartiger Moder
S6L3	yes	yes	no	Dysmull (Amphi)	
S6G1	partial	yes	no	Dysmull (colluvic)	
S6G2	yes	yes	Yes	Pachyamphi folic (albic)	
S6G3	partial	yes	Yes	Eumesoamphi (albic)	
S7G1	yes	yes	Partial	Hemimoder	
S7G2	yes	yes	partial	Eumesoamphi	Mullartiger Moder
S7G3	yes	yes	partial	Leptoamphi	
S8L1	partial	partial	yes	Dysmoder	
S8L2	yes	yes	no	Hemimoder	
S8L3	yes	yes	partial	Hemimoder	Mullartiger Moder/ Typischer Moder
S8G1	yes	yes	yes	Dysmoder	
S8G2	yes	yes	no	Hemimoder	
S8G3	no	yes	no	Hemimoder (erodic)	



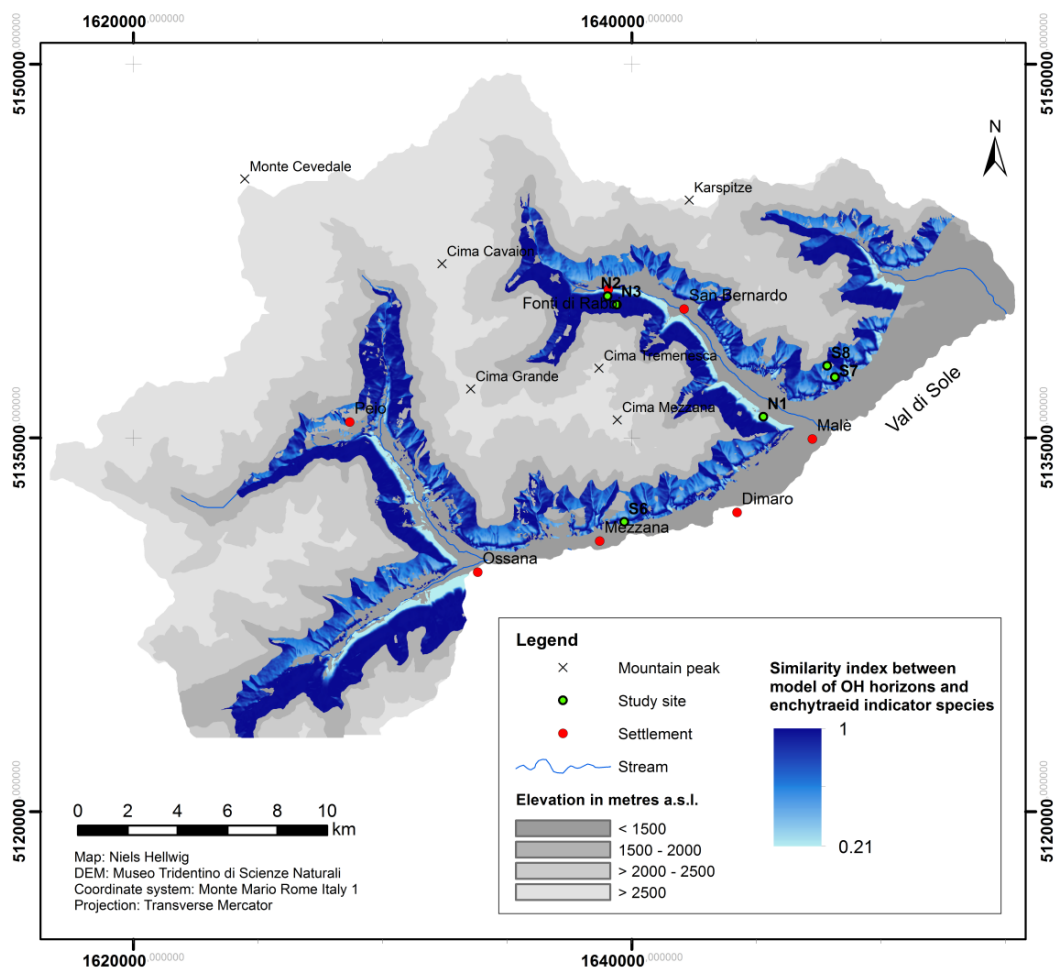


**Figure S1** Similarity between the models of the spatial distribution of enchytraeid indicator classes and the occurrence of humus forms showing an OH horizon.

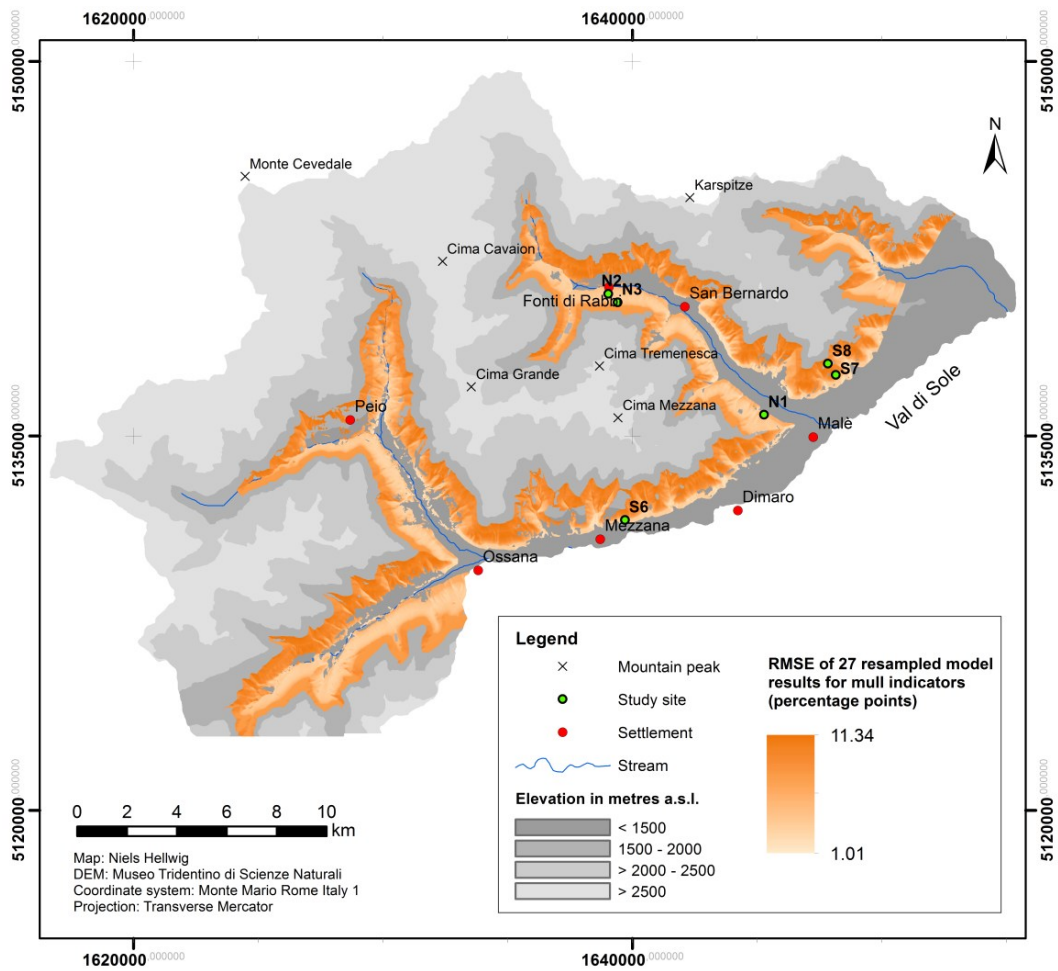


**Figure S2** Spatial distribution of RMSE values of 27 resampled model results for mull-indicating enchytraeids.

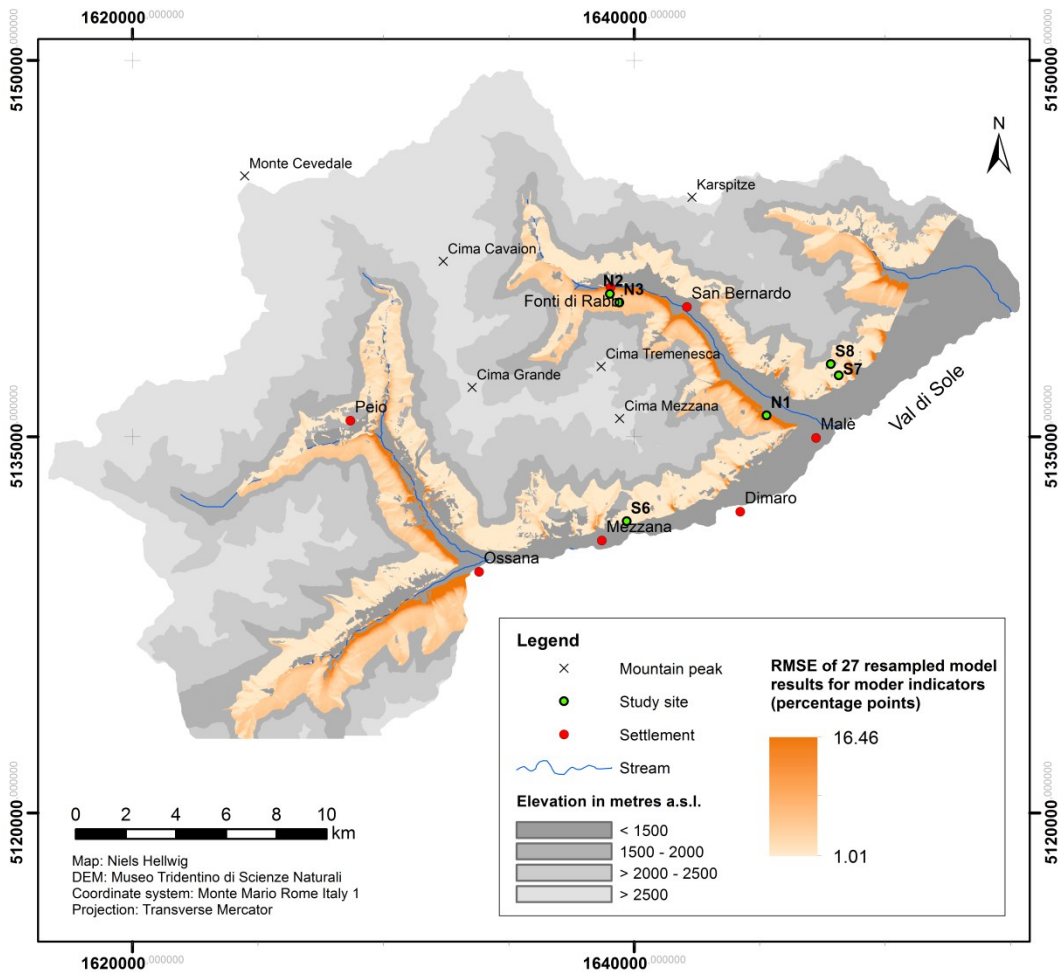


**Figure S3** Spatial distribution of RMSE values of 27 resampled model results for moder-indicating enchytraeids.

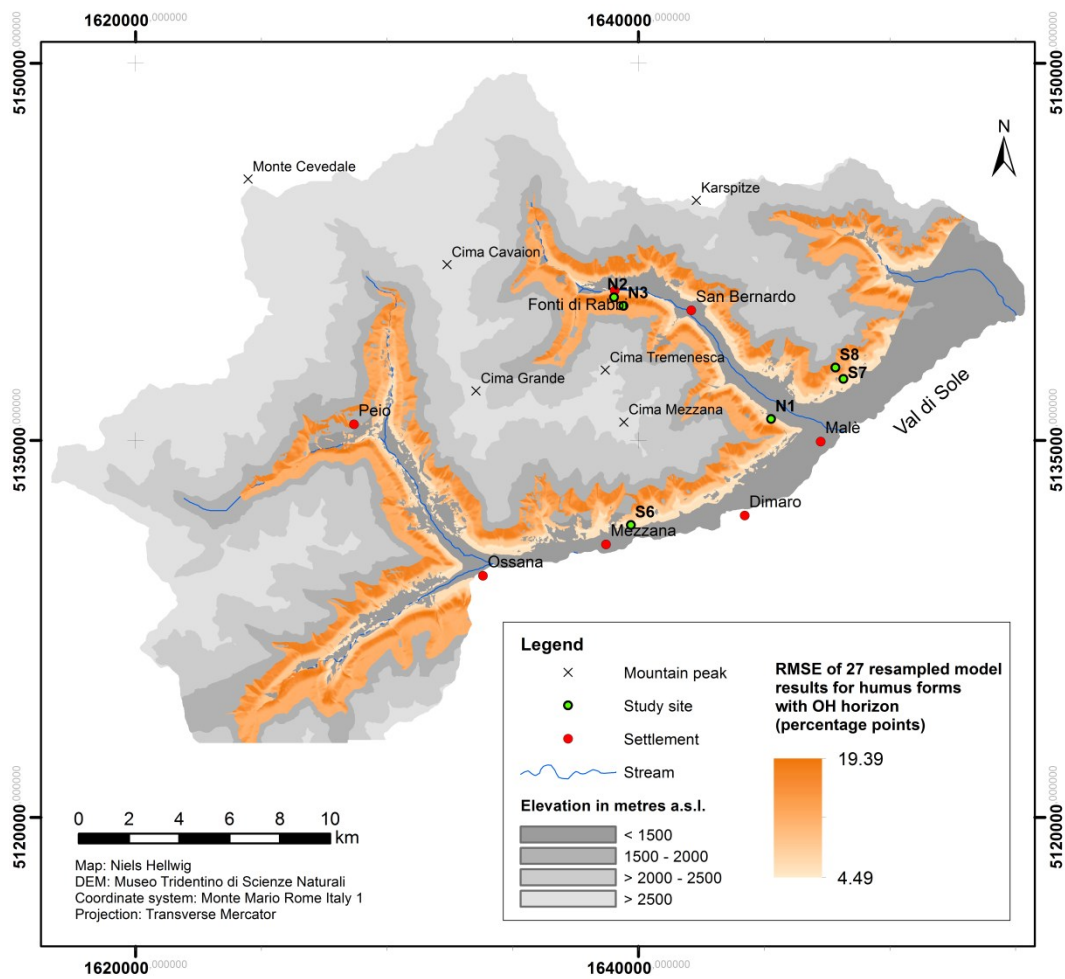


**Figure S4** Spatial distribution of RMSE values of 27 resampled model results for forest humus forms showing an OH horizon.



## Appendix 3: Supplementary material of Chapter 4

**Table S1.** Input data for linear models of soil C/N ratio and enzyme activities depending on pH values

Site	Soil depth (cm)	Soil horizons covered by the sample	pH H <sub>2</sub> O (1:10)	Leucine-amino-peptidase activity (nmol MUF g <sup>-1</sup> dry soil h <sup>-1</sup> )	Ratio alkaline/acid phospho-monoesterase activity	Soil C/N ratio
N1a-1	5-10	A	4.39	147.9	0.01	26.5
N1a-2	5-10	A	4.47	87.6	0.00	21.3
N1a-3	5-10	AE/Bs	4.54	96.2	0.01	19.3
N1a-4	5-10	AE	4.83	144.7	0.03	16.4
N1a-5	5-10	AE/Bs	4.39	123.7	0.00	19.4
N1b-1	0-5	O/A	4.35	180.4	0.16	25.8
N1b-2	5-10	A/Bs	4.43	54.5	0.00	23.6
N1b-3	0-5	O/A	4.22	141.5	0.01	36.6
N1b-4	5-10	A/Bs	4.67	23.7	0.00	22.5
N1b-5	0-5	O/A	4.43	227.7	0.02	35.1
N1c-1	5-10	AE/Bs	5.23	126.0	0.24	17.8
N1c-2	5-10	AE/Bs	5.29	116.8	0.23	21.7
N1c-3	5-10	AE	5.45	128.5	0.37	17.5
N1c-4	5-10	AE/Bs	5.38	105.6	0.26	17.4
N1c-5	5-10	AE/Bs	4.94	58.7	0.08	18.2
S6a-1	5-10	Ah	5.43	72.7	0.22	22.8
S6a-2	5-10	Ah	5.33	66.4	0.59	21.3
S6a-3	5-10	Ah	4.96	30.6	0.03	17.3
S6a-4	5-10	Ah	5.94	149.1	0.57	21.0
S6a-5	5-10	Ah	5.60	61.0	0.23	19.7
S6b-1	0-5	OF/Ah	6.76	438.6	2.17	15.5
S6b-2	0-5	Ah	6.60	285.8	1.72	18.5
S6b-3	10-15	Bw	6.16	58.9	0.80	13.9
S6b-4	0-5	OF/Ah	6.53	148.5	1.60	14.2
S6b-5	0-5	OF/Ah	6.36	130.6	1.79	18.5
S6c-1	0-5	OF/Ah	5.53	192.4	0.13	22.5
S6c-2	0-5	OF/Ah	5.74	337.5	0.13	22.0
S6c-3	0-5	OF/Ah	5.77	588.3	0.65	19.4
S6c-4	0-5	OF/Ah	5.84	351.8	0.39	19.3
S6c-5	0-5	OF/Ah	5.93	266.2	0.71	20.7
N2a-1	10-15	OH/AE	3.82	50.7	0.00	20.5
N2a-2	10-15	OH/AE	3.87	56.1	0.00	24.2
N2a-3	10-15	OH/AE	3.86	48.5	0.00	21.9
N2a-4	10-15	OH/AE	3.97	57.3	0.00	19.9
N2a-5	10-15	OH/AE	3.81	27.8	0.00	22.2
N2b-1	10-15	AE/Bs	5.07	37.3	0.07	18.1
N2b-2	5-10	AE/Bs	4.94	92.5	0.09	18.8
N2b-3	5-10	AE/Bs	5.17	351.4	0.23	17.4
N2b-4	5-10	AE/Bs	4.89	78.3	0.04	23.6
N2b-5	5-10	AE/Bs	4.63	92.9	0.03	23.8
N2c-1	10-15	AE/C	4.53	38.7	0.00	20.4
N2c-2	10-15	AE/C	4.50	24.6	0.00	18.0
N2c-3	10-15	AE/C	4.75	43.6	0.04	20.1
N2c-4	10-15	AE/C	4.48	19.6	0.00	25.3
N2c-5	10-15	AE/C	4.66	26.0	0.00	20.2

Table S1. *Continued*

Site	Soil depth (cm)	Soil horizons covered by the sample	pH H <sub>2</sub> O (1:10)	Leucine-amino-peptidase activity (nmol MUF g <sup>-1</sup> dry soil h <sup>-1</sup> )	Ratio alkaline/acid phospho-monoesterase activity	Soil C/N ratio
S7a-1	10-15	Bs	5.93	209.9	1.10	14.0
S7a-2	10-15	Bs/C	5.99	121.9	0.88	14.1
S7a-3	10-15	Bs/C	5.99	131.8	0.94	14.4
S7a-4	10-15	Bs/C	6.00	141.7	0.95	10.8
S7a-5	10-15	Bs	5.81	166.5	0.94	13.2
S7b-1	5-10	AE	5.89	367.5	0.73	19.4
S7b-2	5-10	AE	5.76	187.7	0.60	17.2
S7b-3	5-10	AE	6.15	356.6	0.86	15.7
S7b-4	5-10	AE	5.93	286.5	0.77	18.5
S7b-5	5-10	AE	5.96	213.4	0.81	15.5
S7c-1	5-10	AE	5.80	145.4	0.56	17.8
S7c-2	5-10	AE	5.56	93.4	0.24	16.5
S7c-3	5-10	AE	5.55	97.5	0.33	16.6
S7c-4	5-10	AE	5.58	120.1	0.30	16.5
S7c-5	5-10	AE	5.60	177.9	0.34	14.4
N3a-1	5-10	OF/AE	4.14	NA <sup>1</sup>	NA <sup>1</sup>	25.9
N3a-2	10-15	OF/AE	4.56	71.5	0.03	20.1
N3a-3	10-15	OF/AE	4.55	81.5	0.03	20.7
N3a-4	5-10	OF/Bs	4.39	92.6	0.02	22.2
N3a-5	10-15	E/C	4.48	67.5	0.02	25.6
N3b-1	10-15	OH/C	4.31	86.7	0.02	19.7
N3b-2	5-10	OF(/C)	4.32	0.0	NA <sup>1</sup>	20.1
N3b-3	10-15	OH/C	4.24	70.5	0.01	18.9
N3b-4	10-15	E/C	4.09	100.3	0.01	NA <sup>1</sup>
N3b-5	10-15	E/C	3.95	28.4	0.00	NA <sup>1</sup>
N3c-1	10-15	AE	4.04	57.1	0.02	22.1
N3c-2	10-15	AE	4.06	75.4	0.01	23.5
N3c-3	10-15	AE	4.07	59.2	0.01	19.5
N3c-4	10-15	AE	3.89	98.9	0.01	NA <sup>1</sup>
N3c-5	10-15	AE	4.07	143.1	0.01	25.5
S8a-1	5-10	OF/Bs	5.52	99.5	0.04	21.2
S8a-2	5-10	Ah/Bs	4.98	142.5	0.03	23.8
S8a-3	5-10	OF/Bs	5.62	892.5	0.09	10.9
S8a-4	5-10	Ah/Bs	5.41	260.7	0.06	18.8
S8a-5	5-10	Ah/Bs	5.66	1403.9	0.12	10.9
S8b-1	5-10	OL/OF/AE	5.20	70.4	0.05	17.2
S8b-2	5-10	OL/OF/AE	5.27	100.0	0.05	14.0
S8b-3	5-10	OL/OF/AE	5.03	77.7	0.06	17.2
S8b-4	5-10	OL/OF/AE	5.31	118.9	0.10	18.2
S8b-5	5-10	OL/OF/AE	5.28	86.6	0.08	17.6
S8c-1	0-5	Ah/Bs	5.18	143.0	0.03	23.2
S8c-2	0-5	Ah/BA	5.50	192.6	0.15	17.5
S8c-3	0-5	Ah/Bs	5.35	131.1	0.09	18.8
S8c-4	0-5	Ah/Bs	5.46	133.2	0.10	22.4
S8c-5	0-5	Ah/Bs	5.81	127.2	0.15	18.2

<sup>1</sup> No sample. Sample was omitted in the respective regression model.

**Table S2.** Input data for linear model of the ratio bacterial / archaeal abundance depending on pH values

<b>Site</b>	<b>Soil depth (cm)</b>	<b>Dominant soil horizons of subsamples</b>	<b>pH H<sub>2</sub>O (1:10)</b>	<b>Ratio bacterial / archaeal abundance</b>
<b>N1a</b>	5-10	AE/Bs	4.52	4.8
<b>N1b</b>	0-5	O/A	4.45	4.7
<b>N1c</b>	5-10	AE/Bs	5.26	4.0
<b>S6a</b>	5-10	Ah	5.45	29.4
<b>S6b</b>	0-5	OF/Ah	6.58	16.1
<b>S6c</b>	0-5	OF/Ah	5.76	19.1
<b>N2a</b>	10-15	OH/AE	3.87	1.9
<b>N2b</b>	5-10	AE/Bss	4.94	0.5
<b>N2c</b>	10-15	AE/C	4.58	40.2
<b>S7a</b>	10-15	Bs/C	5.94	32.7
<b>S7b</b>	5-10	AE	5.94	660.5
<b>S7c</b>	5-10	AE	5.62	22.0
<b>N3a</b>	10-15	OF/AE	4.53	18.0
<b>N3b</b>	10-15	OH/E/C	4.17	0.1
<b>N3c</b>	10-15	AE	4.03	30.4
<b>S8a</b>	5-10	Ah/Bs	5.44	22.1
<b>S8b</b>	5-10	Ah/Bs	5.22	20.3
<b>S8c</b>	0-5	OL/OF/AE	5.46	24.4



**Table S3.** Humus forms (according to [40,41]) and pH values sampled at 60 sites in Val di Rabbi (RN1–RN30 at a north-facing slope, RS1–RS30 at a south-facing slope). pH values are means from two replicates

Sites	Elevation a.s.l. (m)	Ground cover type (percentage at site)	Humus form	pH in A horizon H <sub>2</sub> O (1:10)
<b>RN1</b>	1215	Grass (100%)	Amphimull (AMU)	6.06
<b>RN2</b>	1211	Grass (100%)	Mullartiger Moder (MOM)	5.18
<b>RN3</b>	1244	Grass (100%)	Rohhumusartiger Moder (MRA)	4.88
<b>RN4</b>	1270	Moss (100%)	Amphimull (AMU)	5.20
<b>RN5</b>	1278	Litter (70%)	Amphimull (AMU)	5.25
		Fern (30%)	F-Mull (MUO)	4.96
<b>RN6</b>	1298	Litter (50%)	Hagerhumus (HMO)	5.11
		Grass (50%)	Rohhumusartiger Moder (MRA)	4.41
<b>RN7</b>	1309	Grass (100%)	Rohhumusartiger Moder (MRA)	4.82
<b>RN8</b>	1340	Litter (100%)	Rohhumusartiger Moder (MRA)	4.63
<b>RN9</b>	1362	Grass (100%)	Graswurzelfilz-Moder (GMO)	5.00
<b>RN10</b>	1411	Grass (80%)	Amphimull (AMU)	4.62
		Litter (20%)	Amphimull (AMU)	- <sup>1</sup>
<b>RN11</b>	1437	Litter (50%)	Rohhumusartiger Moder (MRA)	4.41
		Grass (50%)	Mullartiger Moder (MOM)	4.84
<b>RN12</b>	1442	Grass (80%)	Mullartiger Moder (MOM)	4.48
		Litter (20%)	Rohhumusartiger Moder (MRA)	4.45
<b>RN13</b>	1480	Litter (100%)	Rohhumusartiger Moder (MRA)	4.42
<b>RN14</b>	1496	Grass (70%)	Rohhumusartiger Moder (MRR)	4.39
		Litter (30%)	Rohhumusartiger Moder (MRA)	4.64
<b>RN15</b>	1523	Grass (90%)	Rohhumusartiger Moder (MRR)	4.72
		Litter (10%)	Rohhumusartiger Moder (MRR)	4.45
<b>RN16</b>	1540	Grass (100%)	Rohhumusartiger Moder (MRR)	4.80
<b>RN17</b>	1622	Grass (100%)	Rohhumusartiger Moder (MRR)	4.20
<b>RN18</b>	1648	Grass (100%)	Typischer Moder (MOA)	4.25
<b>RN19</b>	1704	Grass (80%)	Rohhumusartiger Moder (MRA)	4.69
		Litter (20%)	Rohhumusartiger Moder (MRR)	4.58
<b>RN20</b>	1735	Grass (100%)	Rohhumusartiger Moder (MRR)	4.73
<b>RN21</b>	1757	Grass (100%)	Rohhumusartiger Moder (MRR)	4.17
<b>RN22</b>	1805	Grass (100%)	Rohhumusartiger Moder (MRA)	4.24
<b>RN23</b>	1849	Grass (100%)	Rohhumusartiger Moder (MRR)	4.46
<b>RN24</b>	1893	Shrubs (100%)	Rohhumus (ROR)	4.22
<b>RN25</b>	1895	Grass (80%)	Mullartiger Moder (MOM)	4.66
		Shrubs (20%)	Rohhumusartiger Moder (MRA)	4.71
<b>RN26</b>	1908	Grass (100%)	Rohhumusartiger Moder (MRA)	4.74
<b>RN27</b>	1915	Grass (100%)	Rohhumusartiger Moder (MRR)	4.02
<b>RN28</b>	1957	Grass (100%)	Rohhumusartiger Moder (MRR)	4.52
<b>RN29</b>	1964	Grass (80%)	Mullartiger Moder (MOM)	4.71
		Shrubs (20%)	Typischer Moder (MOR)	4.68
<b>RN30</b>	2007	Shrubs (100%)	Rohhumus (ROR)	4.05

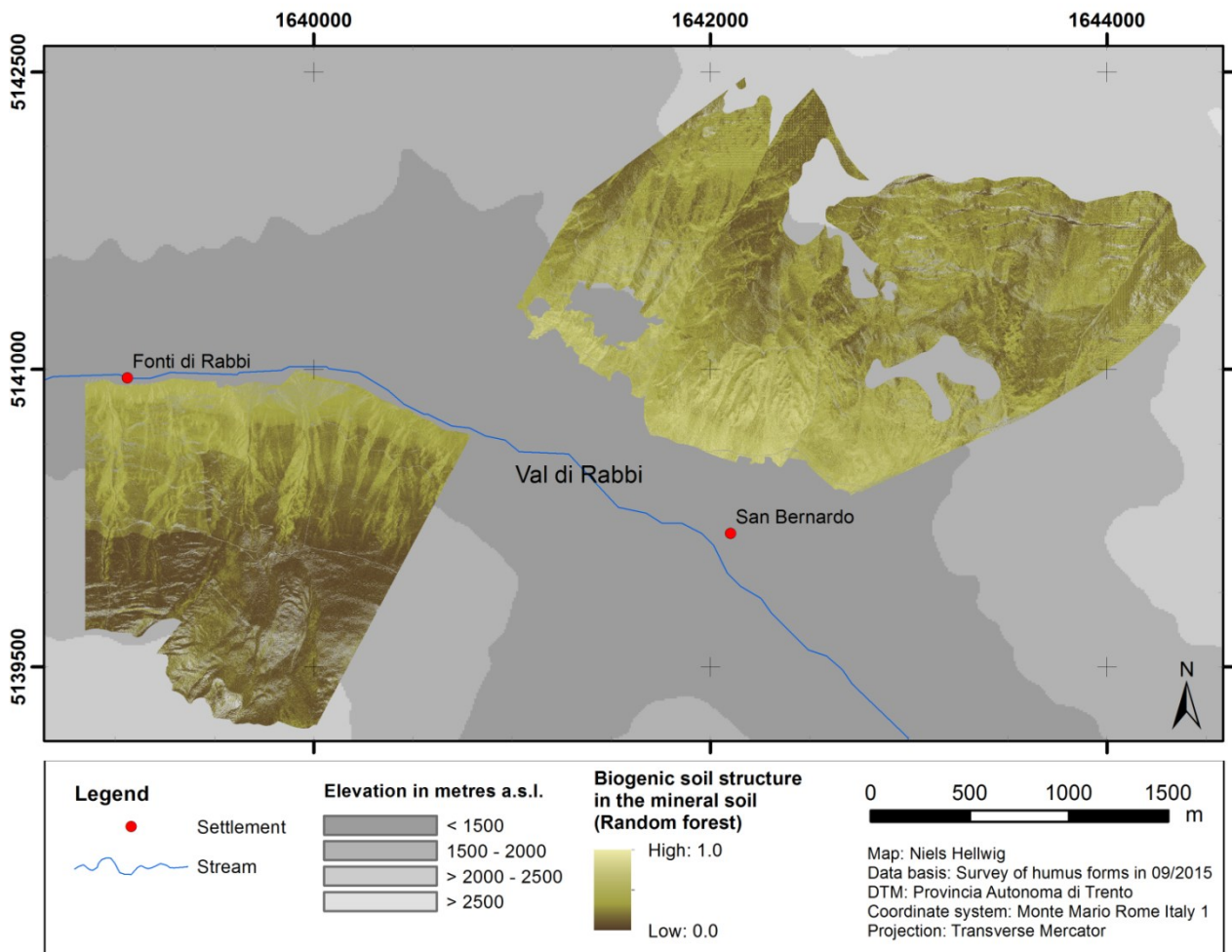
<sup>1</sup> No pH sample was taken under litter at site RN10. For modelling, the pH sample under grass was weighted with 1.0 (instead of 0.8) at this site.

Table S3. *Continued*

Sites	Elevation a.s.l. (m)	Ground cover type (percentage at site)	Humus form	pH in A horizon H <sub>2</sub> O (1:10)
<b>RS1</b>	1229	Grass (100%)	F-Mull (MUO)	5.70
<b>RS2</b>	1310	Grass (100%)	Typischer Moder (MOA)	5.80
<b>RS3</b>	1329	Litter (100%)	Amphimull (AMU)	4.43
<b>RS4</b>	1391	Grass (60%)	Rohhumusartiger Moder (MRA)	4.74
		Litter (40%)	Amphimull (AMU)	4.77
<b>RS5</b>	1415	Grass (100%)	Amphimull (AMU)	5.79
<b>RS6</b>	1421	Grass (100%)	F-Mull (MUO)	5.36
<b>RS7</b>	1459	Litter (70%)	Mullartiger Moder (MOM)	4.67
		Grass (30%)	F-Mull (MUO)	5.36
<b>RS8</b>	1502	Grass (70%)	Rohhumusartiger Moder (MRA)	4.90
		Litter (30%)	Amphimull (AMU)	4.90
<b>RS9</b>	1523	Grass (100%)	Amphimull (AMU)	5.45
<b>RS10</b>	1553	Grass (100%)	F-Mull (MUO)	5.95
<b>RS11</b>	1590	Grass (100%)	Mullartiger Moder (MOM)	5.39
<b>RS12</b>	1621	Litter (60%)	Mullartiger Moder (MOM)	5.05
		Moss (40%)	Mullartiger Moder (MOM)	4.46
<b>RS13</b>	1677	Grass (100%)	Mullartiger Moder (MOM)	5.30
<b>RS14</b>	1719	Grass (100%)	Rohhumusartiger Moder (MRA)	4.61
<b>RS15</b>	1728	Grass (50%)	Rohhumusartiger Moder (MRA)	4.73
		Litter (40%)	Hagerhumus (HMO)	4.92
		Moss (10%)	Rohhumusartiger Moder (MRA)	4.47
<b>RS16</b>	1783	Litter (60%)	Rohhumusartiger Moder (MRA)	4.62
		Grass (40%)	Rohhumusartiger Moder (MRR)	4.74
<b>RS17</b>	1827	Litter (60%)	Rohhumus (ROA)	4.73
		Grass (30%)	F-Mull (MUO)	5.34
		Moss (10%)	Rohhumus (ROA)	<sup>-2</sup>
<b>RS18</b>	1892	Grass (100%)	Rohhumusartiger Moder (MRA)	4.72
<b>RS19</b>	1908	Grass (60%)	Rohhumusartiger Moder (MRA)	4.39
		Litter (40%)	Rohhumusartiger Moder (MRR)	4.72
<b>RS20</b>	1952	Grass (100%)	F-Mull (MUO)	5.30
<b>RS21</b>	1945	Litter (50%)	Rohhumusartiger Moder (MRA)	4.51
		Grass (50%)	F-Mull (MUO)	5.08
<b>RS22</b>	1967	Grass (100%)	Mullartiger Moder (MOM)	5.15
<b>RS23</b>	2010	Grass (100%)	F-Mull (MUO)	5.02
<b>RS24</b>	2029	Shrubs (60%)	Typischer Moder (MOR)	4.94 and 4.98 <sup>3</sup>
		Grass (40%)	Typischer Moder (MOA)	
<b>RS25</b>	2059	Shrubs (80%)	Rohhumus (ROR)	4.75
		Grass (20%)	Rohhumusartiger Moder (MRA)	4.95
<b>RS26</b>	2090	Grass (100%)	Rohhumusartiger Moder (MRA)	5.95
<b>RS27</b>	2130	Shrubs (50%)	Rohhumusartiger Moder (MRA)	4.51
		Grass (50%)	Typischer Moder (MOA)	4.73
<b>RS28</b>	2147	Shrubs (70%)	Rohhumusartiger Moder (MRR)	4.46
		Grass (30%)	Typischer Moder (MOA)	4.92
<b>RS29</b>	2158	Shrubs (80%)	Rohhumusartiger Moder (MRR)	4.61
		Grass (20%)	Typischer Moder (MOA)	5.05
<b>RS30</b>	2212	Shrubs (80%)	Rohhumus (ROR)	4.54
		Grass (20%)	Rohhumusartiger Moder (MRA)	4.86

<sup>2</sup> No pH sample was taken under moss at site RS17. For modelling, the pH samples under litter and grass were weighted with 2/3 (instead of 0.6) and 1/3 (instead of 0.3) at this site.

<sup>3</sup> The labels of ground cover types got lost for pH samples at site RS24.



**Figure S1.** Results of the random forest model for the biogenic soil structure in the mineral soil

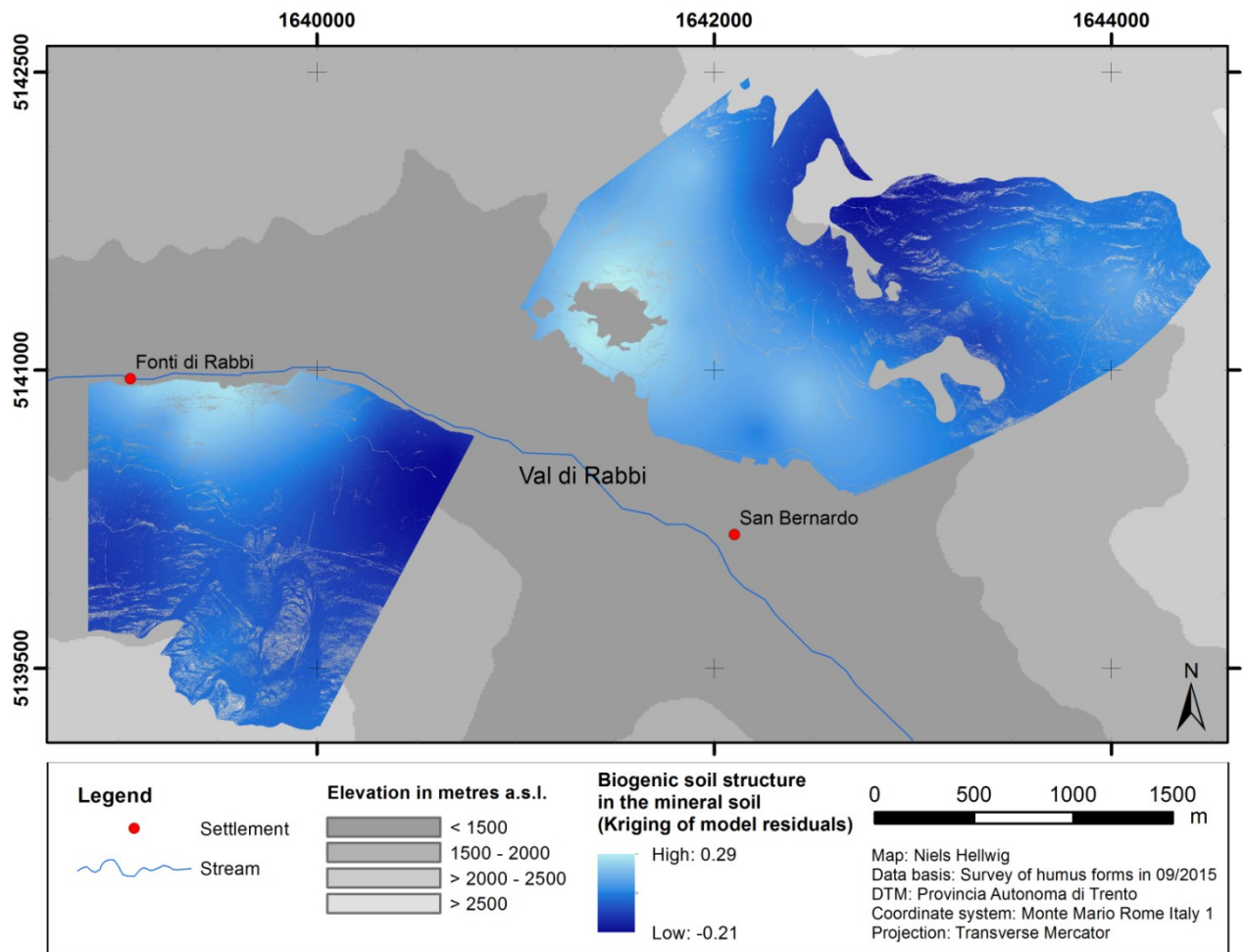


**Figure S2.** Results of the kriging procedure of the model residuals for the biogenic soil structure in the mineral soil

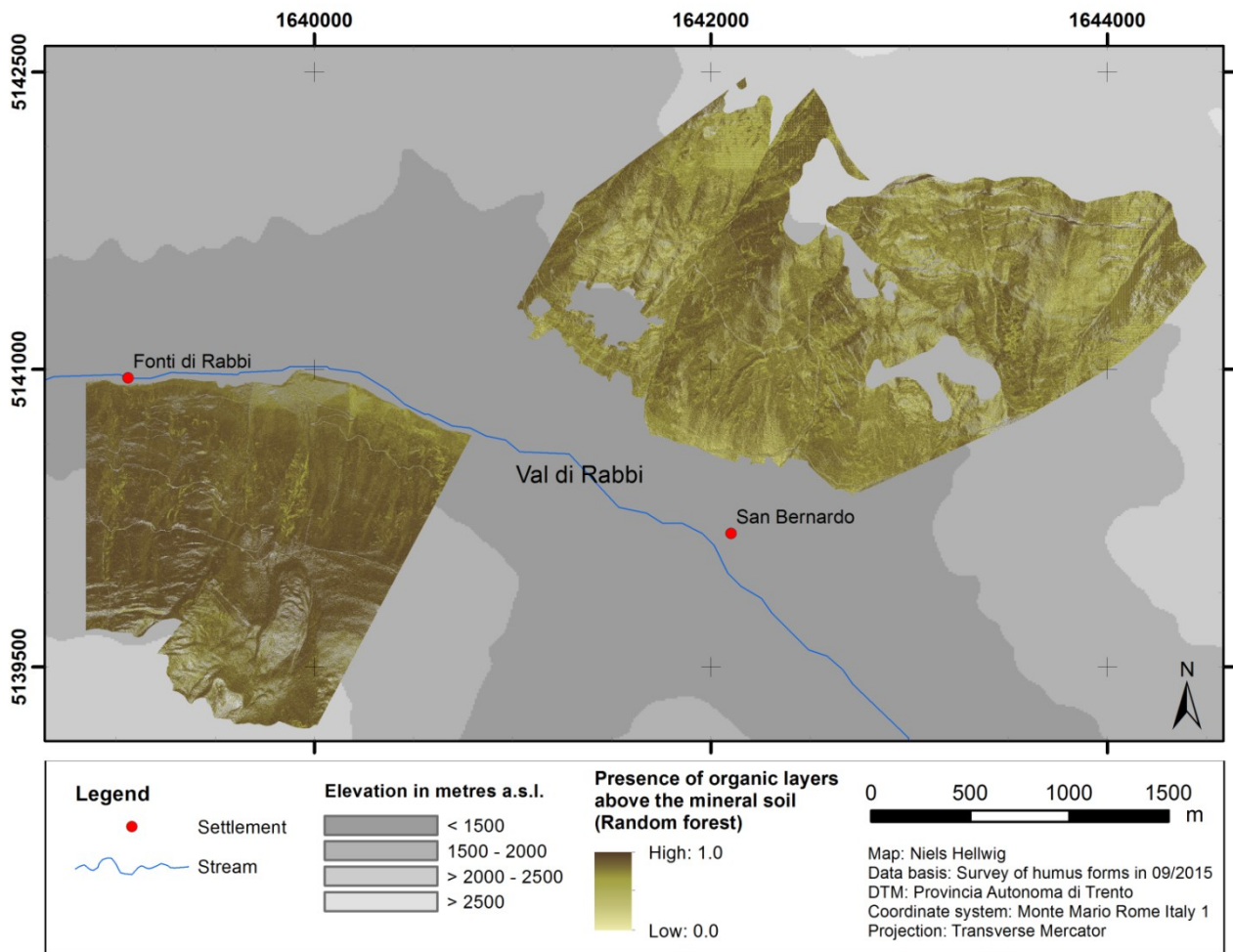


**Figure S3.** Results of the random forest model for the presence of organic layers above the mineral soil

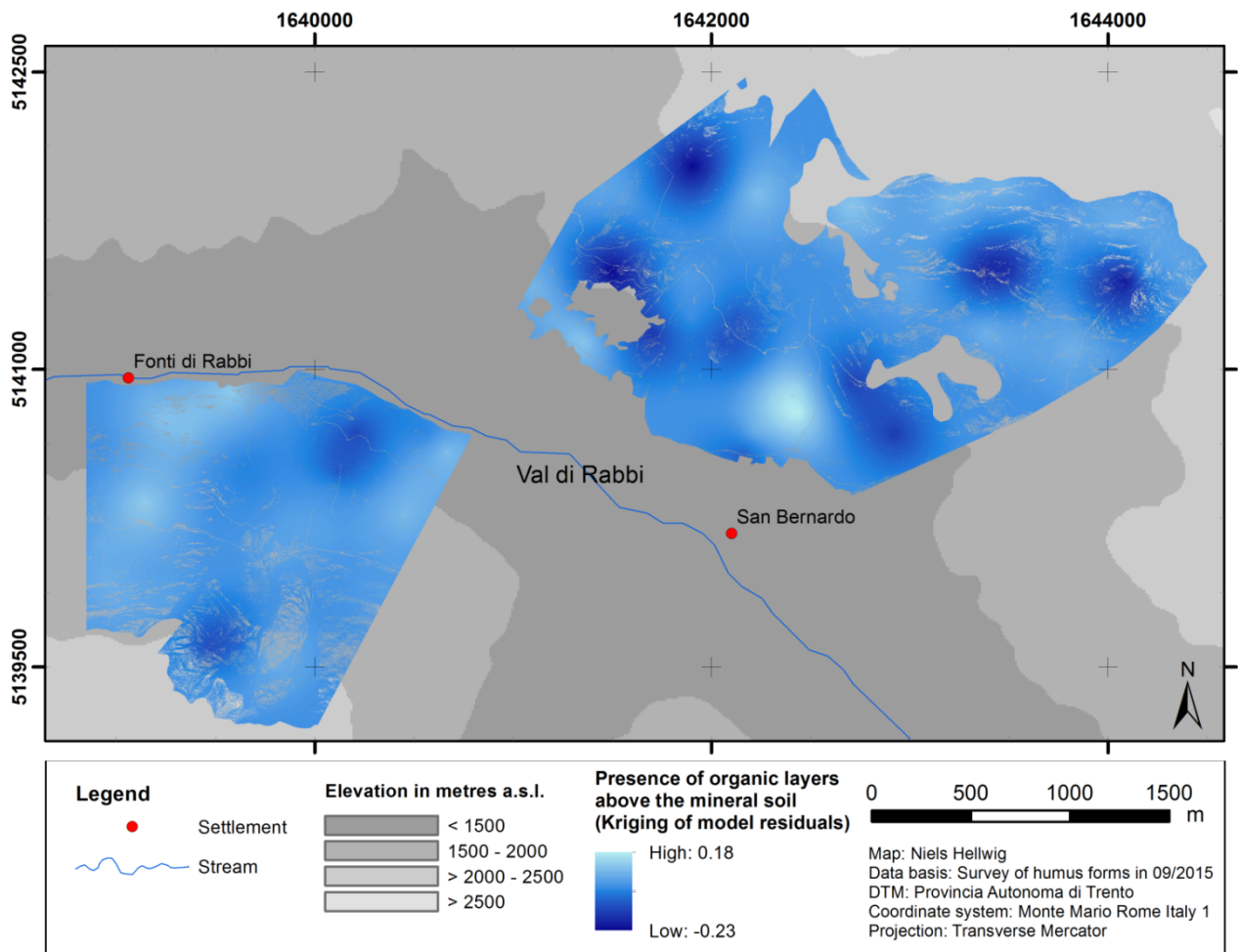


**Figure S4.** Results of the kriging procedure of the model residuals for the presence of organic layers above the mineral soil



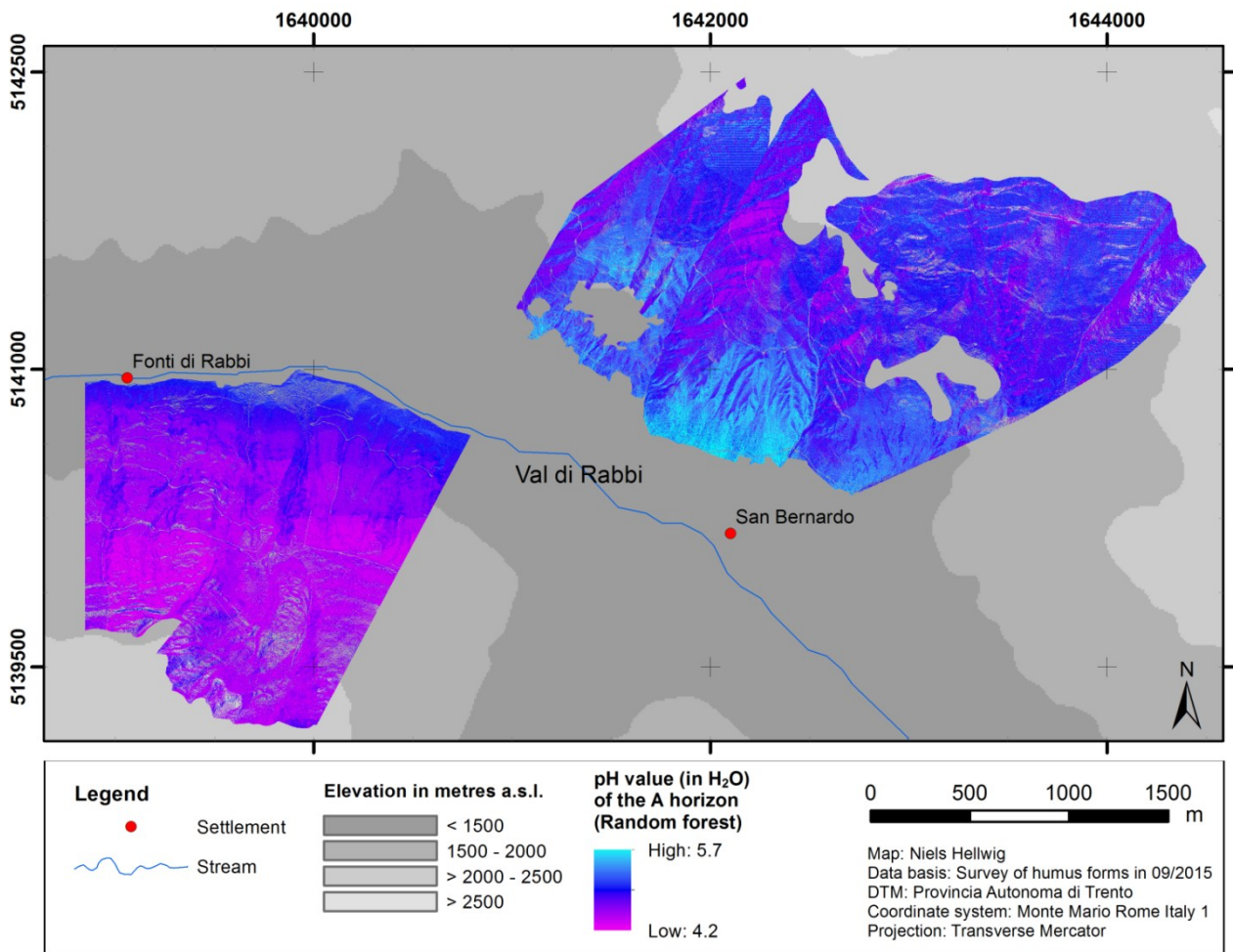


**Figure S5.** Results of the random forest model for the topsoil acidity

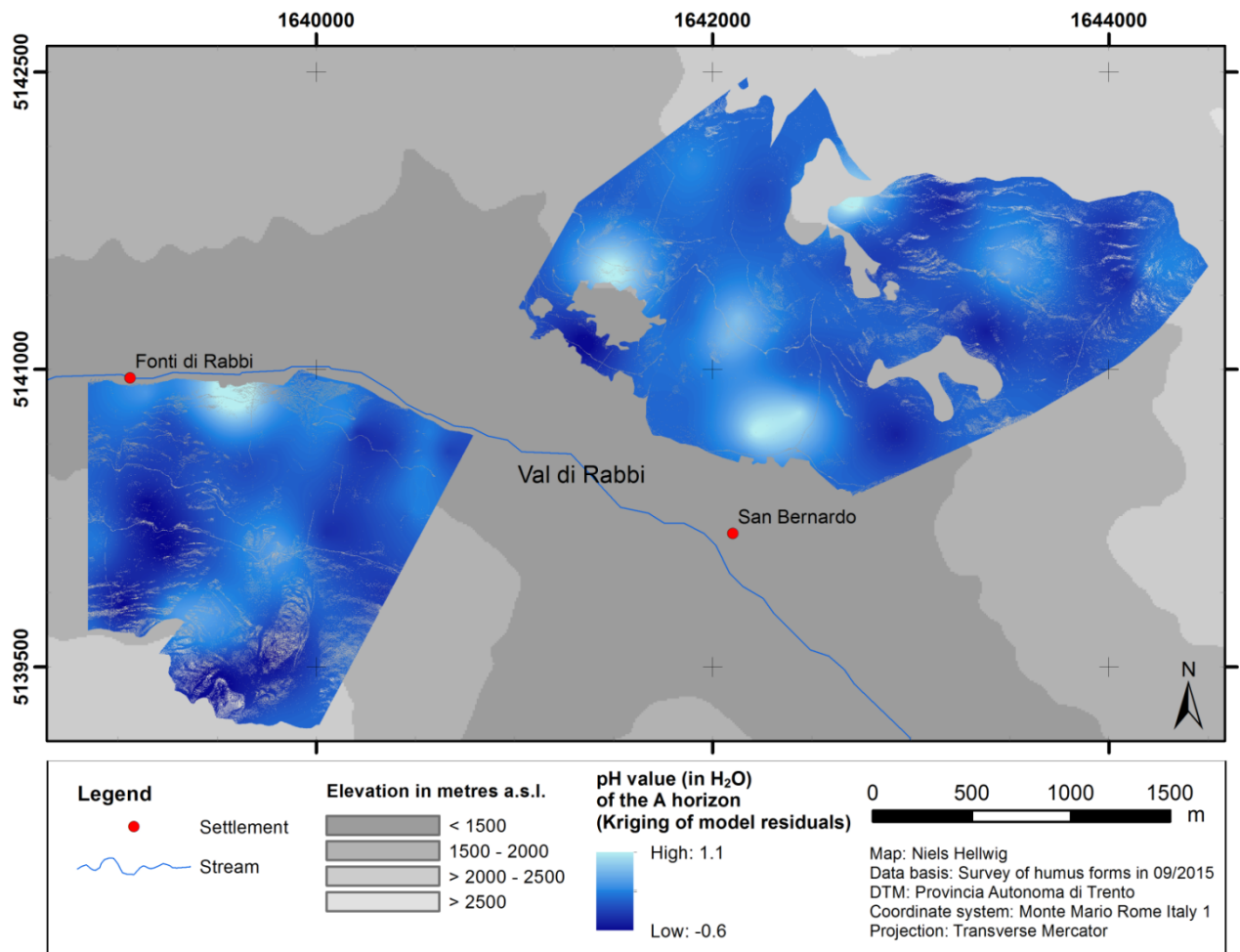


**Figure S6.** Results of the kriging procedure of the model residuals for the topsoil acidity



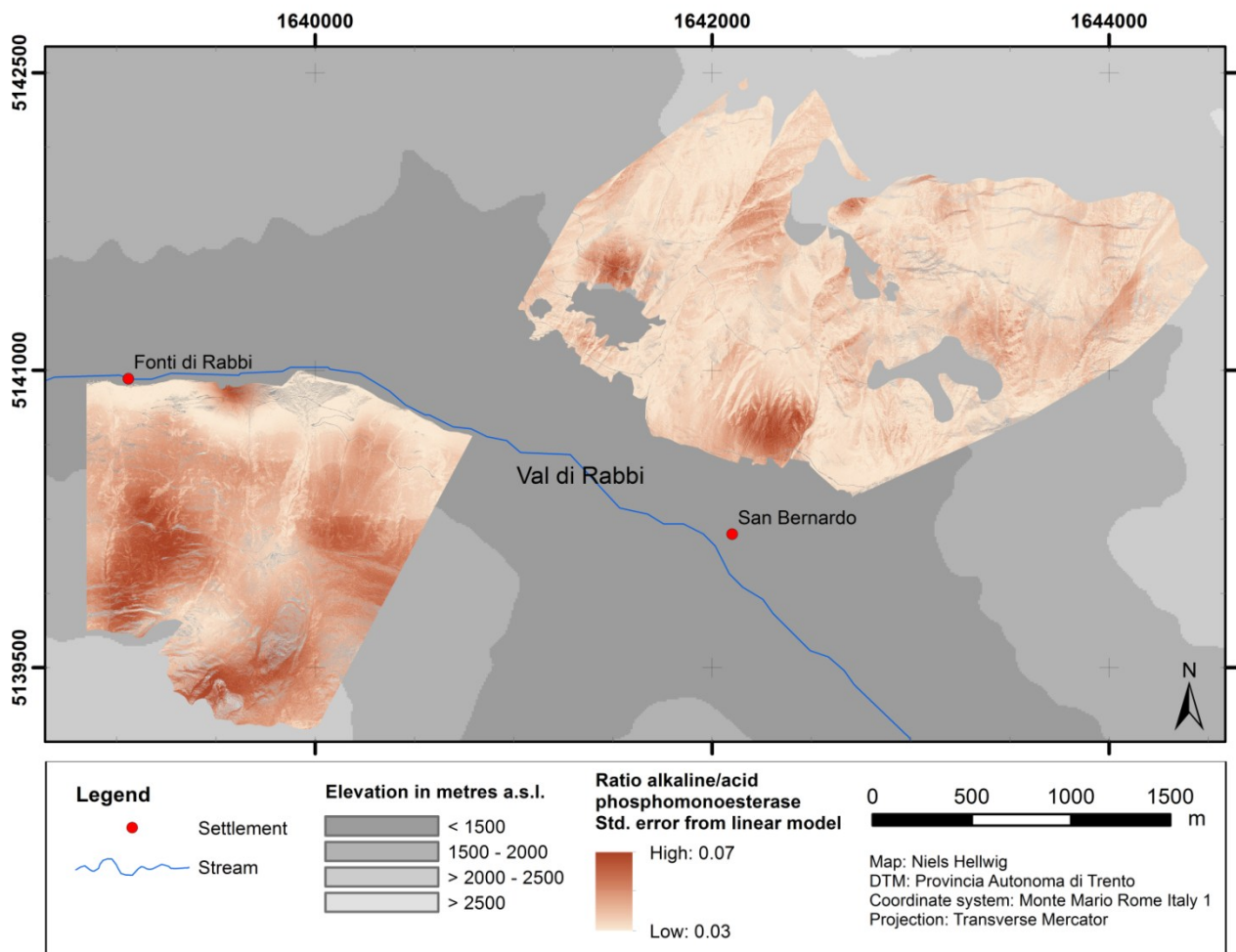


**Figure S7.** Standard error of predictions from linear model of the ratio alkaline/acid phosphomonoesterase activity as a function of the pH value

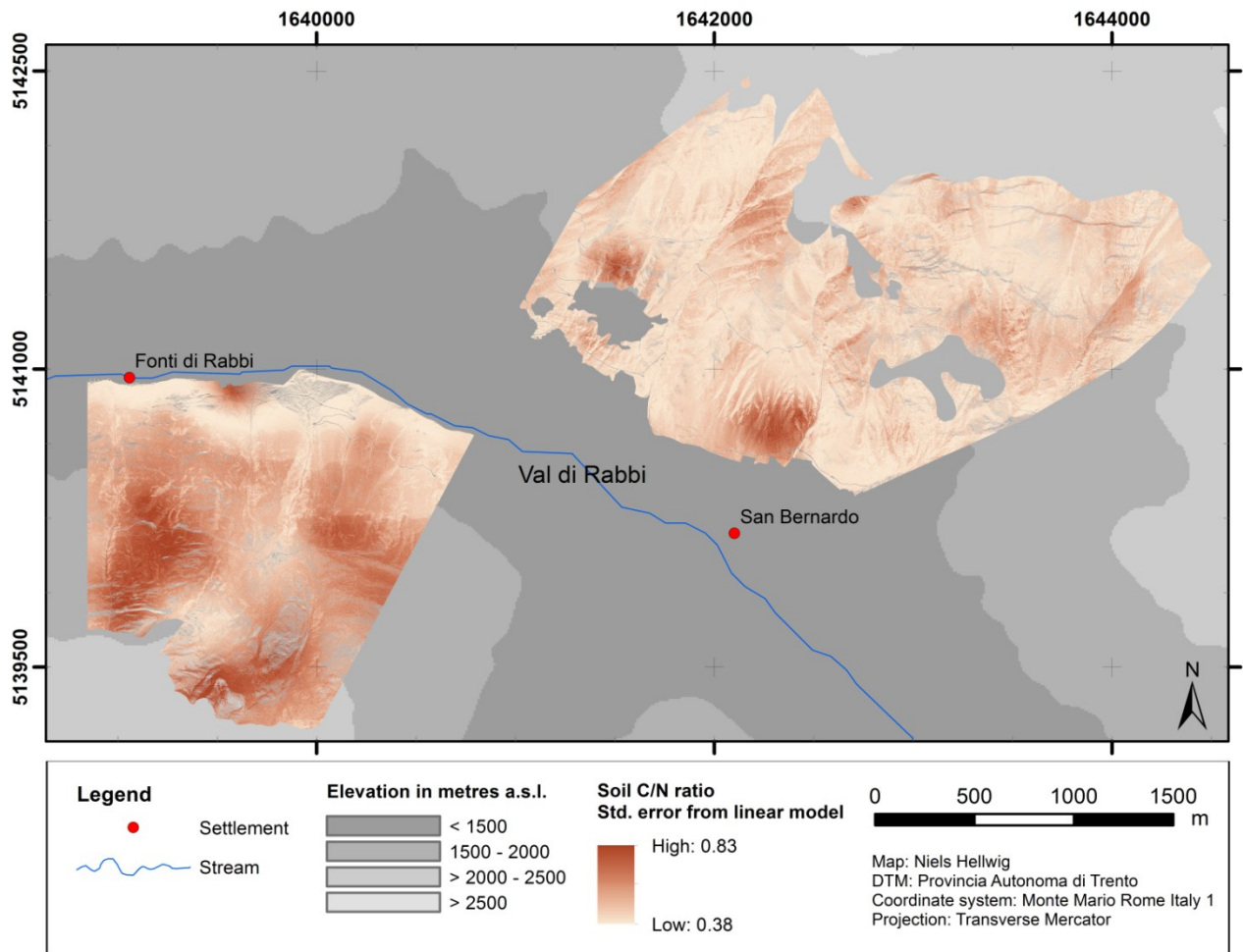


**Figure S8.** Standard error of predictions from linear model of the soil C/N ratio as a function of the pH value



## Appendix 4: Abstract of co-authored article (Anschlag et al. 2017)

*Journal of Mountain Science* 14(4), 2017, 662-673  
<http://dx.doi.org/10.1007/s11629-016-4290-y>

### Vegetation-based bioindication of humus forms in coniferous mountain forests

KERSTIN ANSCHLAG<sup>1,\*</sup>, DYLAN TATTI<sup>2,3</sup>, NIELS HELLWIG<sup>1</sup>, GIACOMO SARTORI<sup>4</sup>, JEAN-MICHEL GOBAT<sup>2</sup>, GABRIELE BROLL<sup>1</sup>

<sup>1</sup> Institute of Geography, University of Osnabrück, Seminarstraße 19ab, 49074 Osnabrueck, Germany

<sup>2</sup> Functional Ecology Laboratory, University of Neuchâtel, Rue Emile-Argand 11, 2000 Neuchâtel, Switzerland

<sup>3</sup> School of Agricultural, Forest and Food Sciences HAFL, Bern University of Applied Sciences, Länggasse 85, 3052 Zollikofen, Switzerland

<sup>4</sup> MUSE, Corso del Lavoro e della Scienza 3, 38122 Trento, Italy

\*Corresponding author

#### ABSTRACT

Humus forms, especially the occurrence and the thickness of the horizon of humified residues (OH), provide valuable information on site conditions. In mountain forest soils, humus forms show a high spatial variability and data on their spatial patterns is often scarce. Our aim was to test the applicability of various vegetation features as proxy for OH thickness. Subalpine coniferous forests dominated by *Picea abies* (L.) H. Karst. and *Larix decidua* Mill. were studied in the Province of Trento, Italian Alps, between ca. 900 and 2200 m a.s.l. Braun-Blanquet vegetation relevés and OH thickness were recorded at 152 plots. The vegetation parameters, tested for their suitability as indicators of OH thickness, encompassed mean Landolt indicator values of the herb layer (both unweighted and cover-weighted means) as well as parameters of vegetation structure (cover values of plant species groups) calculated from the relevés. To our knowledge, the predictive power of Landolt indicator values (LIVs) for humus forms had not been tested before. Correlations between OH thickness and mean LIVs were strongest for the soil reaction value, but indicator values for humus, nutrients, temperature and light were also significantly correlated with OH thickness. Generally, weighting with species cover reduced the indicator quality of mean LIVs for OH thickness. The strongest relationships between OH thickness and vegetation structure existed in the following indicators: the cover of forbs (excluding graminoids and ferns) and the cover of Ericaceae in the herb layer. Regression models predicting OH thickness based on vegetation structure had almost as much predictive power as models based on LIVs. We conclude that LIVs analysis can produce fairly reliable information regarding the thickness of the OH horizon and, thus, the humus form. If no relevé data are readily available, a field estimation of the cover values of certain easily distinguishable herb layer species groups is much faster than a vegetation survey with consecutive indicator value analysis, and might be a feasible way of quickly indicating the humus form.

**Keywords:** Landolt indicator values; OH horizon; Forest ecosystem; Montane forest; Italian Alps

**Received:** 10 November 2016 – **Revised:** 03 February 2017 – **Accepted:** 08 February 2017



## Acknowledgements

This thesis would not have been possible without the support from various people. I am particularly grateful to my supervisor Gabriele Broll. She gave me the opportunity to do research in the context of the DecAlp project and to gain important experience in both international research collaboration and teaching at the university. She enabled me to visit great meetings, conferences and excursions to get connected to national and international colleagues. Finally, she always managed to create a professional setting that stimulated me to focus on the essential tasks. Moreover, I am very grateful to Joachim Härtling and Markus Reichstein for their involvement as referees of the thesis.

Besides, I give many thanks to all members of the working group Agroecology and Soil Science at the Institute of Geography. I thank Kerstin Anschlag very much for the great time that we spent together in the field, at project meetings, at conferences and in the office. In particular, I am thankful to her and to Hans-Jörg Brauckmann for numerous discussions and valuable advice. I thank all students who promoted my research by their assistance in laboratory analyses, in proofreading and in everyday university life: Anne Bienhaus, Theresa Dreier, Mariam El Hourani, Alison Simerly, Janike Wagener and Christian Zimmer.

An excellent multidisciplinary collaboration of the people involved in the DecAlp project was the basis for achieving the parts of this thesis. I am very grateful to all DecAlp colleagues for interesting and inspiring meetings and discussions. Special thanks to those who contributed as co-authors of the three articles of this thesis! I particularly give many thanks to Dylan Tatti, Ulfert Graefe and Giacomo Sartori for their engagement in many insightful discussions in the field.

Additionally, I am thankful to everyone in my professional and private spheres of the last three years. The time that I spent as research assistant at the Institute of Geography was special for me. I gladly remember all those great encounters, conversations, seminars and celebrations with very nice colleagues and students. My family and my friends have always been a support to me and I am grateful for all these vital relations.



# Curriculum vitae

**Niels Hellwig**

born in Osnabrück, Germany

## Professional experience

since 02/2018

**Potsdam University**

Institute of Earth and Environmental Science

**Research Assistant**

- Contribution to EU project ECOPOTENTIAL
- Research on GIS-based statistical modelling of ecosystems in conservation areas

09/2014 - 01/2018

**Osnabrück University**

Institute of Geography

**Research Assistant**

- Contribution to DFG project DecAlp (D.A.CH. network)
- Research on spatial statistical modelling of decomposition processes in the high mountains
- Teaching: seminars, field courses, excursions

08/2011 - 07/2012,  
10/2012 - 08/2014

**Osnabrück University**

Institute of Geography

**Student / Research Assistant**

- Assistance of teaching activities
- Supporting work in research projects
- Support of the conference organization of the German Federal Soil Association in Augsburg

10/2011 - 01/2012,  
10/2012 - 01/2013

**Osnabrück University**

Institute of Computer Science

**Student / Research Assistant**

- Tutor in the lecture Graph Algorithms

## Studies

10/2012 - 09/2014

**Osnabrück University**

School of Mathematics / Computer Science

**Environmental Systems and Resources Management**

- Thesis (**Master of Science**): 'Humusformen und Enchyträen an Hochgebirgsstandorten in den italienischen Alpen – Prognose der räumlichen Verteilung auf der Basis von GIS und Fuzzy-Logik'

10/2009 - 09/2012

**Osnabrück University**

School of Mathematics / Computer Science

**Applied Systems Science**

- Thesis (**Bachelor of Science**): 'Simulation der räumlichen Verteilung von Triclosan im Einzugsgebiet des Mains'



## Scientific publications

- Hellwig, N.,** Gómez-Brandón, M., Ascher-Jenull, J., Bardelli, T., Anschlag, K., Fornasier, F., Pietramellara, G., Insam, H., Broll, G. (2018): Humus Forms and Soil Microbiological Parameters in a Mountain Forest: Upscaling to the Slope Scale. *Soil Systems* 2(1), 12.
- Anschlag, K., Tatti, D., **Hellwig, N.,** Sartori, G., Gobat, J.-M., Broll, G. (2017): Vegetation-based bioindication of humus forms in coniferous mountain forests. *Journal of Mountain Science* 14(4), 662-673.
- Hellwig, N.,** Anschlag, K., Broll, G. (2017): Modellgestützte Analyse räumlicher Dekompositionsmuster im Hochgebirge. *Berichte der DBG (eprints)*, [http://eprints.dbges.de/1232/1/Hellwig%20et%20al\\_2017\\_DBG%20eprints\\_Dekompositionsmuster%20R%C3%A4umliche%20Modelle%20Hochgebirge.pdf](http://eprints.dbges.de/1232/1/Hellwig%20et%20al_2017_DBG%20eprints_Dekompositionsmuster%20R%C3%A4umliche%20Modelle%20Hochgebirge.pdf) (20/01/2018).
- Hellwig, N.,** Graefe, U., Tatti, D., Sartori, G., Anschlag, K., Beylich, A., Gobat, J.-M., Broll, G. (2017): Upscaling the spatial distribution of enchytraeids and humus forms in a high mountain environment on the basis of GIS and fuzzy logic. *European Journal of Soil Biology* 79, 1-13.
- Hellwig, N.,** Anschlag, K., Broll, G. (2016): A fuzzy logic based method for modeling the spatial distribution of indicators of decomposition in a high mountain environment. *Arctic, Antarctic, and Alpine Research* 48(4), 623-635.
- Hellwig, N.,** Graefe, U., Tatti, D., Anschlag, K., Gobat, J.-M., Broll, G. (2015): GIS-basierte Modellierung von Humusformen und Enchyträen in zwei italienischen Alpentälern. *Berichte der DBG (eprints)*, [http://eprints.dbges.de/1142/1/Hellwig\\_et\\_al\\_2015\\_DBG\\_eprints\\_Humusformen\\_Enchy\\_R%C3%A4uml\\_Modell\\_Fuzzy-Logik.pdf](http://eprints.dbges.de/1142/1/Hellwig_et_al_2015_DBG_eprints_Humusformen_Enchy_R%C3%A4uml_Modell_Fuzzy-Logik.pdf) (20/01/2018).

## Teaching

09/2014 - 01/2018

**Osnabrück University**

Institute of Geography

**Self-responsible teaching**

- Proseminar Physische Geographie (3 times, target group: Bachelor, 2nd semester)
- Geländepraktikum Physische Geographie (3 times, target group: Bachelor, 4th semester)
- One day excursion: LIFE-Projekt Emmericher Ward
- One day excursion: Naturschutzgroßprojekt Senne und Teutoburger Wald

**Further teaching activities**

- Teaching activities (partly self-responsible) in the M.Sc. programme Soils, Inland Waters, Contaminated Lands
- Supervision of bachelor and master theses in geography (as second referee)
- Supervision of students' works in the context of interdisciplinary professionalization

10/2016 - 10/2017

**Osnabrück University**

Professional trainings of didactics in higher education and completion of certificate 'Hochschuldidaktische Qualifizierung'

## Attended Conferences

### Talks and Posters

- Hellwig, N., Anschlag, K., Broll, G. (2017): Spatial patterns of organic matter decomposition in a high mountain forest environment. IUFRO 125th Anniversary Congress. Freiburg i. Br., 09/2017.
- Hellwig, N., Anschlag, K., Broll, G. (2017): Modellgestützte Analyse räumlicher Dekompositionsmuster im Hochgebirge. German Soil Science Society, Annual Meeting. Göttingen, 09/2017.
- Hellwig, N., Anschlag, K., Broll, G. (2017): Mapping the patterns of organic matter decomposition in a high mountain environment. Pedometrics. Wageningen, 06/2017.
- Hellwig, N., Anschlag, K., Broll, G. (2017): Modelling spatial patterns of organic matter decomposition in a forest environment in the Italian Alps. 12th YoMos Workshop. Buchenbach, 05/2017.
- Hellwig, N., Anschlag, K., Graefe, U., Tatti, D., Sartori, G., Egli, M., Gobat, J.-M., Broll, G. (2016): Modelling spatial patterns of organic matter decomposition in a high mountain forest environment. Florence Symposium, Italian Academy of Forest Science. Florence, 09/2016.
- Hellwig, N., Anschlag, K., Broll, G. (2016): Spatial patterns of forest humus forms and decomposition processes in two Italian Alpine valleys. The Ecological Society of Germany, Austria and Switzerland, Annual Meeting. Marburg, 09/2016.
- Hellwig, N., Graefe, U., Tatti, D., Anschlag, K., Gobat, J.-M., Broll, G. (2015): Räumliche Modellierung von Humusformen und Enchyträen in zwei italienischen Alpentälern auf der Basis von GIS und Fuzzy-Logik. German Soil Science Society, Annual Meeting. München, 09/2015. [Poster]
- Hellwig, N., Anschlag, K., Broll, G. (2015): Verknüpfung von Entscheidungsbäumen und Fuzzy-Logik zur Modellierung der räumlichen Verteilung von Dekompositionsmerkmalen im Hochgebirge. DBG Workshop Digital Soil Mapping, Tübingen, 03/2015.
- Hellwig, N., Graefe, U., Broll, G. (2015): Spatial modelling of the distribution of enchytraeid species at Val di Sole / Val di Rabbi (Trentino, Italian Alps). Annual Meeting of the Working Group on High Mountains, Hamburg, 01/2015.
- Hellwig, N., Broll, G. (2014): Modellierung der räumlichen Verteilung von Humusformen im Hochgebirge. DBG Workshop Digital Soil Mapping, Tübingen, 04/2014.

### Research Meetings, Workshops and Seminars

- International Conference and Workshop 'Soil classification: a powerful tool for planning Soil Conservation' of the European Society for Soil Conservation and the Soil Science Society of Latvia (Latvia and Estonia, 07/2017)
- Meetings of the D.A.CH. research project „Effect of climate on coarse woody debris decay dynamics and incorporation into the soils of forested Alpine areas“ (DecAlp): Florence (Italy), 09/2016; Osnabrück, 11/2015; Innsbruck (Austria), 03/2015; Neuchâtel (Switzerland), 02/2014
- Joint International Summer School “Advanced methods and new integrated approaches to study soil processes in mountain ecosystems” of the SISS and the EU COST Action SENSFOR (Pieve Tesino / Italy, 06/2016)

- ISRIC Spring School „Hands-on Global Soil Information Facilities“ (Wageningen, 05/2015)
- Workshop “Humusformen von Böden der montanen bis alpinen Stufe der Alpen“ of the Working Group Humus Forms of the German Soil Science Society (Grainau, 05/2014)
- Statistics Workshop “Moderne statistische Verfahren für die Analyse komplexer Datensätze in Bodenbiologie, Bodenökologie und Bodenkunde“ of the Commission III Soil Biology and Soil Ecology of the German Soil Science Society (Osnabrück, 03/2014)
- ERASMUS Intensive Programme „Agents-based modelling for spatial processes in landscape geography“ (Angers / France, 02-03/2013)

### **Memberships**

- Ecological Society of Germany, Austria and Switzerland (GfÖ):  
Specialist group YoMos (Young Modellers in Ecology)
- German Soil Science Society (DBG):  
Working Group Humus Forms and Working Group Digital Soil Mapping
- Working Group on High Mountains of the German Geographical Society (DGfG)



